Cláudia Alexandra Rocha Ferreira

Mestre em Engenharia Civil

Use of Petri Nets to Manage Civil Engineering Infrastructures

Dissertação para obtenção do Grau de Doutor em Engenharia Civil, Especialidade de Estruturas

Orientador: Luís Armando Canhoto Neves,
Professor Auxiliar, FCT/UNL
Co-orientador: José António Campos e Matos,
Professor Auxiliar, EEUM

Júri:

Presidente: Doutor Fernando Manuel Anjos Henriques
Arguentes: Doutor Jorge Manuel Caliço Lopes de Brito
Doutor Luís Miguel Pina de Oliveira Santos
Vogais: Doutor António Abel Henriques
Doutora Maria Paulina Santos Forte Faria Rodrigues
Doutor Eduardo Soares Ribeiro Gomes Cavaco
Doutor Luís Armando Canhoto Neves

FACULDADE DE CIÊNCIAS E TECNOLOGIA
UNIVERSIDADE NOVA DE LISBOA

Dezembro, 2018

Use of Petri Nets to Manage Civil Engineering Infrastructures

To my parents and sister...

Acknowledgements

The completion of this dissertation represents the culmination of an important stage in my life. Its elaboration had the direct and indirect contribution of several people and entities, to which I am deeply grateful.

First and foremost, I would like to express my sincere gratitude to my supervisor, Dr. Luís Neves, for giving me the opportunity to do this work and for the confidence that has always shown from the first day. Without him, this work would not have been possible. For his constant support, friendship, guidance and sharing of knowledge's throughout the entire work, I am truly grateful.

I also would like to express my deeply gratitude to Dr. José Campos e Matos, my co-supervisor, for his support, help and interest over the last few years.

I would also like to extend my thanks to Eng. Ugo Berardinelli, from Ascendi, and to Eng. Luís Marreiro, from BRISA, for all the support and help concerning the access of data relative bridges and road networks needed to carry out this work. As well as, to Dr. Ana Silva for helping with the ceramic claddings.

My appreciation goes also to the members of the Nottingham Transportation Engineering Centre (NTEC) of University of Nottingham for their friendship and how well I have been received. Thanks to all who made my time more enjoyable.

The support of Civil Engineering Department of *Faculdade de Ciências e Tecnologia* is greatly acknowledged. I want to thank all Professor and researchers who helped me and supported me at various stages of this journey. I also would like to thank Maria da Luz and Carla for all helpful support that they gave me. Finally, to my colleagues, I want to thank for their friendship, support, share of ideas, mutual help, and fun over these years. With special thanks to Filipe, Nuno, Hugo and Renato.

I am sincerely grateful to my friends Andreia, Helena and Mafalda for their constant motivation, for being always by my side through good and bad times and above all for wanting me to realize my dreams. I am also truly grateful to Ana Rita for all her help in developing the thesis.

Finally, I wish to thank to my family, parents and sister, for their unconditional love, care and understanding during this period. To them, I am deeply grateful.

Abstract

Over the last years there has been a shift, in the most developed countries, in investment and efforts within the construction sector. On the one hand, these countries have built infrastructures able to respond to current needs over the last decades, reducing the need for investments in new infrastructures now and in the near future. On the other hand, most of the infrastructures present clear signs of deterioration, making it fundamental to invest correctly in their recovery. The ageing of infrastructure together with the scarce budgets available for maintenance and rehabilitation are the main reasons for the development of decision support tools, as a mean to maximize the impact of investments.

The objective of the present work is to develop a methodology for optimizing maintenance strategies, considering the available information on infrastructure degradation and the impact of maintenance in economic terms and loss of functionality, making possible the implementation of a management system transversal to different types of civil engineering infrastructures. The methodology used in the deterioration model is based on the concept of timed Petri nets. The maintenance model was built from the deterioration model, including the inspection, maintenance and renewal processes. The optimization of maintenance is performed through genetic algorithms.

The deterioration and maintenance model was applied to components of two types of infrastructure: bridges (pre-stressed concrete decks and bearings) and buildings (ceramic claddings). The complete management system was used to analyse a section of a road network. All examples are based on Portuguese data.

Keywords: Infrastructure Management Systems; Petri nets; Deterioration; Maintenance; Optimization.

Resumo

Ao longo dos últimos anos, nos países mais desenvolvidos, tem-se assistido a um redirecionamento dos investimentos e dos esforços no sector da construção. Por um lado, estes países, construíram ao longo das últimas décadas infraestruturas capazes de responder às necessidades atuais, diminuindo a necessidade de investimentos em novas infraestruturas no presente e no futuro próximo, por outro, grande parte das infraestruturas existentes apresenta sinais claros de deterioração, tornando-se fundamental investir corretamente na recuperação das mesmas. Assim sendo, o envelhecimento das infraestruturas juntamente com os escassos orçamentos disponíveis para a realização de ações de manutenção e de reabilitação são os principais motivos para o desenvolvimento de ferramentas de apoio à decisão, como meio de maximizar os investimentos.

O presente trabalho tem como objetivo desenvolver uma metodologia de otimização de estratégias de manutenção considerando a informação disponível sobre a degradação das infraestruturas e o impacte das ações de manutenção em termos económicos e de perda de funcionalidade, possibilitando, desse modo, a implementação de um sistema de gestão transversal a diferentes tipos de infraestruturas de engenharia civil. A metodologia utilizada no modelo de deterioração é baseada no conceito de redes de Petri temporais. O modelo de manutenção foi construído a partir do modelo de deterioração, incluído os processos de inspeção, manutenção e renovação. A otimização das ações de manutenção é realizada através de algoritmos genéticos.

O modelo de deterioração e de manutenção foram aplicados a componentes de dois tipos de infraestruturas: obras de arte (tabuleiros de betão armado e pré-esforçado, e aparelhos de apoio) e edifícios (revestimentos cerâmicos). O sistema de gestão completo foi utilizado para analisar um troço de uma rede rodoviária. Todos os exemplos apresentados são baseados em dados portugueses.

Palavras-chave: Sistemas de gestão de infraestruturas; Redes de Petri; Deterioração; Ações de manutenção; Otimização.

Contents

List of Figures

List of Tables

Nomenclature

List of symbols

Upper Roman letters

A	Total area of the façade
A_n	Area of coating affected by an anomaly n
C	Condition index
$C(t)$	Time dependent condition index
C_i	Vehicle capacity of the highway segment i
C_0	Initial condition index
$\mathbf{D}$	Incidence matrix for a Petri net composed only by ordinary arcs
$\mathbf{D}'$	Incidence matrix for a Petri net composed by ordinary and inhibitor arcs
E	Total number of elements present in the database
$E(t)$	Expected value of the system condition at time t
E_i	Expected number of transitions
FT	Firing time
$\mathbf{H}(M)$	Inhibitor matrix
K_e	Total number of transitions observed in the element e in the database
L	Likelihood
L_i	Length of the highway segment i
M	Current marking of the Petri net
$M(p_i)$	Number of tokens in place p_i
M'	New marking of the Petri net
M_i, M_j	Generic marking of the Petri net
M_0	Initial marking of the Petri net
MSE	Within-groups mean squares in the ANOVA statistical test
MSR	Between-groups mean squares in the ANOVA statistical test
N	Total number of transition periods

O_i Observed number of transitions

P   Transition probability matrix

P Finite set of places in the Petri net

$P(\cdot)$ Probability

$P(\cdot|\cdot)$ Conditional probability

P_f Probability of failure

Post   Post-incidence matrix in the Petri net

Pre   Pre-incidence matrix in the Petri net

Q   Transition intensity matrix

Q Load effect

$Q(t)$ Percentage "functionality" (or "quality", or "serviceability") of the system at time t

R Resistance; Resilience

$R(M_0)$ Set of all markings which can be reached from the initial marking M_0

R_L Loss of resilience experienced by the system

R_{Log} Logarithmic resilience

S Safety index; Vector of condition states defined in the performance scale

$S(t)$ Time dependent safety index

S_{cri} Critical speed

$S_{free\,i}$ Limited maximum speed of the highway segment i

$S_i(t)$ Average speed of the highway segment i at time t

S_w Degradation severity of the coating

S_0 Initial safety index

SSE Within-groups sum of squares in the ANOVA statistical test

SSR Between-groups sum of squares in the ANOVA statistical test

T Finite set of transitions in the Petri net; Goodness-of-fit test

T_j Mean sojourn time in condition state j

$TTD(t)$ Total travel distance at time t

$TTT(t)$ Total travel time at time t

V Vector of transitions maximum firing speeds

X Set of nodes of the network

$X(t)$ Condition state of the process at time t

Y Subset of nodes that connect to node x

Lower Roman letters

c_i	Time required to cover the highway segment i with traffic flow rate q_i
c_t	Cost at time t
c_0	Cost at present
df	Number of degrees of freedom
d_j	Delay associated with transition t_j in the Petri net
$f_i(t)$	Traffic flow rate entering the network at input point i at time t
i	Generic highway segment in the traffic model
k	Multiplying factor; Total number of groups tested in the ANOVA statistical test
$k_{a,n}$	Weighting factor corresponding to the relative weight of the anomaly detected
k_e	Generic transition observed in the element e in the database
k_n	Multiplying factor of anomaly n, as a function of their degradation level
$\hat{l}$	Normalized log-likelihood
$\log L$	Logarithm of the likelihood (log-likelihood)
$l_b(t)$	Bridge damage level at time t
m	Total number of transitions in the Petri net
m'	Total number of timed transitions in the Petri net
$m_{p_i}(t)$	Number of tokens in place p_i at time t
n	Total number of places in the Petri net; Total number of observations in each group tested in the ANOVA statistical test
n_i	Total number of components in state i
n_{ij}	Total number of components transitioning from state i to state j
n_i, n_j	Number of observations in group i and j in the ANOVA statistical test
n_{MCS}	Total number of trials in the MCS
$n_{MCS,j}$	Number of trials in the MCS where the condition state predicted is equal to the condition state observed, state j
n_s	Number of elements presents in the sample
p	Randomly generated probability uniformly distributed between 0 and 1; Number of estimated parameters
$p(t)$	Condition vector at time t
p_i	Generic place in the Petri net
p_{ij}	Probability of transition from state i to state j
$post(p_i, t_j)$	Post-condition of the transition t_j; Weight of the arc from transition t_j to place p_i
$pre(p_i, t_j)$	Pre-condition of the transition t_j; Weight of the arc from place p_i to transition t_j
$q_b(t)$	Functionality of the bridge b at time t

$q_i(t)$	Average flow rate of the highway segment i at time t
q_{ij}	Transition intensity from state i to state j
$q_{max\,i}$	Maximum flow rate of transition i
s	Finite state space; Total number of condition states defined in the performance scale
t	Time
t_d	Time during which the deterioration process of performance level is suppressed
t_h	Time horizon
t_i, t_I	Instant of damage initiation; Generic transition in the traffic model
t_{insp}	Time interval between major inspections
$t_{insp,max}$	Upper limit of the time interval between major inspections
$t_{insp,min}$	Lower limit of the time interval between major inspections
t_j	Generic transition in the Petri net
$\cdot t_j$	Pre-set of places of the transition t_j
t_P	Time of reapplication of the maintenance
t_{pd}, t_{PD}	Duration of the effect of the maintenance
t_{PI}	Application time of first maintenance
t_r	Time during which the deterioration rate of the performance level is affected; Time that the recovery of the system is complete
t_0	Time that external event occurs
Δt	Time interval
u	Firing vector
u_j	Firing frequency associated with transition t_j in the Petri net
v	Annual discount rate
$v_i(t)$	Transition firing speed that represents the average flow rate $q_i(t)$ of the highway segment i
v_j	Firing speed associated with transition t_j in the Petri net
$v_{max\,i}$	Maximum firing frequency of the highway segment i
$\bar{y}_i, \bar{y}_j$	Mean of the group i and j in the ANOVA statistical test

Upper Greek letters

$\Gamma(t)$	Performance of the network at time t
Γ^0	Value of $\Gamma(t)$ when none of bridges is in service
Γ^{100}	Value of $\Gamma(t)$ when all bridges are in service
Θ	Deterioration rate vector; Set of parameters of an arbitrary probabilistic distribution
Λ	Firing rate vector

$\Phi(\cdot)$ Cumulative distribution function of the standard normal variate

Lower Greek letters

α Deterioration rate of performance level without maintenance; Significance level

α_i Maximum number of possible simultaneous firings associated with the highway segment i

β Reliability index

β_0 Initial reliability index

$\beta(t)$ Time dependent reliability index

$\Delta\beta$ Variation of the reliability index

γ Improvement of the performance level after the application of the maintenance

γ_D Balancing factor (cost) associated with the distance travelled by the users in the network

γ_T Balancing factor (cost) associated with the time spent by the users in the network

δ Deterioration factor

θ Deterioration rate of performance level during the effect of maintenance

θ_j Parameter of the probabilistic distribution associated with transition t_j

λ_j Scale parameter of the exponential distribution associated with condition state j; Firing rate of the transition t_j that transforms M_i into M_j

$\mu(t)$ Mean of the condition state at time t

$\mu_{cost}(t)$ Mean of the cumulative maintenance cost at time t

ν_{ji} Transition intensity back from state j to state i

ρ_{cri} Critical density

$\rho_i(t)$ Average flow density of the highway segment i at time t

$\rho_{max\,i}$ Jam density of the highway segment i

$\sigma(t)$ Standard deviation of the condition state at time t

$\sigma_{cost}(t)$ Standard deviation of the cumulative maintenance cost at time t

τ Sojourn time

List of acronyms

AASHTO   American Association of State Highway and Transportation Officials

ANOVA   ANalysis Of VAriance

ASCE   American Society of Civil Engineers

BdMS   Building Management System

BMS   Bridges Management System

BREX	Concrete Bridge Rating EXpert system
CDF	Cumulative Distribution Function
CM	Corrective Maintenance
CS	Condition State
CTMC	Continuous Time Markov Chains
CTPN	Continuous Timed Petri Net
DSPN	Deterministic and Stochastic Petri Net
DTMC	Discrete Time Markov Chains
ESPN	Extended Stochastic Petri Net
FCT	Faculdade de Ciências e Tecnologia
FHWA	Federal Highway Administration
GA	Genetic Algorithm
GDP	Gross Domestic Product
GSPN	Generalized Stochastic Petri Net
iCDF	Inverse Cumulative Distribution Function
IMS	Infrastructure Management System
MC	Markov Chain
MCS	Monte Carlo Simulation
MR&R	Maintenance, Repair and Rehabilitation
NBI	National Bridge Inventory
NBIP	National Bridge Inspection Program
NCHRP	National Cooperative Highway Research Project
NDT	Non-Destructive Tests
OD	Origin-Destination matrix
OECD	Organisation for Economic Co-operation and Development
PCI	Pavement Condition Index
PDF	Probability Density Function
PM	Preventive Maintenance
PMS	Pavement Management System
PN	Petri Net
SPN	Stochastic Petri Net
TPN	Timed Petri Net
TSS	Transport Simulation Systems
UNL	Universidade Nova de Lisboa

WMS   Waterwaste Management System

2-D   Two-Dimensional

Petri net symbology

◯   Place

◎   Continuous place

⟶   Directed arc

⟷   Bidirectional arc

⟼○   Inhibitor arc

▮   Immediate transition

▮   Timed transition with deterministic time delay

▯   Timed transition with stochastic time delay

▯   Continuous timed transition

▯   Reset transition

●   Token

Chapter 1

Introduction

1.1 Background and motivation

The paradigm in the construction sector is changing. Economic aspects (ageing of the infrastructures and the scarcity of funding for maintenance and rehabilitation actions) as well as environmental concerns (increase of awareness of the concept of sustainability and the environmental impact of the construction sector) are the main reasons for this change (Scherer and Glagola, 1994; Hovde, 2002; Paulo et al., 2014). This paradigm shift has resulted in an effort to develop decision support tools that maximize the benefits of the investments done in the past by extending the life of existing infrastructures. A more rational approach to decision-making in terms of inspection, maintenance and rehabilitation of the built heritage is required. For this purpose, several steps should be followed. Firstly, it is important to compile an inventory of existing structures and the conservation state of each structure. Secondly, it is essential to develop deterioration models to predict the future performance of these structures. After that, in a third stage, the development of maintenance and optimization models is fundamental to assess the impact of maintenance actions and to optimize better maintenance strategies. Over the past decades, a range of methods have been proposed in the literature for modelling deterioration maintenance and inspections (Thompson et al., 1998; Neves and Frangopol, 2005), as well as, method to optimize inspections and maintenance (Miyamoto et al., 2000; Yang et al., 2006).

The experience gained on the use of these models showed that the uncertainty associated with the deterioration process has to be explicitly included in the decision-making process, since the complexity of the phenomena involved and the limited information available make it impossible to model the deterioration with high precision (Lounis and Madanat, 2002). However, the main difficulty of all these methods is the fit of the inspection data, which is not absolutely reliable. According to Phares et al. (2004), visual inspections are an unreliable method for the evaluation of infrastructures conservation state. Different inspectors under different conditions, evaluate significantly differently the conservation state of the infrastructure, introducing an additional source of uncertainty (Corotis et al., 2005).

Markov Chains (MC) are the most commonly used stochastic technique to predict deterioration profiles in different fields of civil engineering, such as pavements, bridges, pipes, buildings, among others (Butt et al., 1987; Hawk and Small, 1998; Thompson et al., 1998; McDuling, 2006; Ortiz-García et al., 2006; Caleyo et al., 2009; Silva et al., 2016d). Particularly, the use of continuous Markov chains explicitly introduce the uncertainty associated with irregular times between inspections in the model results, while maintaining the simplicity of the traditional Markov processes (Kallen and van Noortwijk, 2006; Morcous, 2006). A continuous Markov chain defines the state of a system[1] in terms

---

[1]Most of the concepts and theory presented here are applicable to a wide range of objects, therefore, the term *system* is used as general description of the object of study.

of a discrete variable (e.g. condition state of a bridge) and the transition between states is defined by an intensity matrix (Kalbfleisch and Lawless, 1985; Kallen and van Noortwijk, 2006; Jackson, 2011). The intensity matrix defines the instantaneous probability of moving from state i to state $j \neq i$ and allows for the transitions between the different states to occur on a continuous timescale, property very useful when the time of observation of each infrastructure is not uniform. In a continuous Markov chain, the time taken to move from one condition state to the next is characterized by an exponential distribution. The simplicity of the exponential distribution (i.e. being a single parameter distribution and the existence of analytical expressions for the probability distribution) is the main advantage of this approach. However, exponential distributions are not very versatile and can result in a gross approximation of the system characteristics. In addition, the Markov chains have other disadvantages, including the inability to build more complex models, namely inspection, maintenance, environmental conditions or uncertainty associated with the decision-making.

To overcome this limitation, models based on net theory can be useful. Petri Nets (PN) are a modelling technique applied successfully in dynamic systems in several fields of knowledge, namely in robotics (Al-Ahmari, 2016), optimization of manufacturing systems (Chen et al., 2014; Uzam et al., 2016), business process management (van der Aalst, 2002), human computer interaction (Tang et al., 2008), among others. This modelling technique has several advantages when compared with the Markov chains. The graphical representation can be used to describe the problem intuitively. It is more flexible and has more capabilities than the Markov chains, it allows the incorporation of more rules in the model to simulate accurately complex situations and it keeps the model size within manageable limits. Moreover, this modelling technique is not restricted to the exponential distribution to simulate the time in the system. As a disadvantage, there are no closed form expressions for the probability distribution used and simulation techniques are required.

Based on these models, it is possible to assess the impact of maintenance actions and to optimize maintenance strategies in order to minimize costs and maximize performance. The massive development of optimization algorithms makes their use relatively simple, and its application to infrastructures management problems has been proposed, among others by Neves et al. (2006) and Orcesi et al. (2010). The main difficulty relates to the quantification of the effects and costs of the maintenance actions and a clear definition of objectives and restrictions. According to Meegoda et al. (2005), the direct costs (labour, equipment, materials) should be supplemented with the indirect costs associated with level of performance, functionality loss, risk of failure, and in the case of transport networks, the growth of the travel time, the growth of the risk of accidents and inaccessibility to areas or equipment. In the case of buildings, indirect costs can be considered in a simplified way, through the duration and the local impact of the maintenance action. In the case of transport network, the service suspension or a reduction affects the entire network, in function of the location, of the alternatives, and the traffic level.

1.2   Objectives

The main aim of this PhD thesis is to develop of methodology for the definition and implementation of an Infrastructure Management System (IMS) that incorporates:

- Assessment of the future performance of infrastructures, considering the uncertainty to the process of deterioration and the errors inherent to the visual inspection process. The assessment of the future performance is carried out through stochastic methodologies including Markov chains and Petri nets;

- Assessment of the direct and indirect costs of preventive and corrective maintenance, assessing its impact on the performance and functionality of the infrastructure; and

- Optimization of maintenance strategies, considering the multiple objectives in terms of different probabilistic indicators of cost and performance. A multi-objective optimization framework based on Genetic Algorithm (GA) is used.

With these developments, it will be possible to implement a transversal management system to different types of civil engineering infrastructures. By minimizing the impact of interventions, the performance level and functionality of infrastructure can be maximized without incurring disproportionate costs. Additionally, the consideration of the inspection data as probabilistic allows a more realistic prediction that consequently leads to better maintenance strategies and a clearer perception of the associated risk.

The main contribution of this work is the development and application of a general civil engineering asset management system, based on Petri-nets. To achieve this, it was necessary to: (i) propose new models for the life-cycle performance of bridges and façades based on Petri nets; (ii) develop a novel calibration procedure for Petri nets using different probabilistic distributions; and (iii) develop and calibrate a macroscopic traffic model, based on Petri nets.

1.3 Methodology

For achieving objective, the PhD program was developed into four main work packages:

- Work Package 1 – Definition, implementation and calibration of Markov chain models;

- Work Package 2 – Definition, implementation and calibration of Petri net models;

- Work Package 3 – Evaluation of the maintenance actions impact on performance and cost;

- Work Package 4 – Implementation of optimization algorithms in asset management.

A description of the work to be developed in each work package is provided in the next sections.

WP1 – Definition, implementation and calibration of Markov chain models

In this first work package, emphasis is placed on the definition and implementation of deterioration and maintenance models based on continuous Markov chains. To achieve this, four main tasks are defined:

- Task 1.1 – Definition;

- Task 1.2 – Implementation;

- Task 1.3 – Calibration;

- Task 1.4 – Maintenance modelling.

In Task 1.1, the main properties of the Markov chain model will be defined. In Task 1.2, the deterioration model will be implemented in MatLab® and extensively tested. In Task 1.3, an algorithm that allows fitting the model to historical data of inspections and maintenance actions is developed. The calibration of the parameters that define the Markov chains will be performed by using maximum likelihood indicators and optimization algorithms, in order that the difference between the predicted and observed values are minimized. In Task 1.4, the most common maintenance strategies are evaluated, considering preventive and corrective maintenance actions. The effect of these maintenance actions in the infrastructure performance is assessed, in the absence of historical data, through expert opinion. The maintenance model is developed based on concept of Markov chains.

WP2 – Definition, implementation and calibration of Petri net models

In WP2, a Petri net formalism will be applied to model the deterioration and maintenance processes of existing assets. This WP can be divided into four tasks:

- Task 2.1 – Definition;

- Task 2.2 – Implementation;

- Task 2.3 – Calibration;

- Task 2.4 – Maintenance modelling.

All tasks will be developed in accordance with the assumptions defined for WP1. In Task 2.1, the main properties of the Petri net model will be defined. In Task 2.2, the deterioration model will be implemented in software MalLab$^{®}$ and extensively tested. In Task 2.3, an algorithm that allows fitting historical data of inspections and maintenance actions to the deterioration model based on concept of timed Petri nets is developed. The sojourn time in each condition level are modelled as probabilistic distributions. The probability distribution that best describes the deterioration process of an infrastructure is that resulting in higher probabilities of occurrence of the observed transitions. In order to assess what are the parameters of the probability distribution that provides a best fit, the parameters are fitted to historical data through maximum likelihood indicators and optimization algorithms. Finally, in Task 2.4, the most common maintenance strategies are evaluated. The maintenance model is developed based in the Petri net formalism.

WP3 – Evaluation of the maintenance actions impact on performance and cost

Maintenance actions imply direct costs to managing agency and indirect costs to users. User cost are usually associated with limitations of use during the application of maintenance actions. For example, in transportation infrastructures these costs correspond to increased travel time and fuel consumption, as well as, overall dissatisfaction. Agency costs are associated with material and labour costs. The consideration of these costs makes it small-scale maintenance solutions more attractive than corrective maintenance actions of greater impact. This approach will also increase the attractiveness of solutions that, although associated with higher costs, result in lower impact on users, like conducting interventions at night or weekend. However, these indirect costs cannot be directly compared to direct cost, since they are allocated to a large number of individuals with little influence in decision-making.

In this work, both direct and indirect costs are considered as two independent impacts. The best maintenance policy is defined as that minimizing both direct and indirect costs or the best balance between them, according to the preferences and financial availability or the decision-maker. This WP, the maintenance model developed in WP2 is applied two different types of infrastructures:

- Task 3.1 – Bridges;

  - Task 3.1.1 – Definition of the traffic model;

  - Task 3.1.2 – Implementation of the traffic model;

  - Task 3.1.3 – Calibration and validation of the traffic model;

- Task 3.2 – Ceramic claddings.

The maintenance model describes the full life-cycle, including not only the deterioration process but also inspections, maintenance and renewal processes. For both types of infrastructures, the maintenance model is used to analyse the consequences of alternative maintenance strategies to control deterioration patterns. In Task 3.1, in order to evaluate the user costs, a traffic model based on Petri net formalism is performed. In Task 3.1.1, the main properties of traffic model will be defined. In

Task 3.1.2, the traffic model will be implemented in software MalLab®. In Task 3.1.3, the traffic will be tested and the calibration and validation will be performed by comparing the values of the basic traffic parameters (speed, density, and flow rate) obtained through the traffic model implemented and a commercial micro simulation software, Aimsun.

WP4 – Implementation of optimization algorithms in asset management

In this last work package, methods to optimize maintenance policies are defined. This WP can be divided into three tasks:

- Task 4.1 – Definition;

- Task 4.2 – Implementation;

- Task 4.3 – Asset management.

In Task 4.1, the constrains and the objective function of the optimization problem will be defined. Constraints should be set for the acceptable average performance level, as well as the probability of violation of performance thresholds. In terms of costs, it should also be defined objectives in terms of the average values of the direct and indirect costs, but additionally measures to minimize the financial risks should be included, namely minimizing the characteristic cost over the life cycle. In Task 4.2, the optimization problem will be implemented in software MalLab® using generic algorithms and evolutionary strategies. Finally, in Task 4.3, the optimization problem is solved considering several objectives of optimization.

1.4 Outline of the dissertation

This dissertation begins with two background chapters, where the state of knowledge regarding Infrastructure Management System, its main components, and the main numerical techniques that enable them to be modelled are presented. In the following chapters, a description of the deterioration and maintenance model developed is presented and analysis of two case study is described. Finally, the impact of maintenance actions on performance and cost is evaluated as a multi-objective optimization problem.

In this way, the present dissertation is divided into nine chapters, including the present one, as follows:

- **Chapter 1:** An introduction to the topic is presented, and the main objectives and methodology of the dissertation are identified.

- **Chapter 2:** A detailed literature review on infrastructure management and maintenance is provided. The chapter begins with definition of an Infrastructure Management System and its main components as an important tool to help managers make informed and optimal decisions based on the analysis of the network data, making reference to several examples of IMS that have been developed over the years. After that, different deterioration models used to predict the future degradation are described and their advantages and limitations are appraised. Special emphasis is given to Markov chain-based deterioration models and to Petri nets-based deterioration models. In the end, a state of the art on maintenance models is presented.

- **Chapter 3:** This chapter is dedicated to Petri nets, describing the fundamental concepts and extensions of the Petri nets used in this project.

- **Chapter 4:** This chapter describes the Infrastructure Management System using the Petri net modelling technique developed. In the first part of this chapter, the time Petri net deterioration

model is presented. After that, the model used to consider maintenance in the system is depicted. The maintenance model was built from the deterioration model, including inspection, maintenance and renewal processes. In this chapter, the computational framework developed to compute the performance profiles are also described.

- **Chapter 5:** The deterioration and maintenance models based on Petri net formalism described in Chapter 4 are applied to two bridge components (pre-stressed concrete decks and bearings), using historical data collected by Ascendi. The chapter starts with the validation of the Petri net deterioration model. After that, the Petri net deterioration model is applied to analyse the deterioration process over time, and the maintenance model is applied to analyse the consequences of alternative maintenance strategies to control deterioration in bridge components.

- **Chapter 6:** The deterioration and maintenance models based on Petri net formalism described in Chapter 4 are applied to ceramic claddings. The deterioration model is used to predict the deterioration of cladding over time and to understand how the different exposure to environmental contribute to degradation. The maintenance model is applied to analyse the consequences of alternative maintenance strategies to control deterioration patters in ceramic claddings. The sample used in this case study is composed by 195 ceramic claddings located in Lisbon, Portugal.

- **Chapter 7:** This chapter focus on evaluate the maintenance impact on performance of a transportation network. The concept of resilience was used to quantify the rapidity of rehabilitation of infrastructure and the restoration of traffic flow. The traffic model implemented is based on the macroscopic approach described by Tolba et al. (2005). The calibration and validation of the traffic model was performed by comparing the values of the basic traffic parameters (speed, density, and flow rate) obtained through the traffic model implemented and the commercial micro simulation software, Aimsun.

- **Chapter 8:** In this chapter, a multi-objective optimization framework based on genetic algorithm for asset management of infrastructures is implemented. The optimization finds the maintenance strategies that minimizes maintenance costs, impact of maintenance on users, and maximizes performance indicators. As an example of application, maintenance strategies for the two bridge components analysed in Chapter 5 are optimized. The indirect costs are evaluated through the traffic model developed in Chapter 7. The case study is part of Portugal's highway network.

- **Chapter 9:** The main conclusions are summarized and recommendations for future research are presented.

Chapter 2

Literature Review

2.1   Introduction

From a civil engineering perspective, the term "infrastructure" is not just about assets, such as roads and bridges. It refers to set of physical systems or facilities which provide the necessary means for society to function, ensuring the delivery of goods and services, promoting prosperity, growth, good quality of life and environment (OECD, 2007). These infrastructures include: buildings, pedestrian and vehicular bridges, tunnels, roadways and railways, factories, conventional and nuclear power plants, offshore petroleum installations, heritage structures, port facilities and geotechnical structures, such as foundations and excavations (Brownjohn, 2007).

Civil infrastructure systems, like buildings, roadways, railways, electricity, and water/sewer networks, play a key role on the economy of a country, being its sustainability a crucial operation. However, a large percentage of existing infrastructure assets in developed countries are deteriorating due to age, harsh environmental conditions, and insufficient capacity (Elbehairy, 2007). In 2017, the American Society of Civil Engineers (ASCE) published one more Infrastructure Report Card on the condition of the United States infrastructure systems (ASCE, 2017). The report card is released every four years and aims to examine trends and assess the progress and decline of America's infrastructure. The 2017 Infrastructure Report Card reveals that the grade for America's infrastructure remains at a "D+" – the same grade received in 2013 – suggesting only incremental progress was made over the last four years. In 2017, sixteen infrastructure categories were assessed, with grades ranging from a "B" for Rail to a "D-" for Transit. While the overall grade did not improve, seven categories did see progress – Hazardous Waste, Inland Waterways, Levees, Ports, Rail, Schools, and Wastewater (Table 2.1). In this Report Card, the ASCE estimated that an investment of $4.59 trillion is needed, over a time period of 10 years, to bring the condition of infrastructure facilities to acceptable levels.

Similar results were obtained by the OECD Report – Infrastructure to 2030 (OECD, 2006, 2007), where it is estimated that, between 2006 and 2030, the annual infrastructure investment requirements for electricity, road and rail transport, telecommunications and water are likely to average around 3.5% of world gross domestic product (GDP).

Due to large size and high cost of infrastructure networks, maintaining such networks is challenging but an important and needed task, to ensure sustainability and growth of the countries. Limited budgets have resulted in an effort to develop new strategies for managing infrastructure assets in order to maximize the benefits of the investments done in the past.

This chapter includes a brief discussion on Infrastructure Management Systems as an important tool to help managers make informed and optimal decisions based on the analysis of the network data. The main components of an IMS are enumerated, and the main management system developed over the

Table 2.1 – Evolution of the condition of the United States infrastructure systems over the years (adapted from ASCE, 2017)

Category	1988	1998	2001	2005	2009	2013	2017
Aviation	B-	C-	D	D+	D	D	D
Bridges	–	C-	C	C	C	C+	C+
Dams	–	D	D	D+	D	D	D
Drinking water	B-	D	D	D-	D-	D	D
Energy	–	–	D+	D	D+	D+	D+
Hazardous waste	D	D-	D+	D	D	D	D+
Inland waterways	B-	–	D+	D-	D-	D-	D
Levees	–	–	–	–	D-	D-	D
Ports	–	–	–	–	–	C	C+
Public parks and recreation	–	–	–	C-	C-	C-	D+
Rail	–	–	–	C-	C-	C+	B
Roads	C+	D-	D+	D	D-	D	D
Schools	D	F	D-	D	D	D	D+
Solid waste	C-	C-	C+	C+	C+	B-	C+
Transit	C-	C-	C-	D+	D	D	D-
Wastewater	C	D+	D	D-	D-	D	D+
GPA	**C**	**D**	**D+**	**D**	**D**	**D+**	**D+**
Cost to improve	**–**	**–**	**$1.3T**	**$1.6T**	**$2.2T**	**$3.6T**	**$4.59T**

years are identified. This is followed by a literature review of the deterioration models used to predict the future degradation, with particular emphasis on Markov chains and Petri net methodologies. In the end of this chapter, a literature review on maintenance models is presented.

2.2   Infrastructure management system

An Infrastructure Management System can be defined as an integrated framework for infrastructure decision-making through its life-cycle, from "cradle to grave", that coordinates its functions in an integrated, data-centred approach to managing the physical systems, in order to maintain the infrastructure elements at an adequate performance level (Grigg, 2012). The life-cycle of an infrastructure can be considered to follow a cyclic chain (Figure 2.1). According to this cycle, the life-cycle starts with the needs assessment procedure, where sections of the infrastructure network that require construction of new infrastructure elements are identified. In the second stage, based on the outcomes of the needs assessment procedures, a master plan is prepared. The items in the master plan are examined in terms of availability of funds and budget restrictions. In the design and construction stage, execution of approved projects is initiated. Once the construction state is completed, the operations and maintenance department ensures that the infrastructure element performs its intended function by performing periodic inspections and repairs. When further repair action is not possible or feasible, or the infrastructure element fails to deliver its required function, renewal (rehabilitation or replacement) or decommissioning of the infrastructure elements takes place (Ryall, 2010; Salman, 2010).

In general, an IMS is developed to help managers and owners make informed and optimal decisions based on the analysis of the network data, and its advantages are clear: when infrastructure works, society has efficient transportation, safe water, reliable and affordable energy, a clean and attractive environment, and other essential support systems; but, on the other hand, when it does not work, the users spend hours in traffic, have bad water or no water, lack electricity, and live in unhealthy conditions (Grigg, 2012; Salman, 2010).
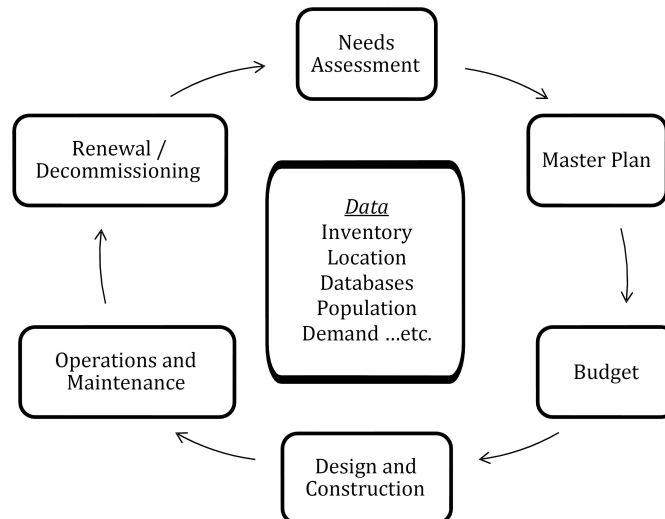
Figure 2.1 – Life-cycle of an infrastructure (Salman, 2010)

With the application of an efficient IMS, costs can be reduced and the consequences associated with ageing of the infrastructure can be mitigated. Systems will last longer and service levels will improve. Therefore, the establishment of an IMS offers multiple benefits, allowing to the manager to (Grigg, 2012):

- Manage capital improvement programs, operations and maintenance practices more efficiently;

- Reduce costs by eliminating unexpected failures;

- Improve service levels.

Therefore, an ideal IMS is not only designed to optimize maintenance and rehabilitation decisions to ensure good levels of safety and service, but is also developed to ensure that such interventions are carried out at key moments in order to keep cost to a minimum.

2.2.1 Main components

To function efficiently any management system must contain as much information as possible about the infrastructure. However, the amount and type of information present will depend on the size and complexity of the system. The American Association of State Highway and Transportation Officials (AASHTO) has developed a list of guidelines for the development of Bridges Management Systems (BMS) where it suggests that any modern BMS should be constituted by the following basic components (AASHTO, 1993): database, deterioration model, optimization model and update functions. In the next points the function of each component is explained in more detail.

2.2.1.1 Database

The database can be considered the heart of any management system. In addition to having the function of storing information such as name, location, age, among other characteristics of all infrastructures (inventory records), it should also store data on all inspections and maintenance actions performed on each infrastructure (inspection records). The database is not a static element, it must be regularly updated throughout the life-cycle of the infrastructures in order to keep up-to-date and to constitute a good historical record of the infrastructures (Elbehairy, 2007).

Inspections aim to evaluate the condition state of an infrastructure, through the identification and classification of defects and anomalies that affect its performance, taking into account its intensity and extension. The inspection record has a fundamental role for monitoring the condition state of the infrastructure and to determine an optimized maintenance plan, allowing prioritizing the maintenance and/or rehabilitation actions for the infrastructures with higher deterioration levels. Maintenance action records are essential for the manager to be informed about the nature of all maintenance actions that were carried out and the costs of the conservation works of each infrastructure (Ryall, 2010).

The condition rating adopted to describe the condition state of the existing infrastructure is not a direct measure of structural safety but rather of the severity of observable defects and is usually based on a discrete scale based on objective and uniform criteria. The scale of condition ratings is not universal and usually each management system develops its own rating scale (Elbehairy, 2007). For example, Table 2.2 shows the condition rating used by the National Bridge Inventory (NBI) as a guide to evaluate bridge elements. However, this lack of consistency across assets and managers is a significant handicap of current IMS, as it increases the complexity of the inspection process, the probability of errors and limits the ability to use information from other networks to improve modelling.

Table 2.2 – Condition rating used by NBI as a guide to evaluate bridge elements (FHWA, 2013)

Rating	Condition category	Description
N	Not applicable	–
9	Excellent	–
8	Very good	No problems noted.
7	Good	Some minor problems.
6	Satisfactory	Structural elements show some minor deterioration.
5	Fair	All primary structural elements are sound but may have minor section loss, cracking, spalling, or scour.
4	Poor	Advanced section loss, deterioration, spalling, or scour.
3	Serious	Loss of section, deterioration, spalling, or scour have seriously affected primary structural components. Local failures are possible. Fatigue cracks in steel or shear cracks in concrete may be present.
2	Critical	Advanced deterioration of primary structural elements. Fatigue cracks in steel or shear cracks in concrete may be present or scour may have removed substructure support. Unless closely monitored, it may be necessary to close the bridge until corrective action is taken.
1	Imminent failure	Major deterioration or section loss present in critical structural components, or obvious loss present in critical structural components, or obvious vertical or horizontal movement affecting structural stability. Bridge is closed to traffic, but corrective action may be sufficient to put the bridge back in light service.
0	Failed	Bridge is out of service and is beyond corrective action.

2.2.1.2 Deterioration model

Deterioration model aim at predicting the degradation process of the infrastructures. Its purpose is to assist the manager in making decisions about the actions to be performed on the structure. In general,

deterioration models can be based on inspection results, estimates obtained through the expert opinion or by combining these two methodologies (Kallen, 2007).

The results provided by the deterioration models are subjective as they are usually associated with a significant level of uncertainty. Firstly, these models are based on inspections records, which, by themselves reveals a high level of uncertainty due to the subjectivity of the inspection procedure. Moreover, uncertainty also arises from the natural variability of the deterioration process, which depends on a large set of factors, such as: material quality, traffic levels, pollution levels, environmental conditions, structural typology, among others (Kallen and van Noortwijk, 2006). To capture the variability of the degradation process, stochastic deterioration models are used by different management systems. This uncertainty should also be taken into account when modelling the effects of the maintenance and rehabilitation actions.

2.2.1.3 Optimization model

The optimization model identifies the best Maintenance, Repair and Rehabilitation (MR&R) activities to be performed on the infrastructures, taking into account the objectives imposed on the management system and the results from the deterioration model. In current models, these objectives are based on minimizing maintenance costs, maximizing structure performance throughout its life-cycle, and in some models, minimizing the impact of maintenance actions on users or a combination of these.

From the predictions of future performance, the definition of optimal strategies is relatively simple through the use of computational means, such as multi-decision processes. The main difficulty in optimizing maintenance strategies is to define optimization conditions, i.e. what is the maximum permissible performance, what should be the maximum probability of a structure presenting this level of deterioration and what maintenance actions to consider (Neves, 2011).

The optimization model can follow one of two approaches: "top-down" or "bottom-up". In the "top-down" approach, an optimal condition distribution is defined for the entire system and then individual elements of the system are selected to undergo maintenance action based on those goals. In the "bottom-up" approach, first the optimal actions for each element of the system are determined and then, based on the network optimization, individual elements will be selected to undergo MR&R activities (Das, 1999). The "top-down" approach works quicker, since the individual projects are determined after the network goals are set. That is, it is not analysed in detail which interventions to perform in all individual projects of the system, the resources are only consumed in the analysis of the previously selected individual projects. The "bottom-up" approach uses more computer time optimizing the individual projects thus the process often proves cumbersome for large populations (Hanji and Tateishi, 2007).

2.2.1.4 Update

Finally, the last of the components of the management system is updating function. These should be updated frequently for two reasons. First, the management system generates reports for planning and programming processes, and uses the information from actions taken the update the deterioration and cost models. Since most of the transition rates used in the deterioration models and improvement costs are based on initial estimates, when inspections or interventions are performed the models need to be updated to make more reflective of actual conditions (Hanji and Tateishi, 2007). Second, because often the optimal maintenance strategy is not followed, requiring changes to correct these failures (Neves, 2011).

2.2.2   Examples of infrastructure management systems

The guidelines previously discussed were defined with bridge management in mind. However, a similar methodology can be applied to any type of infrastructure, as discussed below.

2.2.2.1   Bridge management system

Until the 1960s, bridge MR&R activities were performed on an "as-needed" basis. Owners, when alerted to situations warranting attention, employed the best practices of the day to remedy problem areas. This responsive approach appeared to sufficiently address potential safety issues. This changed in the late 1960s, when a series of bridge failures focused public attention on deterioration of the existing bridge inventory, motivating the governments to mandate standardized bridge inspection procedures (Thompson et al., 1998).

To address this problem, the Federal Highway Administration (FHWA) created the National Bridge Inspection Program (NBIP), with the aim of cataloguing, recording, and tracking in a database the state of all bridges located in the main road of the country. In the beginning, the role of the NBIP was only to inform the authorities about the state of the bridges and the necessities that they demanded in terms of maintenance actions in order not to reach a critical condition state. The interest in the development of a BMS only grew in the 1980's, when the National Cooperative Highway Research Project (NCHRP) began a program with the objective of developing a model for an efficient BMS (Elbehairy, 2007).

In the followings, some of the most relevant BMS developed in the last four decades are discussed. This does not aim at being an exhaustive list, but to describe common and innovate characteristics of different systems. The BMS analysed are the North American systems: Pontis (Thompson et al., 1998) and BRIDGIT (Hawk and Small, 1998); the Japanese system: J-BMS (Miyamoto et al., 2000, 2001); the Danish system: DANBRO (Andersen, 1990); and the Swiss system: KUBA (Hajdin, 2008). The system developed in Portugal include: concrete bridge management system proposed by de Brito (1992), GOA (BETAR, 2017) and SustIMS (Berardinelli et al., 2014).

- **Pontis**

  Pontis was developed in the early 1990s by the FHWA. Pontis is both a software system and an organizing framework to help managers make the transition from collecting and processing raw safety inspection data to a more sophisticated approach of optimizing the economic efficiency of the bridge network. The system provides a defensible and understandable mean of expressing the long-term benefits of keeping bridges in good condition, as well as an objective way for choosing among maintenance, improvement, and replacement opportunities. In order to succeed in this objective Pontis has the capacity of expressing the engineering concerns of deterioration and structural performance in economic terms understandable to a broader audience (Thompson et al., 1998).

  For the deterioration model, Pontis uses a statistical approach based on the Markov chains, to predict the probability of transitions among condition states in each year. A "top-down" approach (from the network-level to the project-level) is employed in the optimization of strategies, favouring the optimization of decision processes at the network-level first, and then uses those results to guide project-level decisions (Thompson et al., 1998).

  To support the data requirements, the condition of each element of each bridge is usually recorded on a biennial cycle. Each element is classified as belonging to one of five discrete condition states, which describe the type and severity of element deterioration in visual terms. Since the number of condition states is limited to five for each element, Pontis includes a translator function to convert the element inspection results into the older 0–9 rating scale for deck,

superstructure, and substructure. Although these older assessments are not used in the Pontis analysis, they are still required by the US Federal Government as a mean of summarizing the condition of each bridge for the NBI (Thompson et al., 1998).

The fundamentals of discounted dynamic programming are used to find the optimal, long-term policy that minimizes expected life-cycle costs while keeping the element out of risk of failure (Thompson et al., 1998).

Nowadays, the Pontis bridge management system is known as AASHTOWare bridge management system, and is considered one of the most complete and popular BMS in the world.

- **BRIDGIT**

  BRIDGIT is a bridge management system released by the NCHRP. The project was initiated in 1985, sponsored by the AASHTO. The goal of the NCHRP was to develop bridge management software tools for transportation agencies, facilitating the organization of bridge data, providing clear, accurate and timely reports, allowing rank bridge populations by a number of user-specified criteria and the identification of critically deficient structures, assisting the track of deterioration trends and repair performance (Hawk and Small, 1998).

  In BRIDGIT, the elements are classified in one of seven categories: decks, superstructures, piers, abutments, joints, railings, and bearings. Protective systems are defined separately from underlying elements. Up to five conditions states are defined for each element and protection system. Quantities of elements in each state are recorded through the inspection process, and each state indicate the physical and functional performance (Hawk and Small, 1998). Markovian deterioration models are used to predict the future condition states of unprotected and protected elements, being formulated separately. For protected elements, the interrelation of the element and the protective system is modelled, assuming that the protection slows the deterioration of the element (Hawk and Small, 1998).

  In the optimization model, a multi-period analysis is performed in two steps. Firstly, life-cycle activity profiles are generated for each bridge in the inventory. The profiles allow estimating the present and future of various MR&R activities, based on element models, improvement scenarios and level-of-service standards. Secondly, optimization is performed to prioritize needs and select the most cost-effective options for given budgets over the planning horizon (Hawk and Small, 1998).

  This BMS is very similar to Pontis in terms of function and capabilities. The main difference between the two systems lies in the optimization model. BRIDGIT uses a "bottom-up" approach to optimization, while Pontis uses the "top-down" approach. The advantage of the former is that BRIDGIT can perform multi-year analyses and consider delaying actions on a particular bridge to a later date (Morcous et al., 2002a).

  Currently, the BRIDGIT bridge management system is not in operation. It was merged into AASHTOWare bridge management system in mid-1999 (Hawk, 1999).

- **J-BMS**

  J-BMS is an academic bridge management system developed by Miyamoto et al. (2000, 2001). The J-BMS records the performance of concrete bridges based on visual inspection, predicts the deterioration processes for existing bridge members and allows maintenance plans for repairs and/or strengthening to be created based on maintenance cost minimization and quality maximization (Miyamoto et al., 2000, 2001).

  The performance of the bridge elements is evaluated using the inspection data obtained from visual inspections and the technical specifications of the bridge. The evaluation is performed through a system called BREX (concrete Bridge Rating EXpert system), which assesses the

performance of the bridge elements in terms of load-carrying capability and durability through a scale of 0–100, where 100 indicates that the bridge is in perfect condition and 0 indicates that the bridge should be removed from service and requires rebuilding (Miyamoto et al., 2000, 2001).

Based on the results of the BREX system, the present deterioration can be characterized and the remaining life of the bridge can be estimated using the predicted function of deterioration. The deterioration curves for load-carrying capacity and durability are described by biquadratic and cubic functions, respectively (Miyamoto et al., 2000, 2001).

As a preliminary step, the effect of repairs and strengthening is estimated, and the cost of each maintenance action is determined. The BMS analysis is obtained from the prediction curve according to the cost and effects of repairs and strengthening. The strategy includes various maintenance plans provided by the cost minimization or quality maximization (Miyamoto et al., 2000, 2001).

The main limitation of the J-BMS is that the prediction of the deterioration is performed with a deterministic analysis, when in other systems stochastic analysis are the methodology most commonly used. In fact, the deterioration of the load-carrying capacity and durability are estimated through predefined deterioration curves, which are fitted using the data from inspection, but which are difficult to justify.

- **DANBRO**

    DANBRO is a bridge management system implemented in Denmark (Andersen, 1990). This management system has been in operation since the 1980s. DANBRO has a modular structure, allowing different bridge owners to choose the individual modules which better meet their needs. The system is organized in: inventory, inspection, optimization of rehabilitation works, long-term budgeting, price catalogue, and administration of heavy transports (Andersen, 1990; Das, 1999).

    The inventory module stores all documentation regarding the design and construction of bridges. The inspection module is considered the main module, allowing the monitoring of the condition of the bridge. Its purpose is to maintain an overview of the general condition of the stock of bridges and to detect significant damage in due time. From this rehabilitation works can be carried out in the optimized way and at the optimum time, taking safety and economic aspects into consideration. In DANBRO, a bridge can be divided into 15 main components, where inspectors can report condition states and recommend maintenance actions individually. The scale of the condition used by this management system varies between 0 and 5, where 0 means a good condition and 5 a bad condition (Andersen, 1990; Das, 1999).

    In the optimization module, the prioritization of maintenance actions is a process of examining the trade-offs between agency costs (related to construction) and traffic costs (related to delays). The long-term budgeting module, based on: average repair intervals, average repair costs, and average service lives, allows computing of total future budgets. In the price catalogue module, the unit prices of common rehabilitation works are, in a systematic way, updated in order to improve the estimates for repair works. Finally, the administration of heavy transport module assigns load bearing capacity classes to bridges and to the vehicles, defining if a special vehicle can use the bridge (Andersen, 1990; Das, 1999).

- **KUBA**

    KUBA is a road structure management system developed for the Swiss Federal Road Authority, with the aim of ensuring fast, safe, and reliable passage between any two points in the road network for the users and minimizing their maintenance cost, while maintaining traffic capacity for the road operators. This management system is divided in four components, a road structure

inventory (KUBA-DB), a preservation planning tool (KUBA-MS), a reporting tool (KUBA-RP), and a heavyweight transport evaluation tool (KUBA-ST) (Hajdin, 2008).

The KUBA-DB component manages the inventory of all information related to structures such as features, inspections and maintenance actions performed, serving as the basis for the other components of the system. The KUBA-MS component uses Markov deterioration models, being the module in charge of optimizing the decision processes related to road network infrastructures. The KUBA-RP component allows the consultation and reporting of all data and analysis results from the system. Finally, the KUBA-ST component is a tool that evaluates the ability of a bridge or several bridges to withstand the passage of special vehicles. Finally, the function of the KUBA-ST is to define is a special vehicle can use the bridge (Hajdin, 2008).

- **Concrete bridge management system**

Concrete bridge management system is an academic expert system developed by de Brito (1992) in his doctoral thesis. The expert system was developed considering the activities performed at the bridge site and the office work, with a special emphasis on rationalizing procedures (de Brito et al., 1997). The functionality of this management system depend on two computer modules. The inspection module (BRIDGE-1) relies on a periodic acquisition of field information complemented by a knowledge-based interactive system. The second module, BRIDGE-2, allows optimizing management strategies and includes three submodules: inspection strategy, maintenance and repair (de Brito et al., 1997).

In BRIDGE-1, the inspection strategy is based on two types of periodic inspections: current (performed at 15-month periods) and detailed (replaces a current inspection at 5-year intervals) and, eventually, complemented with special inspections (structural assessments) performed when bridge safety falls below standard levels. To standardize the inspection procedures, a defect classification system was implemented. All defects likely to be found in concrete bridges were classified according to geographical/functional/materials criteria. The possible causes (direct or indirect) of these defects were then classified according to chronological criteria. The in situ diagnosis methods used to detect or analyse the defects were also classified, according to their functioning principle and the type of results provided. Finally, the repair techniques used to eliminate or prevent the defects were classified in the same groups as the defects (de Brito et al., 1994, 1997; Branco and de Brito, 2004).

To help the inspector in making decisions at the bridge site, BRIDGE-1 has knowledge-based correlation matrices relating defects to causes, defects to diagnosis methods and defects to repair techniques. Each of these matrices is organized so that each row represents a defect and each column a possible cause (or diagnosis method or repair method). The intersection of each row and column represents the correlation between each defect and the other element. The rating of the correlation as: high (2), low (1) or non-existent (0) was defined according to expert knowledge criteria, obtained from technicians in the design and constructions fields (de Brito et al., 1994, 1997; Branco and de Brito, 2004).

BRIDGE-2 contains the bridge database and a decision system to perform the optimal strategies for management. That is, after a periodic inspection i (current or detailed) the inspector classifies the defects leading to maintenance activities. The maintenance submodule is then used to rate the defects and to implement the maintenance works. After every inspection, a reliability analysis (inspection strategy submodule) of the bridge is performed. Based on an analysis of the structural safety evolution (reliability index β), this submodule indicates if a structural assessment should be performed before the next scheduled periodic inspection. When the structural assessment has been completed, the repair submodule is used to perform an economic and reliability analysis and to decide on the type and time of the repair work to be implemented (de Brito and Branco, 1994; de Brito et al., 1997).

- **GOA**

  In Portugal, the *Sistema de Gestão de Obras de Arte* (GOA) is the most popular bridge management system. This system was developed by BETAR Consultores, having been is implemented by several road managers, including IP - Infraestruturas de Portugal, BRISA - Autoestradas de Portugal, Câmara Municipal de Lisboa and Câmara Municipal do Porto (BETAR, 2017).

  GOA provides a detailed inventory of all bridge elements, keeping the database always upgradeable to new information. This BMS allows recording inspection results and planning for future inspection and maintenance actions, estimation of costs of maintenance actions to be performed and prioritization interventions according to available financial resources (GOA, 2008). However, GOA does not allow modelling future performance of the bridge elements.

- **SustIMS**

  SustIMS is an infrastructure management system that is the result of a joint project by Portuguese highway concessionaire ASCENDI, Universidade do Minho, and Universidade Nova de Lisboa. This project intended at developing a management system for all highway assets (bridges, pavements, slopes/retaining walls, and telematics equipment) to support highway operators' decisions, improving not only their competitiveness but also users' satisfaction (Berardinelli et al., 2014).

  The framework of this platform is divided in three main modules: data warehouse, analysis tool, and reporting mechanism. Data warehouse contains all information collected for each element of the road infrastructure. The analysis component consists of a series of tools for condition assessment and performance modelling, allowing the identification and prioritization of needs to achieve the optimal preservation and rehabilitation strategies. Finally, the platform's outputs are a set of customizable reports on the infrastructure condition and the strategic investment planning (Berardinelli et al., 2014).

  The performance evaluation of physical assets is expressed by performance indicators that evaluate the extension of damage of the individual elements of the road infrastructure. This evaluation is performed through regular visual inspections or more reliable Non-Destructive Tests (NDT). The deterioration models for each road component were developed using Markov processes, and the maintenance model was developed to define a set of maintenance actions that lead to the implementation of an effective program to increase the assets' lifetime. Finally, for the optimization model, a multi-objective optimization problem that treats the overall system performance and life-cycle maintenance cost as separate objective functions is formulated, aiming at developing an automated procedure that provides, for a given time horizon, optimal maintenance strategies that improve the system performance while reduce the present value of the life-cycle maintenance cost (Berardinelli et al., 2014).

2.2.2.2 Pavement management system

As described for bridges, several Pavement Management System (PMS) have been developed and implemented in the last three decades. They have some elements in common with bridge management systems such as pavement distress ratings, selection of appropriate MR&R strategies, decision policy to establish priority scheduling, and dealing with fund limitations. However, according to Abaza et al. (2004), there are two additional basic elements necessary for inclusion in a PMS to address the pavement management process in its totality when considering a pavement system. First, a prediction mechanism capable of predicting future pavement conditions especially in the presence of an active MR&R program, and an optimization process designed to yield optimum pavement conditions based on a defined decision policy.

Some of the major developed PMS's deploy stochastic prediction models, which are mainly Markovian, statistical regression, and Bayesian models (Shahin and Kohn, 1982; Golabi et al., 1982; Butt et al., 1987; Harper and Majidzadeh, 1991; Abaza et al., 2004). Others simply do not use prediction models and rely mostly on experience and engineering judgement, and use simple decision trees and "prescription" procedures (Hill et al., 1991; Tavakoli et al., 1992). Optimization of a pavement system according to a defined effective decision policy has been attempted by some of the developed systems (Harper and Majidzadeh, 1991; Hill et al., 1991; Pilson et al., 1999; Abaza et al., 2004). Selection and integration of an appropriate prediction model and optimization method into an effective decision policy are essential for the successful design of any pavement management system. The following points some of the most relevant PMS are described.

- **PAVER**

  PAVER is a pavement management system developed by the U.S. Army Corps of Engineers during the 70s for use of military installations, cities, and counties. It provides the user with practical management tools, including data storage and retrieval, pavement network definition, pavement condition rating, project prioritization, inspection scheduling, determination of present and future network condition, determination of MR&R needs, performance of economic analysis, and budget planning (Shahin and Kohn, 1982).

  PAVER system uses the Pavement Condition Index (PCI) to evaluate the pavements' condition state. It is a numerical index from 0 to 100, where 100 represents an excellent condition. The PCI is determined based on quantity, severity, and type of distress, being divided in seven condition categories: excellent (100–86); very good (85–71); good (70–56); fair (55–41); poor (40–26); very poor (25–11); and failed (10–0). The future PCI for a pavement section is predicted by a linear extrapolation (Shahin and Kohn, 1982).

  A first-level decision of the MR&R activities is made based on the PCI value, type of distress, and deterioration rate. If the value of these variables does not exceed the predefined values, the pavement section does not require further analysis and routine maintenance practices can be continued. On the other hand, if the value of the variables exceeds the predefined values, a further analysis of the pavement section is required. This analysis is based on the evaluation of the structural capacity, roughness, skid resistance, and other relevant factors. Economic analysis is used to help the manager to select the appropriate repair alternative (Shahin and Kohn, 1982).

- **Arizona Pavement Management System**

  This PMS was developed for maintaining roads in the State of Arizona. The management system recommends the best preservation policies that achieve long-term and short-term standards for road conditions at the lowest possible cost (Golabi et al., 1982).

  The optimization model consists of two interrelated models, a short-term model and a long-term model, both using linear programming to find the optimal solution. The long-term model seeks a maintenance policy that minimizes the expected long-term average cost. The requirements are that the proportion of roads in state i is above a number ε_i if i is an acceptable level, and below a number γ_i if i is an unacceptable level, where the parameters ε_i and γ_i are the long-range performance standards. The short-term model seeks a maintenance policy over a planning horizon T that minimizes total expected discounted costs in the first T years subject to short-term standards and to the requirement that the long-term standards would be achieved within the first T years (Golabi et al., 1982).

  Markov processes are used to capture the dynamic and probabilistic aspects of the pavement management problem. In the model, transition probabilities link current road conditions and maintenance actions to future road conditions. The road condition states are defined as a com-

bination of the specific levels of the following variables: roughness (3 levels), present amount of cracking (3 levels), change in amount of cracking during previous year (3 levels), and index of first crack (5 levels) (Golabi et al., 1982).

2.2.2.3   Building management system

As previously referenced, in the context of bridges and pavement, management systems have been developed in the last 30 years and are already implemented around the world. A much larger variety of maintenance problems and a reduced number of buildings per owner mean that Building Management Systems (BdMS) are still quite rare (Paulo et al., 2014). However, in this area, the work developed at Instituto Superior Técnico, Universidade de Lisboa, has defined a new standard for the service life prediction of non-structural components of existing buildings, such as: cement-rendered façades (Gaspar and de Brito, 2008a,b; Gaspar, 2009; Silva et al., 2013; Sá et al., 2014; Silva et al., 2015; Vieira et al., 2015; Silva et al., 2016a,b,d), adhesive ceramic claddings (Silvestre and de Brito, 2009; Bordalo et al., 2011; Galbusera et al., 2014; Silva et al., 2016b,c), natural stone wall claddings (Neto and de Brito, 2011; Silva et al., 2011a,b; Neto and de Brito, 2012; Silva et al., 2012a,b; Emídio et al., 2014; Silva et al., 2016c,e; Mousavi et al., 2017), exterior wall painting (Pires et al., 2013; Chai et al., 2013; Dias et al., 2014; Magos et al., 2016; Silva et al., 2016b,c), ETICS (Amaro et al., 2013; Ximenes et al., 2015; Marques et al., 2018), architectural concrete surfaces (Silva et al., 2017; Serralheiro et al., 2017), and external claddings in pitched roofs (Garcez et al., 2012; Morgado et al., 2017; Ramos et al., 2018). In the following point the most relevant BdMS is described.

- **BuildingsLife**

    BuildingsLife is a building management system developed by Paulo et al. (2014, 2016). This model was created because the need of investing in building rehabilitation and maintenance strategies in order to optimize the social and economic benefits of the built environment. The planning of such works involves the prediction of the moment that critical elements of the built assets will reach degradation levels that exceed acceptable standards (Paulo et al., 2014).

    In this sense, BuildingsLife was developed to provide the building managers information allowing more efficient maintenance of building. This platform helps the building manager to choose the best option for maintenance but it can also help the designer to choose the best constructive solutions and materials, based on their service life under specific environmental conditions. Furthermore, this BdMS also considers a database of building defects, the best repair techniques for them and the costs involved (Paulo et al., 2014).

    BuildingsLife is supported by degradation data on real buildings. A performance scale of six levels was created for each building defect, based on standards and checked experimentally on site. The estimation of degradation is based on two possible approaches: deterministic and stochastic. The deterministic model is used as a first approach, associating with fitting curves related to building components degradation levels. The evolution of the anomalies is simulated considering a birth/death law known as the Gompertz Law. The stochastic method based on Markov chains was implemented alongside the deterministic models to predict the service life of building components, making it possible to estimate the probabilities of a building component to achieve a degradation level (Paulo et al., 2014).

    This platform uses genetic algorithms to find the best balance between performance and costs. In the genetic algorithm approach, the user can pick an acceptable degradation limit level and the period, and then analyse the best solution. Maintenance is analysed for each defect and it can be characterized according to the associated degradation factors (Paulo et al., 2014).

2.2.2.4 Waterwaste management systems

Managers of waterwaste systems face challenges daily in the operation and maintenance of this type of infrastructures. Population growth and stringent regulations require more effective management of the systems, while the continuous ageing of these systems has resulted in the loss of serviceability. Similarly, to other assets, funds to maintain the sewer networks have not increased at the required levels (Jeong et al., 2005).

Waterwaste management systems (WMS's) are similar to bridge and pavement systems. In these three types of management systems, the performance scale is composed of several degradation levels, and the condition state is monitored over time albeit to a lesser extent in the WMS's, due to the difficulty of access (Kielhauser et al., 2017). To overcome these limitations, Fenner (2000) proposed a GIS-based model to calculate "critical grid squares" where algorithms were developed to predict the likelihood of sewer failure in each square. This allowed the determination of geographical "hotspots", as well as finding grids that have the best cost-benefit ratio if the sewers requiring intervention in this grid were repaired or replaced. In this methodology, it is possible, when, enough information is available, to use risk-based models widely recognized as more robust (Kielhauser et al., 2017).

Also, life-cycle cost analysis has been developed in order to identify optimal MR&R alternatives for wastewater systems using the dynamic programming optimization technique (Abraham et al., 1998; Wirahadikusumah et al., 1999; Wirahadikusumah and Abraham, 2003). Several deterioration models have been used to predict condition ratings of infrastructure elements. The methods used in these studies include regression analysis (Ariaratnam et al., 2001; Chughtai and Zayed, 2008), Markov chains (Wirahadikusumah et al., 2001; Micevski et al., 2002; Jeong et al., 2005), artificial neural networks (Najafi and Kulandaivel, 2005), and survival functions (Baur and Herz, 2002).

2.2.2.5 Other types of management systems

Electricity, gas, and water distribution networks show some differences relative bridge or pavement systems. They are characterized by a binary state (work/not-work) with limited inspection possibilities. In this type of systems, interventions plans are essentially based on the probability of failure of the system elements (Kielhauser et al., 2017).

For electricity distribution networks, Stillman (2003) proposed to classify interventions on elements in two classes: emergency maintenance, which involves replacement or repair of the damaged element as soon as possible, and preventive maintenance, where an element is inspected, repaired or replaced at a prearranged point in time. Combining costs for both types of maintenance and service interruptions, as well as a safety constraint (maximum allowed risk of failure), allows the computation of optimal replacement time interval (Kielhauser et al., 2017). More recently, Dehghanian et al. (2013) defined a practical methodology making use of reliability centred maintenance techniques to determine intervention plans for electricity networks. The proposed methodology consists of three stages. In the first stage, the model to be used in the methodology is set up, including a check for data availability, system boundaries and system goals. In the second stage, the critical network components are identified by means of a reliability analysis. In the third stage, intervention plans are created to fit the reliability boundary conditions (Kielhauser et al., 2017).

For gas distribution networks, the development of intervention plans is also based on the methodology proposed by Dehghanian et al. (2013). However, to improve upon the limited inspection possibilities, Pandey (1998) proposed a probabilistic model for gas and oil pipelines that uses magnetic-flux-leakage sensors to update the failure probability by locating irregularities in the pipeline wall, such as corrosion or mechanical dents (Kielhauser et al., 2017).

For water distribution networks, due to inspection difficulties, most research has been focused on how

to predict water main breaks using statistical models (Shamir et al., 1979; Walski and Pelliccia, 1982; Wang et al., 2009). More recently, Zayed and Mohamed (2013) used simulation to define budget allocation and renewal plans for the rehabilitation of water distribution systems. The condition level is defined based on utility functions of pipes' attribute (age, size, water pressure, break rate, number of breaks, and population served). The interventions selected for each pipe section included in the work program were done taking into consideration the condition of the pipe sections and the costs of the intervention (Kielhauser et al., 2017).

2.3   Deterioration models

Deterioration can be defined as the process of decline in the condition of the infrastructure resulting from normal operating conditions, excluding damage from extreme events like: earthquakes, accidents, or fires (Elbehairy, 2007). Due to constant interaction with the environment, civil engineering assets are exposed to different types of actions, including environmental stressors and loads, which directly or indirectly contribute to their deterioration over time.

As observed in Section 2.2, a major challenge in IMS is to establish maintenance programs in order to avoid structural failures. Predictions of repair demands of the infrastructure in the future have to be made along with appropriate budget plans that cover maintenance and repair requirements. Estimations of both life-cycle cost and repair demands are determined by deterioration models (Kobayashi et al., 2010).

Deterioration models can be divided in two main categories (Morcous et al., 2002b): (i) Deterministic models; and (ii) Stochastic models. Deterministic models are simple models that predict the future condition states deterministically by fitting a straight-line or a curve to establish a relationship between the condition and age, ignoring the random error in prediction. Fundamentally, deterministic models are not very robust since they do not capture the natural variability of the process of deterioration. Stochastic models described the deterioration process through one or more random variables or processes to take into account the randomness and uncertainty of the process.

The recognition of the stochastic nature of the deterioration process represents a major step forward in the infrastructure management systems research. For this reason, we will only focus on stochastic models. In the following sections several types of deterioration models currently available in the literature will be presented.

Furthermore, in order to establish an optimal maintenance program, proper performance indicators must be defined. The performance of existing infrastructures can be defined in terms of condition indicators or through safety indicators.

The condition indicators are adopted to describe the condition of existing infrastructures. The condition is usually assessed by means of visual inspections, providing an overall characterization of the general condition of the system. However, this performance indicator cannot be used to assess the structural performance of infrastructure. An example of a classification system based on condition indicators is presented in Table 2.2. The NBI condition rating describes the conditions of bridge deck, superstructure, and substructure using a scale of 0–9, where a highway bridge is classified as structurally deficient if the deck or superstructure or substructure has a condition rating of 4 or less (Chen and Duan, 2014).

On the other hand, safety indicators define the performance in terms of structural performance like the load-carrying capacity and the failure probability of the structure, resulting in a true measure of the infrastructure safety. The safety analysis is based on the comparison between the load effects, Q, and the resistance of the structure, R. It is based on quantification and prediction of the reliability index, β, a function of the probability of failure, P_f:

$$\beta = -\Phi^{-1}\left(P_f\right) \tag{2.1}$$

where $\Phi^{-1}\left(\cdot\right)$ indicates the inverse CDF of the standard normal variate.

In short, there are two main approaches that can be used to model the deterioration process: reliability-based models and condition-based models. However, none of these approaches has shown evidence of being able to be applied in a generic way: both methodology have their advantages and disadvantages. The condition-based model is more suitable to incorporate information from visual inspections, but it cannot be used to assess the reliability of a structure in terms of strengths and stresses. On the other hand, reliability-based models deal with the reliability index, and they are able to quantify physical parameters such as material properties, stress conditions, structural behaviour, among others. However, such models cannot be used to analyse every structure due to the cost of collecting all required information.

2.4 Reliability-based deterioration models

Thoft-Christensen (1998) proposed a deterioration model where the reliability index is used as a performance indicator of an individual bridge under no maintenance:

$$\beta\left(t\right) = \begin{cases} \beta_0, & 0 \leq t \leq t_i \\ \beta_0 - \alpha\left(t - t_i\right), & t > t_i \end{cases} \tag{2.2}$$

where $\beta\left(t\right)$ is the time-dependent reliability index, β_0 is the initial reliability index (i.e. $t = 0$), t_i is the time of initiation of deterioration, α is the deterioration rate of reliability index, and t is time.

This model assumes that under no maintenance the reliability index has a bilinear progression, as shown in Figure 2.2 – Case 1. The first segment models the period after construction during which there is no (significant) deterioration of the reliability index. After this period, the deterioration of reliability index is considered linear (Neves and Frangopol, 2005).

From a mathematical point of view, the linear deterioration model is a very simple. However, the assumption of linear deterioration profiles can be considered a limitation of the deterioration model. For example, Gaal (2004) shows that a parabolic curve has a good fit to the observed spalling data of 81 bridges in the Netherlands. For this reason, to capture the non-linear effect of reliability deterioration is clearly of paramount importance. Therefore, the linear model was extended into the non-linear range by Petcherdchoo and Frangopol (2004). In order to exemplify the effect of non-linear deterioration of the mean reliability index, Figure 2.2 shows four cases of non-linear deterioration (Cases 2 to 5). These cases are all associated with the mean reliability index profile of steel/concrete composite bridges in bending under no maintenance (Frangopol and Neves, 2004).

The models proposed by Petcherdchoo and Frangopol (2004) and Neves and Frangopol (2005) used simple analytical expressions to model the evolution of performance. One advantage of this approach, relative to other commonly used methods like Markov chains, is its ability to incorporate the effects of maintenance in a consistent and intuitive manner. In fact, by changing the form of the curve when maintenance is applied and for a period of time after application, these methods can incorporate the effect of improvement in performance when maintenance is applied, but also the reduction or suspension of maintenance for a period of time after application. However, this methodology does not consider information resulting from visual inspections on bridges, causing reluctance by the managers in abandon the condition states as a performance indicator in the management systems (Frangopol and Neves, 2004).
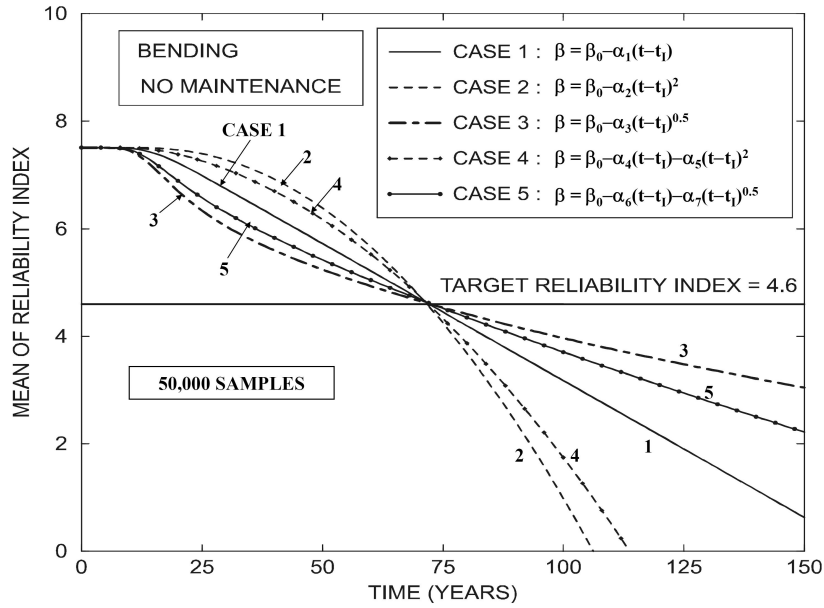
Figure 2.2 – Linear and non-linear reliability profiles without maintenance (Petcherdchoo and Frangopol, 2004)

Later, Neves and Frangopol (2005) proposed a model that integrates both condition and safety indicators, producing a more consistent measure of the effect of deterioration on serviceability and safety of existing structures. The condition index and safety index profiles under no maintenance are each defined using three random variables: initial condition and safety, C_0 and S_0, respectively; time of initiation of deterioration of condition and safety, t_{ic} and t_i, respectively; and deterioration rate of condition and safety, α_c and α, respectively, as shown in Figure 2.3. The deterioration of condition and safety index is considered linear as follows:

$$C(t) = \begin{cases} C_0, & 0 \leq t \leq t_{ic} \\ C_0 - \alpha_c (t - t_{ic}), & t > t_{ic} \end{cases} \tag{2.3}$$

$$S(t) = \begin{cases} S_0, & 0 \leq t \leq t_i \\ S_0 - \alpha (t - t_i), & t > t_i \end{cases} \tag{2.4}$$

where $C(t)$ and $S(t)$ are the time-dependent condition and safety index, respectively; and t is time. In this model, each variable is modelled by a probability density distribution in order to capture the variability associated with the deterioration process.

2.5   Condition-based deterioration models

2.5.1   Markov chain-based models

A Markov chain is a stochastic process used widely by researchers in several fields of civil engineering (Butt et al., 1987; Hawk and Small, 1998; Thompson et al., 1998; McDuling, 2006; Ortiz-García et al., 2006; Caleyo et al., 2009; Silva et al., 2016d), that describes the transitions between a finite state space, s, and satisfies the Markovian property. The Markovian property states that the future state only depends on the present state, not being influenced by the process up to the present state (Sánchez-Silva and Klutke, 2016).

(a) Condition index profile   (b) Safety index profile
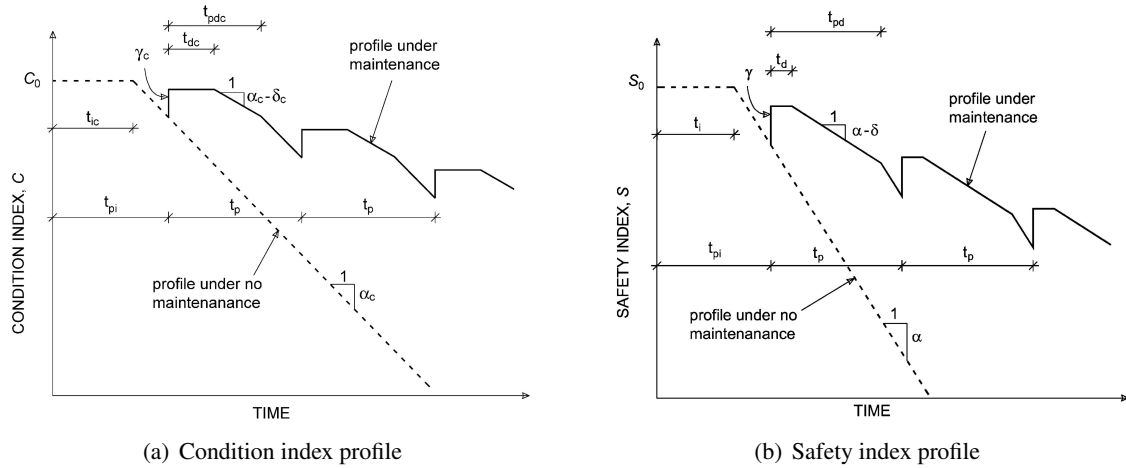
Figure 2.3 – Condition and safety index profiles under no maintenance and under maintenance (Neves and Frangopol, 2005)

In Markov chains, time can be considered to evolve into two ways: by discrete time intervals (discrete time Markov chains, or DTMC) or continuously (continuous time Markov chains, or CTMC).

2.5.1.1 Discrete time Markov chains

Consider a stochastic process $\{X(t), t = 0, 1, 2, ...\}$ that takes values in a countable state space, s. The index set $\{t = 0, 1, 2, ...\}$ will be taken to represent time, and $X(t)$ refers to the condition state of the process at time t. For example, Figure 2.4 shows a sample path of a discrete variable. From this figure it can observe that the process is in state 6 in interval 1, in state 4 in interval 2, and so on.
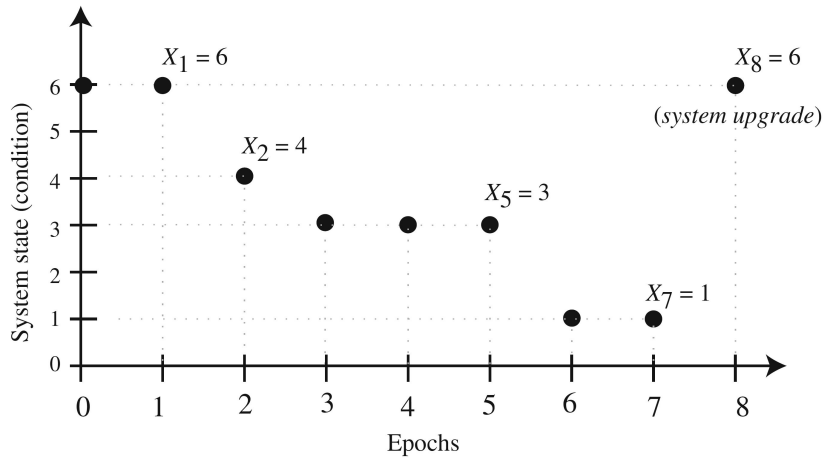
Figure 2.4 – Sample path of a discrete time Markov chain (Sánchez-Silva and Klutke, 2016)

The Markov property for a discrete time process is satisfied if:

$$P(X(t+1) = j | X(t) = i, X(t-1) = i_{t-1}, ..., X(1) = i_1, X(0) = i_0)$$
$$= P(X(t+1) = j | X(t) = i) \tag{2.5}$$

where i, i_t, and $j \in s$ and $P(\cdot | \cdot)$ denotes the conditional probability of any future state given the present and past state. In other words, the Markov property states that, for any reference time t, the "future" of the process (all states subsequent to t) is conditionally independent of the "past" (all states prior to

t), given the "present" (the state at *t*). Considering only time homogeneous Markov chains (i.e. for fixed time intervals), the Equation 2.5 can be simplified to:

$$p_{ij} = P\left(X\left(t + \Delta t\right) = j | X\left(t\right) = i\right) \tag{2.6}$$

where p_{ij} denotes the transition probability from state i to state j during a fixed time interval, Δt. It represents the probability that, given the process is currently in state i, the process will be in state j at the next instant, $t + \Delta t$ (Sánchez-Silva and Klutke, 2016). The transition probabilities can be expressed by a matrix of order $s \times s$ called the transition probability matrix, **P**, where s represents the total number of states.

$$\mathbf{P} = \begin{bmatrix} p_{11} & p_{12} & \cdots & p_{1s} \\ p_{21} & p_{22} & \ddots & p_{2s} \\ \vdots & \ddots & \ddots & \vdots \\ p_{s1} & p_{s2} & \cdots & p_{ss} \end{bmatrix} \tag{2.7}$$

The **P**-matrix is stochastic; therefore, the elements in **P** are nonnegative and each row sums to 1. For a time homogeneous DTMC, the **P**-matrix is called the one-step transition probability matrix.

Deterioration process

The deterioration process of systems where maintenance is not taken into account can be classified as a sequential process. Consider a performance scale where state 1 represents the most favourable condition and state s denotes the worst condition. The condition of the infrastructure deteriorates continuously over time until it reaches the state s, and all condition states defined in the performance scale must be obligatorily covered one after another (Butt et al., 1987). Based on these assumptions, the structure of the **P**-matrix in Equation 2.7 can be simplified to:

$$\mathbf{P} = \begin{bmatrix} p_{11} & p_{12} & \cdots & p_{1s} \\ 0 & p_{22} & \ddots & p_{2s} \\ \vdots & \ddots & \ddots & \vdots \\ 0 & 0 & \cdots & 1 \end{bmatrix} \tag{2.8}$$

Considering that the elements belonging to the lower triangle are null, is equivalent to say that the infrastructure deteriorates naturally without improvement of its condition state. The element p_{ss} takes the value of 1, and represents the absorbent state of the performance scale. Once an asset reaches this condition, it remains in that condition state forever unless a maintenance action is carried, and its condition state is improved (Sánchez-Silva and Klutke, 2016).

In many of the developed deterioration models, the one-step transition probability matrix, **P**, is constructed for 1-year intervals, i.e. $\Delta t = 1$ (Butt et al., 1987; Cesare et al., 1992). In these situations, the authors state that in a 1-year interval it is unlikely that the condition state of the infrastructure decreases more than one condition state, simplifying **P**-matrix to:

$$\mathbf{P} = \begin{bmatrix} p_{11} & 1-p_{11} & 0 & \cdots & 0 & 0 \\ 0 & p_{22} & 1-p_{22} & \ddots & 0 & 0 \\ \vdots & \ddots & \ddots & \ddots & \ddots & \vdots \\ 0 & 0 & 0 & \ddots & 1-p_{s-2,s-2} & 0 \\ 0 & 0 & 0 & \ddots & p_{s-1,s-1} & 1-p_{s-1,s-1} \\ 0 & 0 & 0 & \cdots & 0 & 1 \end{bmatrix} \qquad (2.9)$$

where p_{ii}, with $i = 1, 2, ..., s-1$ is the probability of the system staying in state i during the 1-year interval, and $1 - p_{ii}$, with $i = 1, 2, ..., s-1$ is the probability of the system transiting for the next condition state $i + 1$ during the 1-year interval.

Parameter estimation

To estimate the parameter of the transition probability matrix, $\mathbf{P}$, two methods are commonly used (Morcous, 2006): the regression-based optimization method and the percentage prediction method. The regression-based optimization method estimates transitions probabilities by solving the nonlinear optimization problem that minimizes the absolute distance between the observed condition states and the conditions predicted using the Markov chain model. The objective function and the constraints of this optimization problem can be formulated as follows (Butt et al., 1987; Morcous, 2006):

$$\text{Minimize:} \quad \sum_{t=1}^{N} |C(t) - E(t)|$$

$$\text{Subject to:} \quad 0 \le p_{ij} \le 1 \qquad \text{for } i, j = 1, 2, 3, ..., s \qquad (2.10)$$
$$\sum_{i=1}^{s} p_{ij} = 1$$

where N is the total number of transition periods; $C(t)$ is the system condition at transition period number t; and $E(t)$ is the expected value of the system condition at transition period number t based on Markov chains, which is calculated as follows:

$$E(t) = p(t) \cdot S \qquad (2.11)$$

where $p(t)$ represents the condition vector at transition time period t, and S is the vector of condition states.

On the other hand, the estimate of the transition probability matrix, $\mathbf{P}$, through the percentage prediction method is obtained by the following equation (Jiang et al., 1988; Morcous, 2006).

$$p_{ij} = \frac{n_{ij}}{n_i} \qquad (2.12)$$

where n_{ij} is the number of transitions from state i to state j within a given time period; and n_i represents the total number of infrastructures in state i before the transition.

Both methods have advantages and disadvantages. If, on the one hand, the percentage prediction method is a method of easy application, once it is not required the definition of objective function and constraints for the optimization problem. On the other hand, with the regression-based optimization method reliable results can be obtained with a smaller sample.

Performance prediction

The prediction of the condition state of an infrastructure over time is computed with the aid of the transition probability matrix, **P**. Let us assumed that $p(t_i)$ is a probability condition vector at transition time period t_i, and $\mathbf{P}_{\Delta t}$ the transition probability matrix that reproduce the deterioration of the infrastructure in the time interval Δt. The probability distribution at transition time period $t_f = t_i + \Delta t$ is given by (Morcous, 2006):

$$p(t_f) = p(t_i) \cdot \mathbf{P}_{\Delta t} \tag{2.13}$$

where $p(t_f)$ is the condition vector at transition time period t_f.

A generic probability condition vector, $p(t)$, for a given time t takes the following form:

$$p(t) = \begin{bmatrix} p_1 & p_2 & \cdots & p_s \end{bmatrix} \tag{2.14}$$

where p_i represents the probability of the infrastructure being in state i at time t.

In the discrete Markov chains, the **P**-matrix is formulated for a constant time interval, Δt. However, it is possible to obtain transition probability matrices for time intervals greater by geometric progression with ratio k.

$$\mathbf{P}_{\Delta t}^{final} = (\mathbf{P}_{\Delta t})^k \tag{2.15}$$

2.5.1.2 Continuous time Markov chains

Consider a stochastic process $\{X(t), t \geq 0\}$ with countable state space s. The Markov property for a continuous time Markov chain can be expressed by:

$$\begin{aligned} P(X(t+\Delta t) = j | X(t) = i, X(u) = x(u), u < t) \\ = P(X(t+\Delta t) = j | X(t) = i) \end{aligned} \tag{2.16}$$

where i, j, and $x(u) \in s$ and $t, \Delta t \geq 0$. It is assumed that, in transitions between condition states, the length of time spent in condition state i during the initial sojourn respects the memoryless property; i.e. the length of time spent in the condition state i before marking a transition is an exponentially distributed random variable with parameter λ_i that depends only on condition state i. When the sojourn time in condition state i expires, the process instantaneously enters a different state (Figure 2.5). Just prior to a state change, the next state ("future") can depend only on the current state ("present") and neither on any previous states nor on the length of time spent in the current state ("past") (Sánchez-Silva and Klutke, 2016).

Therefore, Markov chains are considered a simple way to predict the future condition state of elements over time in situations where the full history of the elements is not available (Kalbfleisch and Lawless, 1985; Morcous, 2006). This assumption allows overcoming the problem of lack of records in civil infrastructures due to the fact that infrastructures are usually not continually monitored (Kalbfleisch and Lawless, 1985; Kallen and van Noortwijk, 2006).

In CTMC the movement between the condition states is governed by transition intensities q_{ij} with $i, j = 1, 2, 3, ..., s$, where s represents the total number of condition states. The transition intensities, q_{ij}, represent the instantaneous probability of moving from state i to state j, where $i \neq j$ (Jackson, 2011):
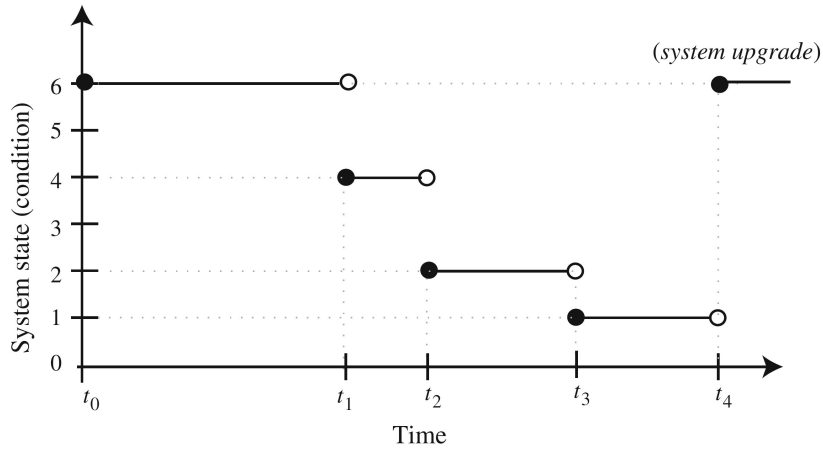
Figure 2.5 – Sample path of a continuous time Markov chain (Sánchez-Silva and Klutke, 2016)

$$q_{ij} = \lim_{\Delta t \to 0} \frac{P\left(X\left(t + \Delta t\right) = j | X\left(t\right) = i\right)}{\Delta t} \tag{2.17}$$

The q_{ij} coefficients can be arranged in a matrix of order $s \times s$ called the transition intensity matrix, **Q**, where $q_{ij} \geq 0$ to $i \neq j$, and $q_{ii} = -\sum_{i \neq j} q_{ij}$.

Physically, an intensity matrix corresponding to a transition rates matrix, independent of Δt, which is directly related to any transition probability matrix, **P**, through the Kolmogorov equation (Kalbfleisch and Lawless, 1985; Kallen and van Noortwijk, 2006):

$$\frac{\partial}{\partial t} \mathbf{P}\left(t\right) = \mathbf{P}\left(t\right) \cdot \mathbf{Q} \tag{2.18}$$

By solving the Kolmogorov equation, the relationship between **Q**-matrix and **P**-matrix is given by:

$$\mathbf{P} = e^{\mathbf{Q} \cdot \Delta t} \tag{2.19}$$

Equation 2.19 allows the computation of the transition probability transition for any time interval between observations.

Deterioration process

To simulate the deterioration process of a system without maintenance, the transition intensity matrix, **Q**, is presented in Equation 2.20. The structure of the matrix is defined taking into consideration the assumption that the deterioration process is sequential. In other words, during the deterioration process, at each infinitesimal time interval, the system can remain in the same condition state or to transit to the next condition state (Kalbfleisch and Lawless, 1985; Jackson, 2007).

$$\mathbf{Q} = \begin{bmatrix} -q_{12} & q_{12} & 0 & \cdots & 0 & 0 \\ 0 & -q_{23} & q_{23} & \ddots & 0 & 0 \\ \vdots & \ddots & \ddots & \ddots & \ddots & \vdots \\ 0 & 0 & 0 & \ddots & q_{s-2,s-1} & 0 \\ 0 & 0 & 0 & \ddots & -q_{s-1,s} & q_{s-1,s} \\ 0 & 0 & 0 & \cdots & 0 & 0 \end{bmatrix} \qquad (2.20)$$

Parameter estimation

The optimal intensity matrix is that resulting in higher probabilities of occurrence of the observed transitions. The most commonly method used to estimate the $\mathbf{Q}$-matrix is the maximum likelihood method described by Kalbfleisch and Lawless (1985). The likelihood, L, measures the distance between the real observations and the one predicted by the model. Let K_e be the total number of transitions observed in element e, and E the total number of elements in the database. The likelihood, L, can be defined by (Kalbfleisch and Lawless, 1985):

$$L = \prod_{e=1}^{E} \prod_{k_e=1}^{K_e} p_{ij} \qquad (2.21)$$

where p_{ij} is the probability of occurrence of the observed transition, as predicted by Equation 2.19.

An initial estimate of the $\mathbf{Q}$-matrix can be computed through (Jackson, 2007):

$$q_{ij} = \frac{n_{ij}}{\sum \Delta t_i} \qquad (2.22)$$

where n_{ij} is the number of elements that moved from state i to state j, and $\sum \Delta t_i$ is the sum of the time intervals between observations.

The optimal $\mathbf{Q}$-matrix can be computed through an optimization problem that maximizes the logarithm of the likelihood, $\log L$. The objective function and the constraints can be formulated as follows:

$$\begin{aligned} \text{Maximize:} \quad & \log L = \sum_{e=1}^{E} \sum_{k_e=1}^{K_e} \log p_{ij} \\ \text{Subject to:} \quad & q_{ij} \geq 0 \qquad\qquad \text{to } i \neq j, \text{ with } i,j = 1,2,3,...,s \\ & q_{ii} = -\sum_{i \neq j} q_{ij} \end{aligned} \qquad (2.23)$$

From a numerical point of view, using the logarithm of the likelihood of occurrence is more robust.

2.5.1.3   Background on Markov chain-based deterioration models

The first deterioration models based on Markov process were developed by Golabi et al. (1982) to describe pavement condition changes over time. In this work, a PMS was developed for the State of Arizona to identify optimal maintenance policies for each mile of the 7 400 mile (approximately, 12 000 km) network of highways. The Markov decision model developed considers both short-term and long-term management objectives, as well as physical road conditions, traffic densities, environmental characteristics, and types of roads.

Butt et al. (1987) applied Markov chains in a pavement performance and prediction model. In this study, the PCI rating is used as performance measure of the existing pavement. The PCI, ranging from 0 to 100, with 100 being excellent condition, was divided into ten equal condition states. To model pavement deterioration, a zoning scheme was defined, each zone representing a period of 6 years. Within each zone, the deterioration rate of a duty cycle is assumed to be constant, i.e. a homogeneous Markov chain and a separate transition matrix have been developed for each zone. However, it is assumed that the deterioration rate of a duty cycle varies from one zone to another, a nonhomogeneous Markov chain has been used for transition from one zone to another. A duty cycle for a pavement is defined as one year's duration of weather and traffic.

Although deterioration models in PMS differ from those in BMS, as a result of the differences in construction materials, structural functionality and the types of loads carried, similar deterioration models have been employed in the development of bridge deterioration (Hatami and Morcous, 2011).

Cesare et al. (1992) is one of the first studies applying Markov chains to bridge deterioration modelling. The authors used a database of 850 bridges in New York State with a total of 2 000 individual spans. The condition scale adopted is of 1 to 7 with 1 being potentially hazardous condition and 7 being new condition. Initially, the study considers the deterioration of each element of the bridge (e.g. superstructures, decks, and piers) is independent of the other elements of the bridge. However, the study also shows that correlation between the elements exists. In general, the developed deterioration model is applied to predict the evolution of average condition of all bridges and shows the effect of repairs performed annually on the average condition state of the network.

Scherer and Glagola (1994) explore the applicability of the Markov process as a stochastic model for bridge deterioration in Virginia, USA. The authors focus on exploring two critical issues associated with the use of Markov decision process models. The first issue involves state-space explosion, and the second is the compliance with the Markovian property. The Virginia Department of Transportation is responsible for the maintenance of, approximately, 13 000 bridges, and each individual bridge is classified into one discrete condition state between 9 (new condition) and 3 (poor condition). The authors states that the model would be computationally intractable because the number of possible states for a relatively complete description of the state of the system is $7^{13\,000}$. The solution found to reduce the state-space was classifying all the bridges into groups that have similar performance characteristics (bridge type, environmental conditions, traffic loading, age, etc.). This approach reduced the number of states to 7^{216}. In the second part of the paper, the authors pointed out that often the Markovian property is assumed without verification, resulting in a model of questionable quality. To verify the Markovian assumption, a frequency analysis of sequence occurrence is employed, i.e. two possible transition sequences, with the same present and future states but different past states, are tracked to determine if there is a difference in occurrence dependent of past state history. An inference analysis using a chi-square statistic is used to test the significance of the Markovian assumption. The results revealed that the Markovian property is a good assumption for bridge deterioration, at least for the data used.

According to Morcous (2006), the use of Markov chain model to predict the performance in BMS main advantages are:

1. Ability to reflect the uncertainty from different sources such as uncertainty in initial condition, uncertainty in applied stresses, presence of condition assessment errors, and inherent uncertainty of the deterioration process;

2. Incremental model that account for the present condition in predicting the future condition; and

3. Ability to manipulate networks with large number of facilities because of their computational efficiency and simplicity of use.

However, the author also states that these models have some limitations that may affect the reliability

of their predictions:

1. These models use discrete parameter Markov chains that assume discrete condition states and constant inspection period for all bridge components. This assumption was made to eliminate the computational complexity and simplify the decision-making process.

2. Models using the first-order Markov chains assume that the future condition of a bridge component depends only on its present condition and not on its past condition, which is called the state independence assumption. This assumption was also made for simplicity purposes despite the fact that bridge deterioration is a nonstationary process, which means that the time elapsed in the initial state affects the probability of transition to the following state.

Morcous (2006) tried to evaluate the impact of these two limitations on the performance prediction of bridge deck system using data from 9 678 structures of 57 different types of highway structure in Québec, Canada. To evaluate the impact of variation in inspection periods, Bayes' rule was used to adjust the developed transition probabilities. Comparing the developed performance prediction models before and after adjustment indicated that the variation in the inspection period may result in a 22% error in estimating the service life of a bridge deck system. To assess the validity of the state independence assumption a frequency test and an inference test were used. The results showed that the state independence assumption is acceptable for the network level analysis with a 95% level of confidence.

As mentioned before, Markov-based models are the most common stochastic technique used to modelling deterioration in bridge elements. However, many of the management systems developed are based on discrete Markov chains. A limitation of these models is the fact that they are based on the assumption that the time period between inspections is constant. Nowadays, it is well known that transportation agencies may inspect their bridges more or less often according to the severity of the conditions and the relative costs and benefits associated with performing these inspections in time. Consequently, the condition data resulting from inspections are not equally spaced and cannot be used to develop and/or update the transition probability matrix, $\mathbf{P}$ (Morcous, 2006). One way to overcome this problem is through the use of continuous Markov chains.

Kallen and van Noortwijk (2006) applied continuous-time Markov process to model the stochastic process that describes the uncertain bridge condition over time. Contrary to a discrete-time Markov process, a continuous-time Markov process allows transitions to occur on a continuous timescale. The authors argue that a discrete-time Markov process is often chosen over continuous-time Markov process because the calculations are simpler. However, the authors state that the difference in complexity is small and does not warrant the loss of generality resulting from the restriction to a discrete timescale; in particular avoids the need to consider constant time intervals between inspections. The main difference between the two processes is focused on the transition probability matrix, $\mathbf{P}$. In discrete-time Markov process, the transition probability matrix, $\mathbf{P}$, is estimated for a predetermined and fixed time intervals. In continuous-time Markov process, a transition intensity matrix, $\mathbf{Q}$, is defined. The aim of this work is on the analyse of four types of continuous-time Markov processes using bridge condition data in the Netherlands. The differences between these processes are based on the dependence on time (age) and on the dependence of state.

More recently, Silva et al. (2016d) applied probabilistic models based on continuous Markov chains to predict the evolution of render façade deterioration according to outdoor environmental conditions. From the results obtained, the authors state that the model is suitable and able to classify correctly the cases analysed, once the mean relative error obtained for the estimated number of cases belonging to each degradation condition is 7.55%, which is considered acceptable.

The main advantage of Markov chains is its simplicity, the use of exponential distribution to describe the transition between condition state, and the existence of analytical expressions for the probability distribution. However, exponential distributions are not very versatile and can result in a gross ap-

proximation of the system characteristics. To overcome this limitation, models based on Petri nets can be useful.

2.5.2 Petri net-based models

The original concept of Petri nets was introduced by Carl A. Petri (Petri, 1962), who, in his doctoral thesis, developed a new model of information flow in systems without the explicit consideration of time. The model was based on the concept of asynchronous and concurrent operation by the parts of a system and the realization that relationships between the parts could be represented by a graph, or net (Peterson, 1977). Petri nets are considered a mathematical and graphical tool suitable for the formal description of systems whose dynamics are characterized as being concurrent, asynchronous, distributed, parallel, nondeterministic, and/or stochastic (Murata, 1989; Marsan et al., 1994). As a graphical tool, Petri nets can be used as a visual-communication aid similar to flowcharts, block diagrams, and networks, being the tokens used to simulate the dynamic and concurrent activities of systems. And, as a mathematical tool, it is possible to set up state equations, algebraic equations, and other mathematical models governing the behaviour of systems (Murata, 1989).

Due to their flexibility, Petri nets can be used in a wide variety of applications. They can be applied to any area or system that can be described graphically like flowcharts and that need some means of representing parallel and concurrent activities (Murata, 1989). During the last decades, in order to investigate new fields of applications, several extensions and modifications have been developed to improve the capabilities of ordinary Petri nets, being all of them based on the basic Petri net formalism, but presenting very different characteristics and assumptions, in order to adapt themselves to the phenomena under analysis (Girault and Valk, 2013).

2.5.2.1 Original concept of Petri nets

A Petri net can be defined as a directed, weighted, and bipartite graph with an initial state called initial marking, M_0 (Peterson, 1977; Murata, 1989; Schneeweiss, 2004). It is considered a bipartite graph because it comprises two kinds of nodes: places and transitions, being both nodes linked by directed edges, which are called arcs. An arc can only connect a place with a transition or vice-versa, and is labelled with a weight (positive integer number), where a k-weighted arc can be interpreted as a set of k parallel arcs (labels for unity weight are usually omitted). Each place has the ability to store a varying number of dots, denoted tokens. The distribution of the tokens on the places represent the present state of the system and can be called the marking of the network, M.

A simple PN is illustrated in Figure 2.6. The places are denoted by circles while a transition is represented by a rectangle. Transition t_1 has two input places (p_1, p_2) and one output place (p_3). The arcs that connect the input places to the transition and the transition to the output place represent the pre- and post-conditions of the transition, respectively. Two tokens are present in places p_1 and p_2.
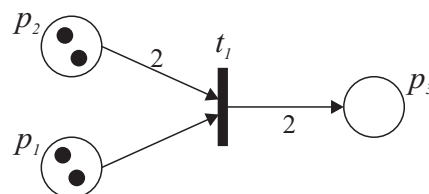
Figure 2.6 – Example of a Petri net

According to the type of application that is given to a Petri net, different interpretations can be given to places and transitions (Peterson, 1977). However, in a simple way, places can represent resources

or a possible condition state of the system while transitions can represent actions which cause the change of the system (Murata, 1989).

Transitions together with tokens are responsible for the evolution of the system, from one state to another. Tokens are stored in places and transitions govern the movements of the tokens between places. In order to simulate the dynamic behaviour of the system, the marking of the Petri net is changed according to the transition (firing) rule (Murata, 1989):

1. A transition t_j is said to be enabled if each input place p_i of t_j is marked with at least $pre(p_i, t_j)$ tokens, where $pre(p_i, t_j)$ is the weight of the arc from p_i to t_j (pre-conditions);

2. An enabled transition may or may not fire, depending on whether or not the event actually takes place;

3. A firing of an enabled transition t_j removes $pre(p_i, t_j)$ tokens from each input place p_i of t_j, and adds $post(p_i, t_j)$ tokens to each output place p_i of t_j, where $post(p_i, t_j)$ is the weight of the arc from t_j to p_i (post-conditions).

Figure 2.7 represents an example of a transition (firing) rule. In Figure 2.7(a), transition t_1 is enabled because the two pre-conditions are respected. After firing, Figure 2.7(b), the marking of the net has changed, and transition t_1 is no longer enabled.

(a) Marking before transition t_1 fires   (b) Marking after transition t_1 fires
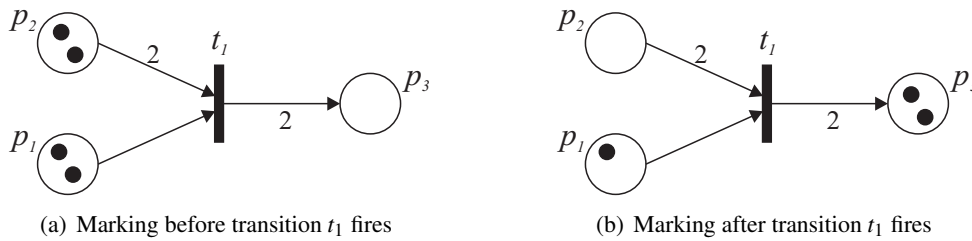
Figure 2.7 – Example of a transition (firing) rule (adapted from Murata, 1989)

Mathematically, a Petri net with n places and m transitions can be denoted by $\langle PN, M_0 \rangle$ that represents a Petri net of dimension $n \times m$ with an initial marking, M_0. The structure of a Petri net is defined by a four-tuple (Peterson, 1977):

$$PN = (P, T, \textbf{Pre}, \textbf{Post}) \tag{2.24}$$

where $P = \{p_1, p_2, ..., p_n\}$ is a finite set of places, $T = \{t_1, t_2, ..., t_m\}$ is a finite set of transitions, **Pre** and **Post** are the pre- and post-incidence matrices, respectively, of dimension $n \times m$. More precisely, the element $pre(p_i, t_j)$ is equal to the weight of the directed arc between p_i and t_j if an arc exists and 0 otherwise; the element $post(p_i, t_j)$ is equal to the weight of the directed arc between t_j and p_i if an arc exists and 0 otherwise. The state of a Petri net is given by its current marking, M, where M is described by a vector of dimension n and the ith component of M, indicated by $M(p_i)$, represents the number of tokens in the ith place $p_i \in P$.

A transition t_j is enabled at a marking M if and only if for each place $p_i \in \cdot t_j$, $M(p_i) \geq pre(p_i, t_j)$, where $\cdot t_j$ represents the pre-set of places of the transition t_j at a marking M. When fired, transition t_j gives a new marking M', for each place p_i it given by:

$$M'(p_i) = M(p_i) + post(p_i, t_j) - pre(p_i, t_j) \tag{2.25}$$

for $i = 1, 2, ..., n$ and $j = 1, 2, ..., m$.

Currently, several extensions such as timed, stochastic, coloured, and object-oriented Petri nets have been successfully used to model the behaviour of systems in different fields of knowledge, namely in robotics (Al-Ahmari, 2016), optimization of manufacturing systems (Meng, 2010; Chen et al., 2014; Uzam et al., 2016), business process management (van der Aalst, 2002), human computer interaction (Tang et al., 2008), management of equipment availability and scheduling of tasks (Cheng et al., 2011), wind turbines maintenance (Le and Andrews, 2016; Leigh and Dunnett, 2016), railway infrastructure asset management (Andrews, 2013; Rama and Andrews, 2016; Yianni et al., 2017), traffic control (Fanti et al., 2014; Di Febbraro et al., 2016), among others. These extensions have been developed in order to improve the capabilities of ordinary Petri nets. All extensions and components used in this work are described in more detail in Chapter 3.

2.5.2.2 Background on Petri net-based deterioration models

The first works that show that Petri net are suitable for modelling the deterioration process of civil engineer assets are from the beginning of this decade (Andrews, 2013; Rama and Andrews, 2013). In these works, an approach to model the railway infrastructure asset management based on Petri net is proposed. A sequential Petri net scheme is used to model the deterioration process that is integrated in the management system. In these two studies, the degradation model is composed by four places (represented by circles in Figure 2.8); each one represents a different condition state of the infrastructure. The change of condition state is model by stochastic transitions (represented by rectangles in Figure 2.8) where the time that the infrastructure remains in a given condition state is derived from a random sample taken from an appropriate distribution.
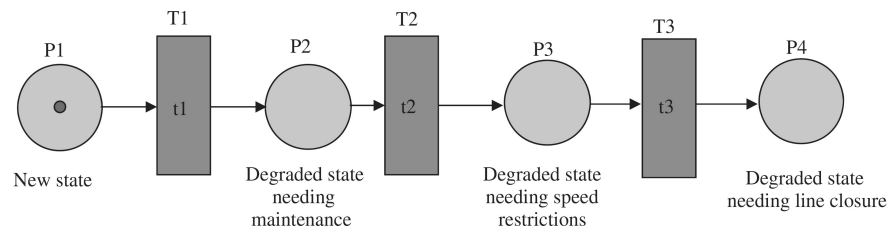
Figure 2.8 – Petri net scheme of the deterioration model proposed by Andrews (2013)

Le and Andrews (2015) developed a bridge asset management model based on the Petri net approach. The method allows for detailed modelling of the individual components in the structure (abutment, girder and deck) whilst maintaining the size of the analytical problem to a manageable size. The model is formed from sub-models of each of the bridge components and takes into consideration the component deterioration process, the interaction and dependency between different component deterioration processes, along with the inspection and maintenance processes. The state residence times between changes in state resulting from deterioration and maintenance are governed by Weibull distributions. The parameters for these distributions are obtained from the historical records on the maintenance actions applied to structures, which can be regarded as similar and from a homogeneous sample.

Finally, Yianni et al. (2017) proposed a Petri net based modelling approach to railway bridge asset management. The model presented tries to reunite a disjointed system by combining deterioration, inspection and maintenance models. In the deterioration model, a 2-D condition scale is used. This condition scale comprising the defect type and the severity of the defect. Yianni et al. (2017) referred that this approach enhances the realism of the deterioration because a structure can fail by multiple failure modes and different defects at different rates are more or less likely to lead into other type of defects.

These works show the flexibility and capability of the Petri nets. This modelling technique allows the incorporation of many rules in the model to simulate accurately complex situations and keeping the model size within manageable limits. Moreover, with this modelling technique, time simulation is not restricted to the exponential distribution.

2.6   Maintenance

According to van Noortwijk and Frangopol (2004), maintenance can be differentiated into two types: preventive and corrective. Preventive maintenance (PM) is associated with low impact on the safety of the infrastructure and low cost, resulting in reduction of the deterioration rate or even delay in the deterioration process. On the other hand, corrective maintenance (CM) is associated with significant impacts on the performance of the infrastructure and high direct and indirect costs. In general, it can be said that corrective maintenance is applied to maintain the structure in a good level of conservation, while preventive maintenance reduces costs over the life-cycle of the structure by delaying corrective maintenance.

Depending on the maintenance application time, maintenance can be classified as time-based or performance-based. Time-based maintenance actions are applied at regular intervals, regardless of the performance indicators, while performance-based maintenance actions is applied when the structure performance indicators cross a pre-defined threshold value (Neves and Frangopol, 2005; Bocchini and Frangopol, 2011a). Usually, preventive maintenance is time-based and corrective maintenance is performance-based.

The impact of a maintenance action on an infrastructure can be modelled by one or more than one of the following effects: improvement in performance at application time; reduction of the deterioration rate for a period of time after application; and delay of the deterioration rate for a period of time after application (Frangopol et al., 2001; Kong and Frangopol, 2003; Neves and Frangopol, 2005).

2.6.1   Reliability-based models

In the maintenance model proposed by Frangopol (1998) and Frangopol et al. (2001), effects of the preventive maintenance are described by five random variables (Figure 2.9): application time of first preventive maintenance, t_{PI}; time of reapplication of preventive maintenance, t_P; duration of the effect of preventive maintenance, t_{PD}; performance rate during the effect of preventive maintenance, θ; and improvement of the performance level after the application of preventive maintenance, γ. In this model, each variable is modelled by a probability density distribution in order to capture the variability associated with the deterioration process (Frangopol et al., 2001).

Kong and Frangopol (2003) proposed a maintenance model where the performance index profile for a structure is built based on superposition of the profiles of the various actions over the lifetime of the structure. Anything that might influence the performance index profile of a structure, such as a maintenance, rehabilitation, inspection, accident or earthquake, is defined as an action. The effect of each action is described by one additional performance profile (Figure 2.10(a – j)). These additional profiles are defined by random parameters in order to consider the uncertainty associated with the deterioration process.

Figure 2.10(a – j) presents examples of additional profiles associated with different actions, where $\Delta\beta$ represents the variation of the performance index; t_s, t_i, and t_e are starting, intermediate, and ending times of the effect of an action; and γ_s and γ_e are the initial and final values of $\Delta\beta$, respectively. Figure 2.10(k) shows the effect of an action on an existing performance index profile. Using the superposition method, the effect of any type of action can be obtained. For instance, Figure 2.10(a) represents a
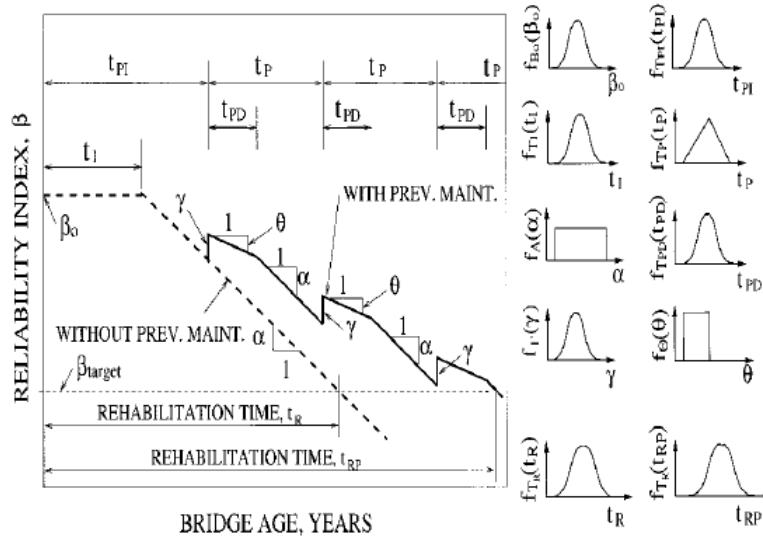
Figure 2.9 – Identification of the variables that describe the effects of preventive maintenance (Frangopol et al., 2001)
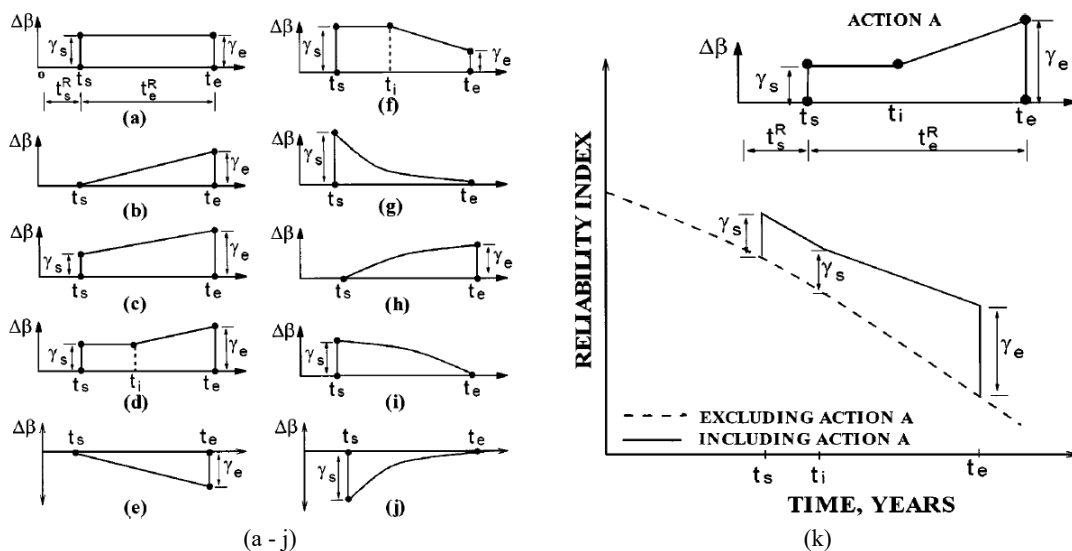
Figure 2.10 – Maintenance model proposed by Kong and Frangopol (2003): (a – j) examples of additional profiles used to describe the actions, and (k) illustration of the effect of the additional profile of an action on the performance index profile

corrective maintenance intervention that improves the performance index during the time interval t_e - t_s; and Figure 2.10(b) represents a preventive maintenance action that reduces the performance index deterioration rate during the time period t_e - t_s. Figure 2.10(e) represents an increase in the performance index deterioration rate due to external actions, and Figure 2.10(j) represents the sudden drop of the system reliability index due to an extreme event (e.g. earthquake) followed by repair effects over a certain time period.

Neves and Frangopol (2005) proposed an extension of the model described by Frangopol (1998), considering both condition and safety indicators. Furthermore, a new parameter defining a period during which no deterioration occurs after the application of maintenance is also included. In this model, the effects of maintenance on the performance profiles are also based on the superposition of profiles. Each maintenance action can lead to one, several, or all of the following effects: (a)

increase in the condition index and/or safety index immediately after application; (b) suppression of the deterioration in condition index and/or safety index during a time interval after application; and (c) reduction of the deterioration rate of condition index and/or safety index during a time interval after application. These effects are modelled through several random variables as follows: (a) increase in condition index and safety index immediately after application, γ_c and γ, respectively; (b) time during which the deterioration processes of condition index and safety index are suppressed, t_{dc} and t_d, respectively; (c) time during which the deterioration rate in condition index and safety index are suppressed or reduced, t_{pdc} and t_{pd}, respectively; and (d) deterioration rate reduction of condition index and safety index, δ_c and δ, respectively. All these random variables are presented in Figure 2.3.

2.6.2   Condition-based models

2.6.2.1   Markov chain-based models

Kallen (2007) uses Markov chains to model deterioration and maintenance of bridges in the Netherlands. The author proposes two maintenance models. In the first model the condition of the structure is improved one condition state, allowing the transitions back to the previous condition state, while in the second model the condition of the structure is improved to the perfect maintenance state. The author also refers that the purpose is simply to observe the behaviour of the data with respect to backward transitions, because there are no detailed records of maintenance in the database used.

Considering a classification system composed by four condition states, where 1 represents a perfect condition state and 4 a very poor condition state, the structure of the transition intensity matrix, $\mathbf{Q}$, for the first model proposed by Kallen (2007) is given by:

$$\mathbf{Q} = \begin{bmatrix} -q_{12} & q_{12} & 0 & 0 \\ \nu_{21} & -\nu_{21}-q_{23} & q_{23} & 0 \\ 0 & \nu_{32} & -\nu_{32}-q_{34} & q_{34} \\ 0 & 0 & \nu_{43} & -\nu_{43} \end{bmatrix} \tag{2.26}$$

where the elements q_{ij} with $i < j$ represent the transition intensities for more deteriorated condition states and the elements ν_{ij} with $i > j$ represent the transition back to the previous state. In the second model, where perfect maintenance is considered, the structure of the transition intensity matrix, $\mathbf{Q}$, is:

$$\mathbf{Q} = \begin{bmatrix} -q_{12} & q_{12} & 0 & 0 \\ \nu_{21} & -\nu_{21}-q_{23} & q_{23} & 0 \\ \nu_{31} & 0 & -\nu_{31}-q_{34} & q_{34} \\ \nu_{41} & 0 & 0 & -\nu_{41} \end{bmatrix} \tag{2.27}$$

Le (2014) also used the concept of continuous-time Markov chains to develop a bridge management model. The transition intensity matrix, $\mathbf{Q}$, for a system containing only one element with four condition states is given by:

$$\mathbf{Q} = \begin{bmatrix} -\lambda_1 & \lambda_1 & 0 & 0 & 0 & 0 & 0 & 0 \\ 0 & -\lambda_2 & \lambda_2 & 0 & 0 & 0 & 0 & 0 \\ 0 & 0 & -\lambda_3 & \lambda_3 & 0 & 0 & 0 & 0 \\ 0 & 0 & 0 & 0 & 0 & 0 & 0 & 0 \\ 0 & 0 & 0 & 0 & 0 & 0 & 0 & 0 \\ \nu_1 & 0 & 0 & 0 & 0 & -\nu_1 & 0 & 0 \\ \nu_2 & 0 & 0 & 0 & 0 & 0 & -\nu_2 & 0 \\ \nu_3 & 0 & 0 & 0 & 0 & 0 & 0 & -\nu_3 \end{bmatrix} \tag{2.28}$$

where λ_1, λ_2 and λ_3 are the deterioration rate between two adjacent condition states and v_1, v_2 and v_3 are the repair rates that bring the system from the good, poor, and very poor condition state back to the perfect condition state.

In this model, the **Q**-matrix is composed by eight condition states, where the first four represent the deterioration process and the last four the inspection process. In this work, all bridges and their components are assumed to be inspected regularly. At this point, the current state of the system is identified. If a change in the state of the system happens in between two inspections, the failure is unrevealed until the second inspections. For this reason, four more states are added to represent the states where the actual condition of an element is revealed following an inspection. After an inspection, a maintenance decision can be made to repair the system or it can be left to deteriorate to a poorer state. The option to carry out repair is achieved by enabling the repair process represented in the **Q**-matrix by the repair rates v_1, v_2 and v_3. Figure 2.11 shows the Markov state diagram for a single bridge element. Based on the same concept as the elemental model, the bridge model can be built (Le, 2014).
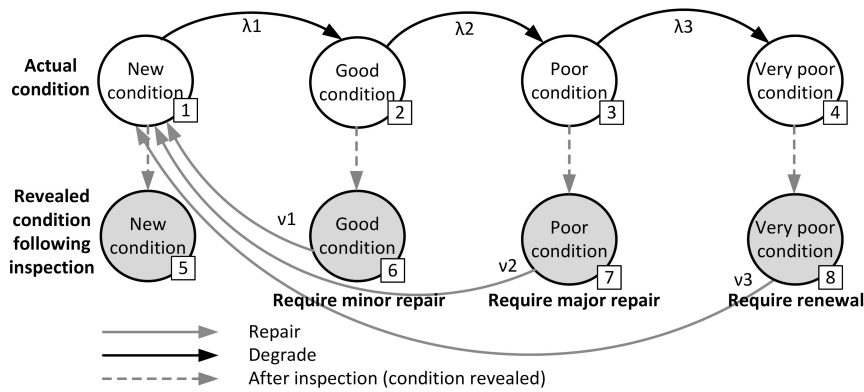
Figure 2.11 – Markov state diagram for a single bridge element (Le, 2014)

2.6.2.2 Petri net-based models

Andrews (2013) proposed an approach to model the railway infrastructure based on Petri nets, considering both deterioration and maintenance. In this approach, a track section model is proposed which incorporates the deterioration, inspection, maintenance and renewal processes, providing a means to predict the condition of the ballast section over time. In this model, as in the Markov chain-based models, only the improvement of the performance at the application time is considered.

The deterioration process is modelled considering four states (Figure 2.8). The condition of a system is not continuously known, and is only revealed following an inspection. The inspection process, depicted by Figure 2.12(a), allows the detection of the current condition of the system. The inspection will take place at intervals of θ time units and will allow assessing the true condition of the system. The inspection process is represented by the loop $P5$ - $T5$ - $P6$ - $T4$ - $P5$. A token in place $P5$ means that it is not time to conduct an inspection along this section. Transition $T5$ manages the times of realization of the inspections. This transition is enabled due to the token present in place $P5$ and fires at every θ time units; when it fires, the token is removed from place $P5$ and one token is added to place $P6$. A token in place $P6$ signifies that inspection is being performed, enabling two transitions. It enables the transition $T4$, if the inhibitor arc constraints are checked which causes token to return to place $P5$ to wait for the next inspection. Moreover, it enables the transition $T6$. The firing of this transition removes the token from the deterioration process (place $P2$) and reveals the true condition of the track. After the inspection, transition $T4$ is enabled to fire and the token presents in place $P6$ returns to place $P5$, waiting for the next inspection (Andrews, 2013).

After the true condition is revealed (Figure 2.12(b)), the appropriate maintenance work will be requested with the appropriate priority. Place $P7$ feeds through transition $T7$ into place $P10$. A token in place $P10$ indicates that maintenance has been carried out on the section. The time that it takes to conduct the maintenance, $t6$, is sampled from a probability distribution. Maintenance improves the condition of the ballast but does not return the condition to as-good-as-new. Therefore, the output from transition $T7$ cannot be back to state $P1$. A new place, $P10$, is added to the PN to represent the condition of the ballast following tamping. From this improved state from where deterioration will occur and will again, at some point, result in a condition where maintenance is required. However, at some point in time the condition of the system will reach the point where it is cheaper to replace the ballast rather to than continue to maintain it. So, after a predetermined life time L, all the system is renewed (Figure 2.12(c)). At the point that the new ballast state is entered, $P1$ is marked, both transitions $T1$ and $T11$ are enabled. $T11$ fires immediately and places a token in its two output places, $P1$ and $P12$. Returning the token to $P1$ enables the normal ballast degradation process to be followed. A token in $P12$ effectively starts the lifetime clock for the ballast on this section. Once the token is in place $P12$, it inhibits the transition $T11$ so that it does not keep on firing (Andrews, 2013).

(a) Inspection process

(b) Maintenance process

(c) Renewal process
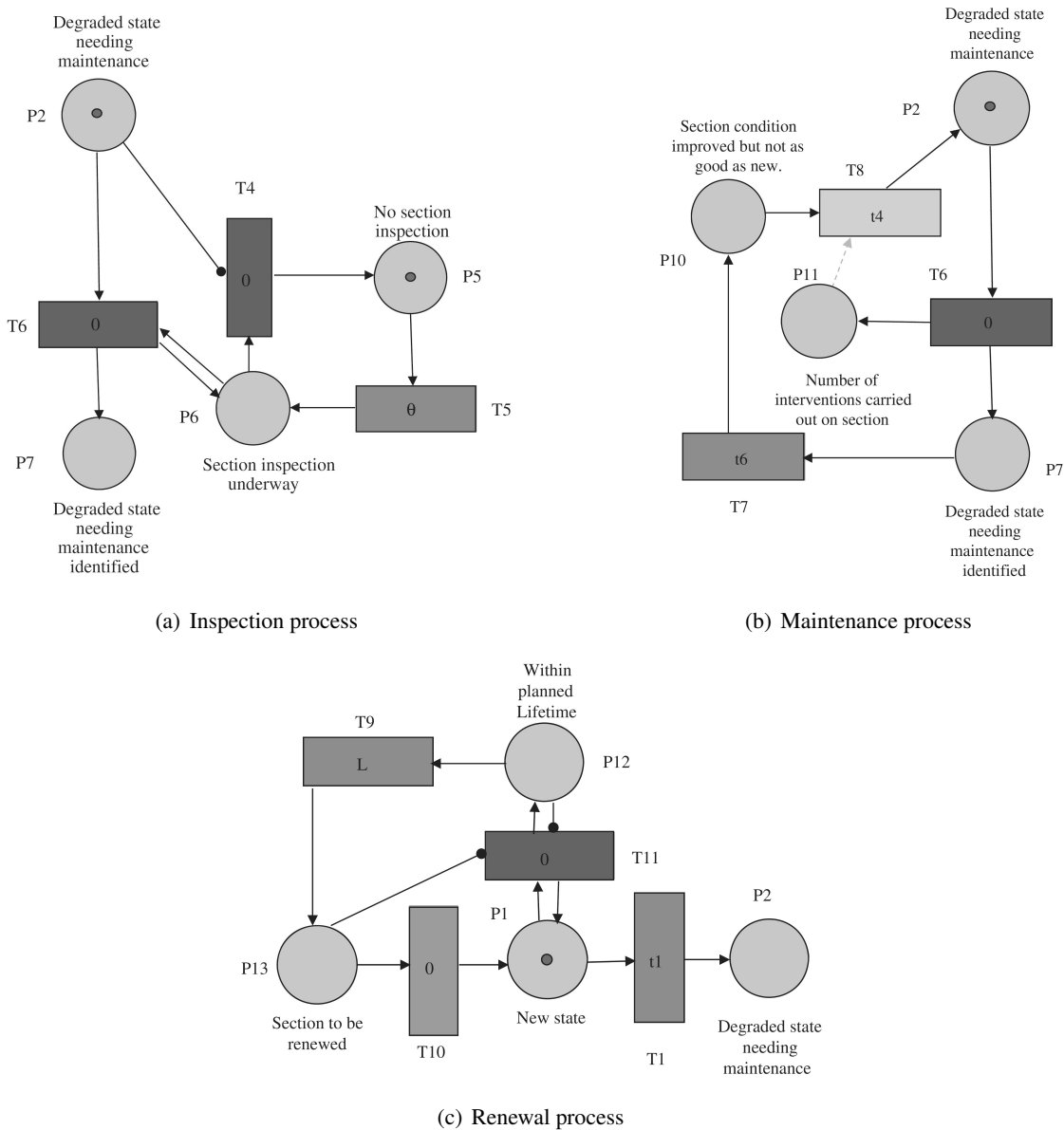
Figure 2.12 – Petri net scheme of the maintenance model proposed by Andrews (2013)

2.7 Summary

In this chapter, it was shown that in last three decades the concern with the development of a more rational approach to decision-making in terms of inspection, maintenance and rehabilitation of the built heritage has increased. It was observed that research on management systems is not restricted to bridges, as there is a reasonable amount of research in other areas, such as buildings, pavements, wasterwater, among others. In addition, it was possible to see that the methodologies used by the different management systems and their basic components are similar for all types of infrastructures.

Deterioration models are considered a critical component of a management system. This component has the function of simulating the degradation process of the infrastructure. However, the results provided by the deterioration models are subjective, because they are usually associated with a significant level of uncertainty. To capture the variability of the degradation process, stochastic deterioration models are used to predict the future performance of the structures. The majority of deterioration models is based on Markov chains. There are also a considerable number of studies based on reliability-based approaches and, recently, the Petri net formalism has been used to model deterioration process.

The main advantage of Markov chains is its simplicity, the use of exponential distribution to describe the transition between condition state, and the existence of analytical expressions for the probability distribution. However, exponential distributions are not very versatile, can result in a gross approximation of the system characteristics, the model size increases exponentially with the increasing number of condition state or number of modelled components, and the effects of maintenance is not directly captured by the transition probability matrix.

The application of Petri nets to degradation models is a recent development which has shown several advantages relative to the more traditional Markov chains. The graphical representation can be used to describe the problem in an intuitive way; Petri nets are more flexible than the Markov chains, allowing incorporating many rules in the model to accurately simulate complex situations and keeping the model size within manageable limits. Moreover, with this modelling technique, transition times are not required to be exponential distributed.

Chapter 3

Petri Nets Theory

3.1 Introduction

As referred in Section 2.5.2, the original concept of Petri nets was introduced by Carl A. Petri (Petri, 1962), who in his doctoral thesis developed a new model of information flow and control in systems. An ordinary Petri net is considered a directed, weighted, bipartite graph with an initial state called the initial marking, M_0 (Peterson, 1977; Murata, 1989; Schneeweiss, 2004). It is denoted by a bipartite graph because nodes are divided into two different types: places, usually represented by circles, and transitions, usually represented by rectangles. Both nodes are linked by directed arcs. A place can represent a particular state of the system while a transition can represent actions which cause changes to the system, modelling its dynamic behaviour. The last element of a Petri net, tokens, usually represented by black dots, are located in places, indicating the present state of the system. Figure 3.1 depicts a simple Petri net including all major elements.
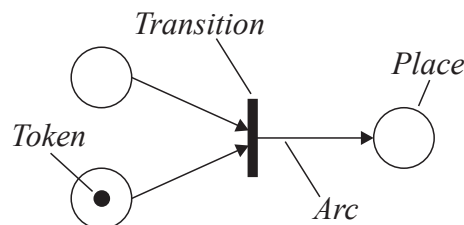
Figure 3.1 – Petri net

Petri net models described in this work are an extension of the original concept. These extensions correspond to models to which functioning rules have been added, in order to enrich the initial model, thereby enabling a greater number of applications to be treated (David and Alla, 2010), allowing making the model more concise and efficient (Le and Andrews, 2015). In the following sections, all extensions and components of the PN implemented in this project are discussed.

3.2 Extensions of the Petri nets

3.2.1 Timed Petri nets

In the original definition of Petri nets, the concept of time is not explicitly included (Murata, 1989). However, for many applications where the behaviour depends on time, introduction of time delays must be considered. Time delays can either be associated with places or transitions. Most modellers

assigned time to transitions, since these can be used to model activities, so that transition enabling periods correspond to activity executions and transitions firings correspond to activity completions, modelling the activities in a more natural way (Marsan et al., 1994; Bowden, 2000).

For example, consider the timed Petri nets (TPN) illustrated in Figure 3.2(a). When a token is generated in place p_1, transition t_1 becomes enabled, and the associated timer is set to an initial value. The timer is then decremented at constant rate, and the transition fires when the timer reaches the value zero. The timer associated with the transition can thus be used to model the duration of an activity whose completion induces the state change that is represented by the change of marking produced by the firing of transition t_1, Figure 3.2(b).

(a) Marking before transition t fires   (b) Marking after transition t fires
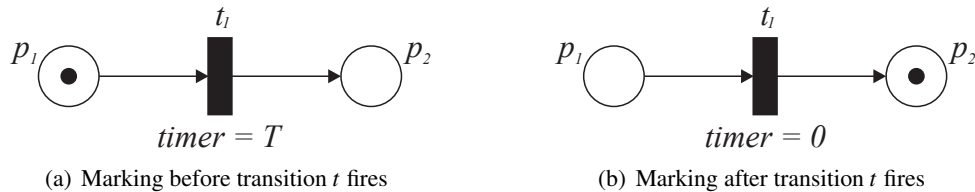
Figure 3.2 – Example of a timed Petri net (adapted from Marsan et al., 1994)

According to Bowden (2000), there are three basic ways of representing time in PN: firing durations, holding durations, and enabling durations. In firing durations, each transition has a time delay associated with it. When a transition becomes enabled, input tokens are immediately removed but output tokens are not created until the firing duration has elapsed. On the other hand, holding durations classifies the tokens into two types: available and unavailable. Available tokens can be used to enable a transition, whereas unavailable tokens cannot. Each transition is assigned a duration, and when a transition fires, the action of removing and creating tokens is done instantaneously. However, the created tokens are not available to enable new transitions until they have been in their output place for the time specified by the transition that created them. Holding durations and firing durations represent time in the same way. The only difference is that in one case the tokens are "held" in the transitions, while in the other they are "held" in the places. Finally, in enabling durations, the firing of the transition is done immediately. Tokens are removed and created in the same instant, and time delays are represented by forcing transitions to be enabled for a specified period of time before they can fire. In this work, this last approach is used.

3.2.2   Stochastic Petri nets

Timed Petri nets were initially introduced through the works of Ramamoorthy and Ho (1980) and Zuberek (1980). In these two works, a deterministic time is assigned for each transition. However, we live daily with random phenomena, like unpredictable weather changes or equipment failures. To overcome this difficulty a stochastic process was introduced in Petri nets. Molloy (1982) proposed Stochastic Petri Net (SPN) assigning an exponentially distributed firing rate to each transition for continuous time systems or a geometrically distributed firing rate to each transition for discrete time systems.

After that, several classes of SPN's have been proposed for performance and reliability analysis of systems, in order to meet the diverse needs of different application fields. The most relevant are:

- **Generalized Stochastic Petri Nets (GSPN)**

    Generalized stochastic Petri nets were introduced by Marsan et al. (1984). The main difference between SPN's and GSPN's is that the latter type allows the use of two different classes of transitions: immediate transitions and timed transitions. An exponentially distributed firing

rate is associated only with timed transition, while immediate transition has no firing delay (Marsan et al., 1984).

- **Extended Stochastic Petri Nets (ESPN)**

  Extended stochastic Petri nets were developed by Dugan et al. (1984). In ESPN the firing rate is assigning to each transition as proposed by Molloy (1982), however, it is allowed that firing rates may belong to an arbitrary distribution (Dugan et al., 1984). According to Dugan et al. (1984), the ESPN greatly enhances the modelling power and flexibility of stochastic Petri nets, but also increases the complexity of the model.

- **Deterministic and Stochastic Petri Nets (DSPN)**

  The concept of deterministic and stochastic Petri nets was introduced by Marsan and Chiola (1986). DSPN's are an extension of GSPN models, which allows firing delays of timed transition to be either constant, or exponentially distributed random variable (Marsan and Chiola, 1986).

From a mathematical point of view, the theory behind any class of SPN is the same as the PN; their mode of operation is identical, applying the same firing rules. The only difference lies on the fact that a transition can only fire sometime after it becomes enabled. A stochastic Petri net with n places and m transitions can be denoted by $\langle SPN, M_0 \rangle$, which represents a stochastic Petri net of dimension $n \times m$ with an initial marking, M_0. The structure of any class of SPN can be defined by a five-tuple:

$$SPN = (P, T, \mathbf{Pre}, \mathbf{Post}, \Lambda) \tag{3.1}$$

where P, T, **Pre**, **Post** have the same meaning of the original Petri nets (Equation 2.24) and Λ is the firing rate vector. It is a vector of dimension m and the jth component of Λ, indicated by λ_j, represents the firing rate of the transition $t_j \in T$. In situations where the Petri net has immediate transitions, the vector Λ contains only m' elements, on what m' is the number of timed transition (Marsan et al., 1984).

Due to the memoryless property of the exponential distribution, Molloy (1982) has proved that there is an isomorphism between bounded stochastic Petri net with exponentially distributed firing rates and a finite Markov chain. A Markov chain can be obtained from a reachability graph of a given SPN by applying the following two rules (Murata, 1989):

1. The Markov chain state space is the reachability set $R(M_0)$ of the stochastic Petri net;

2. The transition intensity from state M_i to state M_j is given by $q_{ij} = \lambda_j$, where λ_j is the firing rate of transition t_j transforming M_i into M_j ($q_{ij} = \lambda_{j1} + \lambda_{j2} + ...$ if there are two or more transitions, t_{j1}, t_{j2}, ..., transforming M_i into M_j); $q_{ij} = 0$ if no transition transforming M_i into M_j, for $i \neq j$; and q_{ii} is determined in order to satisfy $\sum_j q_{ij} = 0$. The square matrix $\mathbf{Q}$ is known as the transition intensity matrix.

The reachability set is fundamental for studying the dynamic properties of any system. The firing of an enabled transition will change the marking in a network according to the transition rules. So, a reachability set, $R(M_0)$, can be defined as the set of all markings that can be reached from the initial marking M_0 (Peterson, 1977; Murata, 1989).

For example, Figure 3.3 illustrates a marked SPN with four places and five transitions. Transitions t_1, t_2, t_3, t_4 and t_5 have marking-independent firing rates λ_1, λ_2, λ_3, λ_4 and λ_5, respectively. From the initial marking $M_0 = (2; 0; 0; 0)$, transitions t_1, t_3 and t_5 are enabled. The firing of t_1 and t_5 leads to the same marking, $M_1 = (1; 1; 0; 0)$, while the firing of t_3 leads to marking $M_2 = (1; 0; 1; 1)$. Now, analysing M_1, transitions t_1, t_2, t_3 and t_5 are enabled. The firing of t_1 and t_5 leads to marking $M_3 = (0; 2; 0; 0)$, the firing of t_3 leads to marking $M_4 = (0; 1; 1; 1)$, while the firing of t_2 leads

the Petri net to the initial marking M_0. This methodology is followed until all possible markings and firing transitions are covered. The reachability graph of the SPN is shown in Figure 3.4 and the corresponding Markov chain state space is given by Figure 3.5. From these two figures it is observed that the bounded SPN illustrated in Figure 3.3 is isomorphic to a Markov chain of six states.
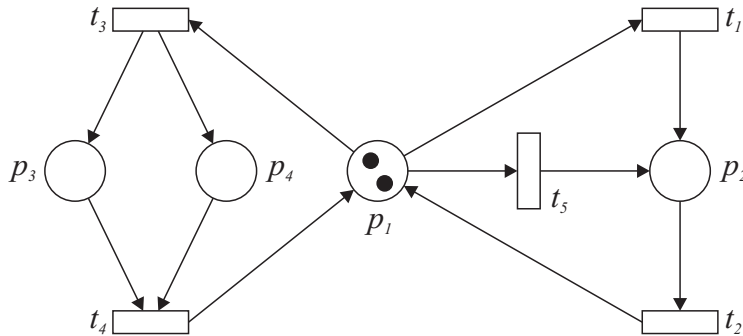
Figure 3.3 – Example of a stochastic Petri net (Murata, 1989)
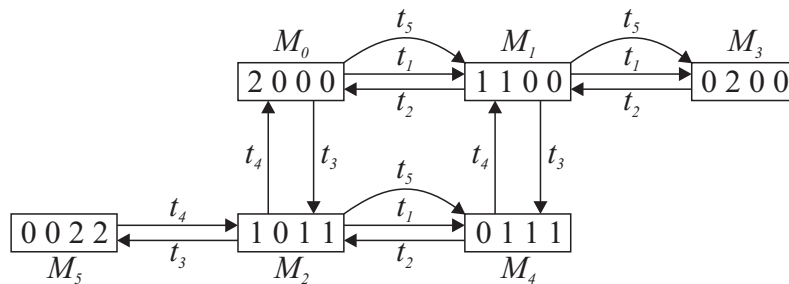
Figure 3.4 – Reachability graph of the SPN shown in Figure 3.3
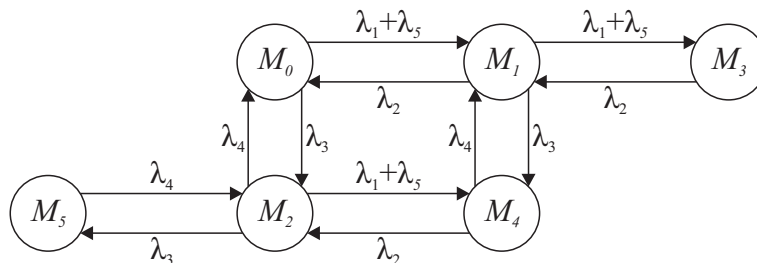
Figure 3.5 – Markov chain state space of the SPN shown in Figure 3.3

The transition intensity matrix $\mathbf{Q}$ of dimension $s = |R(M_0)|^1$ is given by Equation 3.2.

$$\mathbf{Q} = \begin{bmatrix} -\lambda_{15} - \lambda_3 & \lambda_{15} & \lambda_3 & 0 & 0 & 0 \\ \lambda_2 & -\lambda_{15} - \lambda_2 - \lambda_3 & 0 & \lambda_{15} & \lambda_3 & 0 \\ \lambda_4 & 0 & -\lambda_{15} - \lambda_3 - \lambda_4 & 0 & \lambda_{15} & \lambda_3 \\ 0 & \lambda_2 & 0 & -\lambda_2 & 0 & 0 \\ 0 & \lambda_4 & \lambda_2 & 0 & -\lambda_2 - \lambda_4 & 0 \\ 0 & 0 & \lambda_4 & 0 & 0 & -\lambda_4 \end{bmatrix} \tag{3.2}$$

where $\lambda_{15} = \lambda_1 + \lambda_5$.

---

[1]Note that symbol $|A|$ is used to denote the cardinality of a generic set A.

3.2.3 Continuous timed Petri nets

Continuous Timed Petri Nets (CTPN) are another extension derived from the original concept of Petri nets (David and Alla, 2010). In a timed Petri net, the marking of a place is made through an integer number and the firing of a transition occurs at times while, in a CTPN, the marking of a place becomes a non-negative real number and the firing of a transition becomes a continuous flow.

The CTPN was obtained as a relaxation of the discrete Petri nets and this formalism is useful for modelling continuous systems such as handling of fluids (Alla and David, 1998). In order to better understand the basic operation of CTPN, consider the following example. An hourglass (Figure 3.6(a)) is initialized at time t_0. Its behaviour from t_0, from a discrete point of view, can be described by PN illustrated in Figure 3.6(b). The tokens in places p_1 and p_2 represent the number of grains in the upper part and in the lower part of the hourglass, respectively. The delay d_1 corresponds to the average time between two successive grain passages from top to bottom. Let $m_1(t_0) = C$ and $m_2(t_0) = 0$ the initial marking of the Petri net.

A continuous model, where the passing of grains is considered a continuous flow, can be constructed from the discrete PN of Figure 3.6(b) by replacing the delay d_1 by a firing frequency $u_1 = 1/d_1$. This gives the CTPN of Figure 3.6(c) in which the markings of places p_1 and p_2 are non-negative real number at any time. A firing speed v_1 is associated with the transition t_1, which means that the "quantity of tokens" passing from p_1 to p_2 between time t and $t + dt$ is $v_1 dt$. The comparison of the marking evolution of both models is represented in 3.6(d). For both models, all the marks have passed from p_1 to p_2 at time $t_h = C/u_1$.

From a mathematical point of view, a continuous Petri net can be denoted by $\langle CTPN, M_0 \rangle$, which represents a continuous timed Petri net (CTPN) with an initial marking, M_0. The structure of a continuous timed Petri net can be defined by a five-tuple (Alla and David, 1998; Tolba et al., 2005):

$$CTPN = (P, T, \mathbf{Pre}, \mathbf{Post}, V) \tag{3.3}$$

where P, T, $\mathbf{Pre}$, $\mathbf{Post}$ have the same meaning of the original Petri nets (Equation 2.24) and V is real positive vector of transitions maximum firing speeds.

3.2.4 Coloured Petri nets

Coloured Petri nets belong to the class of high-level nets. This class is more powerful and able to describe more complex system of the real-world in a manageable way (Jensen, 1992).

In coloured Petri net, tokens carry information through the Petri net. Each token has attached its own characteristics, called the token colour, and has the ability to carry a large number of different types of information (e.g. the first field of the record can be a real number, the second a text string, while the third is a list of integer pairs). Transitions in this kind of Petri nets are also more complex. In addition to being necessary to satisfy the number of tokens required by pre-conditions, it is necessary that the tokens present in the input places satisfy the transition criteria, called guard. Only when these two types of constraints are satisfied are the transitions enabled (Jensen, 1992).

An example of a coloured Petri net is shown in Figure 3.7. Places p_1 and p_2 contain a token each. The token present in place p_1 has associated an integer which has a value equal to 3, while the token in place p_2 has two types of information: an integer (value = 2) and a string "abc". The transition t_1 is basically a function, the input edge of the transition provides the input for the function and the output edge of the transition produces the output of the function. The input and output constraints are shown by the arcs that connect the transition to the places. When the transition fires, the tokens in place p_1 and p_2 are consumed and a token in place p_3 is produced with the properties of an integer (value =

(a) Hourglass (Gandelheid, 2007)

(b)   Timed Petri net

(c) Continuous timed Petri net

(d) Marking evolution
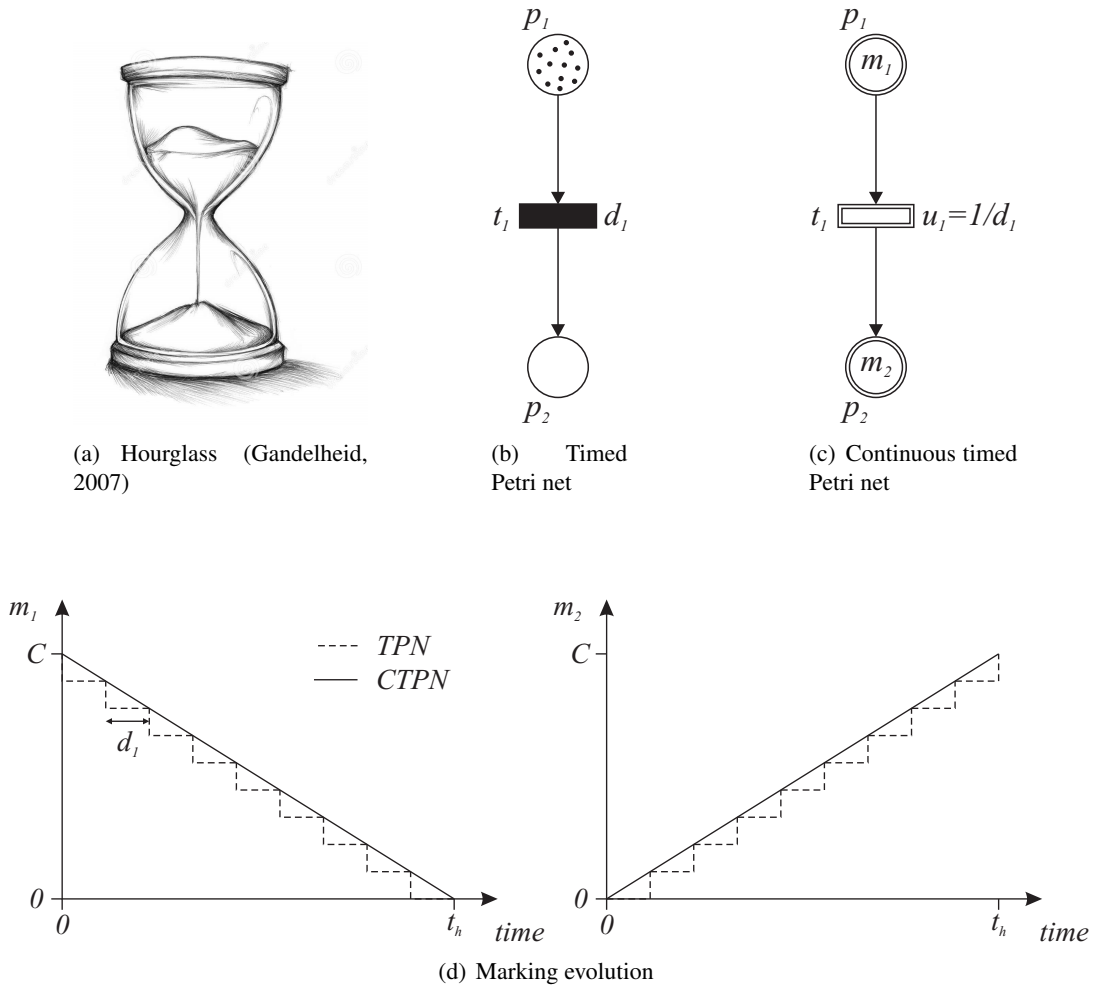
Figure 3.6 – Example of a continuous timed Petri net (adapted from Alla and David, 1998)

9) and a string "abc". The transition t_1 also has a condition on the firing, i.e. only when the token in place p_1 and p_2 have the integer value of greater than 0 is the transition enabled (Le, 2014).

(a) Before the transition t fires

(b) After the transition t fires
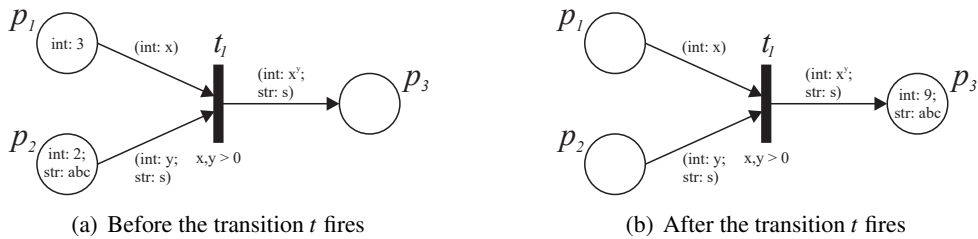
Figure 3.7 – Simple example of a coloured Petri net (adapted from Le, 2014)

In coloured Petri nets, the basic concept of the original Petri net is preserved. The main difference between both methods is the transitions in coloured Petri net are a function that allows the characteristics of the token to change once it passes through a transition, whereas, in traditional Petri nets, the tokens are simply consumed at the input and reproduced at the output of a transition. The flexibility of the coloured Petri net comes from the ability to transform part of the Petri net into a function. This transformation, besides other advantages, allows reducing, in a considerably way, the size of the network (Jensen, 1992; Le, 2014).

3.3 Petri net component nomenclature

In Section 3.2 several extensions of the original concept of PN were presented and several components were added to improve the graphical formulation of Petri nets. Over the years, a convention was proposed by several authors (Marsan et al., 1984; Marsan and Chiola, 1986; Schneeweiss, 2004). The main purpose of this section is to describe the convention adapted to represent the different types of components in this work.

3.3.1 Transitions and places

Transitions can be divided into five types (immediate, timed with deterministic delay, timed with stochastic delay, continuous timed and reset) while places can be divided into two types (ordinary and continuous).

In timed transitions with deterministic time delay there is a constant time delay associated with the transition. This type of transitions allows modelling discrete processes and changing the qualitative behaviour of the model with respect to the untimed Petri nets (Marsan and Chiola, 1986). On the other hand, timed transitions with stochastic time delay are defined to be random variables with given statistical distributions. This type of transitions is very useful to model random processes, and the firing rate can be defined from different probabilistic distributions (Dugan et al., 1984; Marsan and Chiola, 1986). Immediate transitions are associated with the original concept proposed by Petri (1962) where, by definition, the firing delay is equal to zero. This transitions are used to represent logical control or an activity whose delay is negligible when compared with those associated with timed transitions (Marsan et al., 1984; Murata, 1989). Continuous timed transitions are associated with CTPN and are used to model continuous systems (Alla and David, 1998). Finally, reset transitions have associated a list of places and number of tokens that each place will contain after the Petri net resets. A reset action can be performed using the original concept of PN but would require a large number of transitions and places to be added to the model that would increase the size and complexity, confusing the engineering process that is being modelled (Andrews, 2013; Le and Andrews, 2015).

Regarding places, the distinction between ordinary and continuous is made through the type of marking. In models where the marking of the Petri net is made through integer numbers, ordinary places are used, while in models where the marking of the Petri net is made through non-negative real numbers continuous places are used. In order to simplify the nomenclature, in this document, ordinary places are only called places.

In this work, it was adapted that immediate transitions, Figure 3.8(a), are drawn as thin bars; timed transitions with deterministic time delay, Figure 3.8(b), as black rectangular boxes; timed transitions with stochastic time delay, Figure 3.8(c), as white rectangular boxes; continuous timed transitions, Figure 3.8(d), as a double white rectangular boxes; and , reset transition, Figure 3.8(e), as white thin bars. Ordinary places, Figure 3.9(a), are drawn as circles; and continuous place, Figure 3.9(b), as a double circle.

(a) Immediate transition

(b) Timed transition with deterministic time delay

(c) Timed transition with stochastic time delay

(d) Continuous timed transition
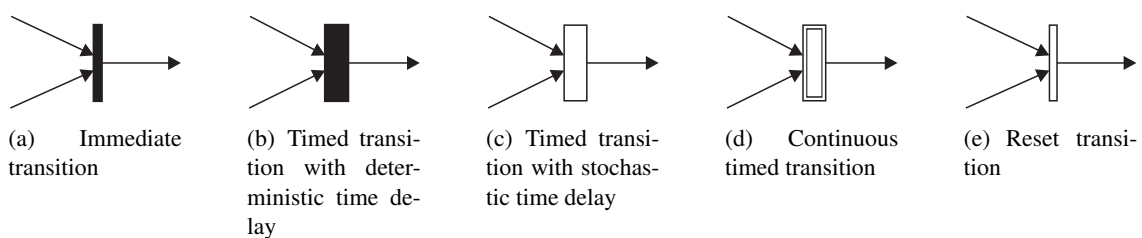
(e) Reset transition

Figure 3.8 – Symbols often used to represent different types of transitions

(a) Ordinary place   (b) Continuous place
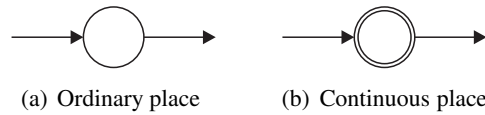
Figure 3.9 – Symbols often used to represent different types of places

3.3.2 Inhibitor arc

Inhibitor arcs are a second type of edges that can be used. This type of edge allows prioritizing the firing of transitions into PN. In situations where two or more transitions connected to a common place exist and it is needed to specify which transition takes precedence, inhibitor arcs change the firing rules and disable some of the transitions. In other words, an inhibitor arc allows defining negative conditions and prevent the firing of a particular transition (Peterson, 1977; Baskocagil and Kurtulan, 2011).

In a Petri net with inhibitor arcs, the firing rule is changed as follows: a transition is enabled to fire when there are tokens in all of its (normal) input places and there are no tokens in the inhibiting input places. When the transition fires, the tokens are removed from the normal input places and deposited in the output places as usual, but the number of tokens in the inhibiting input place (place p_2 in Figure 3.10) remains nil (Dugan et al., 1984). An inhibitor arc (Schneeweiss, 2004) can only go from a place to a transition and, graphically, it is representing by a tiny circle replacing the arrow head, directly touching the transition that it is possible to block (Figure 3.10).

Figure 3.10 illustrates an example of a simple Petri net with one inhibitor arc. Transition t_2 is blocked if and only if there is one or more tokens in place p_2 (Figure 3.10(b)), otherwise, the prioritization rules of the original Petri net method apply.

(a) Transition t_2 available   (b) Transition t_2 unavailable
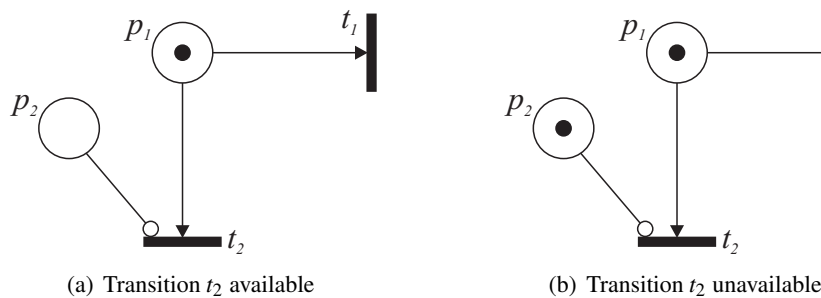
Figure 3.10 – Example of a Petri net with inhibitor arcs

In order to use inhibitor arcs in a computerized environment, it is necessary to incorporate the behaviour of inhibitor arcs into the state equation (Baskocagil and Kurtulan, 2011). The state equation for a Petri net composed only by ordinary arcs, in matrix form, is given by:

$$M' = M + u\mathbf{D} \tag{3.4}$$

where M is the current system state; u is an m-dimensional firing vector, and m is the total number of transitions. In this vector, all of the elements assume a value of zero except the jth element; this element assumes a value of one that means the jth transition will be fired. Finally, $\mathbf{D}$ denotes the incidence matrix:

$$\mathbf{D} = \mathbf{Post} - \mathbf{Pre} \tag{3.5}$$

The state equation for a Petri net composed for both type of arcs is defining by:

$$M' = M + u\mathbf{H}(M)\mathbf{D}' \tag{3.6}$$

where $\mathbf{H}(M)$ is an inhibitor matrix, a diagonal matrix of dimension $m \times m$ whose off-diagonal elements are either 0 or 1. This matrix is variable and depends on the current system state, M, and allows identifying the transitions that are blocked by the inhibitor arc.

$$\mathbf{H}(M) = \begin{cases} \mathbf{H}_{ij}(M) = 0, & i = 1,...,m, \quad j = 1,...,m, \quad \text{if } i \neq j \\ \mathbf{H}_{jj}(M) = 1, & j = 1,...,m, \quad \text{if } t_j \text{ is not blocked by the inhibitor arc} \\ \mathbf{H}_{jj}(M) = 0, & j = 1,...,m, \quad \text{otherwise} \end{cases} \tag{3.7}$$

In Equation 3.6, $\mathbf{D}'$ denotes the new incidence matrix. The inhibitor matrix itself is not enough to model the behaviour of the inhibitor arc, i.e. the incidence matrix also has to be modified. When a transition triggers, no tokens are removed from the place that is connected to this transition by an inhibitor arc. The new incidence matrix changes the token transfer mechanism, in order to make it suitable for the inhibitor and ordinary arcs. The new incidence matrix for inhibitor arc is given by:

$$\mathbf{D}' = \begin{cases} d'_{ij} = 0, & i = 1,...,n, \quad j = 1,...,m, \quad \text{if there is an inhibitor arc between } p_i \text{ and } t_j \\ d'_{ij} = d_{ij}, & i = 1,...,n, \quad j = 1,...,m, \quad \text{otherwise} \end{cases} \tag{3.8}$$

where n denotes the total number of places in the Petri net.

3.4 Conflicts

An important concept in PN's is that of conflict. A conflict occurs when two or more transitions are enabled from a common place and the firing of one transition disables the other transitions (Bowden, 2000). In the literature several ways of resolving conflicts is proposed; they can be solved in a deterministic way, for example through the introduction of a priority transition by the user, or in a probabilistic way, by assigning probabilistic properties to the conflicting transitions (David and Alla, 2010).

The PN in Figure 3.11 presents a structural conflict between transitions t_1 and t_3, $\langle p_5, \{t_1, t_3\} \rangle$. There is an effective conflict when p_1, p_3, and p_5 are marked (both t_1 and t_3 are enabled). In this example, it can consider there is a resource shared by two kinds of customers: the resource is available when there is a token in p_5, and the tokens in p_1 and in p_3 model the customers are waiting for a service. Allocating the resource to the left side customers or to the right side customers corresponds to firing t_1 or t_3, respectively. The conflict resolution consists of choosing the transition that is fired when both are enabled (David and Alla, 2010).

One way of resolving conflicts is by transition priority. This methodology is considered deterministic and consists in introducing prioritization of transitions by the user. In our example, the priority may be given to t_1 over t_3. This is denoted by $t_1 < t_3$. In this situation, as long as there is a token in p_1, t_3 cannot be fired. For example, consider Figure 3.12(a), there are two resources (two tokens in p_5) and both transitions are enabled. Since $t_1 < t_3$, both tokens present in p_5 must be assigned to firing of t_1 because of the priority rule. But, on the other hand, if it consider Figure 3.12(b), one token must be assigned to firing of t_1, and the other may be used to fire t_3 (David and Alla, 2010). This type of conflict can also be solved by introducing an inhibitor arc (Figure 3.13).
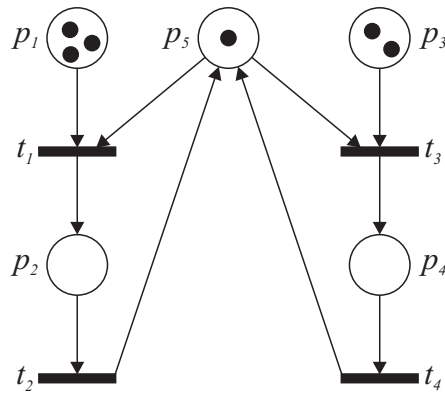
Figure 3.11 – Example of a Petri net with conflict (adapted from David and Alla, 2010)
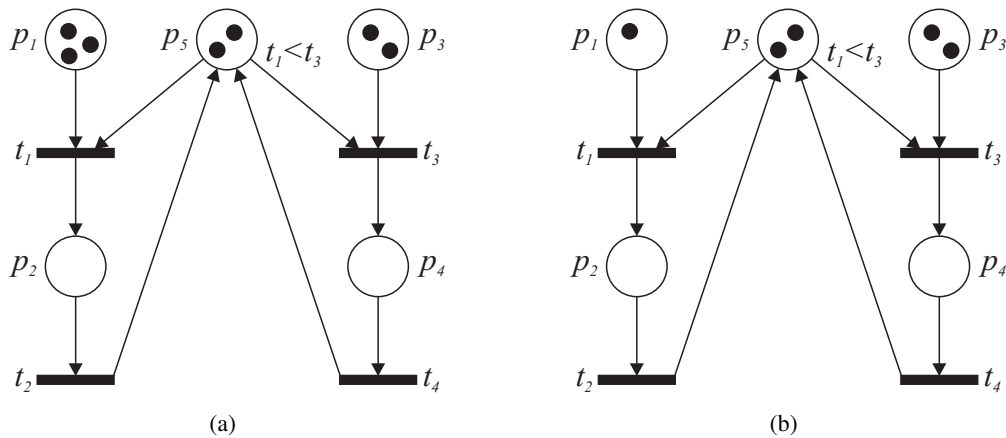
Figure 3.12 – Example of a Petri net with conflict (adapted from David and Alla, 2010) – Transition priority
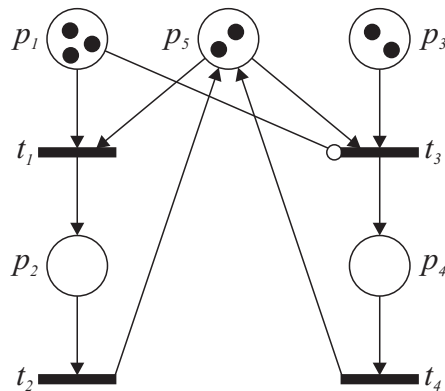
Figure 3.13 – Example of a Petri net with conflict (adapted from David and Alla, 2010) – Inhibitor arc

A second methodology for resolving conflicts is by assigning probabilistic properties to each conflicting transitions. For example, consider that t_1 should fire with a probability of 0.75 while t_3 should fire with a probability of 0.25. When both transitions are enabled, a random drawing is performed such that $P(firing\ t_1 | t_1\ and\ t_3\ are\ enabled) = 0.75$. This random drawing is such that t_1 will be fired roughly 3 times more often than t_3. If a probability of 0.5 is assigned to both transitions, it corresponds practically to the absence of constraint. The probabilities could be functions of other variables (David and Alla, 2010).

Finally, another methodology present in the literature to resolve conflicts is the alternate firing. Two places, p_6 and p_7 have been added to the PN (Figure 3.14) such that t_1 and t_3 will be fired in turn. There is a token in p_6; after firing of t_1 there will be no token in p_6 but a token in p_7, allowing t_3 to be fired when p_3 and p_5 are marked, and so on. However, with this change in the PN, it can be said that there is no longer any effective conflict (David and Alla, 2010).
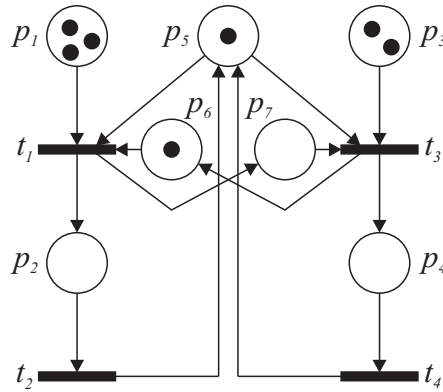
Figure 3.14 – Example of a Petri net with conflict (adapted from David and Alla, 2010) – Alternate firing

3.5 Summary

This chapter discusses, in detail, the modifications in the original Petri net modelling technique to suit the problem of infrastructure management. It should be mentioned that there are many more applications for Petri nets than those presented here. However, we have chosen to refer only the main types of Petri nets and the extensions implemented throughout the work.

Chapter 4

Petri Net Model

4.1 Introduction

This chapter describes the model used to predict the deterioration on civil engineering infrastructures based on the Petri net approach. In the proposed model the uncertainly associated with degradation of existing structures, as well as, the effect and the time of application of maintenance actions is considered through the use of probability distributions and the Monte Carlo Simulation (MCS).

In the first section of this chapter, the Petri net deterioration model is presented. The methodology used to develop the deterioration model is based on the ESPN formalism proposed by Dugan et al. (1984), where the firing rate assigned to each transition can be modelled by a variety of probabilistic distributions, and time is represented by enabling durations. After that, the model used to consider maintenance in the system based on Petri nets is depicted. The maintenance model was built from the deterioration model, including inspection, maintenance and renewal processes. In the following section, the computational platform developed to compute the performance profiles is described. The combination of the Petri net formulation with the Monte Carlo simulation allows different maintenance strategies to be investigated.

4.2 Petri net deterioration model

The deterioration process can be modelled with Petri nets through a linear sequence of places and stochastic timed transitions. Each place represents a condition state of the classification system adapted and each stochastic timed transition defines the movement between condition states (Andrews, 2013; Yianni et al., 2017). Pictorially, an example of the PN scheme of the deterioration model can be depicted by Figure 4.1. The transitions are located between places and the position of the token in the network indicates the current condition state of the system.
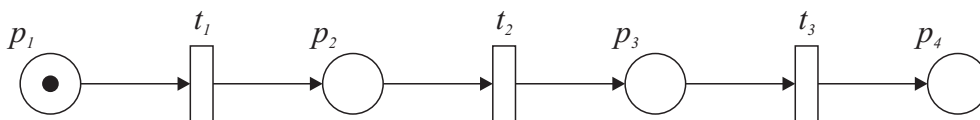
Figure 4.1 – Petri net scheme of the deterioration model

In situations where maintenance is not considered, the condition state of the system deteriorates continuously over time until it reaches the worst condition state defined in the performance scale. The first place defined in the PN scheme of the deterioration model (Figure 4.1) represents the best condition state while the last place represents the worst condition state. The remaining places represent the

intermediate condition states. In this example, the model is composed by four places (p_1 to p_4) and three transitions (t_1 to t_3). Places p_1 and p_4 represent, respectively, the best and worst condition state of the performance scale. Since the token is in place p_1, the system is currently in the best condition state.

The notion of time is assigned through the stochastic timed transitions. As mentioned above, these elements have the function of modelling the changes between the different condition states and the assignment of time delays to transitions are the most natural way of modelling the deterioration process. When time is assigned to transitions, it is assigning to each transition the sojourn time of the system in each condition state, i.e. the time specified by transition t_i, with $i = 1, 2, 3$, represents the time that the system spends in condition state i before moving to condition state $i + 1$.

4.2.1 Estimation of the firing rates

The parameter estimation from a set of data is essential to model degradation. Herein, it is considered that the probability distribution that best describes the deterioration process of a system is that resulting in higher probabilities of occurrence of observed transitions. So, in order to identify the parameters of the probability distribution that provide a better fit, a parameter estimation is required. The parameters of the probability distribution are fitted to historical data through the maximum likelihood method described by Kalbfleisch and Lawless (1985). The likelihood, L, measures the difference between the real observations and those predicted by the model, and can be defined as:

$$L = \prod_{e=1}^{E} \prod_{k_e=1}^{K_e} p_{ij} \qquad \text{(2.21 revisited)}$$

where E is the total number of elements present in the database, K_e is the total number of transitions observed for element e, and p_{ij} is the probability of occurrence of the observed transition where i indicates the condition state in the initial instant and j the condition state in the final instant. From a numerical point of view, using the logarithm of the likelihood of occurrence is more robust. Therefore, Equation 4.1 is used as a measure of the fit quality:

$$\log L = \sum_{e=1}^{E} \sum_{k_e=1}^{K_e} \log p_{ij} \qquad \text{(4.1)}$$

The optimal firing rates can be computed through an optimization problem that maximizes the logarithm of the likelihood, $\log L$.

The maximum likelihood method was chosen over other estimation methods such as regression methods (Butt et al., 1987; Cesare et al., 1992; Morcous, 2006) because it is more robust and uses the probability of occurrence to compute the likelihood.

4.2.2 Monte Carlo simulation

The probability of occurrence of the observed transition, p_{ij}, is estimated by Monte Carlo simulation. MCS is an helpful approach to compute numerical approximations in situations where it is not feasible to obtain analytical solutions and can be used to consider the propagation of uncertainties during the lifetime of the system. This method allows generating random sojourn times to each condition state from the inverse cumulative distribution function (iCDF) of a probability distribution.

The proposed procedure for computing the probability of occurrence of the observed transition, p_{ij}, is illustrated in the flowchart in Figure 4.2. The procedure depicted is repeated for each observed

transitions in the historical database. From each observed transition in the database, the following parameters are recorded: time interval between observations, t_h; condition state in the initial instant, i; and condition state in the final instant, j. The condition state in the initial instant, i, is used to define the initial marking, M_0, of the Petri net and to define the first transition to fire, t_i; the time interval between observations constitutes the time horizon of the analysis, t_h; and the condition state in the final instant, j, is used to compute the probability of occurrence in the end of the procedure.
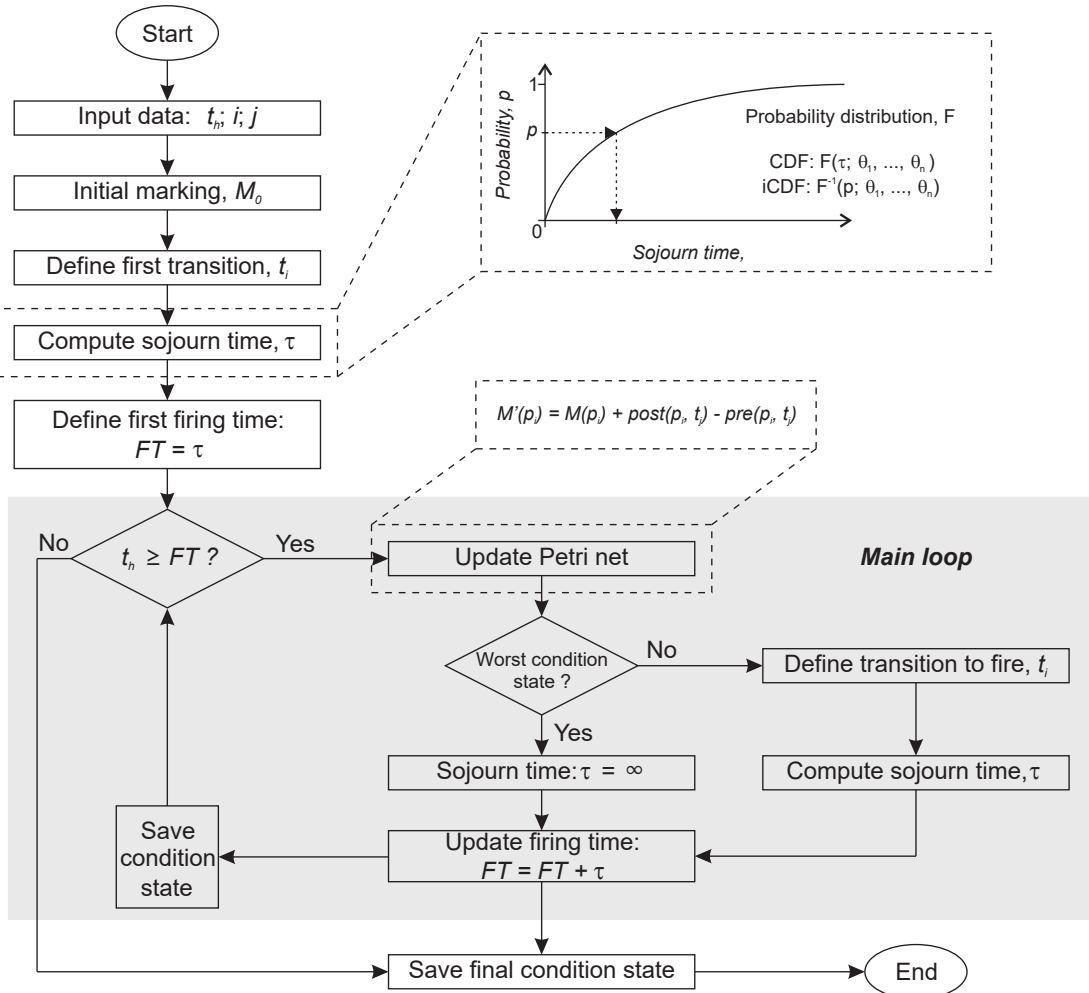
Figure 4.2 – Procedure to compute the probability of occurrence of the observed transition

In the next analysis step, the sojourn time, τ, in the initial condition state is computed. A uniformly distributed random variable, p, between 0 and 1 is randomly generated. The inverse CDF is used to calculate a random sample from the objective distribution. It should be noted that parameters θ_1, ..., θ_n of the probability distribution are state-dependent, because deterioration rate is not the same for all condition states. After that, it is possible to define the instant in which the first transition fires, FT.

The main loop of the procedure begins with a verification. If the time horizon, t_h, is greater than or equal to the firing time, FT. The enabled transition fires and the Petri net is updated through Equation 2.25. After that, it is verified if the system is in the worst condition state defined in the performance scale. If this is true, it is assumed that the system will remain infinitely in this condition state because it is considered that there is no application of maintenance actions to improve the condition state of the system. Otherwise, a new transition to fire, t_i, is defined and the sojourn time τ in the new condition state is computed. After that, the variable firing time, FT, is update and the condition state of the system is saved in a vector. It is assumed that until the next firing time, the system remains in the same condition state. If, on the other hand, the time horizon, t_h, is smaller than or equal to the

firing time, FT, all intermediate steps are ignored, and the following step is the saving of the final condition state.

The output of the procedure, at the time horizon, is a condition state where the sojourn time in each condition state is computed stochastically. The repetitive calculation of this procedure (Monte Carlo simulation) allows estimating the probability of occurrence of the observed transitions, p_{ij}, that is given by:

$$p_{ij} = \frac{n_{MCS,j}}{n_{MCS}} \tag{4.2}$$

where n_{MCS} is the total number of trials of the MCS and $n_{MCS,j}$ is the number of trials of the MCS where the final condition state predicted is equal to the condition state observed, state j.

4.2.3   Genetic algorithm optimization

In engineering, the choice of the best design alternative or optimal strategy depends, sometimes, on our ability to model the system performance over time, which is uncertain by nature (Sánchez-Silva and Klutke, 2016). The simpler way to find the optimum solution is by exhaustive search, i.e. to evaluate all possible solutions, in order to find the fittest one. However, in complex engineering problems, the evaluation of each potential solution is a time consuming task. This is particularly true when there is a large dimensioned search space, making the search for the optimal solution, one by one, impossible. Therefore, an optimization technique should be implemented to find the best solution (Le, 2014).

In the literature, there is a wide variety of optimization techniques available, including gradient-based or gradient-free optimization algorithms. Gradient-based optimization techniques are more efficient at finding local minima. However, when used with Monte Carlo simulation the numerical errors associated with the simulation can result in erroneous gradients, and severely limit the ability of the algorithm to find a good solution. On the other hand, gradient-free optimization algorithms do not need to compute gradient and can be used with MCS, however, these optimization algorithms are slow.

In this work, the optimization of the parameters of the probability distributions is performed using genetic algorithm (Holland, 1992). The genetic algorithm is an optimization and search technique based on the Darwin theory of evolution, where search procedures aim to find the best and fittest solutions as a sequence of generations where each new generation is defined based on the properties of the individuals of the previous generation. The advantage of GA's over other optimization techniques lies on the fact multiple solutions to the problem (i.e. population) are stored and probabilistic rules (crossover and mutation) to generate new and better populations are used, which is more efficient and increases the odds of finding optimal solutions. Further, GA's use only information of the objective function, not requiring any information on its gradients, which greatly simplifies the problem (Man et al., 1999; Morcous and Lounis, 2005).

The GA used for optimization of the parameters of the probability distributions is simply depicted in the flowchart in Figure 4.3. The optimization procedure begins with the definition of three important elements of the algorithm: problem parameters, objective function, and constraints. The problem parameters are all variables that must be optimized. The objective function measures the degree of "goodness" of each individual of the population (Man et al., 1999; Morcous and Lounis, 2005). The aim of this problem is to find the parameters of the probability distributions that best fit the historical data, i.e. that maximize the log-likelihood (Equation 4.1). So, all parameters of the probability distributions are defined as problem parameters, while Equation 4.1 and the entire procedure explained

in the above section defines the objective function. Finally, the constraints of the problem are related with the parameters of the probability distributions.
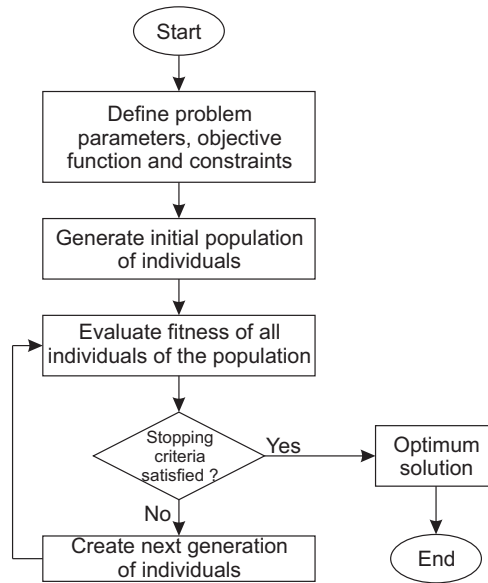
Figure 4.3 – Procedure to optimize the parameters of probability distributions (adapted from Morcous and Lounis, 2005)

In the following step, the initial population is randomly generated. A population is composed of a set of individuals, where each individual is a solution of the problem. All individuals of the initial population are evaluated through the objective function. These individuals are then ranked according to their fitness value. At each step of the optimization process, the GA uses the current population to create the offsprings that make up the next generation. A group of individuals of the current population that have the better fitness values are selected as parents, who contribute their genes to their offsprings. Children are produced either by mutation or crossover. In crossover, there is the combination of the properties of parents in the current population in order to obtain two new offsprings. In mutation there is a disturbance of the properties of an individual, allowing the inclusion of characteristics that were not present in the initial population and ensure that the algorithm explores a broader search space (MatLab, 2017). The new population generated is then evaluated using the objective function and used as a new parent population. This process is repeated iteratively until a predefined stopping criteria is satisfied.

In this study, the optimization of the parameters was performed using genetic algorithm available in software MalLab$^®$ (MatLab, 2017). The analytical formulation of the problem is:

> **Find:** The parameters of the probabilistic distributions

> **So that:** $\log L = (\sum \sum \log p_{ij})$ is maximized

The parameters used in the GA are the following:

- Size of the population: 50 individuals when the number of optimization variables is less than or equal to 5; and 200 individuals otherwise;

- Stopping criteria: the algorithm stops if the average relative change in the best fitness function value over 50 generations is less than or equal to 10^{-6};

- Mutation procedure was performed using the Gaussian algorithm implemented in MalLab$^®$;

- Crossover procedure was performed using the Scattered algorithm implemented in MalLab$^®$.

4.3   Petri net maintenance model

Figure 4.1 illustrates the Petri net scheme used herein for modelling the deterioration process. In this particular example, the system begins in a *Very good condition* and degrades continuously until reaches a *Very poor condition*, since maintenance is not considered. However, in reality, when the deterioration leads the system to a *Poor* or *Very poor condition*, performing maintenance is required in order to maintain the system operating in a safety condition state.

4.3.1   Inspection process

The condition of a system is not continuously known; it must be detected. Its true condition is only revealed after a major inspection is being performed. The major inspections are periodic and carried out within the maintenance program defined for the system. In general, these are visual inspections, carried out by specialized staff, with the objective of evaluating the degradation state of the system, through the identification of anomalies that may affect performance. The exposure of the true condition will enable the most appropriate maintenance work to be requested for existing anomalies with the appropriate priority. The part of Petri nets that is responsible for managing the moments that the major inspections are carried out in the system is shown in Figure 4.4 through the cycle formed by the following places and transitions: p_5 - t_5 - p_6 - t_4 - p_5 (Andrews, 2013).
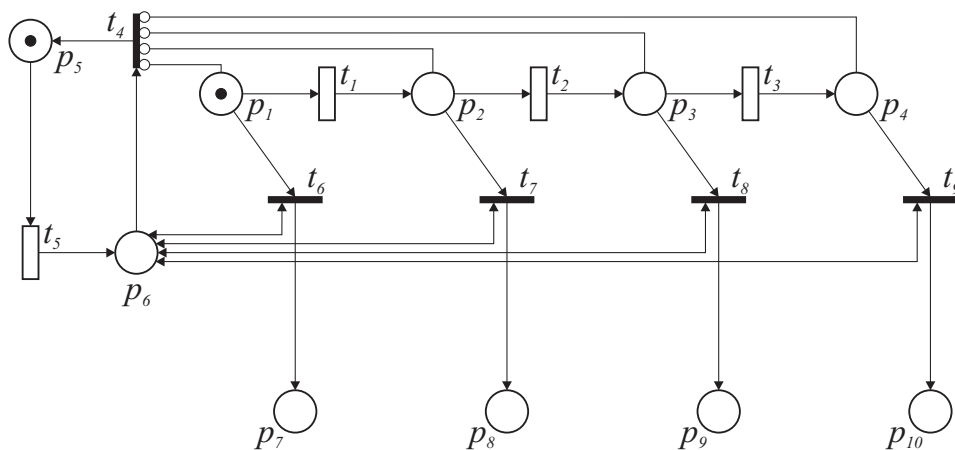
Figure 4.4 – Introduction of the inspection process on the Petri net scheme of the maintenance model

A token in place p_5 means that it is not time to conduct a major inspection. Transition t_5 is a timed transition and manages the moments of realization of the major inspections. This transition is enabled due to the token present in place p_5 and fires at regular time intervals; when it fires, the token is removed from place p_5 and one token is added in place p_6.

A token in place p_6 signifies that the major inspection is being performed, enabling several other transitions. It enables the immediate transition t_4, if the inhibitor arcs constraints are checked, which causes the token to return to place p_5 to wait for the next major inspection. Moreover, it enables one of the following transitions: t_6, t_7, t_8, or t_9. The firing of one of these transitions removes the token from the deterioration process (places p_1 - p_4) and reveals the true condition of the system by depositing it in one of the following places p_7 - p_{10}, respectively. In this example, a token in places p_7, p_8, p_9 or p_{10} means, respectively, that the true condition of the system is *Very good*, *Good*, *Poor*, or *Very poor*. Place p_6 is connected to transitions t_6, t_7, t_8, and t_9 by bidirectional arcs, representing a simplification for two unidirectional arcs. This ensures that the token on place p_6 is not removed at this stage.

4.3.2 Maintenance process

Once the true condition of the system is revealed, it is decided if maintenance work is required. Figure 4.5[1] shows the Petri net scheme with the maintenance process.
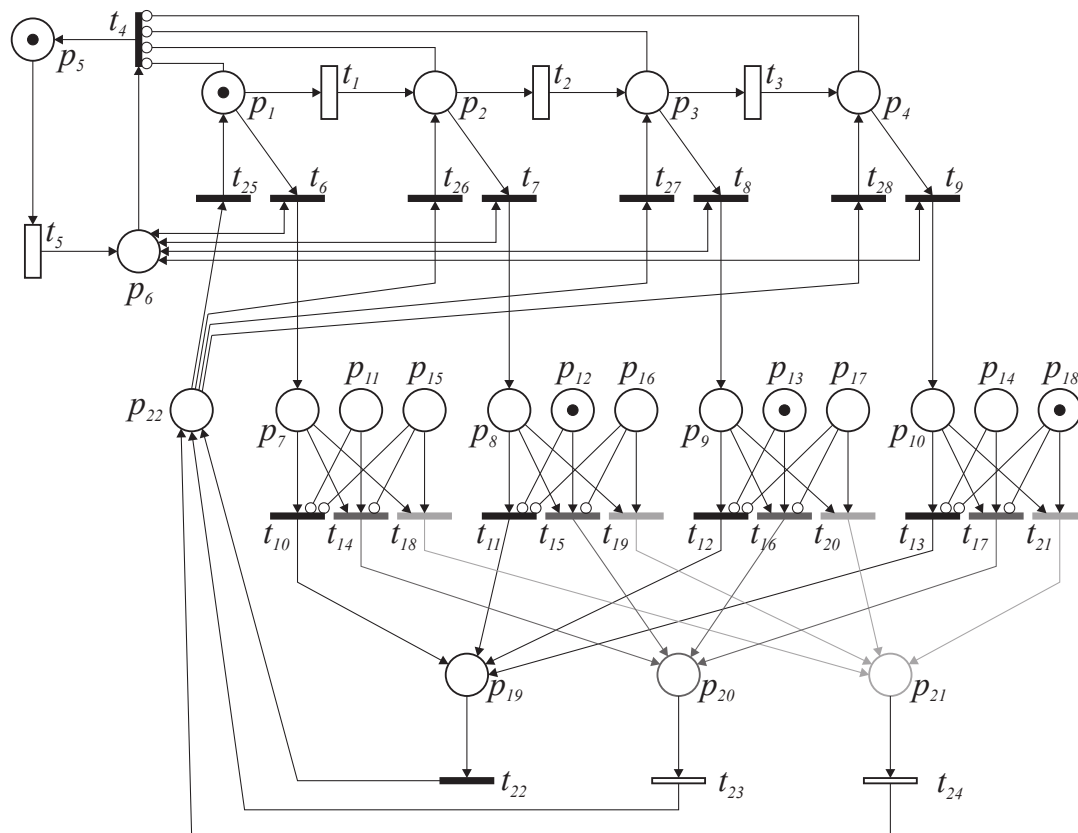
Figure 4.5 – Introduction of the maintenance process on the Petri net scheme of the maintenance model

As mentioned above, the existence of a token in one of the places p_7 - p_{10} means that the condition of the system is known and maintenance can be initiated. The first step is to analyse what types of maintenance are available in the maintenance program for the system under study for the respective true condition. This information is introduced in the model through places p_{11} - p_{18}. A token in places p_{11} - p_{14} means that preventive maintenance must be performed while a token in places p_{15} - p_{18} means that corrective maintenance must be performed. If there is no token in these places, there is no maintenance involved. On the other hand, in the cases where there is a token in both types of maintenance, corrective maintenance is performed, since this type of maintenance is more effective and usually covers the same maintenance works that the PM.

After that, depending on the action to take, one of the following transitions may be fired:

- Transitions t_{10} - t_{13}: No maintenance is performed, the token is removed from places p_7 - p_{10} and it is deposited in place p_{19};

- Transitions t_{14} - t_{17}: Preventive maintenance, the token is removed from places p_7 - p_{10} and it is deposited in place p_{20};

- Transitions t_{18} - t_{21}: Corrective maintenance, the token is removed from places p_7 - p_{10} and it is deposited in place p_{21}.

---

[1]The different colours that are in the Petri net scheme has no special meaning, its function is only to help understand better the direction of the arcs

For example, according to the marking of Figure 4.5, if major inspection reveals that the system has a *Very good condition*, transition t_6 fires, removing the token from place p_1 and depositing it in place p_7. Since, places p_{11} and p_{15} have no marks, no maintenance is performed in this condition state, enabling transition t_{10} to fire, which leads the token from place p_7 to place p_{19}. But, if on the other hand, major inspection reveals that the system has a *Good condition*, transition t_7 fires, removing the token from place p_2 and depositing it in place p_8. Since place p_{12} is marked, preventive maintenance is required, enabling transition t_{15} to fire, which leads the token from place p_8 to place p_{20}. For the case in which major inspection reveals that the system is in a *Poor condition*, transition t_8 fires, removing the token from place p_3 and depositing it in place p_9. Since only place p_{13} has a token, preventive maintenance is required, enabling transition t_{16} to fire, which leads the token from place p_9 to place p_{20}. Finally, if major inspection reveals that the system has a *Very poor condition*, transition t_9 fires, removing the token from place p_4 and depositing it in place p_{10}. Since only place p_{18} is marked, corrective maintenance is required, enabling transition t_{21} to fire, which leads the token, from place p_{10} to place p_{21}.

Places p_{19} - p_{21} enable, respectively, transitions t_{22} - t_{24}, which move the token to place p_{22}. This place is a decision place, since it enables four immediate transitions t_{25} - t_{28} that are in conflict with each other. The choice of the transition to fire is performed in a deterministic way, according to the effect that the maintenance had on the system. More concretely, firing the transition relative to the condition that the system is in. In this model, it was considered that the application of preventive and corrective maintenance is "instantaneous" through the use of immediate reset transitions t_{23} and t_{24}, respectively. However, this transitions can be replaced by timed transitions in order to model, in a more realistic way, the time that maintenance interventions take.

4.3.3   Maintenance

A successful maintenance program seeks a balanced between of preservation and rehabilitation activities. Therefore, two main types of maintenance actions can be defined: preventive and corrective maintenance. Preventive maintenance is associated with a lower impact on the system safety and a lower cost. However, these strategies are cost-effective, since the deterioration rate is often reduced with a lower life-cycle cost, keeping the system in a safe condition state. On the contrary, corrective maintenance is associated with significant improvement in the performance at time of application and higher both direct and indirect cost. Nevertheless, they are required to restore an adequate condition state (van Noortwijk and Frangopol, 2004). A combination of both maintenance actions is required to achieve a cost-effective life-cycle performance, considering budget limitations.

4.3.3.1   Effect of maintenance actions

In the proposed maintenance model, the impact of a maintenance action in a system can be modelled by one or combination of the following effects (Neves and Frangopol, 2005; Bocchini and Frangopol, 2011a):

  (i) Improvement of the condition state of the system after the application of the maintenance action;

  (ii) Suppression of the deterioration process or reduction of the deterioration rate for a period of time after the application of the maintenance action.

The different impacts of the maintenance actions on the system are illustrated in Figure 4.6. When a maintenance action that improves the condition state of the system is applied, this effect is described by the indication of the condition state for which the system improves immediately after the main-

tenance action, γ, as illustrated in Figure 4.6(a). Numerically, after the application of maintenance action, the new condition state at instant t is defined by Equation 4.3.

$$C(t) = \gamma \qquad (4.3)$$

On the other hand, if the maintenance action suppresses the deterioration process, this is characterized only by the time period in which the process is suppressed, t_d. During this time, it is assumed the performance indicator of the system remains unchanged, as shown in Figure 4.6(b). Computationally, after the application of maintenance action, the sojourn time in a condition state i, t_i, is defined by Equation 4.4.

$$t_i = t_i^w + t_d \qquad (4.4)$$

In this situation, the sojourn time in condition i, t_i, is extended t_d years, where t_i^w represents the sojourn time of the system in condition state i without maintenance.

Finally, reduction in rate of deterioration can be modelled by two parameters: period of time that the deterioration rate is affected, t_r; and deterioration factor, δ. The meaning of these two parameters is depicted in Figure 4.6(c). Numerically, after the application of maintenance action, the sojourn time in a condition state i, t_i, is defined by Equation 4.5.

$$t_i = \begin{cases} t_i^w + t_i^w \cdot \delta & \text{and} \quad t_r = t_r - t_i^w, & t_i^w \leq t_r \\ t_i^w + t_r \cdot \delta, & & t_i^w > t_r \end{cases} \qquad (4.5)$$

That is, it is assumed that when this type of maintenance is applied, the change of the condition state is not restrained; what is done is to extend the length of time that the system is in each condition state by a total of $t_r \cdot \delta$ years.

Furthermore, each maintenance action is associated with an applicability range, which is defined as a range of performance indicators for which the maintenance action is effective; outside this range, the effect of the maintenance action on the system is not complete, leading to alternative maintenance actions more effective.

In the present model, the decision to apply a maintenance action, either preventive or corrective, is always the consequence of a major inspection, where the true condition of the system is revealed. In this methodology it can be interpreted that both types of maintenance actions are condition-based, considering as preventive maintenance all actions that directly reduce future costs related to the failure while the system is in a satisfactory state of operation and as corrective maintenance the interventions required once the system fails or reaches a predetermined deterioration level (Sánchez-Silva and Klutke, 2016).

4.3.3.2 Modelling of maintenance actions

The Petri net scheme used to model the effects of maintenance actions, previously identified, is illustrated in Figure 4.7 for preventive maintenance and Figure 4.8 for corrective maintenance.

For the example of preventive maintenance (Figure 4.7), when a token arrives at place p_{20} from Figure 4.5, it means that the major inspection has already been performed, that the true condition of the system has been revealed and that it has been verified that the system presents the requirements for a preventive maintenance action to be taken.

(a) Improvement of the condition state

(b) Suppression of the deterioration process

(c) Reduction of deterioration rate
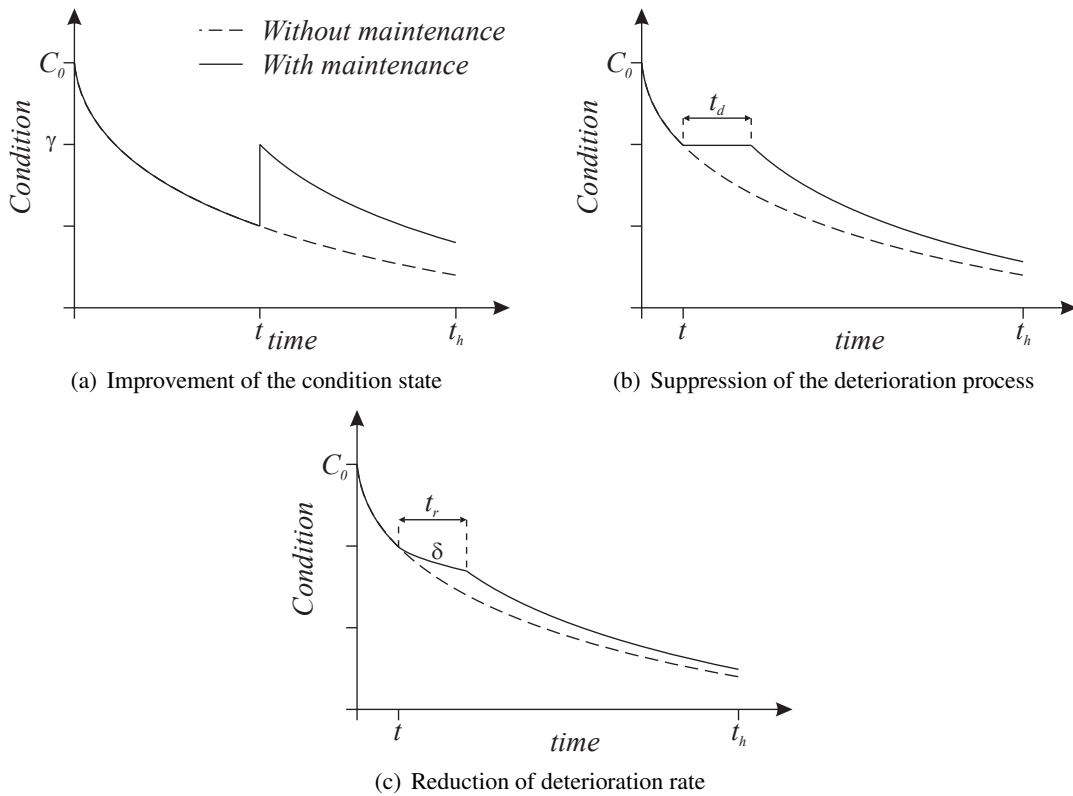
Figure 4.6 – Effects of the maintenance actions

The characteristics of the preventive maintenance action are introduced in the maintenance model through the places p_{23} - p_{25} and the transitions t_{29} - t_{33}. The marking of places p_{23}, p_{24} or p_{25}, means, respectively, that the maintenance action, when applied, has the effect of improving the condition of the system, suppressing the deterioration process or reducing the deterioration rate. Then, depending on the impact that the maintenance action has on the system, only one of the following immediate transitions can fire by removing the token from place p_{20} and depositing it in place p_{26}:

- Transition t_{29}: Improvement the condition state of the system only;

- Transition t_{30}: Suppression the deterioration process over a period of time only;

- Transition t_{31}: Improvement of the condition state and suppression the deterioration process over a period of time;

- Transition t_{32}: Reduction the deterioration rate over a period of time only;

- Transition t_{33}: Improvement the condition state and reduction the deterioration rate over a period of time.

The values of the parameters needed to model the maintenance actions are "attached" to the tokens present in places p_{23} - p_{25}. When the transition fire occurs, this information is transmitted to the token that is deposited in place p_{26}, which is responsible for introducing the characteristics of the maintenance action implemented in the deterioration process of the maintenance model.

For the construction of the Petri nets scheme of corrective maintenance actions (Figure 4.8), the same methodology was followed as in preventive maintenance actions. When a token arrives at place p_{21} from Figure 4.5, it means that the major inspection has already been performed, that the true condition of the system has been revealed and that a corrective maintenance action is required in the system.

The characteristics of the maintenance action are introduced in the maintenance model through places
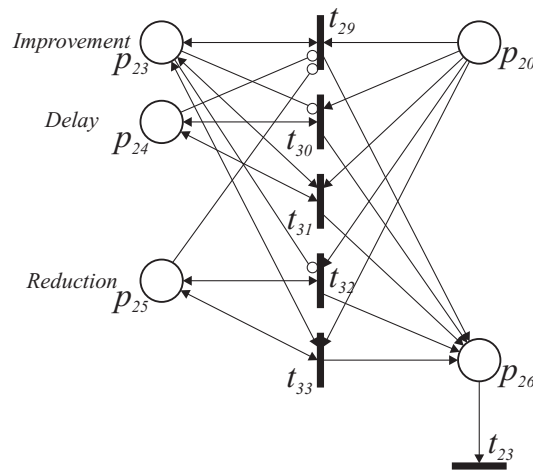
Figure 4.7 – Petri net scheme for preventive maintenance actions

p_{27} - p_{29} and transitions t_{34} - t_{36}. In the same way as in preventive maintenance actions, the marking of places p_{27}, p_{28} or p_{29}, means, respectively, that the maintenance action, when applied, has the effect of improving the condition of the system, suppressing the deterioration process or reducing the deterioration rate. Then, depending on the impact that the maintenance action has on the system, only one of the following immediate transitions can fire by removing the token from place p_{21} and depositing it in place p_{30}:

- Transition t_{34}: Improvement the condition state of the system only;

- Transition t_{35}: Improvement the condition state and suppression the deterioration process over a period of time;

- Transition t_{36}: Improvement the condition state and reduction the deterioration rate over a period of time.
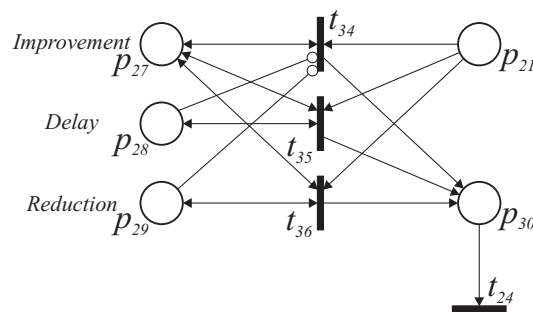
Figure 4.8 – Petri net scheme for corrective maintenance actions

The Petri net scheme for the corrective maintenance actions is different of the Petri net scheme for the preventive maintenance actions because it is assumed that corrective maintenance has the function of putting the system back into service. I.e. it is considered that corrective maintenance improves always the condition state of system, so there will be a smaller combination of effects.

It should be mentioned that other combinations of effects of maintenance actions can be added to both the Petri net scheme of preventive and corrective maintenance. This can be accomplished by introducing more transitions. The combinations of effects of the maintenance actions present in these two figures represent only one example of the capacities of Petri nets.

4.3.3.3 Periodicity of the preventive maintenance

As mentioned in Section 2.6, depending on the maintenance application time, maintenance can be classified as time-based or performance-based. Usually, preventive maintenance actions are timed-based.

In this model, the periodicity of the preventive maintenance is considered through the places p_{31} - p_{34} and the deterministic timed transitions t_{37} - t_{40} shown in Figure 4.9. The introduction of information that this maintenance is available in a given condition level is performed by placing tokens in places p_{31} - p_{34}. Transitions t_{37} - t_{40} are associated with a delay that allows, at the end of θ time units, the tokens present in places p_{31} - p_{34} to be removed and added to places p_{11} - p_{14}, allowing the preventive maintenance to be performed at the next inspection time, if the imposed constrains are verified.
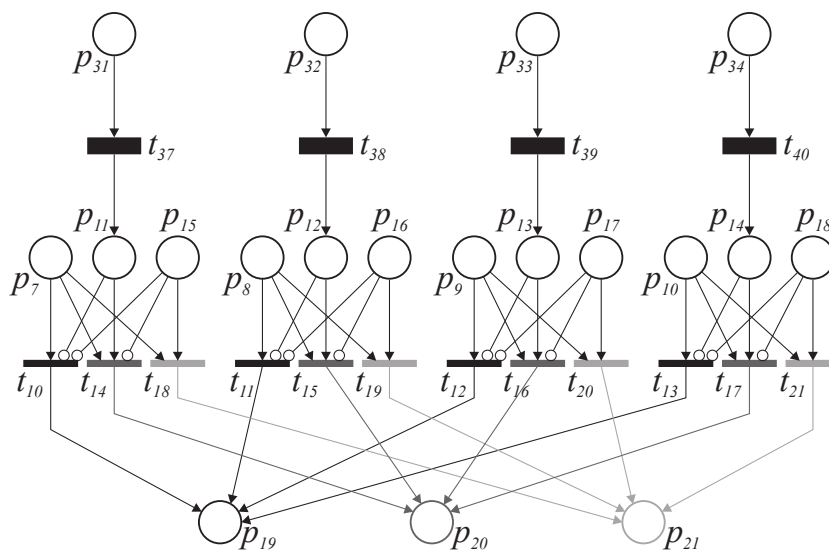
Figure 4.9 – Petri net scheme for periodicity of the preventive maintenance

4.3.4 Renewal process

At some time, the deterioration of the system will reach a point where a specific maintenance is no longer effective and a more effective maintenance needs to be applied. There are many possibilities as to how this instant can be defined. It can be after a predetermined lifetime, after the condition level is deemed to be too poor or after a set number of maintenance actions (Le and Andrews, 2015). Any of these approaches can be implemented in a PN model.

In the maintenance model, the renewal is performed after a certain number of a specific maintenance actions is carried out. These constrains are introduced in the model by adding to places p_{31} - p_{34}, if it is a preventive maintenance, and to places p_{15} - p_{18}, if it is a corrective maintenance, the number of tokens equal to the maximum number of maintenance allowed. When the maximum limit of a maintenance actions is reached, this action is no longer available causing the system to continue the deterioration process until it reaches worst condition levels where more effective maintenance actions are applied. It should be noted that the transitions t_{23} and t_{24} are reset transitions which, when fired, initialize the tokens in places p_{31} - p_{34} and p_{15} - p_{18}, according to the constrains imposed.

4.4 Complete maintenance model

The combination of all parts of the Petri net schemes together results in the Petri net is shown in Figure 4.10. For a performance scale with four condition states, the maintenance model is composed by 34 places and 40 transitions, being four stochastic (t_1, t_2, t_3, and t_5), four deterministic (t_{37}, t_{38}, t_{39}, and t_{40}), and two reset (t_{23} and t_{24}). The stochastic transitions t_1, t_2, and t_3 have sample times from the probability distribution that define the movement between condition states and stochastic transition t_5 have sample times from a triangular distribution that manages the timing of major inspections.
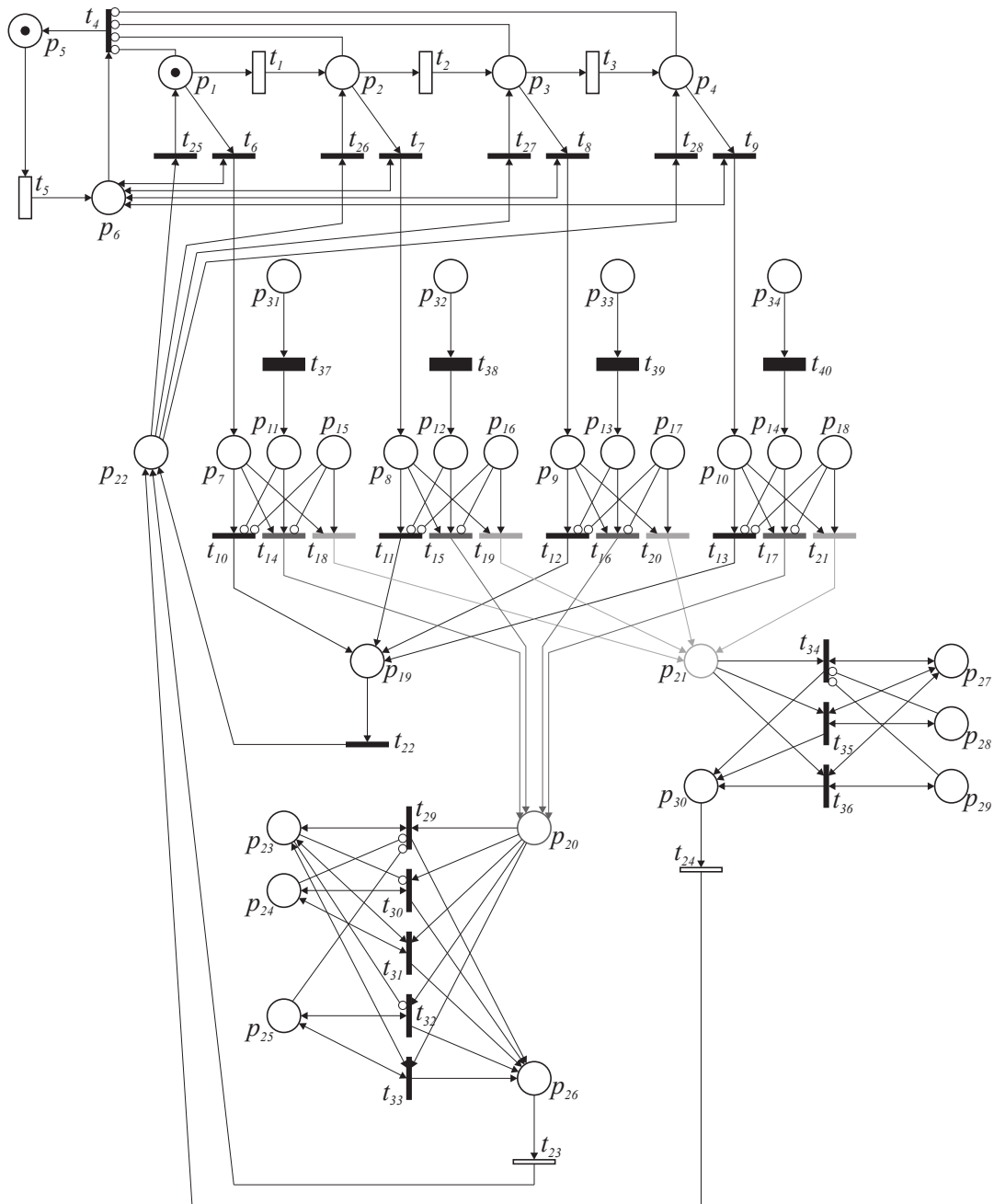
Figure 4.10 – Petri net scheme of the complete maintenance process

A full list with the description of the places and transitions included in the maintenance model is provided in Appendix A.

4.5   Computation of the performance profiles

Since there is significant uncertainty related to the assignment of a condition state to a system, as well as, on the definition of the effects of maintenance actions, Monte Carlo simulation is used to consider the propagation of uncertainties during the system's lifetime and to compute the performance profiles.

4.5.1   Performance profile without maintenance

The procedure used in simulating each Monte Carlo sample to compute the performance profile without maintenance is described in the flowchart shown in Figure 4.11 and in Section 4.2.2. The performance profile is characterized by an initial condition state C_0; a deterioration rate vector, $\Theta = \{\theta_1, ..., \theta_{s-1}\}$, where element θ_i corresponds to parameters of the probability distribution associated with transition t_i that models the sojourn time that the system spends in condition state i before moving to condition state $i+1$ and s denotes the total number of condition states defined in the classification system adapted; and, finally, a time horizon, t_h. The initial condition, C_0, is defined as the condition of the system in the last major inspection, being used to define the initial marking of the Petri net, M_0, and to define the first transition to fire, t_i, in the deterioration process. The deterioration rate vector, Θ, is composed by the optimal parameters of the probability distribution used to model the deterioration process.
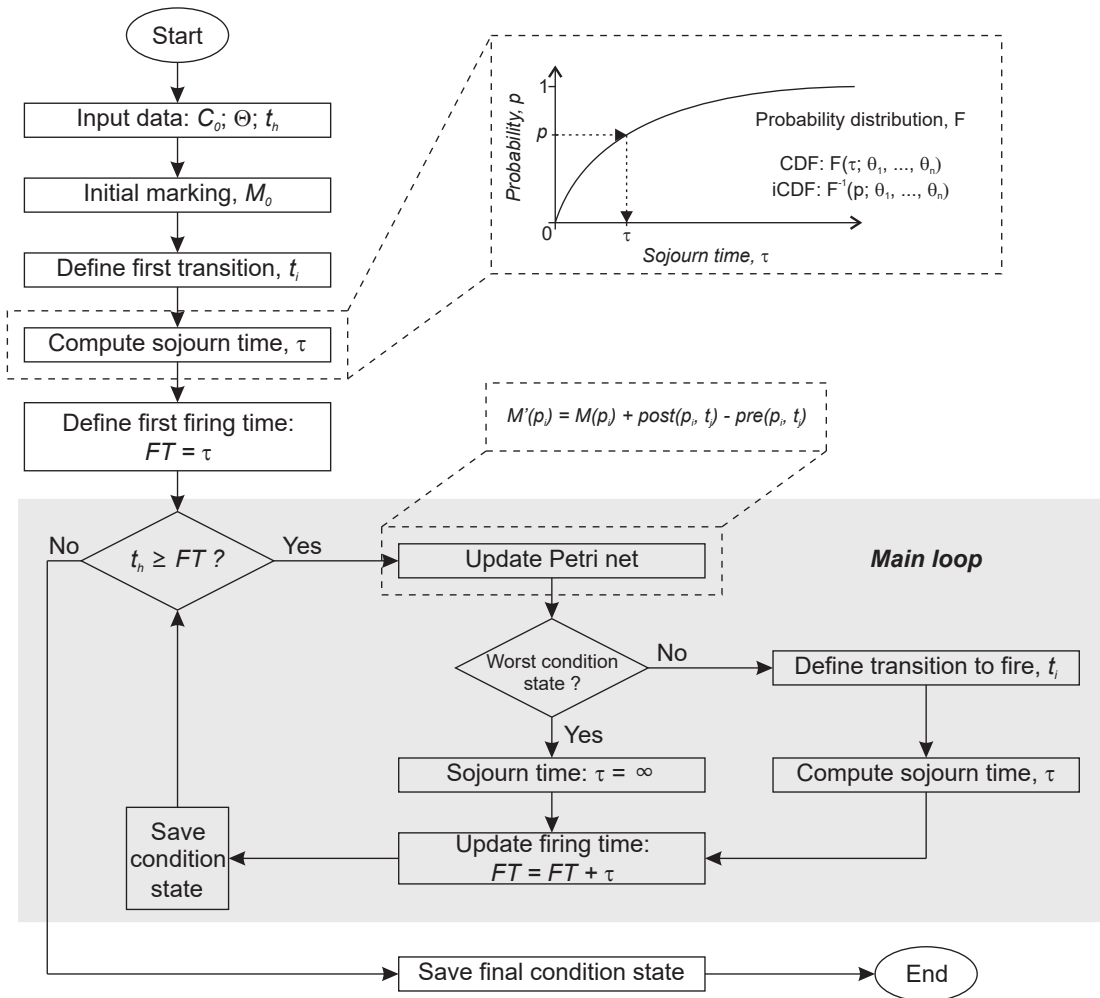
Figure 4.11 – Procedure to compute the performance profile of the system over time horizon for the situation without maintenance

The output of this procedure, at time horizon, is a condition state vector, where the condition state of the system is defined for all years from the beginning of the analysis until the time horizon. The repetitive calculation from procedure (Monte Carlo simulation) allows computing the mean, $\mu(t)$, and standard deviation, $\sigma(t)$, of the condition state in each instant, as follows:

$$\mu(t) = \frac{\sum_{i=0}^{n_{MCS}} C(t)}{n_{MCS}} \tag{4.6}$$

$$\sigma(t) = \sqrt{\frac{\sum_{i=0}^{n_{MCS}} C(t)^2}{n_{MCS}} - \mu(t)^2} \tag{4.7}$$

where $C(t)$ is the condition state of the system at time t and n_{MCS} is the total number of trials of the MCS.

4.5.2 Performance profile with maintenance

Since there is significant uncertainty associated with the attribution of the effects of maintenance action on the system, maintenance actions are usually better modelled using a probabilistic approach. In this model, it is assumed that all random variables are modelled by triangular distributions. The choice of this probability distribution is motivated by the fact that the triangular distribution is one of the easiest ways to introduce randomness into the model, with a minimum and a maximum defining a range of possible values and a mode, corresponding to the most probable value. In addition, the triangular distribution is one of the easiest ways to treat the information provided by experts (Denysiuk et al., 2016). The random variables used in the Monte Carlo simulation are identified in Table 4.1.

Table 4.1 – Variables used in the maintenance model for defining the application of maintenance actions

Random variable	Variable definition
t_{insp}	Time interval between major inspections
γ	Condition state for which the system improves immediately after the maintenance action
t_d	Time period during which the deterioration process is suppressed
δ	Deterioration factor
t_r	Time period during which the deterioration rate is affected

The procedure used to determine the performance profile of the system for the situation where maintenance is considered is shown in Figure 4.12. In this situation, in addition to the initial condition state, C_0, the deterioration rate vector, Θ, and the time horizon, t_h, it is necessary to introduce information regarding preventive and corrective maintenance actions and the interval between major inspections. As before, the initial condition state, C_0, is used to define the initial marking of the Petri net, M_0, and the first transition of the deterioration process to fire, t_i; and the deterioration rate vector is used to compute the sojourn time in each condition state. The time interval between major inspections is used to define the time that inspections should be performed on the system, t_{insp}, and the information regarding to the maintenance actions are used to define the application range and the effects that these have on the system.

The first step in the procedure is the determination of the first transition to be fired, t_i, in the deterioration process and the sojourn time of the system in the current condition state, τ, followed by the determination of time of the first inspection of the system, t_{insp}. After that, it is possible to compute the first firing time and its transition through Equation 4.8.
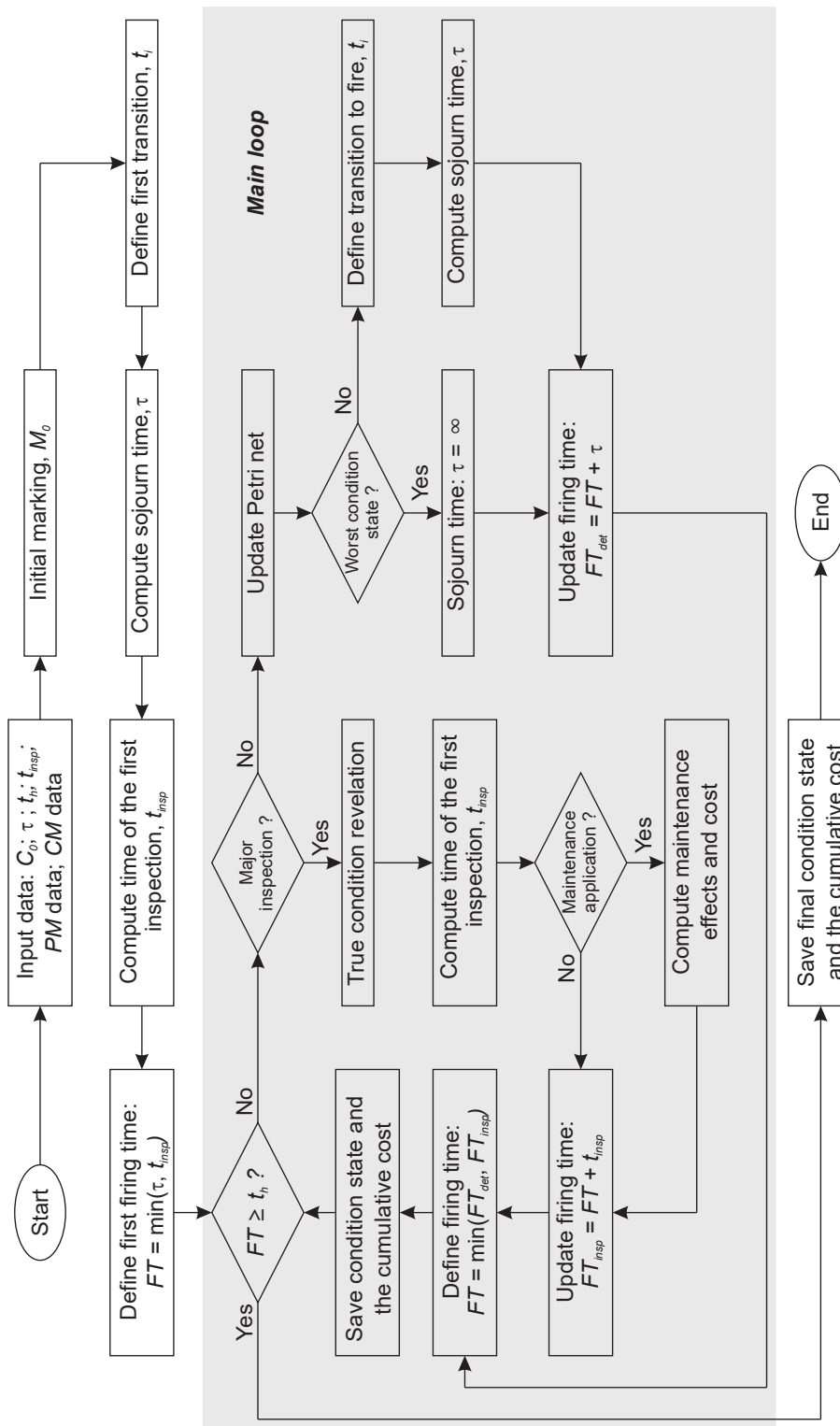
Figure 4.12 – Procedure to compute the performance profile of the system over time horizon for the situation with maintenance

$$FT = \min\left(\tau, t_{insp}\right) \tag{4.8}$$

The main loop starts by checking if the next firing time, FT, occurs after the time horizon, t_h, in which case the computation ends. Otherwise, the next transition to be fired can be either a major inspection

or a deterioration step. In the latter case the enabled deterioration transition fires and the Petri net is updated using Equation 2.25.

The procedure is run until the next firing time, FT, is larger than the time horizon. In each step, the first branch checks if a major inspection occurs in that year. If so, the true condition is revealed, the time of next inspection is computed and the relevant maintenance actions are applied. If no inspection occurs in that year, the next deterioration transition time is activated. The condition is updated and the next deterioration firing time is computed. If the system is in the worst condition state, the transition time until the next deterioration step is taken as ∞.

The output of this procedure, at time horizon, is a condition state vector, where the condition state of the system is defined for all years from the beginning of the analysis until the time horizon. The repetitive calculation from procedure (Monte Carlo simulation) allows computing the mean and standard deviation of the condition state in each year. The mean, $\mu(t)$, and the standard deviation, $\sigma(t)$, of the condition state in each year are computed through Equations 4.6 and 4.7, respectively.

4.5.3 Cost of maintenance actions

For investments over long time periods, it is necessary to take into account the cost of opportunity. If investments are made later, the funds can be invested during this interval, raising a profit. This is taken into account herein by considering a discounted value as money as:

$$c_0 = \frac{c_t}{(1 + v/100)^t} \tag{4.9}$$

where c_t is the cost at time t and v is the annual discount rate (Frangopol et al., 2004).

The output of this procedure, at time horizon, is a cumulative maintenance cost vector. The repetitive calculation from procedure (Monte Carlo simulation) yields the mean and the standard deviation of the cumulative maintenance cost in each year. The mean, $\mu_{cost}(t)$, and the standard deviation, $\sigma_{cost}(t)$, of the cumulative maintenance cost in each year are computed as:

$$\mu_{cost}(t) = \frac{\sum_{i=0}^{n_{MCS}} c_0(t)}{n_{MCS}} \tag{4.10}$$

$$\sigma_{cost}(t) = \sqrt{\frac{\sum_{i=0}^{n_{MCS}} c_0(t)^2}{n_{MCS}} - \mu_{cost}(t)^2} \tag{4.11}$$

4.6 Summary

This chapter describes the development of a probabilistic model based on a Petri net formulation to assess the deterioration of civil engineering infrastructure under no maintenance, preventive and corrective maintenance. This modelling technique is increasingly being used in modelling dynamic systems, but only recently it has been applied to model deterioration in civil engineering assets. The flexibility and capability of the technique have been demonstrated with regard to the requirements and complexity of a civil asset management model. The model is considerably more detailed than others found in the literature.

The uncertainly related with the deterioration process and the effect of the maintenance actions is considered through the use of probability distributions and the Monte Carlo simulation.

Chapter 5

Case Study 1: Application to Bridges

5.1 Introduction

In this chapter, the deterioration and maintenance model based on Petri net formalism described in the previous chapter is applied to two bridge components, pre-stressed concrete decks and bearings. In a first part of this chapter, validation of the Petri net deterioration model is performed. The validation is accomplished taking into account the existing isomorphism between bounded Petri net with exponentially distributed transition rates and a finite Markov process. After that, the Petri net deterioration model is applied to analyse the deterioration process over time, and the maintenance model is applied to analyse the consequences of alternative maintenance strategies to control deterioration patterns in bridge components. The maintenance model described can be considered a full life-cycle model that includes not only the deterioration process, but also inspections and maintenance processes.

The historic data used was procured from a Portuguese highway manager, Ascendi, which is responsible for the management of a road network with, approximately, 1 300 km located in the north and center of the country. The data used are based in major bridge inspection historic information and include the data of inspection and the condition state of the various components constituting the bridge.

5.2 Classification system adapted

The condition state, a variable that quantifies the deterioration level of a structure, in the classification system adapted by Ascendi is a discrete variable and its value varies between 0–5, where zero means that the structure is in an excellent condition state while index five means that the structure demonstrates a poor condition state.

The overall bridge condition is based on the evaluation of the visual condition of each bridge, using a component-based system. It is considered that the individual elements of the asset and the entire asset (Table 5.1) are inspected and rated, individually, from zero to five according to the classification present in Table 5.2. The global condition is obtained by a weighted sum of each contribution (Barros, 2013; Berardinelli et al., 2014). Each condition state of the classification system has the following purpose (GOA, 2008):

- To classify the damages suffered by the component in terms of severity, extension, and cause;

- To assess if the damages compromise the function of the component and to what degree and if it has consequences for other components.

Table 5.1 – List of the bridge components (GOA, 2008; Barros, 2013)

Number	Bridge component
1	Bridge
2	Wing walls
3	Slope
4	Abutments
5	Bearings
6	Pier/column
7	Bridge deck
8	Cornice
9	Railings
10	Safety barrier
11	Sidewalks
12	Pavement
13	Drainage system
14	Expansion joints
15	Other components

Table 5.2 – Condition state classification for bridge components (Barros, 2013; Berardinelli et al., 2014)

Condition State		Description
CS0	Excellent	Fully operational / No damage / No action is needed
CS1	Very good	Operational / Damages with no evolution / No action is needed
CS2	Good	Operational / Damages which can progress / Observation
CS3	Reasonable	Operational / Damages in progress / Long-term actions
CS4	Bad	Operational / Damages which can affect the durability / Short-term actions
CS5	Poor	No operational / Damages which can affect the structural safety / Immediate actions

The use of the condition state index, based on visual inspections only, is often imprecise and subjective. However, the funding available for the inspection, testing, monitoring and safety assessment of the entire bridge stock, is always extremely limited. As a result, in spite of the limitation of assessing the structures based only on visual inspections, this is the only information for the vast majority of existing structures and, consequently, the only source of a representative sample of observations of structural deterioration. Furthermore, the application of a single measure of performance to characterize complex components, like the bridge decks or bearings, is a severe limitation of the bridge classification system currently in use in Portugal, as well as, in most other European and North American countries.

5.3 Historical databases

The database used contain all information regarding major inspection performed over the last decades in a large set of reinforced and pre-stressed concrete bridges located in Portugal. The major inspection is a rigorous and systematic survey of all visible bridge components, carried out periodically (at intervals of 1–6 years) by specialized technicians, in order to create a register that allows monitoring

the development of damages and anomalies in the infrastructures. The major inspections historic records include: data of inspection, condition and maintenance state of each bridge component, as well as global condition and maintenance state of the infrastructure.

To build the databases, all bridge components for which there are two or more observations were considered as initial data. The date of construction was considered as an inspection record, assuming that, at this moment, the bridge component presents an excellent condition state. However, throughout the history of a bridge, it is possible to see an improvement in the condition state from one inspection to the next, associated with a maintenance action or by some error occurred in one of the major inspections. Since this study intends only to analyse the deterioration process without the application of maintenance actions, in these situations the bridge component record is divided from the point that revealed the improvement of the condition state. For example, consider Bridge B with a history of five inspections shown in Table 5.3.

Table 5.3 – Example of a bridge with five inspections

Bridge	Observation date	Condition state
B	2001	3
B	2002	3
B	2006	2
B	2009	3
B	2015	4

As it can be seen, at some point Bridge B is rehabilitated from condition state 3 to condition state 2. So, the procedure is to subdivide the records of Bridge B into two bridges as shown in Table 5.4.

Table 5.4 – Division of Bridge B into two records

Bridge	Observation date	Condition state
B1	2001	3
B1	2002	3
B2	2006	2
B2	2009	3
B2	2015	4

After split of the records, two "bridges", B1 and B2, are considered without improvement of the condition state. In situations where the division of registers gives rise to "bridges" with one observation moment, this is ignored as for the deterioration model it is necessary that each "bridge" has at least two observation moments.

In this work, the deterioration process was only analysed for two bridge components: pre-stressed concrete decks and bearings. Each bridge component is analysed separately. Table 5.5 shows the total number of components and transitions for each bridge component analysed.

Table 5.5 – Number of components and transitions for each bridge element

Component	Number of components	Number of transitions
Pre-stressed concrete decks	362	425
Bearings	301	360

It should be mentioned that the databases are composed by a large set of bridges with similar characteristics, which were all built over a period of less than two decades, according to the same structural

design codes and the same construction techniques, and they are located, approximately, in the same region of the country. Furthermore, the bridges are relatively young, which makes the more advanced deterioration states rare or non-existent.

5.4   Validation of the Petri net deterioration model

The Petri net deterioration model for bridge components is illustrated in Figure 5.1. The Petri net scheme is composed by six places and five transitions, where each place represents one of the six discrete condition states that constitute the classification system adopted for bridge components as defined in Section 5.2. Transitions, which are located between places, have the function of modelling the sojourn time of the component in a given condition state before it moves to the next higher condition state. The sojourn time in each condition state is randomly computed from a probability distribution. In this model, the distributions that best fits the historical data are considered as appropriate.
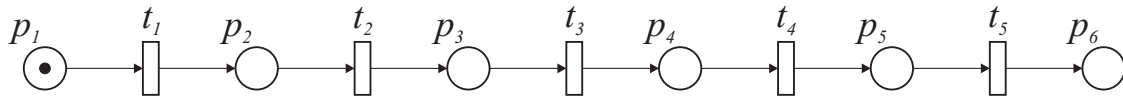
Figure 5.1 – Petri net scheme of the deterioration model for bridge components

Since Markov chains are widely used to evaluate the deterioration process over time and taking into account the isomorphism between Markov chains and stochastic Petri net, in a first phase it is assumed that the deterioration process follows an exponential distribution with parameters $(\lambda_0, \lambda_1, \lambda_2, \lambda_3, \lambda_4)$. The comparison of these results with the results obtained by the Markov chains model allows the validation of the Petri net deterioration proposed, and the evaluation of the efficiency of the numerical procedure and the optimization algorithm described in Section 4.2.1.

The pre-stressed concrete decks and bearings databases, identified above, were used as case studies herein.

5.4.1   Markov chains deterioration model

The optimal transition rates for the Markov chains deterioration model were obtained using the methodology described in Section 2.5.1.2. The estimation of the **Q**-matrix has the purpose of obtaining the q_{ij} coefficients so that a **P**-matrix can be calculated with the maximum possible rigour and for any time interval. The coefficients are estimated from the historical database.

The model adopted for the **Q**-matrix for the deterioration process is presented in Equation 2.20. Based on Equation 2.19, the **P**-matrix can be defined for any time interval between observations. There are essentially two uses for this approach. Firstly, it allows the computation of the likelihood of a set of given observations, independently of the time interval between inspections. This is fundamental to adjust the prediction model to the available data. Secondly, it allows the prediction of performance at a given instant in the future with limited computational cost.

The best deterioration model is that resulting in higher probabilities of occurrence of the observed transitions. The likelihood of occurrence can be defined by Equation 2.21. However, from a numerical point of view, using the logarithm of the likelihood of occurrence is more robust. Therefore, Equation 4.1 is used as a measure of the fit quality.

The optimal **Q**-matrix is computed through an optimization problem that maximizes the logarithm of the likelihood. In this study, the optimization of the parameters was performed using genetic

algorithm available in software MalLab® (MatLab, 2017). The analytical formulation of the problem is given by:

Find: The parameters of the **Q**-matrix

So that: $\log L = (\sum \sum \log p_{ij})$ is maximized

The parameters used in the GA are the following:

- Size of the population: 50 individuals;

- Stopping criteria: the algorithm stops if the average relative change in the best fitness function value over 50 generations is less than or equal to 10^{-6};

- Mutation procedure was performed using the Gaussian algorithm implemented in MalLab®;

- Crossover procedure was performed using the Scattered algorithm implemented in MalLab®.

Table 5.6 shows the optimal transition rates for both bridge components, as well as, the log-likelihood computed for each set of optimal parameters.

Table 5.6 – Optimal parameters of the Markov chains deterioration model

Bridge component	Optimal parameters					$-\log L$
	λ_0	λ_1	λ_2	λ_3	λ_4	
Pre-stressed concrete decks	0.2241	0.0563	0.0574	0.0035	0.2987	394.3773
Bearings	0.2520	0.0614	0.0536	0.0535	0.0008	313.1235

In order to assess the quality of fit of the Markov chains, the approach described by Aguirre-Hernández and Farewell (2002) was adapted. According to Aguirre-Hernández and Farewell (2002), the goodness-of-fit test is suitable to assess the quality of fitting because this test statistic is appropriate for data in which the spacing between the responses and the total number of observations vary from one individual to another.

The goodness-of-fit test, T, measures the discrepancy between the observed number of transitions of each time, O_i, and the expected number of transitions according to the statistic model, E_i, as (Aguirre-Hernández and Farewell, 2002):

$$T = \sum_{i=1}^{C} \frac{(O_i - E_i)^2}{E_i} \qquad (5.1)$$

where C represents the total number of different transitions. The deterioration process is considered as sequential, i.e. only transitions from a condition i to a condition j, with $i \leq j$ are possible. For a countable state space s, C is given by:

$$C = \frac{s(s+1)}{2} - 1 \qquad (5.2)$$

The transition corresponding to the absorbent state, $s \rightarrow s$, is ignored.

It is considered, as null hypothesis, that the deterioration model based on continuous time Markov chains describe properly the inspections data. It is reasonable to assume that the distribution of the goodness-of-fit follows a χ^2_{df} distribution, with $df = C - 1 - p$ degrees of freedom, where p is the number of estimated parameters (Aguirre-Hernández and Farewell, 2002). The rejection or no rejection of the null hypothesis is determined by the comparison between the observed goodness-of-fit test and the $\chi^2_{df:\alpha}$ distribution, where α is the significance level.

Table 5.7 presents the predicted and observed values from both bridge components analysed. From these results it is possible to determine the value of goodness-of-fit test, T, through Equation 5.1, while Table 5.8 presents the results of goodness-of-fit test, T, for both bridge components.

Table 5.7 – Observed and predicted values from both bridge components analysed

Transition type	Pre-stressed concrete decks		Bearings	
	Observed values	Predicted values	Observed values	Predicted values
$0 \to 0$	61	79.7	74	78.1
$0 \to 1$	138	117.7	128	121.9
$0 \to 2$	40	35.4	37	40.5
$0 \to 3$	6	12.0	11	10.1
$0 \to 4$	0	8.8×10^{-2}	3	2.5
$0 \to 5$	0	1.1×10^{-1}	0	7.9×10^{-3}
$1 \to 1$	119	122.7	53	56.5
$1 \to 2$	22	18.7	14	9.7
$1 \to 3$	2	1.6	0	7.6×10^{-1}
$1 \to 4$	0	4.7×10^{-3}	0	4.2×10^{-2}
$1 \to 5$	0	1.1×10^{-3}	0	2.6×10^{-5}
$2 \to 2$	26	27.2	34	30.3
$2 \to 3$	5	3.8	1	4.3
$2 \to 4$	0	1.4×10^{-2}	0	3.5×10^{-1}
$2 \to 5$	0	4.3×10^{-3}	0	2.8×10^{-4}
$3 \to 3$	6	6.0	5	4.5
$3 \to 4$	0	2.8×10^{-2}	0	4.7×10^{-1}
$3 \to 5$	0	1.2×10^{-2}	0	4.5×10^{-4}
$4 \to 4$	0	0	0	0
$4 \to 5$	0	0	0	0

Table 5.8 – Results of goodness-of-fit test, T

Bridge component	T
Pre-stressed concrete decks	12.97
Bearings	7.74

The null hypothesis is rejected with a significance level of 5 % if:

$$T > \chi^2_{df:\alpha} = \chi^2_{20-1-5:0.05} = 23.69 \tag{5.3}$$

Comparing the values of goodness-of-fit test in Table 5.8 to the value of $\chi^2_{df:\alpha}$ distribution, it is possible to verify that the goodness-of-fit test, T, of the two elements are smaller than the $\chi^2_{df:\alpha}$ distribution value. This mean that the null hypothesis is not rejected and there is an adequacy between the sample and the model. In other words, the model describes adequately the original data for the pre-stressed concrete decks and bearings.

5.4.2   Pre-stressed concrete decks

The optimal transition rates obtained for both deterioration models, Markov chains and stochastic Petri nets, through the historical data of pre-stressed concrete decks, as well as, the log-likelihood

computed for each set of optimal parameters, are shown in Table 5.9. By comparing the results, it can be observed that the values of the parameters obtained for both models are very similar. The main difference is obtained for λ_4. This difference results the reduce size of the sample. The differences observed in the other parameters are due to sampling errors associated with Monte Carlo simulation. In the Petri net deterioration model, the Monte Carlo simulation is used to compute the probability of occurrence of the observed transition, p_{ij}, while in the Markov chain model the probability of occurrence have an analytical solution (Equation 2.19). In this study, 50 000 Monte Carlo samples were used.

Table 5.9 – Comparison of the optimal parameters of the Markov chains and Petri nets models – Pre-stressed concrete decks

Model	Optimal parameters					$-\log L$
	λ_0	λ_1	λ_2	λ_3	λ_4	
Markov chains	0.2241	0.0563	0.0574	0.0035	0.2987	394.3773
Petri nets	0.2242	0.0543	0.0644	0.0033	1.0321	392.3649
Error [%]	0.04	3.55	12.20	5.71	245.53	0.51

From the transitions rates obtained for these two models, it is possible to determine the mean sojourn time in each condition state, T_j, by:

$$T_j = \frac{1}{\lambda_j} \tag{5.4}$$

The results obtained are shown in Figure 5.2. It is possible to verify that the sojourn times in each condition state are similar in both models. The main differences are observed for condition state 3 and 4. However, it must be kept in mind that the bridges are relatively young and advanced deterioration states are unusual. Consequently, the calibration procedure is less accurate.
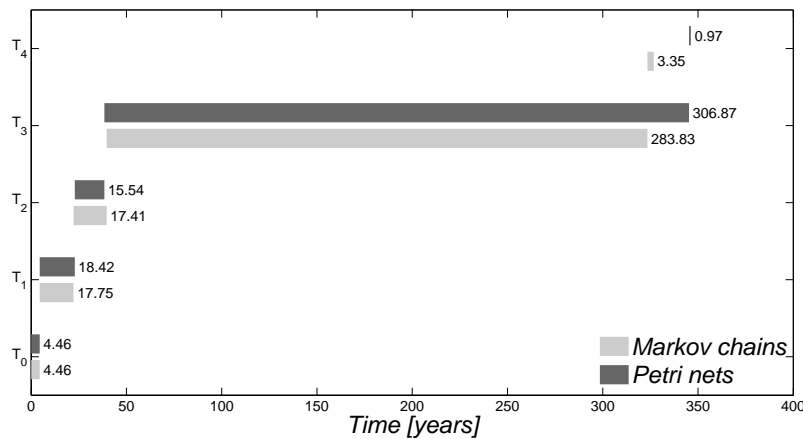
Figure 5.2 – Comparison of the mean sojourn times for both methodologies in each condition state – Pre-stressed concrete decks

Table 5.10 shows the number of observed and predicted pre-stressed concrete deck elements in each condition state, as well as the relative error obtained for each model used between the observed and predicted data, and the relative error between the predicted data by Markov chains model and by Petri nets model.

For the first group of results (columns 5 and 6 of Table 5.10), it can be observed that both models are relatively well suited to model the deterioration process. Both models present errors greater than

Table 5.10 – Number of observed and predicted bridge components in each degradation condition and the relative error obtained for both models – Pre-stressed concrete decks

Condition state	Observed	Predicted		Relative error		
		MC	**PN**	**MC [%]**	**PN [%]**	**MC / PN**
CS0	61	79.65	79.63	30.6	30.5	1.00
CS1	257	240.35	242.39	6.5	5.7	0.99
CS2	88	81.31	78.01	7.6	11.3	1.04
CS3	19	23.42	24.71	23.3	30.0	0.95
CS4	0	0.13	0.06	–	–	2.23
CS5	0	0.13	0.20	–	–	0.66

20% for CS0 and CS3, but the relative error for the intermediate condition states is less than 8% for Markov chains and less than 12% for Petri nets. For CS4 and CS5, the relative error was not calculated because there are no observed elements in these two condition states. With the second group of results (column 7 of Table 5.10), it is intended to compare the results predicted by the two deterioration models. These results reinforce the previous conclusions, that the results obtained by the two models are quite similar.

Finally, Figure 5.3 compares the predicted condition profile of pre-stressed concrete decks over time using the Markov chains model and the Petri nets model. In this analysis, a 150-year time horizon was considered and it was assumed that the pre-stressed concrete deck begins with a perfect condition (Condition State 0). Throughout the entire simulation period, a good agreement is observed between the two curves, that are practically overlapping (Figure 5.3(a)). In terms of dispersion of the results (Figure 5.3(b)), from the year 25, the values of the standard deviation vary, approximately, between 0.8 and 1.

5.4.3   Bearings

For bearings, the optimal transition rates as well as the log-likelihood computed for each set of optimal parameters, for both deterioration models, from the historical data are present in Table 5.11. Similarly to previous bridge component, the values of the parameters obtained for models are quite similar. There are little differences that are associated with sampling errors of the Monte Carlo simulation. In this study, 50 000 Monte Carlo samples were used.

Table 5.11 – Comparison of the optimal parameters of the Markov chains and Petri nets models – Bearings

Model	Optimal parameters					$-\log L$
	λ_0	λ_1	λ_2	λ_3	λ_4	
Markov chains	0.2520	0.0614	0.0536	0.0535	0.0008	313.1235
Petri nets	0.2603	0.0572	0.0488	0.0601	0.0008	310.7728
Error [%]	3.29	6.48	8.96	12.34	0.00	0.75

Figure 5.4 presents the mean sojourn times in each condition state for both models. The mean sojourn times are computed through Equation 5.4. The plotted results show that the sojourn times in each condition state have the same magnitude. As before, the values obtained for the CS4 are not representative, as they are computed based on a very small sample.

Table 5.12 shows the number of observed and predicted bearings elements in each condition state, relative error obtained for each model, and the relative error between the predicted data by Markov
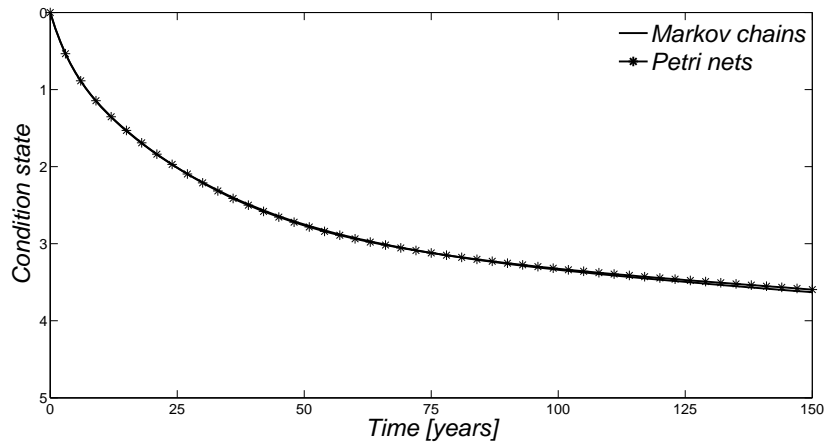
(a) Mean condition
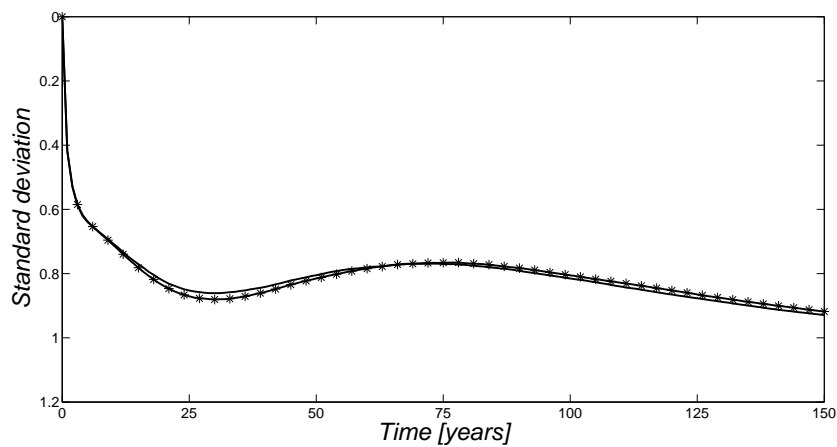
(b) Standard deviation of condition

Figure 5.3 – Comparison of the predicted future condition profile over time for both models – Pre-stressed concrete decks
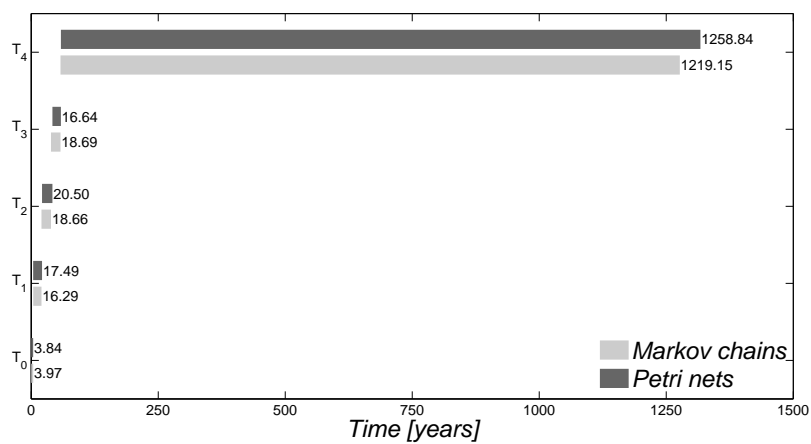
Figure 5.4 – Comparison of the mean sojourn times for both methodologies in each condition state – Bearings

chains and Petri nets models. In Figure 5.5, the predicted condition profile of bearings over time using

the Markov chains model and the Petri nets model are compared. From these results, it is possible to observe a good agreement between the two deterioration models. Furthermore, both models are well suited to model the deterioration process, as both present relative errors smaller than 16%.

Table 5.12 – Number of observed and predicted bridge components in each degradation condition and the relative error obtained for both models – Bearings

Condition state	Observed	Predicted		Relative error		
		MC	**PN**	**MC [%]**	**PN [%]**	**MC / PN**
CS0	74	78.12	76.20	5.6	3.0	1.03
CS1	181	178.30	183.06	1.5	1.1	0.97
CS2	85	80.54	79.61	5.2	6.3	1.01
CS3	17	19.67	17.77	15.7	4.5	1.11
CS4	3	3.35	3.36	11.8	11.9	1.00
CS5	0	0.01	0.01	–	–	1.06
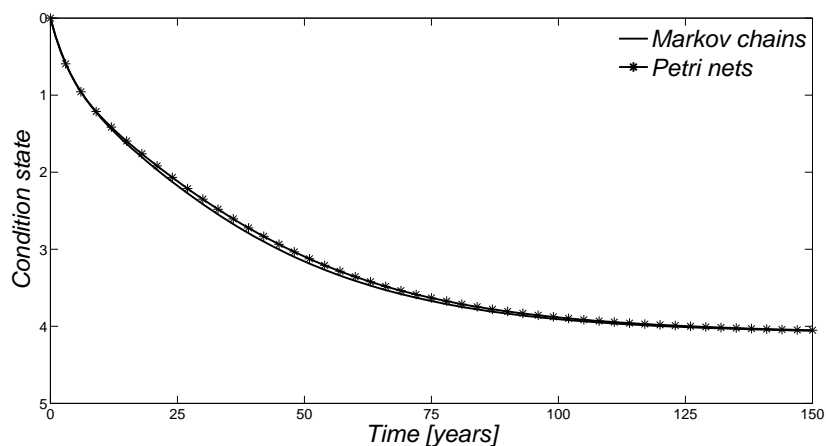
(a) Mean condition
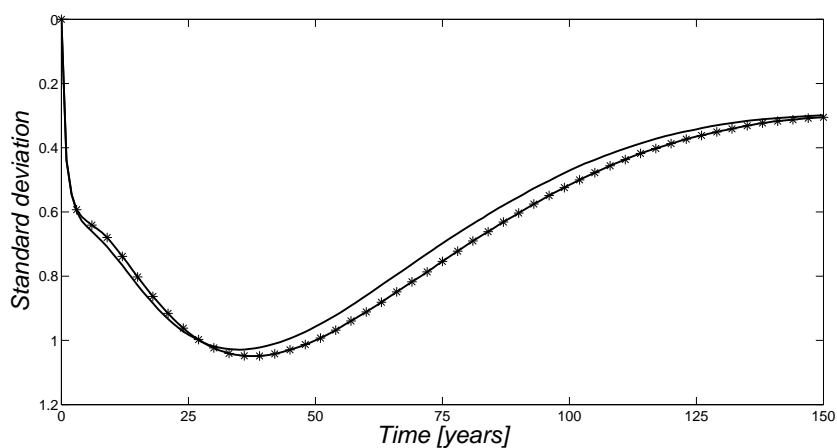
(b) Standard deviation of condition

Figure 5.5 – Comparison of the predicted future condition profile over time for both models – Bearings

5.5 Probabilistic analysis

In Petri net deterioration model, in addition to the Exponential distribution, four two-parameters distributions were studied: Weibull, Gumbel, Normal, and Lognormal. The expression for each probability density function is presented in Table 5.13.

Table 5.13 – Probability density function

Distribution	Probability density function	Parameters
Exponential	$f(t\|\lambda) = \lambda e^{-\lambda t}$	$\lambda > 0$ – scale parameter
Weibull	$f(t\|\alpha, \beta) = \frac{\beta}{\alpha} \left(\frac{t}{\alpha}\right)^{\beta-1} e^{-\left(\frac{t}{\alpha}\right)^{\beta}}$	$\alpha > 0$ – scale parameter $\beta > 0$ – shape parameter
Gumbel	$f(t\|\alpha, \beta) = \frac{1}{\beta} e^{\left(-\frac{t-\alpha}{\beta}\right)} e^{-e^{\left(-\frac{t-\alpha}{\beta}\right)}}$	$\alpha \in \mathbb{R}$ – location parameter $\beta > 0$ – scale parameter
Normal	$f(t\|\alpha, \beta) = \frac{1}{\beta\sqrt{2\pi}} e^{\frac{-(t-\alpha)^2}{2\beta^2}}$	$\alpha \in \mathbb{R}$ – location parameter $\beta > 0$ – scale parameter
Lognormal	$f(t\|\alpha, \beta) = \frac{1}{t\beta\sqrt{2\pi}} e^{\frac{-(\ln t - \alpha)^2}{2\beta^2}}$	$\alpha \in \mathbb{R}$ – location parameter $\beta > 0$ – scale parameter

A Normal distribution was used since it is usually adequate to model the average of several independent random variables. If the deterioration in the bridge component is seen as a set of areas, deteriorating independently, then the average condition can be modelled as a normal distribution. However, a significant drawback of the normal distribution is the non-null probability of negative values, which in the present context, is not physically possible. Alternatively, the Lognormal distribution can be used to model the transition times, avoiding negative values. If, on the other hand, the condition is mostly characterized by the deterioration of the most critical areas of the bridge component, extreme distributions like the Weibull and Gumbel might be more adequate.

In this study, the condition, standard deviation and probabilistic distribution profiles are computed using the Monte Carlo simulation with 50 000 samples.

5.5.1 Pre-stressed concrete decks

Table 5.14 shows the optimal parameters obtained for all probability distribution analysed in terms of mean and standard deviation of time in each condition state, as well as, the log-likelihood computed for each set of optimal parameters. Table 5.15 shows the number of observed and predicted pre-stressed concrete decks in each condition state for each probability distribution, as well as, the relative error obtained for each case. The light and dark gray cells indicate the distributions with smaller and larger relative errors, respectively, for each condition state.

From the results shown in Tables 5.14 and 5.15, two main conclusions can be drawn. The first one is that distributions with null probability of negative values, as Exponential, Weibull and Lognormal distributions, show better log-likelihood values than distributions with non-null probability of negative values, as Gumbel and Normal distributions. These results are in agreement with the literature, since these three distributions (Exponential, Weibull and Lognormal) are the most commonly used in reliability and survival analysis (Sánchez-Silva and Klutke, 2016).

The second conclusion is that two-parameter distributions (Weibull and Lognormal) have a better fit to the historical data than the Exponential distribution (Table 5.14). The good agreement between these two distributions and the historical data is also visible when the number of observed and predicted

Table 5.14 – Optimal parameters obtained for all probability distribution analysed in terms of mean and standard deviation of time in each condition state – Pre-stressed concrete decks

Parameters		Exponential	Weibull	Gumbel	Normal	Lognormal
Mean	t_1	4.46	7.32	4.36	5.39	9.53
(years)	t_2	18.42	27.66	15.13	12.41	142.45
	t_3	15.54	18.26	10.35	7.89	141.47
	t_4	306.87	10.61	9.63	8.57	57.24
	t_5	0.97	3.48	9.24	4.87	27.36
Standard	t_1	4.46	19.61	3.83	0.89	68.44
deviation	t_2	18.42	36.60	12.94	5.54	1036.05
	t_3	15.54	21.19	8.39	4.37	1012.01
	t_4	306.87	1.57	3.71	3.25	14.40
	t_5	0.97	0.58	7.27	2.46	99.76
$-\log L$		392.3649	361.5791	407.1832	425.3420	363.1665

Table 5.15 – Number of observed and predicted pre-stressed concrete decks in each condition state for each probability distribution and relative error [%] obtained for each probability distribution – Pre-stressed concrete decks

Probability distribution		CS0	CS1	CS2	CS3	CS4	CS5
Observed		61	257	88	19	0	0
Predicted	Exponential	79.63	242.39	78.01	24.71	0.06	0.20
	Weibull	66.64	244.57	83.93	27.78	1.26	0.81
	Gumbel	81.91	216.87	81.16	35.54	6.36	3.16
	Normal	98.49	228.43	70.84	25.15	1.39	0.71
	Lognormal	63.03	254.45	83.42	24.09	0.00	0.00
Relative	Exponential	30.5	5.7	11.3	30.0	–	–
error [%]	Weibull	9.3	4.8	4.6	46.2	–	–
	Gumbel	34.3	15.6	7.8	87.0	–	–
	Normal	61.5	11.1	19.5	32.4	–	–
	Lognormal	3.3	1.0	5.2	26.8	–	–

pre-stressed concrete decks in each state are compared (Table 5.15). These two distributions are those with the smallest relative errors for all condition states. The relative error for CS0, CS1 and CS2 for most situations is less than 5%. The condition state 3 is the one that presents the largest relative errors, approximately, 27% for Lognormal distribution and 46% for Weibull distribution. The relative error for the most advanced condition states was not computed, since these two condition states are not represented in the database used. However, if the mean relative error for all condition states is analysed, Lognormal distribution is the one that has lower mean relative error (9.1%, Table 5.15). But, on the other hand, Weibull distribution is the one that has lower log-likelihood value ($-\log L = 361.5791$, Table 5.14).

Figure 5.6(a) shows the mean condition profile over time for all probability distributions analysed. The profiles obtained for the five distributions can be divided into three groups. The first group contains only the Exponential distribution, as the profile obtained using this distribution is quite different from the other four profiles, associated a simple parabolic shape without inflection points. The second group is constituted by Weibull, Gumbel and Normal distributions. The profiles obtained by these three distributions present very similar characteristics throughout the time horizon analysed, although they show some differences in the scale. In these three profiles, even if slight, it is possible to observe changes in the concavity when there is transition of condition state. Finally, the third group is formed

by Lognormal distribution. In the profile obtained by this distribution it is also possible to see con-cavity changes when there is transition of condition state, however the profile is quite different from the profiles obtained by distributions of the group 2. Finally, it should also be noted that differences in probability distributions can be explained by the fact that only real data exists for a small time interval (approximately, between year 0 and 25).

In terms of dispersion of results, Figure 5.6(b), distributions from the second group show higher dispersion values in the interval between year 25 and 50. However, from this point the dispersion values begin to decrease, obtaining values very close to zero for the Gumbel and Normal distribution. For the Exponential distribution, from year 25 the dispersion values remain, sensitively, constant until the end of the time horizon. Finally, for the Lognormal distribution, during the analysed time period, shows a growth of standard deviation. Moreover, should it be mentioned that in the database only data for the period of 25-30 years exists and, consequently, the results are very influenced by the higher deterioration states.
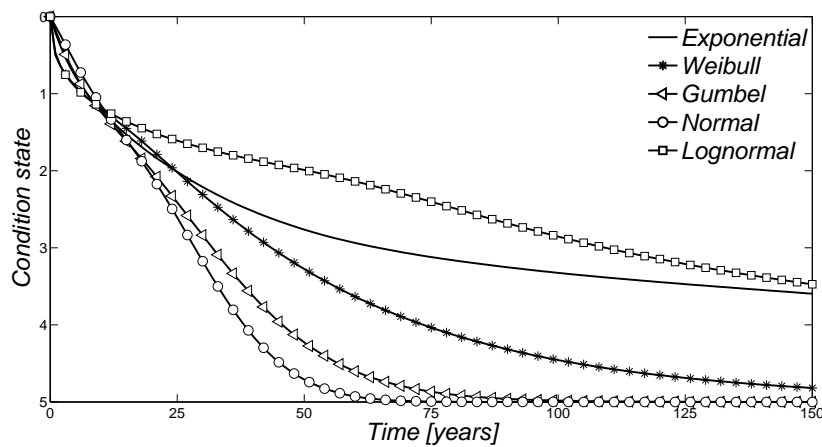
(a) Mean condition
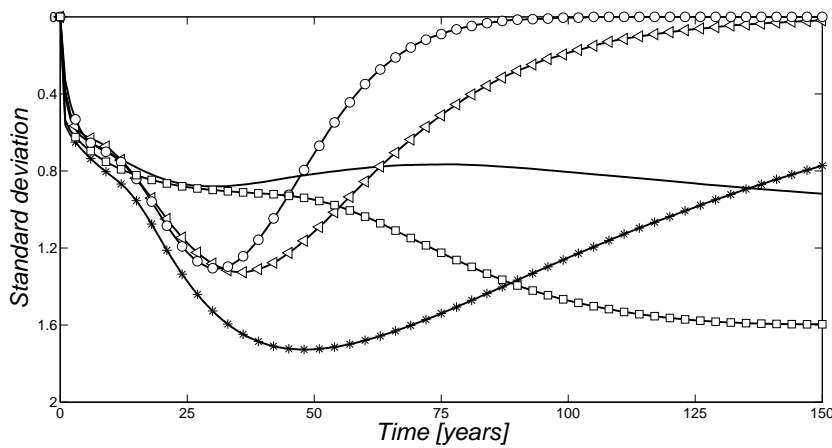
(b) Standard deviation of condition

Figure 5.6 – Comparison of the predicted future condition profile over time for all probability distri-bution analysed – Pre-stressed concrete decks

Figure 5.7 compares the probabilistic distribution of all distributions over time for each condition state. For CS0 (Figure 5.7(a)), CS1 (Figure 5.7(b)) and CS2 (Figure 5.7(c)), the behaviour of the predicted probabilities profile for all distributions is quite similar. There are some differences in terms of scale, but the profiles of the five distribution have the same shape. For example, for CS0 (Figure

5.7(a)), the predicted probabilities for all distributions begins with probability equal to 1 and decreases over time and at year 25 the probability of a pre-stressed concrete deck being at CS0 is near zero for Exponential, Gumbel and Normal distributions while for Weibull and Lognormal distributions there is, approximately, a probability of 10%. Furthermore, it can be observed that between years 1 and 5 the probability of belonging to either CS0 or CS1 is very similar, for all distributions. For CS1 (Figure 5.7(b)), the maximum probability for all distributions occurs between years 5 and 11, and the maximum probability value obtained for all distributions has the same order of magnitude. The major differences are that Weibull and Lognormal distribution shows a bigger right-tail. The same observations can be made with respect to Figure 5.7(c).

For CS3 (Figure 5.7(d)), CS4 (Figure 5.7(e)) and CS5 (Figure 5.7(f)), it is possible to observe significant differences between the distributions analysed. The differences observed for CS3 occur mainly as there are few samples in the database for this condition state. The results for CS4 and 5 will not be discussed because there are not samples to evaluate the results.

(a) Condition State 0

(b) Condition State 1

(c) Condition State 2

(d) Condition State 3

(e) Condition State 4
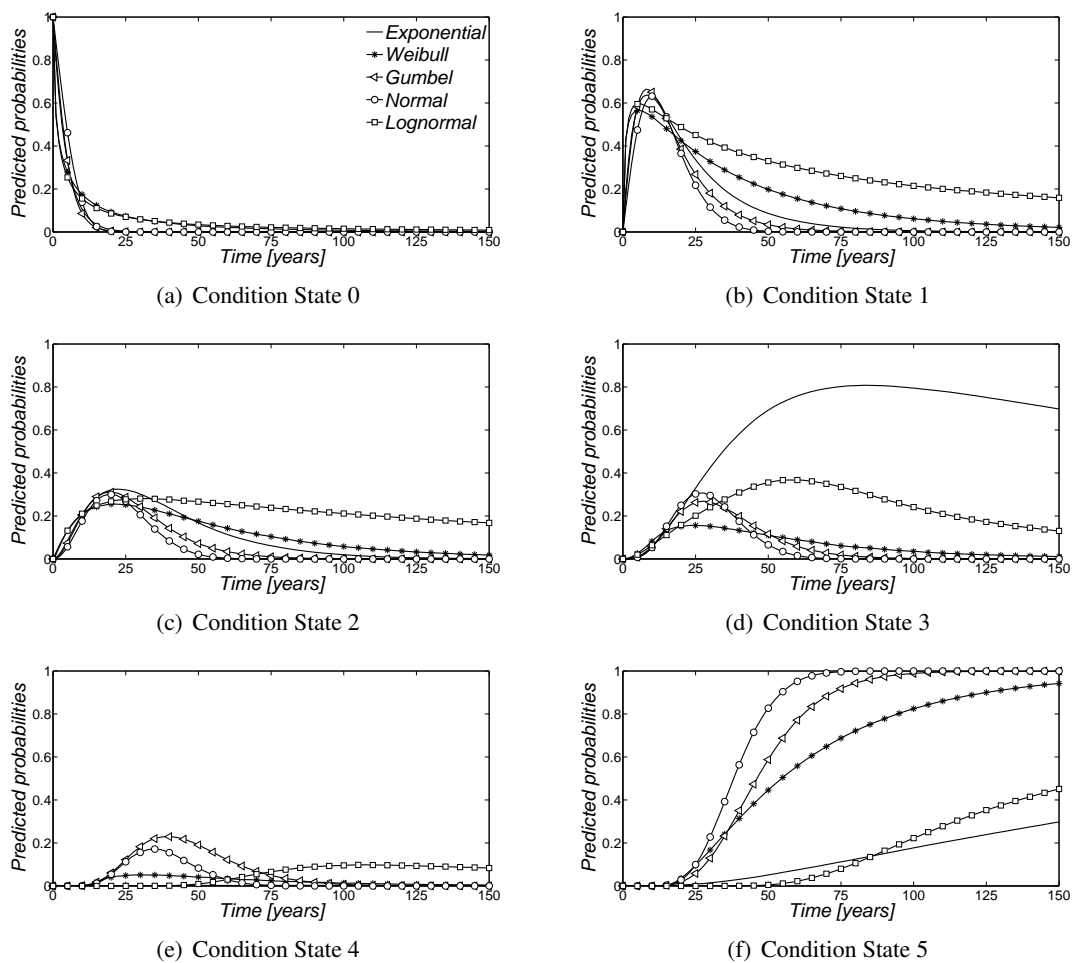
(f) Condition State 5

Figure 5.7 – Comparison of the probabilistic distribution for each condition state over time – Pre-stressed concrete decks

From Figures 5.6 and 5.7 can be seen that the results obtained from the five probabilistic distributions are widely dispersed. It Gumbel and Normal distributions not describe adequately the deterioration process. According to these results, the decks reach CS5 approximately at year 50. Eurocode 0 (CEN, 2002) indicates that bridges should have a project lifetime of 100 years, period during which it is expected that a structure or part thereof may be used for its intended purpose, with expected maintenance, but without need for major repairs. According to the classification used (Table 5.2), when the deck reaches CS5 it means that the damage can affect structural safety and that the bridge

is not operational. Furthermore, Exponential and Lognormal distributions also do not describe adequately the deterioration process. According to these distribution the lifetime of the deck is over 150 years. Finally, for pre-stressed concrete decks, the Weibull distribution is the one that shows a minor log-likelihood value and, consequently, a better fit to the historical data (the deck reaches CS5 approximately at year 104). For this reason, this distribution will be used to sample the transitions times that specify the movement between different condition states of the decks.

5.5.2 Bearings

For bearings, Table 5.16 shows the optimal parameters obtained for all probability distribution analysed in terms of mean and standard deviation of time in each condition state, as well as, the log-likelihood computed for each set of optimal parameters. Table 5.17 compares the number of observed and predicted bearings in each condition state for each probability distribution, as well as, the relative error obtained for each case. The light and dark gray cells indicate the distributions with smaller and largest relative errors, respectively, for each condition state.

Table 5.16 – Optimal parameters obtained for all probability distribution analysed in terms of mean and standard deviation of time in each condition state – Bearings

Parameters		Exponential	Weibull	Gumbel	Normal	Lognormal
Mean	t_1	3.84	4.26	4.13	4.83	4.75
(years)	t_2	17.49	17.88	13.26	12.14	118.91
	t_3	20.50	9.77	10.78	11.04	47.62
	t_4	16.64	7.12	6.30	6.98	8.07
	t_5	1258.84	7.50	6.21	7.51	388.93
Standard	t_1	3.84	4.70	3.60	1.00	9.17
deviation	t_2	17.49	21.87	10.79	5.69	865.13
	t_3	20.50	5.78	6.79	6.47	143.43
	t_4	16.64	1.96	0.85	3.57	0.61
	t_5	1258.84	1.39	0.60	3.05	532.49
$-\log L$		310.7728	306.9696	315.2972	323.9939	307.3837

Table 5.17 – Number of observed and predicted bearings in each condition state for each probability distribution and relative error [%] obtained for each probability distribution – Bearings

Probability distribution		CS0	CS1	CS2	CS3	CS4	CS5
Observed		74	181	85	17	3	0
Predicted	Exponential	76.20	183.06	79.61	17.77	3.36	0.01
	Weibull	79.66	167.60	87.45	21.71	3.20	0.39
	Gumbel	84.36	176.14	79.99	17.07	2.10	0.34
	Normal	96.90	168.57	74.26	18.09	1.97	0.21
	Lognormal	73.62	183.63	80.37	20.25	2.14	0.00
Relative	Exponential	3.0	1.1	6.3	4.5	11.9	–
error [%]	Weibull	7.7	7.4	2.9	27.7	6.7	–
	Gumbel	14.0	2.7	5.9	0.4	30.0	–
	Normal	30.9	6.9	12.6	6.4	34.2	–
	Lognormal	0.5	1.5	5.5	19.1	28.7	–

Similarly to the previous bridge component, it is important to stress that distributions with null probability of negative values, as Exponential, Weibull and Lognormal distributions, show better log-likelihood values than Gumbel and Normal distributions and two-parameter distributions (Weibull

and Lognormal) have a better fit to historical data than the Exponential distribution (Table 5.16). However, when the numbers of observed and predicted bearings in each condition state are compared (Table 5.17), a similar mean relative error for all distributions is obtained. For most situations, the relative error is less than 10%. The CS4 is the one that presents the largest relative errors, approximately, 30 − 35% for Gumbel, Normal and Lognormal distributions. For this bridge component, if the mean relative error for all condition states are analysed, Exponential distribution is the one that has lower mean relative error (5.4%, Table 5.17), but Weibull distribution is the one that has lower log-likelihood value ($-\log L = 306.9696$, Table 5.16). It should be referred that the relative error for CS5 was not computed, since this condition state is not represented in the database.

Figure 5.8(a) presents the mean future condition profile over time considering all probability distributions analysed. As described for the pre-stressed concrete decks, the profiles obtained can be divided into three groups: Group 1 - Exponential distribution; Group 2 - Weibull, Gumbel and Normal distribution; and Group 3 - Lognormal distribution. For this bridge component, the profiles obtained by Exponential and Lognormal distribution show more similarities than in pre-stressed concrete decks. However, the shape of these profiles continues to be quite different from the profiles obtained through the Weibull, Gumbel and Normal distribution. These differences in probability distributions can be explained by the fact that only real data exists for a small time interval (approximately, between year 0 and 25).

In terms of dispersion of results (Figure 5.8(b)), the Exponential, Weibull, Gumbel and Normal distributions show higher dispersion values between years 25 and 50. From this point, dispersion values begin decreasing, approaching zero for the Gumbel and Normal distributions. For the Lognormal distribution, dispersion values grow until year 50. However, from this point the dispersion values remain, sensitively, constant until the end of the time horizon. As for pre-stressed concrete decks, the results for higher condition states are very influenced by the small size of dataset for these condition states.

In Figure 5.9 the probabilistic distribution of the five distributions are compared for each condition state. For CS0 (Figure 5.9(a)), CS1 (Figure 5.9(b)), CS2 (Figure 5.9(c)) and CS3 (Figure 5.9(d)), the predicted probabilities profile for all distributions are similar. The profiles of all distributions have the same shape, although they show some differences in terms of scale. For CS4 (Figure 5.9(e)) and CS5 (Figure 5.9(f)) it is possible to observe major differences between the predicted probabilities profiles. These differences can be explained by the fact that there are few components in the database for the most advanced condition states (there is no data for CS5 and the number of elements in CS4 is very reduced), making data fitting very difficult.

As referred before, bridges are often designed for long service life, approximately 100 years (CEN, 2002). Structural bearings are an integral part of the bridge and must guarantee a service life compatible with that of the remaining components. However, in most cases, the service life of bearings is lower than that of the bridge in which they are installed. As a consequence, during the service life of a bridge, it is necessary to carry out several maintenance, repair or replacement operations involving support bearings (Freire et al., 2013, 2014). According to the classification used (Table 5.2), when the bearings reaches CS5 it means that the anomalies affect the integrity of the bearing and jeopardises the safety of the structure, as well as, its in-service capacity, eventually needing traffic conditioning measures; it calls for a an immediate or very fast repair or replacement (Freire et al., 2014). From Figures 5.8 and 5.9, for Gumbel, Normal and Weibull distributions, the results show, respectively, that after 48, 49 and 60 years, the bearings has, on average, reached a condition state of 5, which implies the extensive repair or replacement of the bearings. On the other hand, it is also possible to verify that Exponential and Lognormal distributions do not describe adequately the deterioration process, since according to these distributions the service live of the bearings is over 150 years. From these results, the Weibull distribution will be used to sample the transitions times that specify the movement between different condition states of the bearings, because it is the one that shows a minor

(a) Mean condition

(b) Standard deviation of condition
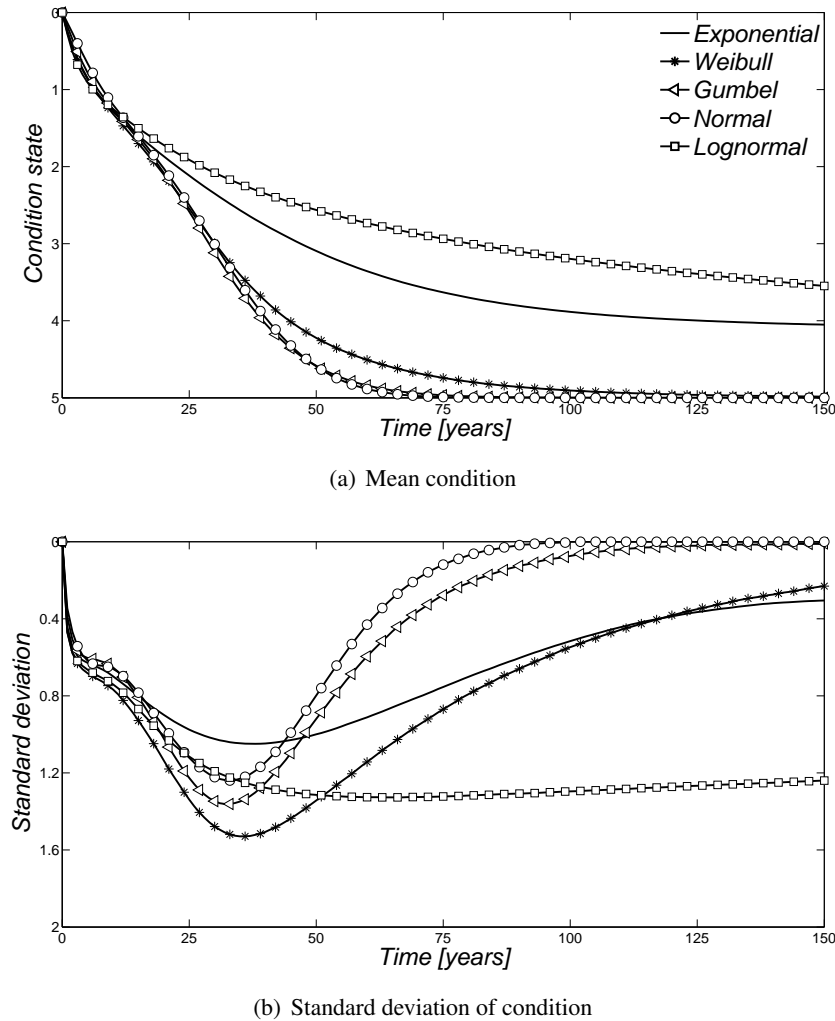
Figure 5.8 – Comparison of the predicted future condition profile over time for all probability distribution analysed – Bearings

log-likelihood value and a good fit to the historical data.

5.6 Maintenance model

The maintenance model proposed in Chapter 4 was applied to analyse the consequences of alternative maintenance strategies to control the effects of deterioration on bridges components. The Petri net maintenance model for bridges components is illustrated in Figure 5.10. The Petri net is composed of 44 places and 54 transitions. The meaning of each place and transition present in the maintenance model has been defined in Chapter 4.

Bridges are designed for long periods of service life. However, as bridges age and volumes of traffic increase, bridges' maintenance has become a significant challenge for the owners that are charged with managing this ageing resource. So, in order to keep them in a safe and serviceable condition, several maintenance activities during their lifetime are required. It is, however, necessary to develop a maintenance model to help decision-making to planning, scheduling and monitoring maintenance activities in a bridge network (O'Connor et al., 2011).

With this aim in mind, a set of applicable maintenance actions throughout the lifetime of pre-stressed

(a) Condition State 0

(b) Condition State 1

(c) Condition State 2

(d) Condition State 3

(e) Condition State 4
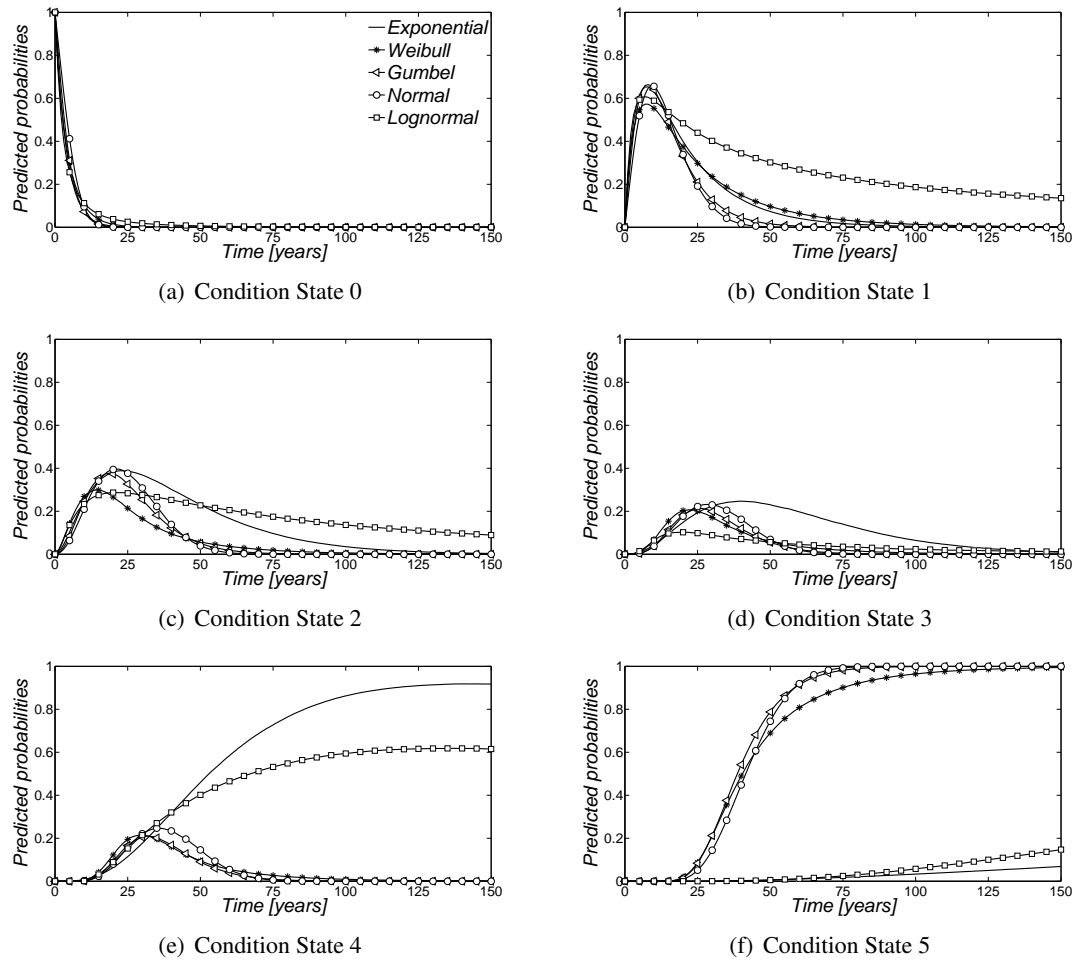
(f) Condition State 5

Figure 5.9 – Comparison of the probabilistic distribution for each condition state over time – Bearings

concrete decks and bearings was compiled. The characterization of the effects of maintenance actions were performed through interviews with the technical staff of Ascendi, a manager of highways in Portugal. However, considering the short life of the bridge stock under analysis (25-30 years), the experience in terms of application of maintenance is limited. In this way, the technical staff express their level of confidence regarding the effects of maintenance actions through a triangular distribution, namely the lower limit, upper limit and mode. Tables 5.18 and 5.19 show, respectively, the effectiveness of the impact of the main maintenance actions for pre-stressed concrete decks and bearings resulting from the experts' beliefs.

For pre-stressed concrete decks, a set of eight main maintenance activities was defined by Ascendi technical staff (Guimarães and Matos, 2015):

- Deck washing is a preventive maintenance that suppresses the deterioration process for a period of time of 1 to 2 years. This maintenance contributes to an effective removal of debris and contaminants, preventing the deterioration of concrete elements;

- Spot painting of concrete elements is a preventive maintenance that reduces the deterioration rate by 40% during a period of time of 4 to 8 years. Spot painting consists of applying a penetrating sealer or a protective coating in concrete elements. By maintaining their waterproofing integrity, it prevents the ingress of water and chlorides into the concrete;

- Complete painting of concrete elements is a corrective maintenance that consists in the application of penetrating sealer or a protective coating to underdeck girders. This maintenance

Table 5.18 – Maintenance activities – Pre-stressed concrete decks

Description	Type	Cost [€/m²]	Application zone	Suppression t_d [years]			Improvement γ[CS]			Reduction t_r [years]			Reduction δ [%]		
				Min	Mod	Max	Min	Mod	Max	Min	Mod	Max	Min	Mod	Max
D1. Deck washing	PM	3	CS1 – CS2	1	1.5	2	–	–	–	–	–	–	–	–	–
D2. Spot painting of concrete elements	PM	54	CS1 – CS2	–	–	–	–	–	–	4	6	8	30	40	50
D3. Complete painting of concrete elements	CM	50	CS3 – CS5	4	5	8	2	1	1	10	12	15	50	70	80
D4. Patching minor spalling concrete	PM	200	CS1 – CS2	1.5	2	3	–	–	–	–	–	–	–	–	–
D5. Partial or full-depth concrete repair	CM	958	CS3 – CS5	–	–	–	2	1	1	–	–	–	–	–	–
D6. Sealing construction joints	PM	30	CS3 – CS5	–	–	–	–	–	–	1	3	5	75	80	90
D7. Crack sealing by injection resin based on epoxy	CM	126	CS3 – CS5	–	–	–	–	–	–	0.5	1.5	3	75	90	100
D8. Replacing overlay with water-proofing	CM	28	CS4 – CS5	1	1.5	2	–	–	–	2	3	4	75	90	100

Table 5.19 – Maintenance activities – Bearings

Description	Type	Cost [€/unit]	Application zone	Suppression t_d [years]			Improvement γ[CS]			Reduction t_r [years]			Reduction δ [%]		
				Min	Mod	Max	Min	Mod	Max	Min	Mod	Max	Min	Mod	Max
B1. Cleaning operations	PM	3	CS1 – CS2	0.5	1	2	–	–	–	–	–	–	–	–	–
B2. Maintenance	PM	120	CS1 – CS2	2	3	4	–	–	–	–	–	–	–	–	–
B3. Total repair	CM	500	CS4 – CS5	–	–	–	2	2	2	–	–	–	–	–	–
B4. Replacement	CM	1576	CS4 – CS5	–	–	–	1	1	1	–	–	–	–	–	–
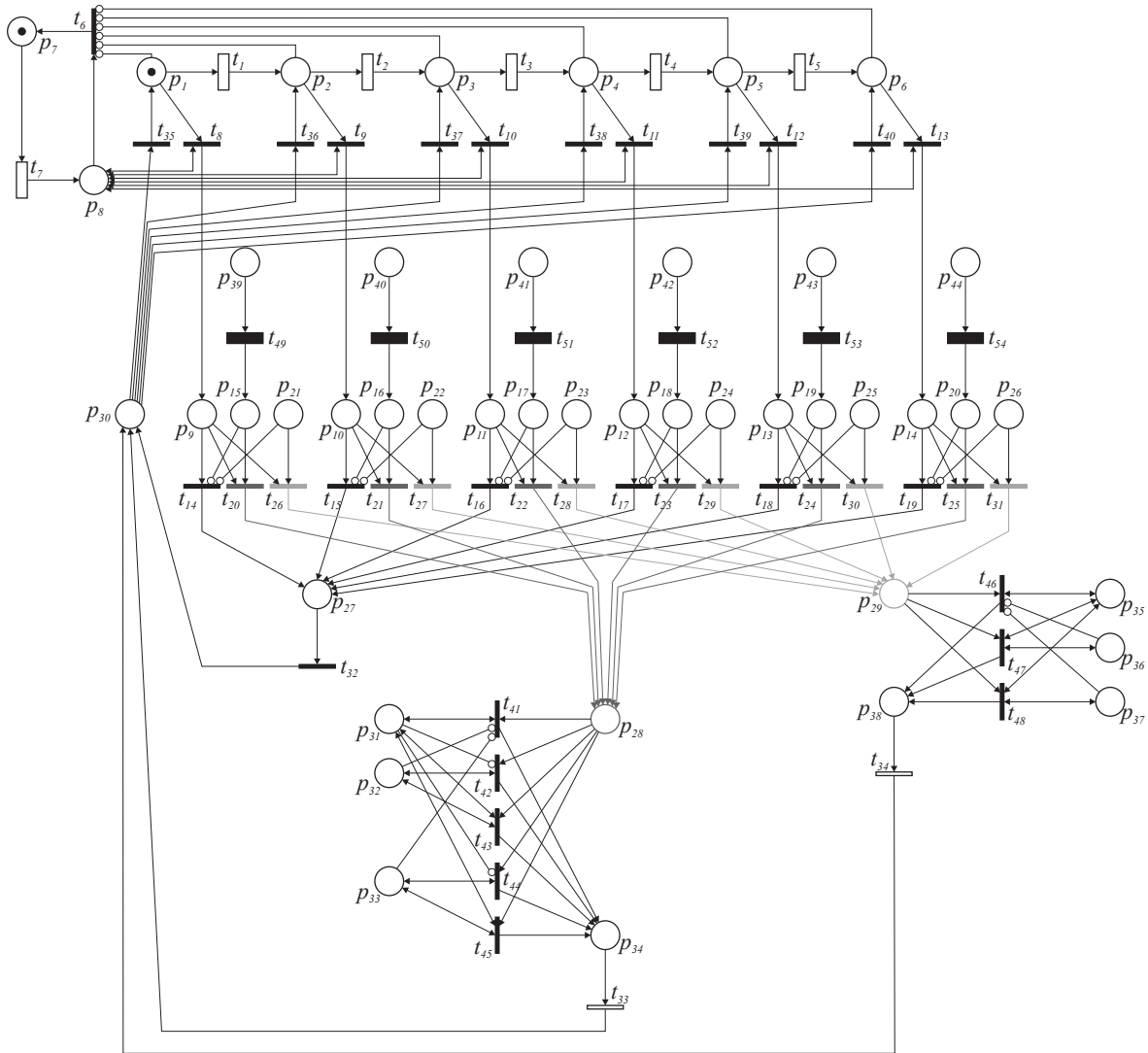
Figure 5.10 – Petri net scheme of the maintenance model for bridges

improves the condition state to CS1 or CS2 and prevents the natural decay process by suppressing the deterioration process during 4 to 8 years and reduces the deterioration rate near 70% for a period of time of 10 to 15 years;

- Minor spalling repair is a preventive maintenance applied when damage severity is relatively low, namely, small defects, mechanical damage, low or null exposure of reinforcing bars. In this type of maintenance, cement or resin-based can be used as patching materials to prevent further deterioration and an effective suppression of the deterioration process can be achieved for a period of time of 1.5 to 3 years;

- Partial or full-depth concrete repair is a corrective maintenance, consisting in removing and replacing damaged portions of concrete and reinforcing steel. It is applied when the concrete is highly contaminated with chlorides or carbonation, causing the despassivation of reinforcing steel. Since the aim of this intervention is to restore the structural integrity of damaged members, an improvement of the condition state CS1 or CS2 is expected;

- Sealing construction joints is a preventive maintenance aiming at to preventing the accumulation of debris, ingress of water and other contaminants. This maintenance leads to a reduction of the deterioration rate 80% during a period of time of 1 to 5 years;

- Crack sealing by injection of epoxy resin-based is a corrective maintenance that aiming at restoring structural integrity of damaged members, should be seen as a remedial measure to prevent further deterioration and additional measures should be performed. With this maintenance, a reduction of the deterioration rate 90% during a period of time of 0.5 to 3 years can be achieved;

- Replacement of waterproof membrane is a corrective maintenance, intending to protect reinforcing steel against water and chloride ingression. This maintenance allows suppressing the deterioration process for a period of time of 1 to 2 years and reducing the deterioration rate 90% during 2 to 4 years.

For bearings, a set of four main maintenance activities was defined by Ascendi technical staff (Guimarães and Matos, 2015):

- Cleaning operations is a preventive maintenance that allows the suppression of the deterioration process for a period of time of 0.5 to 2 years. This intervention includes the removal of debris, contaminants and pressure washing, allowing a proper movement of the superstructure;

- Maintenance of the bearings is a preventive maintenance that allows suppressing the deterioration process for a period of time of 2 to 4 years;

- Total repair of the bearings is a corrective maintenance that allows improving the condition state to CS2;

- Replacement of the bearings is a corrective maintenance that improves the condition state to CS1. This maintenance is applied when there is excessive deformation and the total repair activity is not deemed cost effective.

In this study, the condition, standard deviation and cost profiles are computed using the Monte Carlo simulation with 50 000 samples.

5.6.1 Pre-stressed concrete decks

The results presented in this section describe the effect of three maintenance strategies on the performance of pre-stressed concrete decks. In this study, only maintenance actions that correct spalling defects were analysed.

The three maintenance strategies considered are:

1. Partial or full-depth concrete repair (Maintenance D5);

2. Combination of partial or full-depth concrete repair (Maintenance D5) and minor patching (Maintenance D4);

3. Combination of partial or full-depth concrete repair (Maintenance D5), minor patching (Maintenance D4) and spot painting of concrete elements (Maintenance D2).

The effects of the maintenance actions on the performance of pre-stressed concrete decks, as well as, the range of applicability values and associated costs, are presented in Table 5.18.

In maintenance strategy 1, Maintenance D5 is applied when decks have the highest deterioration level (i.e. exposure of the reinforcement bars). The repair method of the damaged members involves, concrete removal, reinforcement preparation, and concrete placement (Guimarães and Matos, 2015). According to experts' judgement, it is considered that the member achieves a poor condition when it reaches the CS3 or higher.

Maintenance strategy 2 is composed by Maintenance D5 and D4. In this maintenance strategy, Maintenance D4 is applied when the damage severity is low without exposure of the reinforcement bars.

This type of maintenance is applied when an inspection is performed and the component is in CS1 or CS2. Maintenance D5 is applied when the component presents the high level of deterioration, as defined for maintenance strategy 1.

Finally, maintenance strategy 3 is composed by Maintenance D5, D4 and D2. Spot painting (Maintenance D2) is applied in lower deterioration levels (CS1 and CS2). As can be seen from Table 5.18, Maintenance D4 and D2 have the same application zone, however the level of intervention of each maintenance action is different. Maintenance D2 intends to prevent chloride penetration into the concrete, while Maintenance D4 is applied when chloride already penetrated into the concrete but the damage severity is low. So, the aim of Maintenance D4 is to prevent deterioration from reaching the reinforcing bars. Therefore, in this maintenance strategy, the application zones of the three maintenance were slightly altered in relation to those initially defined by the specialists: application zone of Maintenance D2 is the same (CS1 or CS2), Maintenance D4 is applied in CS3, while Maintenance D5 is applied when the component reaches CS4 or CS5. The direct costs of each maintenance action are shown in Table 5.18.

Regarding restrictions, it is assumed that after two consecutive spot painting interventions (Maintenance D2), this maintenance is no longer efficient, making it necessary to apply a minor patching intervention (Maintenance D4). It is also considered that after two consecutive minor patching interventions (Maintenance D4), this maintenance is no longer efficient making it necessary to apply a partial or full-depth concrete repair intervention (Maintenance D5) in order to recover the defect. Regarding the restrictions of the reset transitions, when Maintenance D5 is applied, the number of D4 and D2 interventions is initialized.

The transitions times that specify the movement between different deterioration levels of pre-stressed concrete decks, denoted by transitions t_1 - t_5 in Figure 5.10, are assumed to follow Weibull distributions with parameters (α_i, β_i), with $i = 1, 2, 3, 4, 5$. The parameters are shown in Table 5.20. The Weibull distribution was chosen as the appropriate distribution to sample the transitions times through the study of the deterioration characteristics carried out in Section 5.5.1.

Table 5.20 – Parameters of the Weibull distribution – Pre-stressed concrete decks

Transition	t_1	t_2	t_3	t_4	t_5
α_i	2.8330	23.6165	16.9646	11.2627	3.7143
β_i	0.4419	0.7653	0.8647	7.9990	7.0281

Regarding to periodicity of inspections, it is defined that regular inspections are performed, in order to reveal the true condition of the bridge components. It is assumed the time interval between inspections follows a triangular distribution with 5, 6, and 7 years representing the minimum, mode, and maximum values, respectively. This values were defined based on experts' judgement.

A 150-year time horizon and a deck in a perfect condition at the beginning of the analysis were assumed. Figure 5.11 shows the results computed, in terms of mean and standard deviation of condition state, for the three maintenance strategies previously defined. A fourth maintenance strategy in which the range of applicability of the maintenance strategy 1 is reduced to CS4 – CS5 was added in order to evaluate the consequences of applying a maintenance action sooner or later in terms of mean condition state and costs. In Figure 5.12, the mean and standard deviation of cumulative costs for the three maintenance strategies, considering 0 and 5% annual discount rate are presented, as well as the results obtained when the application zone of the maintenance strategy 1 is reduced to CS4 – CS5. In this work, the mean cumulative costs are used as a simple measure to compare different maintenance strategies.

As shown in Figure 5.11, any of the defined maintenance strategies has a significant impact on the mean condition state in comparison with the profile without maintenance, keeping the mean condition

(a) Mean condition

(b) Standard deviation of condition

Figure 5.11 – Comparison of the predicted future condition profile over time for all maintenance strategies considered – Pre-stressed concrete decks

state almost constant during the entire lifetime. Figure 5.11(a) shows that maintenance strategies 1 and 2 are the most effective in terms of reducing the effect of deterioration on mean condition state. In these two maintenance strategies, the deck has, on average, a condition state of 1.5 and the dispersion of results range, on average, between 0.6 and 0.8.

If, on the other hand, the mean cumulative costs are compared (Figure 5.12), these two maintenance strategies are the most expensive. By observing the effects of these two maintenance strategies (Table 5.18), it is possible to verify the reason of their lack of effectiveness. The higher costs of both maintenance strategies is a direct consequence of the application of the corrective Maintenance D5. Although the application of Maintenance D5 increases the lifetime of the deck, this maintenance is extremely expensive. One way to reduce the costs of this maintenance strategy is the inclusion of preventive maintenance, that will allow the reduction of frequency of application of Maintenance D5 and keep the deterioration level at acceptable levels. However, in maintenance strategy 2, Maintenance D4 is not very effective, since the period of time that the deterioration process is suppressed, t_d, is short, reducing its impact on the average condition state of the deck.

This can be verified by the results present in Figures 5.13 and 5.14. These figures show, respectively, the distribution of the number of interventions for the maintenance strategy 1 and 2. According to these results, for a time horizon of 150 years, there are, on average, 3.2 partial or full-depth concrete

(a) 5% discount rate

(b) 0% discount rate

Figure 5.12 – Cumulative cost profiles for three maintenance strategies considered. Black/green lines represent the mean cumulative cost and the gray/light green lines the standard deviation of the mean cumulative cost – Pre-stressed concrete decks

repair interventions (Maintenance D5) for the maintenance strategy 1, and, for the maintenance strategy 2, there are, on average, 6.8 minor patching interventions (Maintenance D4) and 3.3 partial or full-depth concrete interventions (Maintenance D5). As it can be seen, the combination of the preventive Maintenance D4 with the corrective Maintenance D5 does not reduce the number of application of Maintenance D5.

However, if results obtained for maintenance strategy 3 are compared with those obtained for maintenance strategy 1 and 2, it is clear that the inclusion of Maintenance D2 leads to a reduction of the number of applications of Maintenance D5 and, consequently, of the mean cumulative costs. By observing Figure 5.11, it can be seen that mean condition state of the component is worse than for maintenance strategy 1 and 2. For this maintenance strategy, the deck has, on average, a condition state of 2.2 and the dispersion of results are between 0.9 and 1.0. However, the components continue to present acceptable deterioration levels, and the mean cumulative costs is about 60% lower than that observed for maintenance strategy 2 and about 20% lower than that for maintenance strategy 1 (Figure 5.12(a)).

Figure 5.15 shows the distribution of the number of interventions for the maintenance strategy 3. For a time horizon of 150 years, there are, on average, 4.6 spot painting interventions (Maintenance D2),

Figure 5.13 – Number of interventions for maintenance strategy 1 – Pre-stressed concrete decks
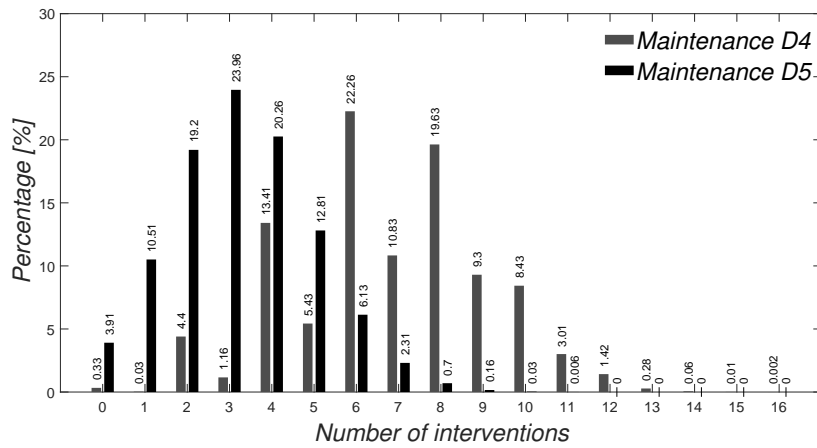
Figure 5.14 – Number of interventions for maintenance strategy 2 – Pre-stressed concrete decks

4.3 minor patching interventions (Maintenance D4) and 1.9 partial or full-depth concrete interventions (Maintenance D5). The inclusion of Maintenance D2 allows reducing, considerably, the number of applications of Maintenance D5 and D4 without a significant impact on the average condition state.
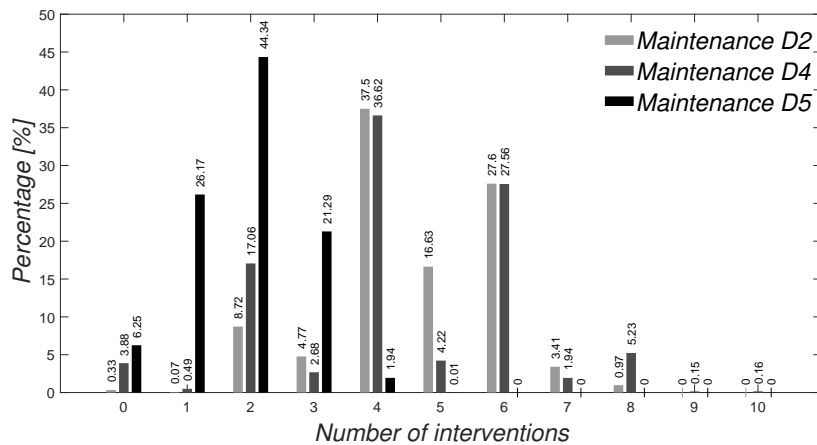
Figure 5.15 – Number of interventions for maintenance strategy 3 – Pre-stressed concrete decks

Finally, if the four maintenance strategies plotted in Figures 5.11 and 5.12 are compared, maintenance strategy 4 shows the best relationship between mean condition state and associated costs. However, maintenance strategy 4 includes only corrective maintenance. Furthermore, if indirect costs are considered small-scale maintenance solutions are more attractive than corrective maintenance actions of greater impact. This approach will increase the attractiveness of solutions that, although associated with higher costs, result in lower impact on users, like conducting interventions at night or weekend.

It should also be mentioned that the cumulative costs have a very significant dispersion, due to the dispersion in the cost of each application, time of application and number of applications. Usually, decision-makers are more interested to knowing the maximum likely cost (i.e. the cost characterized by 5% probability of being exceeded, $C_{0.95}$) than the mean cost, as this allows making maintenance planning with greater level of confidence (Neves and Frangopol, 2005). In Figure 5.16, the 50-, 90-, 95-, and 99-percentiles of the cumulative cost for the four maintenance strategies considering an annual discount rate of 5% are presented. The median cumulative costs are relatively close to the mean. However, when the 95-, and 99-percentiles are considered, the cumulative costs becomes two to five times higher than the mean cost. Furthermore, when the 95-, and 99-percentiles are compared, the maintenance strategy 3 shows lower costs when compared to maintenance strategy 1 and 2, and similar costs comparatively to maintenance strategy 4.

(a) Maintenance strategy 1   (b) Maintenance strategy 2

(c) Maintenance strategy 3   (d) Maintenance strategy 4
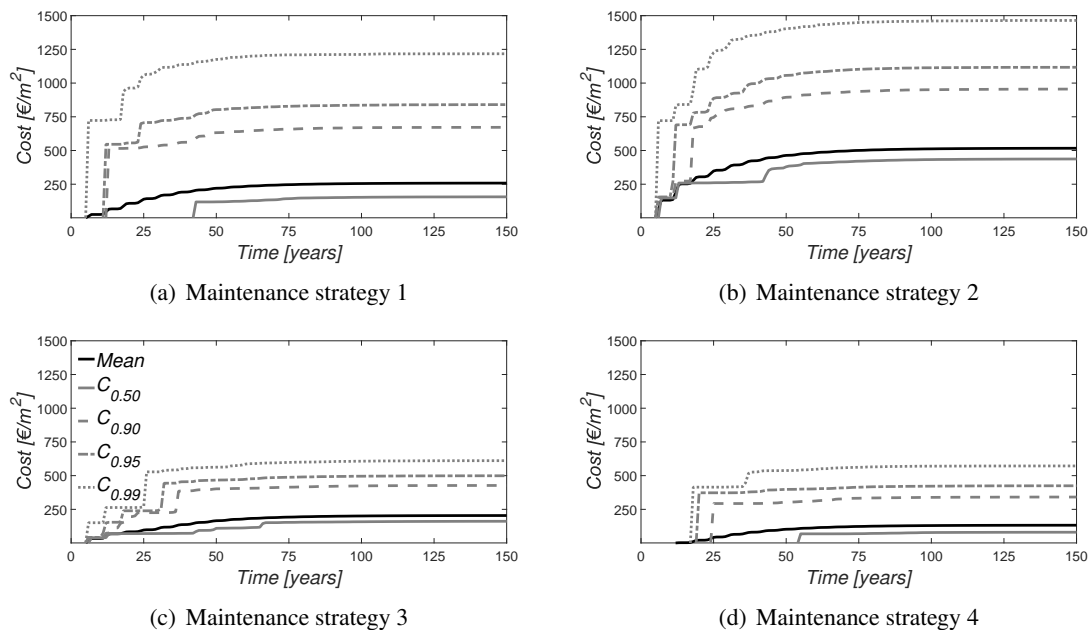
Figure 5.16 – Percentiles of cumulative costs for the four maintenance strategies, where $C_{0.50}$, $C_{0.90}$, $C_{0.95}$, and $C_{0.99}$ are the 50-, 90-, 95-, and 99-percentiles of the cumulative cost, respectively, considering an annual discount rate of 5% – Pre-stressed concrete decks

5.6.2   Bearings

With regard to the performance of the bearings, three maintenance strategies are analysed. In this study, only maintenance actions that correct corrosion defects in metallic bearings were analysed.

1. Replacement of the bearings (Maintenance B4);

2. Combination of replacement of the bearings (Maintenance B4) and repair of the bearings' component (Maintenance B3);

3. Combination of replacement of the bearings (Maintenance B4), repair of the bearings' component (Maintenance B3) and maintenance of the bearings' component (Maintenance B2).

The effects of the maintenance actions on the performance of the bearings, as well as, the range of applicability values and associated cost are presented in Table 5.19.

In strategy 1, Maintenance B4 is applied when bearings have the highest deterioration level and repair of the bearings is no longer effective. In this work, it is considered that the bearings are replaced when the deterioration level reaches CS5. Maintenance strategy 2 is composed by Maintenance B4 and B3. In this maintenance strategy, Maintenance B3 is applied when the bearings have the high deterioration but their functionality can be restored by repairing them. It is composed by a set of cost-effective activities that involve jacking the superstructure, cleaning seats, replacement of failed components, lubricate sliding surfaces and spot paint applying protective coatings against corrosion. This type of maintenance is performed when the deterioration level reaches CS4. Maintenance B4 is applied when repair of the bearings is no longer effective, as explained in maintenance strategy 1. Finally, maintenance strategy 3 is composed by Maintenance B4, B3, and B2. Maintenance B2 includes cleaning and lubrication operations, applied when damage severity is low. This type of maintenance is applied when an inspection is performed and the bearings is in CS1, CS2 or CS3.

It is assumed that after three consecutive maintenance interventions (Maintenance B2), this maintenance action is no longer efficient, making it necessary to perform a total repair of the bearings (Maintenance B3). It is also considered that at the end of two repairs of the bearings (Maintenance B3), this maintenance is no longer efficient, and it is necessary to replace the bearings (Maintenance B4). Regarding the restrictions of the reset transitions: (i) when total repair of the bearings (Maintenance B3) is applied the number of Maintenance B2 is initialized; and (ii) when replacement of the bearings (Maintenance B4) is performed the number of Maintenance B2 and B3 is initialized.

The transitions times that specify the movement between different deterioration levels of bearings, denoted by transitions t_1 - t_5 in Figure 5.10, are assumed to follow Weibull distributions with parameters (α_i, β_i), with $i = 1, 2, 3, 4, 5$. The parameters are shown in Table 5.21. The Weibull distribution was chosen as the appropriate distribution based on results presented in Section 5.5.2.

Table 5.21 – Parameters of the Weibull distribution – Bearings

Transition	t_1	t_2	t_3	t_4	t_5
α_i	4.0684	16.0919	10.9700	7.8474	8.0651
β_i	0.9083	0.8228	1.7448	4.0905	6.2982

Regarding the periodicity of inspections, it is defined that the interval between inspections follows a triangular distribution with 5, 6, and 7 years representing the minimum, mode, and maximum values, respectively. This values were defined based on experts' judgement.

For bearings, the condition profile obtained for the three maintenance strategies and without maintenance are presented in Figure 5.17. Regarding the results obtained, as for the pre-stressed concrete decks, it is possible to stress out that any of the defined maintenance strategies has a significant impact on the mean condition profile, keeping the mean condition state almost constant during the entire lifetime. For all maintenance strategies, the mean condition state of the bearings over time varies between 2 and 2.5. In terms of dispersion of results, the values range, on average, between 0.6 and 1.3, with maintenance strategy 1 resulting in larger dispersion.

Figure 5.18 compares the mean cumulative costs of the three maintenance strategies, considering annual discount rates of 0 and 5%. The direct costs of each maintenance action are shown in Table 5.19. Figures 5.17 and 5.18 show that maintenance strategy 2 leads to lower mean cumulative cost and, consequently, better relationship between performance and cost. However, as mentioned before, the decision-makers are also interested in estimating the maximum likely cost. Figure 5.19 shows
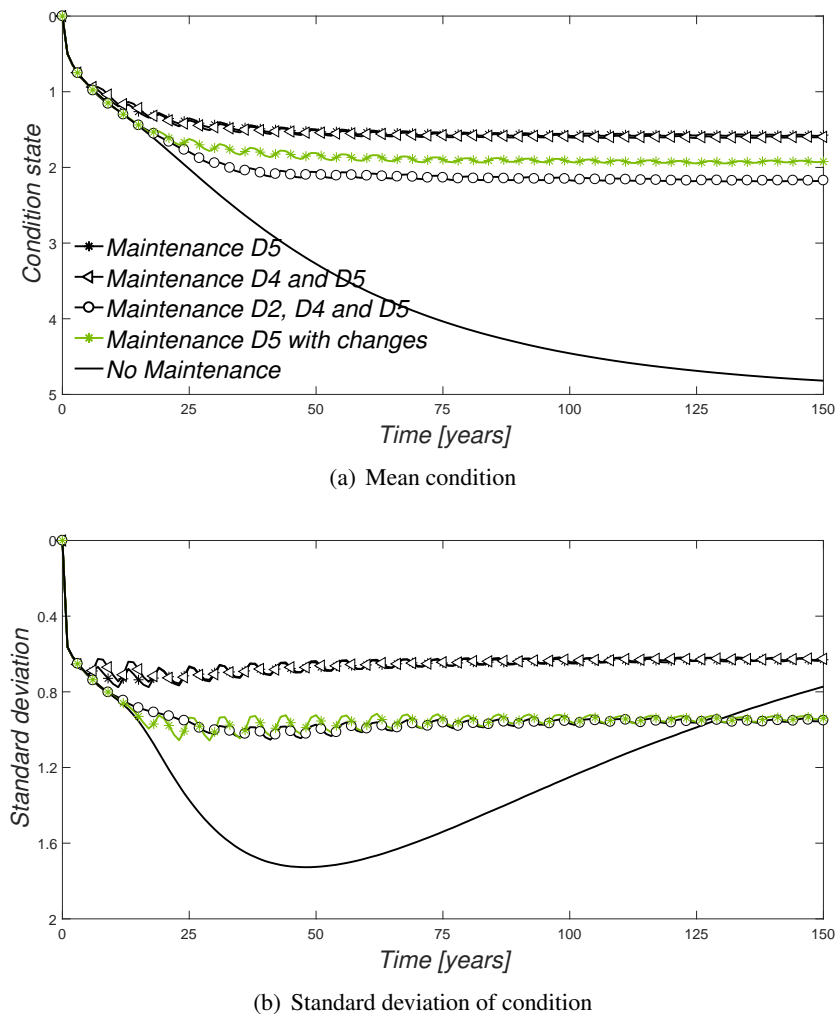
(a) Mean condition

(b) Standard deviation of condition
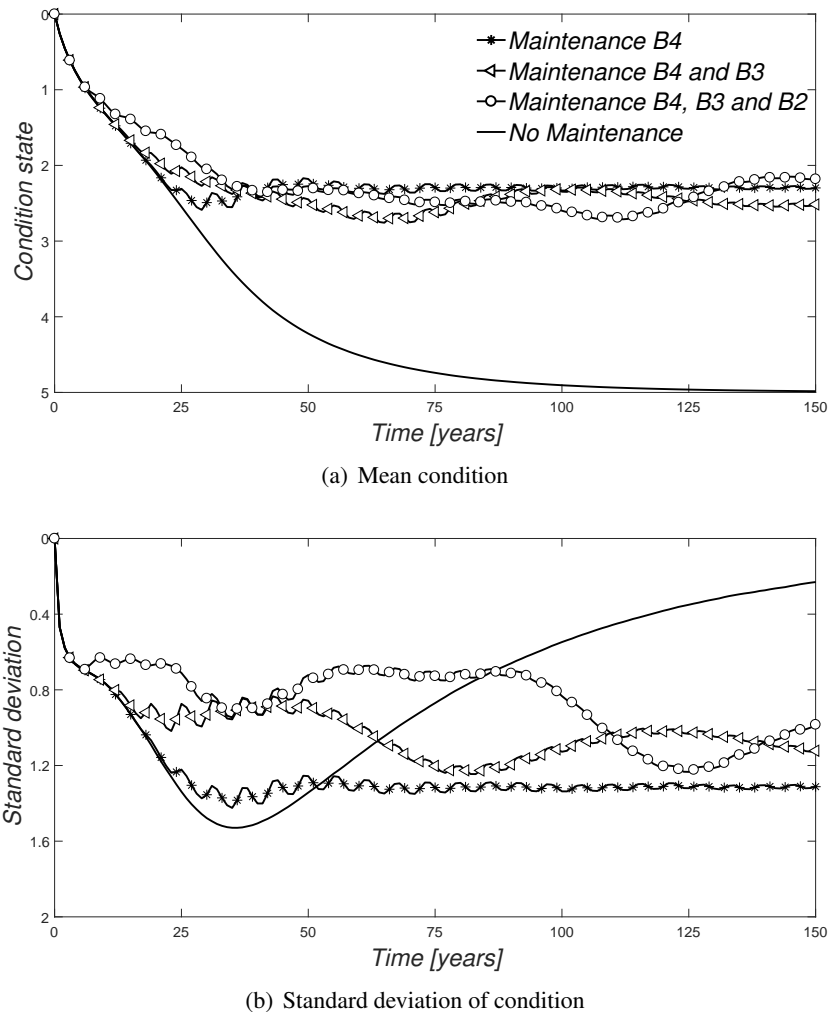
Figure 5.17 – Comparison of the predicted future condition profile over time for all maintenance strategies considered – Bearings

that the medians of the cumulative cost are relatively close to the mean, but, the 95- or 99-percentiles are significantly higher than the mean cost. Furthermore, when 95- or 99-percentiles are compared, the maintenance strategy 3 shows lower costs, showing that the realization of maintenance works is essential to keep the bearings in a serviceable condition during their lifetime.

Figures 5.20, 5.21, and 5.22 show the distribution of the number of interventions for the three maintenance strategies. The combination of preventive and corrective maintenance reduces the number of application of Maintenance B4, and, consequently, the maintenance costs. According to these results, for a time horizon of 150 years, there are, on average, 2.8 bearings' replacement (Maintenance B4) for the maintenance strategy 1. For the maintenance strategy 2, there are, on average, 3.6 bearings' repair (Maintenance B3) and 1.3 bearings' replacement (Maintenance B4). And, for the maintenance strategy 3, there are, on average, 11.1 bearings' maintenance (Maintenance B2), 2.1 bearings' repair (Maintenance B3) and 0.9 bearings' replacement (Maintenance B4).

(a) 5% discount rate

(b) 0% discount rate
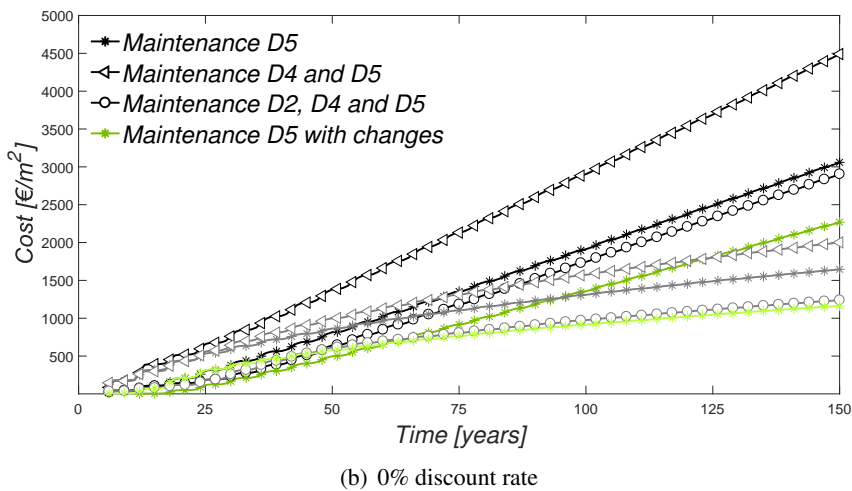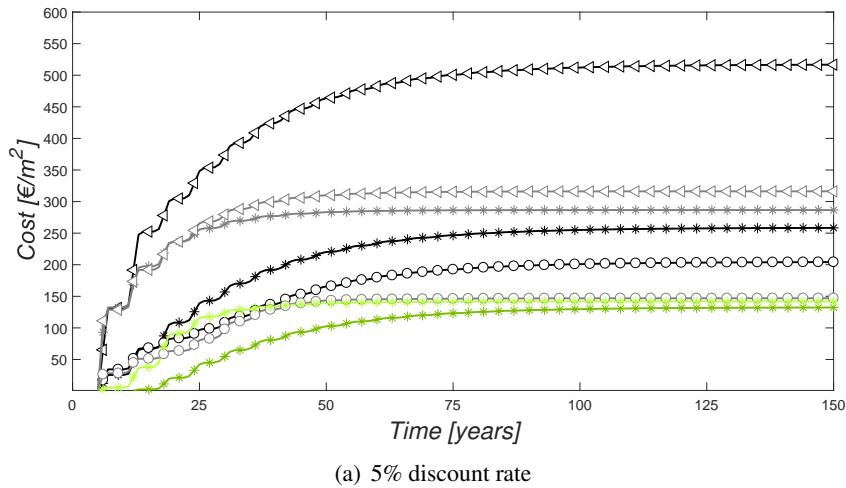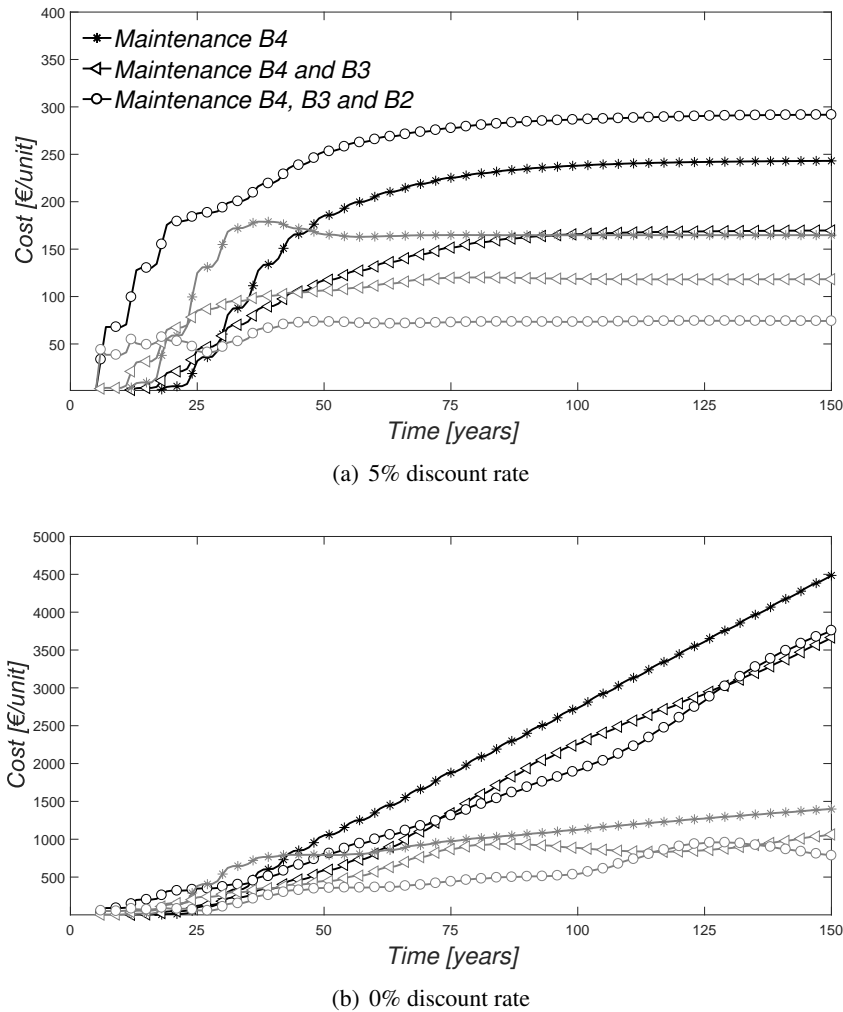
Figure 5.18 – Cumulative cost profiles for three maintenance strategies considered. Black lines represent the mean cumulative cost and the gray lines the standard deviation of the mean cumulative cost – Bearings

5.7   Summary

In this chapter, Markov chains and Petri nets are used to develop deterioration models for bridge components. Markov chains are used to verify the Petri net model and evaluate the size of the samples. The obtained results show that Petri nets allow a more accurate prediction of future deterioration, due to their ability to consider multiple probability distributions. From the results of the probabilistic analysis, four main conclusions can be drawn:

- Firstly, the Exponential distribution do not describe adequately the transition between the more advanced deterioration states. The poor fit of the Exponential distribution can be explained by: (a) the limitation of being a one-parameter distribution that may contribute to the difficulty in modelling the deterioration process; and (b) the rare or non-existent elements in the more advanced deterioration states that influence the performance of the optimization algorithm;

- Secondly, the Lognormal distribution, also, does not describe adequately the transition between the more advanced deterioration states. The poor fit of the Lognormal distribution is, mainly, related with the low number of elements in the database. The Lognormal distribution shows unrealistic mean times in each condition state, which leads to believe that the Lognormal need

(a) Maintenance strategy 1

(b) Maintenance strategy 2

(c) Maintenance strategy 3
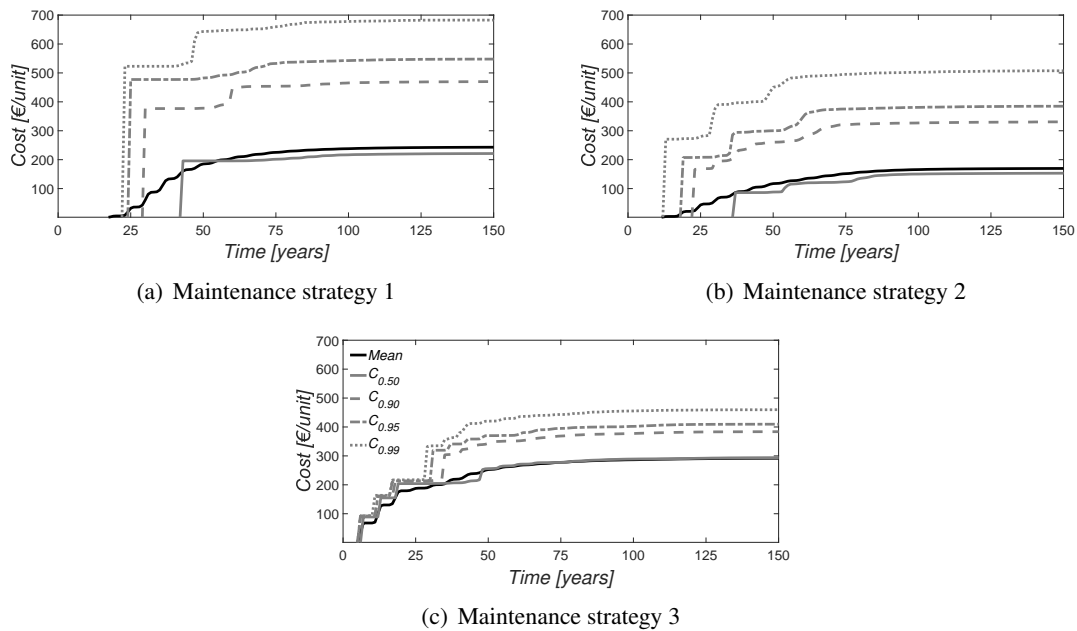
Figure 5.19 – Percentiles of cumulative costs for the three maintenance strategies, where $C_{0.50}$, $C_{0.90}$, $C_{0.95}$, and $C_{0.99}$ are the 50-, 90-, 95-, and 99-percentiles of the cumulative cost, respectively, considering an annual discount rate of 5% – Bearings
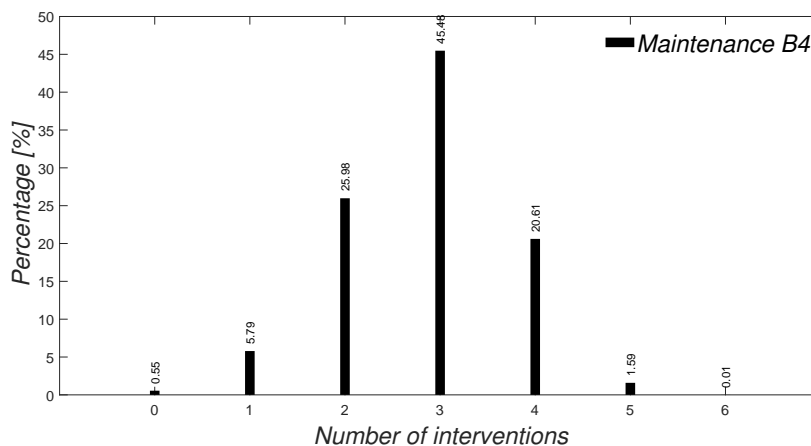
Figure 5.20 – Number of interventions for maintenance strategy 1 – Bearings

much more observations to estimate, properly, the parameters that best describe the process of deterioration;

- Thirdly, in terms of predicted future condition profile and predicted probabilities, Gumbel and Normal distribution show results very close to the results obtained by the Weibull distribution (Figures 5.6 and 5.8). However, the log-likelihood values and the mean relative errors are worse for these distributions;

- Finally, for both bridge elements, the Weibull distribution shows a minor log-likelihood value and, consequently, a better fit to the historical data.

In the maintenance model, to evaluate the performance of bridges' component, four maintenance strategies were considered for pre-stressed concrete decks ad three for bearings. For both bridges' component, the Weibull distribution was chosen as the appropriate distribution to sample the tran-
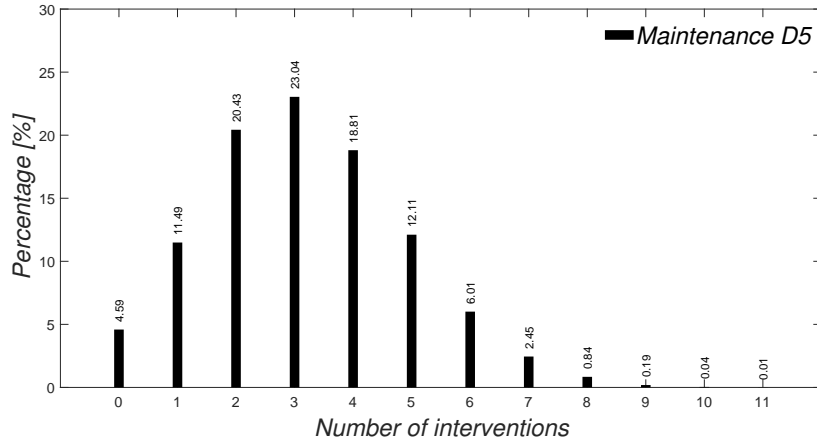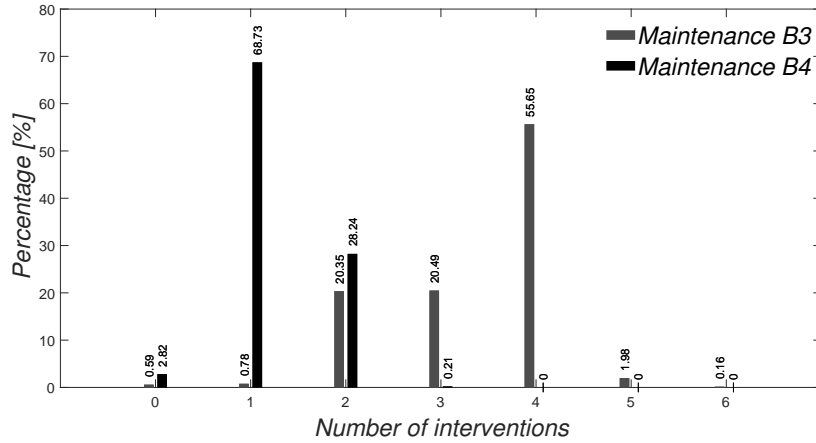
Figure 5.21 – Number of interventions for maintenance strategy 2 – Bearings
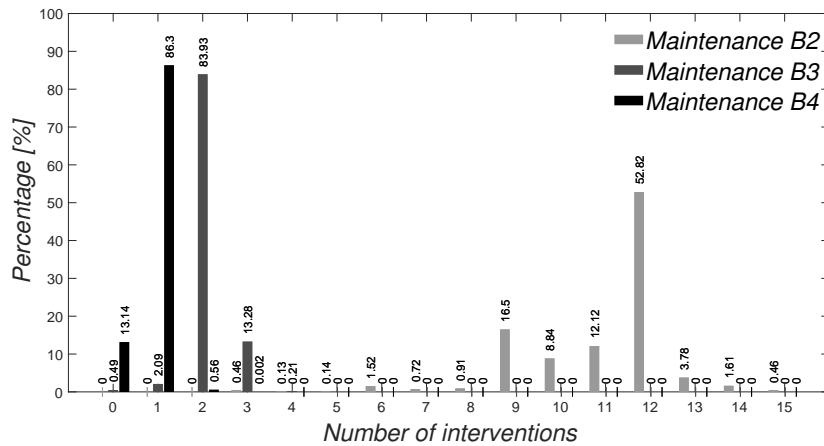
Figure 5.22 – Number of interventions for maintenance strategy 3 – Bearings

sitions times in the deterioration process, and the triangular distribution was chosen as the proper distribution to set the inspections times. The choice of the Weibull distribution was performed based on the results obtained in the probabilistic analysis performed in this same chapter, while the Triangular distribution was defined based on experts' judgement.

Through the analysis of the predicted future condition profiles over time, it is possible to observe that any of the defined maintenance strategies, for both components, has a significant impact on the mean condition level comparing with the profile without maintenance. For pre-stressed concrete decks, maintenance strategy 4 is the one that shows better relationship between performance and cost. However, in order to keep the bridge deck in a safe and serviceable condition during their lifetime, the realization of preventive maintenance is important, because it allows owners to know the correct condition state of the structure and to intervene at the best moment, avoiding that the bridges suffer serious structural damage that endanger the lives of users. Furthermore, when the 95-, and 99-percentiles of the cumulative cost for the four maintenance strategies are compared, it can be observed that maintenance strategy 3 presents minor costs than maintenance strategy 1 and 2, and similar costs to maintenance strategy 4, and continues to present an acceptable deterioration level. Regarding bearings, from Figures 5.17 and 5.18 it can be seen that maintenance strategy 2 is the one that shows better relationship between performance and cost. But, if the 95- or 99-percentiles are analysed (Figure 5.19), it becomes clear that the cumulative costs of maintenance strategy 3 are not too far, and it is likely that, in the long-term, maintenance strategy 3 is the one that presents the best

relation between performance and cost. Furthermore, in order to keep the bearings in a serviceable condition during their lifetime, the realization of maintenance works is fundamental.

Chapter 6

Case Study 2: Application to Ceramic Claddings

6.1 Introduction

The deterioration Petri net model developed in Section 4.2 is applied to analyse the deterioration process of a sample of 195 ceramic claddings. The information present in the database is based only on visual inspection records of adhesive ceramic cladding systems with no cultural value located in Lisbon, Portugal. Each place illustrated in Figure 6.1 represents one of the five deterioration levels proposed by Gaspar and de Brito (2008b, 2011), which classify the degradation condition of ceramic claddings.
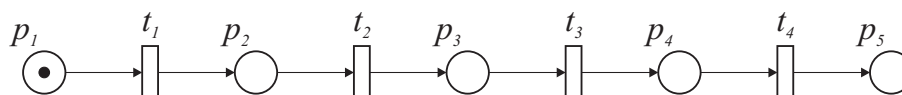
Figure 6.1 – Petri net scheme of the deterioration model for claddings

Firstly, Petri net model is used to predict the deterioration of claddings over time and to understand how the different environmental exposures contribute to the overall degradation. The probabilistic analysis is performed into two phases. In the first phase, the complete sample is analysed. The five probabilistic distribution studied Chapter 5 are fitted to the complete sample and the best distribution is identified. In the second phase, the original sample is divided according to four environmental characteristics: exposure to damp, distance from the sea, orientation and wind-rain action. These four characteristics were considered the most relevant to explain the degradation. Following this, an inference analysis is performed to examine the impact of the environmental characteristics considered. After that, the Petri net maintenance model is applied to analyse the consequences of alternative maintenance strategies to control deterioration patters in ceramic claddings. The maintenance model described can be considered a full life-cycle model that includes not only the deterioration process, but also inspections, maintenance and renewal processes.

It should be noted that, for each cladding described in the historical database, only the initial and final condition level are known. It is assumed that, at time zero, the cladding is in the most favourable condition level (Level A) while the final condition level corresponds to the condition level at the time of inspection. The condition, standard deviation, probabilistic distribution and cost profiles are computed using the Monte Carlo simulation with 50 000 samples.

6.2   Classification of the degradation condition

Nowadays, there are various methods of assessing the deterioration state of façades (Shohet et al., 2002; Shohet and Paciuk, 2004; Gaspar and de Brito, 2008b). The method used in this study to asset the deterioration state is a discrete scale proposed by Gaspar and de Brito (2008b, 2011). The authors propose a qualitative and quantitative scale. The qualitative scale is based on the evaluation of the physical and visual condition of the sample analysed. The defects associated with ceramic claddings are divided into five levels, from Level A (no visual deterioration – most favourable situation) to Level E (worst condition level). The quantitative scale, called severity of degradation, S_w, is obtained as the ratio between the extent of the façade degradation, weighted as a function of the degradation level and the severity of the defects, and a reference area, equivalent to the maximum theoretical extent of the degradation for the façade in question:

$$S_w = \frac{\sum (A_n \times k_n \times k_{a,n})}{A \times k} \tag{6.1}$$

where S_w is the degradation severity of the coating, expressed as a percentage; k_n is the multiplying factor of anomaly n, as a function of their degradation level, within the range $K = \{0, 1, 2, 3, 4\}$; $k_{a,n}$ is a weighting factor corresponding to the relative weight of the anomaly detected ($k_{a,n} \in \mathbb{R}^+$); $k_{a,n} = 1$ by default; A_n is the area of coating affected by an anomaly n; A is the façade area; and k is the multiplying factor corresponding to the highest degradation level of a coating of area A. For more details on the classification system an interested reader is kindly referred to Gaspar and de Brito (2008b, 2011) and Bordalo et al. (2011).

All the defects considered for ceramic claddings such as the qualitative and quantitative scales are summarized in Table 6.1.

6.3   Probabilistic analysis

Similarly to the bridge's component (Section 5.5), for ceramic claddings five distributions were also analysed. The condition, standard deviation and probabilistic distribution profiles are computed using the Monte Carlo simulation with 50 000 samples.

Table 6.2 shows the optimal parameters obtained for all probability distribution analysed, as well as, the log-likelihood computed for each set of optimal parameters. Table 6.3 shows the number of observed and predicted ceramic claddings in each condition level for each probability distribution, as well as, the relative error obtained for each case. The light and dark gray cells indicate the distributions with smaller and larger relative errors, respectively, for each condition level.

One of the main conclusions that can be drawn from these results is that two-parameter distributions (Weibull, Lognormal, Gumbel and Normal) have a better fit to the historical data (Table 6.2). All these four distributions resulted in a better log-likelihood value than the exponential distribution. The good agreement between distributions and historical data also is visible when the number of observed and predicted claddings are compared (Table 6.3). The number of observed and predicted claddings are close, even in the Exponential distribution. In a more detailed analysis, it can be seen that all distributions have a tendency to overestimate the number of claddings in Level A and C, and underestimate those in Level B, D and E.

In terms of relative error (Table 6.3), the values obtained are, in most cases, less than 10%. The extreme conditions levels (Level A and E) are those with larger errors; in Level A, the largest errors occur for Normal distribution (24.3%) and Weibull distribution (11.2%); in Level E, the largest errors occur for Normal distribution (29.1%), Weibull distribution (23.0%) and Gumbel distribution

Table 6.1 – Degradation conditions for ceramic claddings (Silva et al., 2016c)

Degradation level	Defects		% of cladding are affected	Severity of degradation
Level A	No visible degradation			$S_w \leq 1$
Level B	Visual or surface degradation defects	- Small surface craters	≤ 10	$1 < S_w \leq 6$
Level C	Visual or surface degradation defects	- Small surface craters	> 10 and ≤ 50	$6 < S_w \leq 20$
		- Biological growth	≤ 30	
	Cracking	- Cracking with no predominant direction	≤ 30	
	Joint deterioration	- Without loss of filing material	≤ 30	
		- With loss of filing material	≤ 10	
	Detachment	- Loss of adherence	≤ 20	
Level D	Visual or surface degradation defects	- Small surface craters	> 50	$20 < S_w \leq 50$
		- Biological growth	> 30	
	Cracking	- Cracking with no predominant direction	> 30 and ≤ 50	
	Joint deterioration	- Without loss of filing material	> 30 and ≤ 50	
		- With loss of filing material	> 10 and ≤ 30	
	Detachment	- Loss of adherence	> 20	
		- Localized detachment	≤ 10	
Level E	Cracking	- Cracking with no predominant direction	> 50	$S_w > 50$
	Joint deterioration	- Without loss of filing material	> 50	
		- With loss of filing material	> 30	
	Detachment	- Generalized detachment	> 10	

(21.3%). It must be noted that these two condition levels are those less represented in the sample. However, analysing the mean relative error for all condition levels, the Lognormal distribution is the one that has lower mean relative error (5.4%). The Weibull distribution, which is the one with the smallest log-likelihood value, presents a mean relative error for all condition levels of 8.9% (third lower value).

Silva et al. (2016c) used Markov chain models to analyse the same database. The values of the parameters obtained by Markov chains and by Petri nets with the Exponential distribution are very similar (Table 6.4). The largest differences occur for the transition t_4. The reason for this difference is the small number of elements present in the Level E. The differences obtained in the others parameters are due to sampling errors associated with the Monte Carlo simulation. Taking into account the results obtained by Petri nets, it is confirmed that there is a likeness between both models and the proposed

Table 6.2 – Optimal parameters obtained for all probability distribution analysed

Parameters		Exponential	Weibull	Gumbel	Lognormal	Normal
Mean	t_1	6.69	6.84	6.70	6.39	7.70
(years)	t_2	24.88	23.50	22.72	24.51	22.70
	t_3	39.93	22.60	22.72	23.95	22.13
	t_4	317.60	31.46	38.90	3.34×10^4	37.12
Standard	t_1	6.69	6.24	5.57	6.59	5.80
deviation	t_2	24.88	12.37	13.79	17.73	12.08
	t_3	39.93	1.42	2.55	0.54	0.32
	t_4	317.60	1.93	13.07	1.52×10^6	9.53
$-\log L$		180.2441	160.1749	160.8896	162.3466	160.6454

Table 6.3 – Number of observed and predicted claddings in each condition level for each probability distribution and mean error obtained for each probability distribution

Probability distribution		Level A	Level B	Level C	Level D	Level E
Observed		15	70	64	43	3
Predicted	Exponential	16.40	64.88	67.30	43.86	2.56
	Weibull	16.69	67.12	66.76	42.12	2.31
	Gumbel	16.24	64.14	66.95	45.31	2.36
	Lognormal	15.65	66.67	68.32	41.59	2.77
	Normal	18.64	65.63	65.97	42.64	2.13
Relative	Exponential	9.3	7.3	5.2	2.0	14.5
error [%]	Weibull	11.2	4.1	4.3	2.0	23.0
	Gumbel	8.3	8.4	4.6	5.4	21.3
	Lognormal	4.4	4.8	6.7	3.3	7.7
	Normal	24.3	6.2	3.1	0.8	29.1

model is suitable to evaluate the degradation of ceramic claddings.

Table 6.4 – Comparison of the optimal parameters of the Markov chains and Petri nets models (Exponential distribution)

Parameters		Markov chains	Petri nets (Exponential)
Mean	t_1	6.58	6.69
(years)	t_2	24.81	24.88
	t_3	39.68	39.93
	t_4	100.00	317.60
Standard	t_1	6.58	6.69
deviation	t_2	24.81	24.88
	t_3	39.68	39.93
	t_4	100.00	317.60
$-\log L$		183.8355	180.2441

Figure 6.2(a) presents the mean condition profile over time for all probability distributions analysed. The profiles obtained for the five distributions can be divided into three groups. The first group is constituted by Exponential distribution. The profile computed using the Exponential distribution is quite distinct from the other four profiles. This distribution shows a profile with a simple parabolic shape without inflection points. The second group is composed by the Weibull, Gumbel and Normal

distributions. The profiles of these three distributions are very similar throughout the time horizon, with a clear change in concavity when there is transition of condition level. Finally, the third group is formed by Lognormal distribution. The profile obtained by this distribution is a mixture of the two types of profiles refer above. The profile of the Lognormal distribution is very similar to the profiles of the distributions in group 2 during the first transitions (Level A to B, Level B to C and Level C to D). The major difference lies in the transition between Level D and E, where the profile shows more likeness to the profile of the Exponential distribution. In terms of dispersion of results, Figure 6.2(b), the values are low, and any of the two-parameter distributions has lower dispersion values over the time horizon than the exponential distribution.
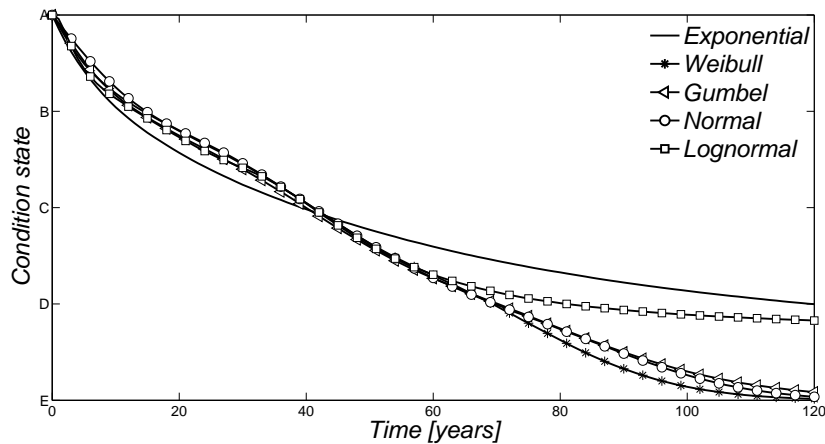
(a) Mean condition
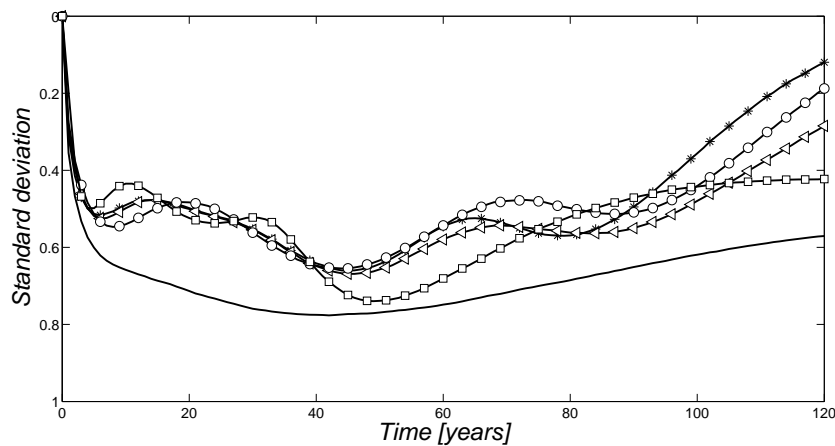
(b) Standard deviation of condition

Figure 6.2 – Comparison of the predicted future condition profile over time for all probability distribution analysed. Mean and standard deviation are computed considering a correspondence between the condition scale and an integer scale between 1 and 5

Figure 6.3 shows the probabilistic distribution of all degradation condition levels over time. The differences between probability distribution identified above are also visible in these plots. For Level A, the predicted probabilities for all distributions are similar; probability is equal to 1 at $t = 0$ and decreases over time; at year 30 the probability of a ceramic cladding be at level A is close to zero (Figure 6.3(a)). Furthermore, it can be observed that between years 5 and 7 the probability of belonging to either Level A or B is practically the same for all distributions, the results show that during this time interval there is a transition from Level A to B. From Level B, it is possible to see differences between the three groups of distribution defined above; between years 12 and 16 the maximum prob-

ability of a cladding belonging to Level B is attained, however the maximum probability obtained through the Exponential distribution is about 15-20% lower (Figure 6.3(b)). When using an Exponential distribution, there is transition from Level B and C around year 22 while to the two-parameter distributions transition between Level B and C occurs six years later (around year 28). The maximum probability of belonging to the Level C is close to 0.50 for the Exponential distribution while for other distributions it varies between 0.70 and 0.80. After the maximum probability is achieved, the slope of the Exponential distribution is relatively softer, when compared with the other distributions. The transition between Level C and D occurs around year 54 for the two-parameter distributions and for Exponential distribution it occurs, approximately, thirteen years later (around year 67). The largest differences between distributions are obtained for Level D (Figure 6.3(d)) and E (Figure 6.3(e)). The Exponential and Lognormal distributions, during the time horizon analysed, never result in a transition between these two condition levels. For the Weibull and Normal distributions, the transition between condition levels occurs around year 84 and for Gumbel distribution occurs around year 90.

(a) Condition Level A

(b) Condition Level B

(c) Condition Level C

(d) Condition Level D

(e) Condition Level E
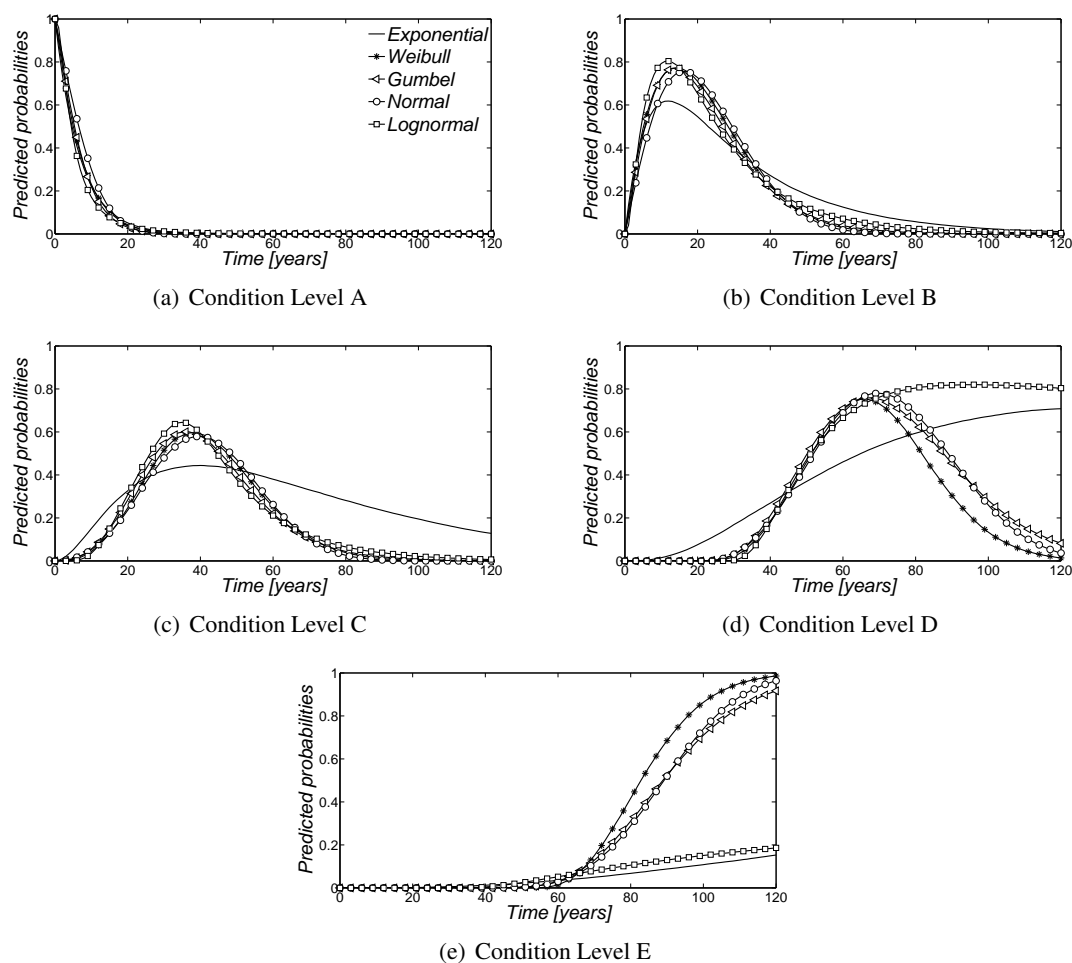
Figure 6.3 – Comparison of the probabilistic distribution for each condition state over time – Claddings

From these results, it can be seen that the Exponential and Lognormal distributions do not describe adequately, principally, the transition between the two worst conditions levels. The poor fit of the Exponential distribution can be explained by a limitation of the distribution. The Exponential distribution has only one parameter and this may contribute to the difficulty in modelling the deterioration process. For the Lognormal distribution, the poor fit is related to the low number of claddings observed in the database in Level E (only 3 elements, Table 6.3). The results show that the low number of observations is insufficient for properly estimate the parameters of the Lognormal distribution. How-

ever, it should be mentioned that the time horizon in the plots is not realistic for ceramic claddings as this type of material is not design for such a long time horizon so great. In terms of durability, it is expected that this type cladding requires maintenance actions around year 50 (Level D represents a minimum accepted level of performance) and until this year there is a good fit of the Lognormal distribution.

6.4 Probabilistic analysis according to exposure

The different environmental exposures that a cladding is subjected have a significant effect on deterioration. To understand how the environment contributes to the overall degradation, the most relevant characteristics influencing the degradation of claddings were analysed: exposure to damp, distance from the sea, orientation and wind-rain action.

The results obtained in the analysis for different characteristics are shown in Table 6.5 and Figures 6.4 to 6.7. Table 6.5 shows the probability of belonging to each condition as a function of the variables considered and Figures 6.4 to 6.7 present the predicted future condition profile over time for each exposure. The predicted future condition profile for each variable is obtained through the distribution that has the lowest normalized log-likelihood value (Table 6.5).

The normalized log-likelihood, $\hat{l}$, is obtained through the division of the logarithm of the likelihood, $\log L$, by the number of elements present in the sample, n_s (Equation 6.2). The obtained value represents the expected log-likelihood of a single element in the model.

$$\hat{l} = \frac{-\log L}{n_s} \qquad (6.2)$$

The differences between the normalized log-likelihood values of all the variables are not very high. The lowest value is obtained for Orientation – South (0.6006) and the largest for Orientation – West (0.8626). These results show that variable Orientation – South is the one that has a better fit to the historical data.

6.4.1 Exposure to damp

Dampness associated with salt leaching can cause aesthetic degradation and/or structural damage to exterior building façades (Rirsch et al., 2011). The presence of moisture on a façade can start cracking of the surface, and biological growth, among other defects (Silva et al., 2016d).

Relatively to exposure to damp, claddings are divided into low and high exposure to damp. The distinction was made between buildings located in areas without the influence of prevailing winds from sea or rivers (low exposure to damp), and buildings located in areas under direct influence of prevailing winds from the sea or from a river front (high exposure to damp) (Gaspar, 2009; Silva et al., 2016d). The samples for low and high exposure to damp are composed by 111 and 84 elements, respectively. The predicted future condition profile according to exposure to damp is shown in Figure 6.4.

The results show that the claddings with low exposure to damp are more prone to remain in lower degradation conditions (Level A and B) and none of these claddings evolves to the worse condition level (Level E). However, claddings with high exposure to damp show higher probability of belonging to the most unfavourable conditions levels ($P(Level \geq C) = 70.6\%$).

Table 6.5 – Probability of belonging to a condition as a function of the variables considered

Variables	Number of samples	Distribution	Level A [%]	Level B [%]	Level C [%]	Level D [%]	Level E [%]	$-\log L$	$\hat{\gamma}$
Complete sample (G)	195	Weibull	8.6	34.4	34.2	21.6	1.2	160.17	0.8214
Exposure to damp									
Low (DL)	111	Weibull	8.8	45.4	29.7	16.1	0.0	87.87	0.7916
High (DH)	84	Normal	7.1	22.3	37.2	30.9	2.5	57.73	0.6872
Distance from the sea									
Less than 1 km (SC)	77	Gumbel	7.8	20.5	37.2	31.1	3.4	52.43	0.6809
Between 1 and 5 km (SI)	62	Normal	3.3	33.9	34.1	28.7	0.0	42.96	0.6929
More than 5 km (SF)	56	Weibull	13.9	56.2	26.9	3.0	0.0	45.88	0.8193
Orientation									
North (ON)	58	Normal	10.3	21.8	44.2	21.9	1.9	44.85	0.7733
East (OE)	40	Lognormal	8.3	33.5	29.6	28.6	0.0	31.54	0.7885
South (OS)	41	Weibull	8.6	38.3	21.9	27.1	4.1	24.63	0.6006
West (OW)	43	Lognormal	8.8	41.3	36.2	13.7	0.0	37.09	0.8626
Wind-rain action									
Low (WL)	45	Normal	2.3	41.6	37.1	18.9	0.2	33.64	0.7476
Moderate (WM)	97	Weibull	10.9	40.0	32.2	16.9	0.0	77.32	0.7972
High (WH)	53	Normal	7.5	18.8	33.9	34.9	4.9	40.14	0.7573
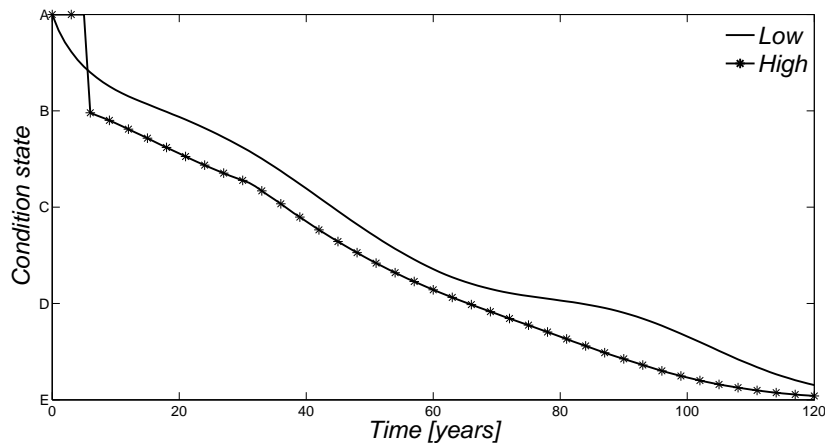
Figure 6.4 – Predicted future condition profile over time – Exposure to damp

6.4.2 Distance from the sea

Proximity to the sea can be particularly damaging to ceramic claddings. Sea spray driven by the wind causes the progressive deposition of ions on the external surfaces of structures which, by ionic diffusion, penetrate the interior of the material. The penetration of the ions causes deterioration of the physical infrastructure, affecting durability and reducing the service life (Hossain et al., 2009; Silva et al., 2016d)

Figure 6.5 presents the predicted mean condition profile according to distance from the sea. For this environmental characteristic, claddings are divided into three sets: close to the sea (less than 1 km), far from the sea (more than 5 km) and an intermediate position (between 1 and 5 km). The samples for the sets less than 1 km, between 1 and 5 km, and more than 5 km are composed by 77, 62 and 56 elements, respectively.

The influence of the sea in the overall condition of the claddings is very clear. The claddings located close to the sea have significantly higher probability of belonging to the most unfavourable conditions levels ($P(Level \geq C) = 71.7\%$). This tendency decreases with the distance from the sea. The probability of a cladding belonging to the most unfavourable conditions are 62.8% and 29.9% for the intermediate and far from the sea, respectively.
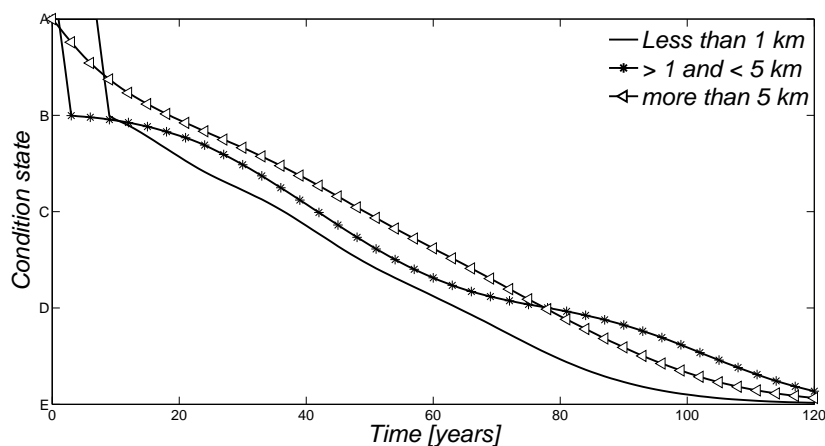
Figure 6.5 – Predicted future condition profile over time – Distance from the sea

6.4.3   Orientation

Regarding orientation, claddings are divided into the four main cardinal directions: North, East, South, and West. The number of elements of each set are, respectively, 58, 40, 41 and 43. In this analysis, claddings in intermediate directions (Northeast, Southeast, Southwest, and Northwest) are ignored because the size of the sample was very small. The predicted mean condition profile according to orientation is shown in Figure 6.6.

According to Gaspar (2009), in Portugal, North and West are the most aggressive directions, because North is more humid and cold and West presents dominant winds and a higher probability of occurrence of wind-rain action. In this study, it was verified that claddings with orientation to North show higher probability of belonging to the most unfavourable conditions levels ($P(Level \geq C) = 68\%$), but claddings with orientation to West are more prone to remain in lower condition levels with a probability of 50.2%.
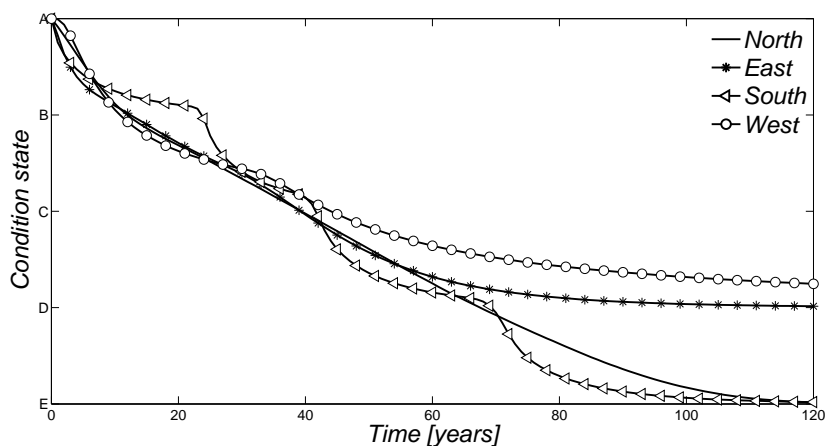
Figure 6.6 – Predicted future condition profile over time – Orientation

6.4.4   Wind-rain action

The combined action of wind and rain changes the trajectory of raindrops, the way they impact the building's façade and the pattern of runoff flow along the surface (Choi, 1999). In this study, the quantification of driven-rain incidence is associated with level of protection of the façade.

According to Gaspar (2009), the level of protection takes into consideration the height of the building and the density of ground occupation in the surrounding area:

- Low exposure – for low-rise buildings (up to two storeys high), in densely populated areas, protected from prevailing winds by other buildings, adjacent hills or vegetation;

- Moderate exposure – for medium-to-high buildings, in populated urban areas, protected from prevailing winds by other buildings, adjacent hills or vegetation;

- High exposure – for buildings with more than four storeys or in open country or crossroads.

The samples for low, moderate and high exposure are composed by 45, 97 and 53 elements, respectively. Figure 6.7 presents the predicted mean condition profile according to wind-rain action.

From the results it can be observed that claddings with high exposure to the combined action of wind and rain have a lower probability of belonging to the most favourable conditions levels ($P(Level \leq B) = 26.3\%$). However, claddings with a moderate wind-rain action have a higher probability of belonging

to the most favourable conditions levels ($P(Level \leq B) = 50.9\%$). The low wind-rain action also is prejudicial to the conservation of the ceramic claddings.
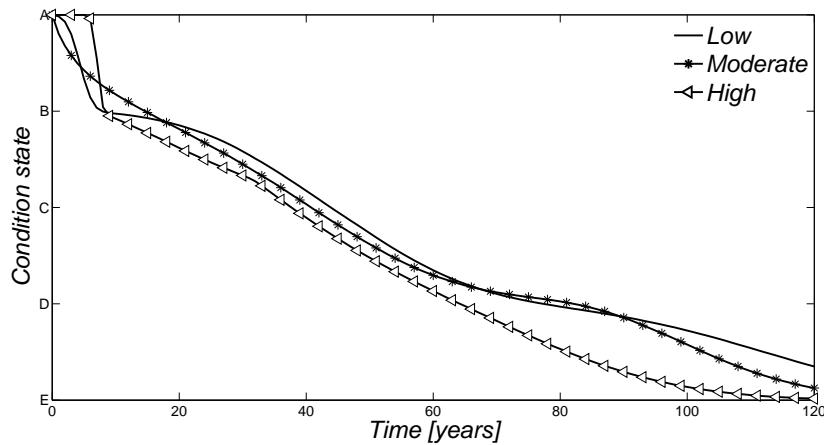
Figure 6.7 – Predicted future condition profile over time – Wind-rain action

6.5 Statistical analysis

To ensure the validity of the models proposed in this study, is it relevant to examine the independence of the variables considered. To do this, a statistical comparison of the results is performed by using an analysis of variance (ANOVA), and subsequent post hoc comparisons are made by using a Tukey multiple comparison test.

The one-way ANOVA test (Neter et al., 1996; Wu and Hamada, 2011) indicated if there are any significant differences between the means of three or more of independent variables. The statistical test compares the means between the variables and determines if any of those means are significantly different from each other, where the hypothesis is defined by:

- H_0: All group means are equal

- H_1: At least one group mean is different from the others

The statistical test can be validated through the comparison of the critical value of the F-ratio with the table F-value. The critical F-value is given by:

$$F_{critical} = \frac{SSR/(k-1)}{SSE/(n \times k - k)} = \frac{MSR}{MSE} \tag{6.3}$$

where *SSR* is the between-groups sum of squares, *SSE* is the within-groups sum of squares, *MSR* is the between-groups mean squares, *MSE* is the within-groups mean squares, k is the number of group tested and n is the number of observations in each group. If the critical F-value is greater than the table F-value or if the p-value is smaller than the significance level considered, the null hypothesis should be rejected. The table F-value has a Fisher distribution with $k-1$ and $n \times k - k$ degrees of freedom.

When the null hypothesis is rejected, it is concluded that at least the mean of one group tested is statistically different from the others. However, the ANOVA test does not indicate what groups are statistically different from that of each other. To determine which specific groups differed from each other, a Tukey multiple comparison test (Hochberg and Tamhane, 1987) must be performed. This test

is based in the studentized range distribution and it is optimal for procedure with equal sample sizes. The Tukey test compares all pairwise possible between groups and it can be stated that the groups compared are statistically different and the null hypothesis is rejected if the following relationship is verified:

$$\frac{\left|\bar{y}_i - \bar{y}_j\right|}{\sqrt{MSE \cdot \left(\frac{1}{n_i} + \frac{1}{n_j}\right)}} > \frac{1}{\sqrt{2}} \cdot q\left(\alpha; k; n \times k - k\right) \tag{6.4}$$

where $\bar{y}_i$ and $\bar{y}_j$ are the mean of groups i and j, respectively; MSE is the within-groups mean squares obtained from the one-way ANOVA test; n_i and n_j are the number of observations in group i and j, respectively; and $q\left(\alpha; k; n \times k - k\right)$ is the upper $100 \times (1 - \alpha)$th percentile of the studentized range distribution with parameter k and $n \times k - k$ degrees of freedom and a significance level α.

The one-way ANOVA test was performed in order to verify whether complete sample and the twelve subsets are independent. In other words, whether for a determined time horizon, the final condition level is influenced by the different exposures considered. The ANOVA test results are presented in Table 6.6. The statistical test was performed for five different time horizons and each variable is composed by 50 000 samples.

Table 6.6 – ANOVA test results

Time horizon (years)	*F*-critical	*p*-value
10	5784.4	0
20	5983.3	0
30	3040.1	0
40	2743.7	0
50	3440.8	0

As mentioned before, the test can be validated through the comparison of the critical *F*-value (Table 6.6) with the table *F*-value or through the comparison of the p-value with the established significance level. For a significance level of 0.05, the table *F*-value is equal to 1.752.

Through the analysis of the results obtained, it is possible to see that for the five time horizons tested the null hypothesis is rejected. This result shows that at least one group mean is statistically different from the others, but it does not identify what groups are statistically different from each other. To determine which specific groups differed from each other, a Tukey test is performed.

The Tukey test compares all possible pairwise between groups and it can state that the groups compared are statistically different and the null hypothesis is rejected if the relationship in Equation 6.4 is verified. The value on the right side of the Equation 6.4 is constant for all analysis and is equal to 3.12. The values on the left side are presented in Table 6.7. Light gray cells identify the pairwise where the null hypothesis is not rejected.

The results obtained in the statistical test can be divided into two parts. In the first part of the analysis, the complete sample was compared with each subset. The results show that the intermediate distance from the sea, SI, is statistically closer to the overall sample the complete sample for year 20, and the moderate wind-rain action, WM, is statistically nearer the complete sample for year 20 and 30. For all other exposures, the differences between the mean of the groups are statistically significant showing that the variables are relevant.

In the second part, a comparison with each family of variables was performed. From the results it can be seen that for year 10 the mean of intermediate distance from the sea (SI) and close to

Table 6.7 – Pairwise comparison

Pairwise		Time horizon (years)				
		10	**20**	**30**	**40**	**50**
G	DL	11.91	45.99	50.99	38.03	25.35
G	DH	118.79	79.18	51.42	48.43	42.96
G	SI	90.37	2.88	11.38	8.04	5.45
G	SF	53.71	53.01	62.77	75.65	82.88
G	SC	87.34	76.64	68.20	48.95	45.46
G	OE	33.98	30.36	20.56	21.35	16.47
G	ON	26.42	37.97	34.13	18.28	6.11
G	OW	51.68	59.23	3.35	22.79	48.50
G	OS	22.97	101.18	12.78	23.39	67.51
G	WH	99.90	60.07	35.40	38.84	37.56
G	WM	6.53	1.31	2.66	5.18	6.13
G	WL	80.33	18.34	39.59	33.58	24.90
DL	DH	130.70	125.17	102.40	86.46	68.30
SI	SF	144.08	55.89	51.39	67.61	77.43
SI	SC	3.02	73.75	79.58	56.98	50.90
SF	SC	141.05	129.64	130.97	124.59	128.34
OE	ON	7.56	7.61	13.57	3.07	10.36
OE	OW	17.70	28.87	17.21	44.14	64.97
OE	OS	56.96	131.54	7.78	44.74	51.04
ON	OW	25.27	21.26	30.78	41.07	54.61
ON	OS	49.39	139.15	21.35	41.68	61.40
OW	OS	74.66	160.41	9.43	0.60	116.01
WH	WM	93.37	61.38	32.74	33.66	31.43
WH	WL	19.58	78.41	74.99	72.42	62.46
WM	WL	73.80	17.04	42.25	38.76	31.03

the sea (SC) are statistically closer, and for year 40 there is a significant dependence between the variables Orientation – East (OE) and Orientation – North (ON) and Orientation – West (OW) and Orientation – South (OS). In the remaining situations, the differences between the mean of the groups are statistically significant showing that the variables are independent.

Finally, from the results obtained in the independence analysis, it can be concluded that the different environmental factors have significantly different impacts on the performance of the façades during their life.

6.6 Maintenance model

The methodology described in Chapter 4 was applied to analyse the deterioration patterns of ceramic claddings. The Petri net maintenance model for claddings is illustrated in Figure 6.8. The Petri net is composed by 39 places and 47 transitions. The meaning of each place and transition present in the maintenance model is defined in Chapter 4.

Maintenance is usually not considered for ceramic claddings, resulting in very deteriorated façades. In fact, this type of building material is frequently assumed to be maintenance free (Thai-Ker and Chung-Wan, 2006). They excel in durability, appearance stability and other important characteristics as hygiene, cleaning ease and efficiency, and resistance to aggressive environment, meaning no main-
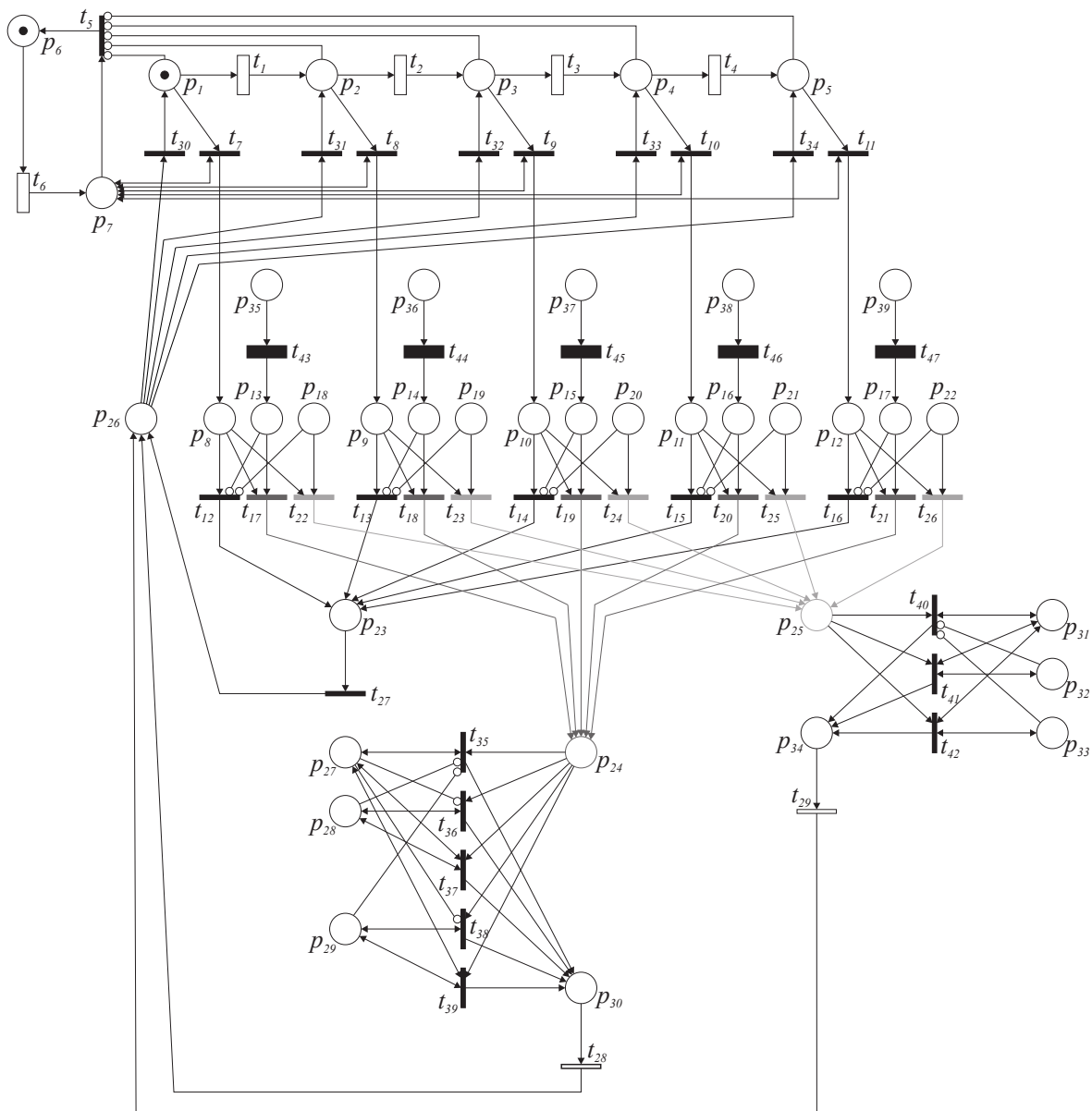
Figure 6.8 – Petri net scheme of the maintenance model for claddings

tenance is required for a long time (Plšková et al., 2011). However, due to exposure to all types of environmental conditions, as well as, faulty design and execution errors, ceramic claddings can deteriorate prematurely and defects start to be visible in the first 2 years after construction (Shohet et al., 2002). These defects can be easily revealed, measured and controlled through regular inspections and an adequate maintenance program. However, regular inspections on buildings are not mandatory and the performance levels of the different building components are defined by the owners (Shohet et al., 2002; Thai-Ker and Chung-Wan, 2006).

According to Silva et al. (2016c), the probabilistic distribution of degradation conditions over time can be seen as an assessment of the risk of performance loss due to deterioration. That is, by establishing a threshold of acceptable risk, a stakeholder may estimate the need for repair based on the probabilistic analysis of a set of data. To illustrate this concept, one can consider that "high", "average" and "low" probabilities of a given condition correspond to "high", "average" and "low" risks associated to the consequences of the defects and the cost of repair and thus produce an indication of the urgency to maintenance and repair actions (Table 6.8).

Table 6.8 – Association of the risk with the extension of the defects and the maintenance actions required (Silva et al., 2016c)

Risk	Action to take	Probabilities
Low	No maintenance is required beyond monitoring the evolution of degradation	Probability higher than 75% of belonging to more favourable condition levels
Average	Repair works are required	Intermediate condition levels
High	Need to extensive repair	Probability higher than 25% of belonging to worst condition levels

Madureira et al. (2017), during fieldwork and based on technical documents and on the literature proposed four intervention levels for ceramic tiling façades: cleaning, minor interventions and major interventions (Table 6.9).

Table 6.9 – Association of the risk with the extension of the defects and the maintenance actions required (adapted from Madureira et al., 2017)

Action type	Description of the maintenance	Frequency
Inspection	– Check for adhesion loss, colour change, cleaning needs, *graffiti*; – Check for localized stains: humidity, laying material, biological colonization, efflorescence; – Check for joints, namely efflorescence, wearing, biological colonization, colour change; – Check for cracks, broken elements, gaps, detachments.	Every 3 years
Cleaning	– Clean with damp sponge. For deep stains, use a detergent and light brushing.	Every 10 years
Minor intervention	– Joints filling material treatment; – Reinforce the laying material; – Repair localizer elements.	Every 13 years
Major intervention	– Replacement of elements with new ones.	Every 26 years

6.6.1 Maintenance strategies

In this work, to evaluate the performance of ceramic claddings, three maintenance strategies were considered:

1. Only major intervention;

2. Combination of minor and major interventions; and

3. Combination of cleaning, minor and major interventions.

The transitions times that specify the movement between different deterioration levels of the ceramic claddings, denoted by transitions t_1 - t_4 in Figure 6.8, are assumed to follow Weibull distributions with parameters (α_i, β_i), with $i = 1, 2, 3, 4$, shown in Table 6.10. The Weibull distribution was chosen based on the results presents in Section 6.3.

Regarding periodicity of inspections, it is assumed that the time interval between inspections is set to follow a triangular distribution with 3, 4, and 5 years representing the minimum, most likely, and

Table 6.10 – Parameters of the Weibull distribution

Transition	t_1	t_2	t_3	t_4
α_i	7.0859	26.5108	23.2276	32.3015
β_i	1.0973	1.9847	19.6844	20.2604

maximum values, respectively. This values were defined based on the studies of Silvestre and de Brito (2005), Thai-Ker and Chung-Wan (2006), and Madureira et al. (2017).

The major intervention is considered a corrective maintenance, and is applied when façades have the highest deterioration level and the lifetime of the façade is reached. In this study, it is considered that ceramic claddings reach the end of their service life when the deterioration level reaches Level D or higher, and their replacement has a probability of 50% of rehabilitating the façade to Level A and a probability of 50% of rehabilitating the façade to Level B.

The minor intervention is also considered a corrective maintenance, and is applied when façades show an intermediate deterioration level. This type of maintenance is performed when deterioration reaches Level C, having a probability of 50% of improving the condition of the façade to Level A and a probability of 50% of rehabilitating the façade to Level B. In the minor intervention, it is assumed that 20% of the ceramic tiles are replaced; 30% of the fissures are filled; 10% of the joint material are filled; and the surface dirt is removed.

The cleaning operation is considered a preventive maintenance and it is applied at regular time intervals. This maintenance action is applied whenever an inspection is performed and the coating is in Level B but the last maintenance action has been applied more than 10 years before. It has a probability of 31.4% of improving the condition of the façade to Level A and a probability of 68.6% of not improving performance. It should be mentioned that the effects of the maintenance actions were defined based on experience and engineering judgement.

In these maintenance strategies it is assumed that after two consecutive cleaning operations this maintenance action is no longer efficient, making it necessary to apply a minor intervention in order to recover the anomalies present in the ceramic cladding. It is also considered that after three minor interventions this maintenance action is no longer efficient, being necessary to apply a major intervention. Regarding the restrictions of the reset transitions: when the cleaning operation is applied, the time delay of transition t_{44} is initialized; when the minor intervention is applied, the number of cleaning operations in place p_{36} and the time delay of transition t_{44} are initialized; and finally, when the major intervention is applied, the number of major interventions in place p_{21} and p_{22}, the number of minor interventions in place p_{20}, the number of cleaning operations in place p_{36} and the time delay of transition t_{44} are initialized.

6.6.2   Results

Considering a 100-year time horizon and a ceramic façade at perfect condition at $t = 0$, the condition profile obtained for the three maintenance strategies and the condition profile for the situation without maintenance are plotted in Figure 6.9.

These results show that all considered maintenance strategies have a significant impact on the mean condition level. In fact, for all maintenance strategies, the mean condition level never goes beyond Level B. In terms of dispersion of results, the values range, on average, between 0.4 and 0.8, with maintenance strategy 1 resulting in larger dispersions.

Maintenance strategy 1 represents the maintenance strategy currently implemented by most owners. The results obtained are in agreement with the information observed in the literature. According to
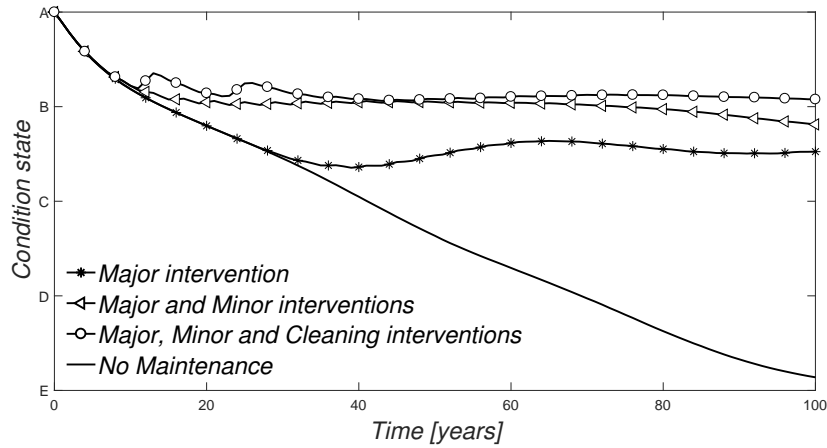
(a) Mean condition
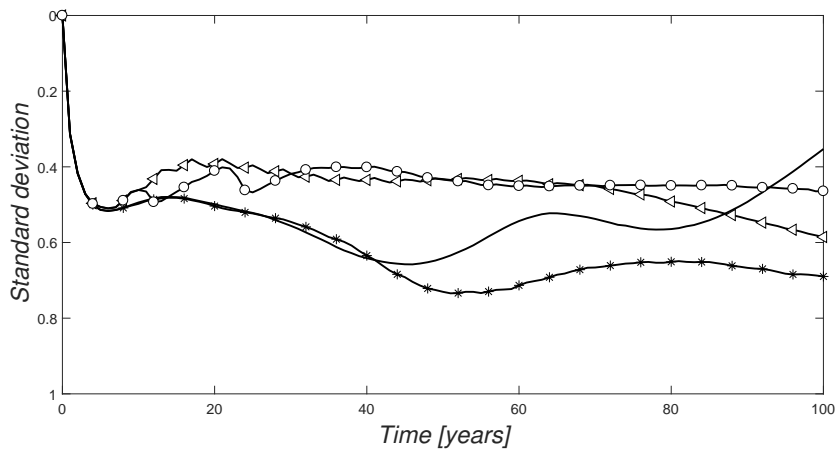
(b) Standard deviation of condition

Figure 6.9 – Comparison of the predicted mean condition profile over time for all maintenance strategies considered. Mean and standard deviation are computed considering a correspondence between the condition scale and an integer scale between 1 and 5

Silva et al. (2016b), the end of the service life of a ceramic cladding varies between 46 and 58 years, at which point maintenance is required. Through Tables 6.11 and 6.12, it can be observed that for the time horizon of 100 years, there are, on average, 1.40 major interventions, and the first intervention is applied approximately at year 55.3. A value that is within the range defined by the literature despite being slightly higher than the value usually adopted for the reference service life of 50 years (Silva et al., 2016c).

Table 6.11 – Number of interventions for maintenance strategy 1

Number of interventions	Major intervention [%]
0	0.400
1	59.692
2	39.710
3	0.198

Tables 6.13 and 6.14 show the distribution of the number of interventions and the statistics of the

Table 6.12 – Statistics of the time of the first intervention (in years) for maintenance strategy 1

Intervention	Minimum	Maximum	Average	Standard deviation
Major	22	100	55.3	13.7

time of the first intervention for maintenance strategy 2, respectively. From these results, it can be observed that for the time horizon of 100 years, there are, on average, 0.05 major interventions and 2.65 minor interventions, and the first major intervention is performed at year 91.9 and the first minor intervention is applied approximately at year 32.8. The results obtained for maintenance strategy 2 are slightly different from the maintenance operations proposal by Madureira et al. (2017). In this paper, the authors suggest that minor interventions should be applied every 13 years, while the results obtained in maintenance strategy 2 suggest that minor interventions should be performed every 33 years, i.e. 20 years later. But the results obtained are consistent with Silva et al. (2016c), that states that light maintenance actions should be performed before year 40. Furthermore, it is possible to verify that the combination of minor and major interventions increases the estimated service life from 55.3 to 91.9 years.

Table 6.13 – Number of interventions for maintenance strategy 2

Number of interventions	Major intervention [%]	Minor intervention [%]
0	94.686	0.006
1	5.314	3.358
2	–	28.590
3	–	67.614
4	–	0.408
5	–	0.024

Table 6.14 – Statistics of the time of the first intervention (in years) for maintenance strategy 2

Intervention	Minimum	Maximum	Average	Standard deviation
Major	55	100	91.9	7.3
Minor	4	98	32.8	13.8

According to the results obtained for maintenance strategy 3, on average, until year 14.9 (Table 6.16) ceramic claddings are only monitored. This result is in agreement with the literature. Silva et al. (2016c) state that ceramic claddings should be monitored until year 13. Furthermore, the combination of cleaning, minor and major interventions increases the estimated service life from 55.3 to 88.9 years, and delays the minor intervention from 32.8 to 46.5 years. From Table 6.15, for a time horizon of 100 years, it is possible to verify that there are, on average, 0.006 major interventions, 1.81 minor interventions and 4.00 cleaning operations.

With the aim of reducing maintenance costs, the costs of the three maintenance strategies are examined. To do so, the life-cycle costs are compared and focus is placed on the influence of direct costs and the discount rate. Figure 6.10 shows the mean cumulative cost for the three maintenance strategies considering 0 and 5% discount rates, while the direct costs of each maintenance strategy are presented in Table 6.17. The mean cumulative cost of maintenance strategy based only in the major intervention is lower than the maintenance strategy based in major, minor and cleaning interventions. However, this difference is lower when the discount rate is equal to 0% (Figure 6.10(b)).

Table 6.15 – Number of interventions for maintenance strategy 3

Number of interventions	Major intervention [%]	Minor intervention [%]	Cleaning operation [%]
0	99.370	0.314	0.002
1	0.630	36.098	0.020
2	–	46.056	3.480
3	–	17.472	13.934
4	–	0.058	63.488
5	–	0.002	17.088
6	–	–	1.986
7	–	–	0.002

Table 6.16 – Statistics of the time of the first intervention (in years) for maintenance strategy 3

Intervention	Minimum	Maximum	Average	Standard deviation
Major	56	100	88.9	9.7
Minor	4	100	46.5	19.0
Cleaning	11	92	14.9	5.2

Furthermore, it should be noted that mean condition profile of these two maintenance strategies is considerably different.

Table 6.17 – Maintenance cost

Intervention	Cost [€/m^2]
Major	52.15
Minor	22.59
Cleaning	9.13

6.7   Summary

In the first part of this chapter, the Petri net model is used to predict the deterioration of ceramic claddings over time and to understand how the different exposure to environmental contribute to the overall degradation. The deterioration rates were estimated from available historical date and five probability distributions (Exponential, Weibull, Gumbel, Lognormal and Normal) were analysed in order to identify which distribution has a better fit to the historical date. The use of the Exponential distribution to model the sojourn time was considered a particular study case. By comparing the results obtained from the Petri net with exponentially distributed transition rates and the results obtained by Silva et al. (2016c) using Markov chains, it was possible to validate the deterioration model proposed. The use of the other four distributions (Weibull, Gumbel, Lognormal and Normal) showed the limitation of the exponential distribution to model the deterioration phenomenon and, consequently, the limitation of the Markov chains. From the results of the probabilistic analysis performed, it was found that the use of distributions with two parameters improves the value of the log-likelihood. The log-likelihood values of the four distributions are quite similar; however, the Weibull distributions shows a minor log-likelihood value and, consequently, a better fit to the historical date. In addition, when comparing the results of the probabilistic analysis of the ceramic claddings and the bridge elements, it is verified that the Weibull distribution is the one that shows a better fit in the three situations.

(a) 5% discount rate

(b) 0% discount rate
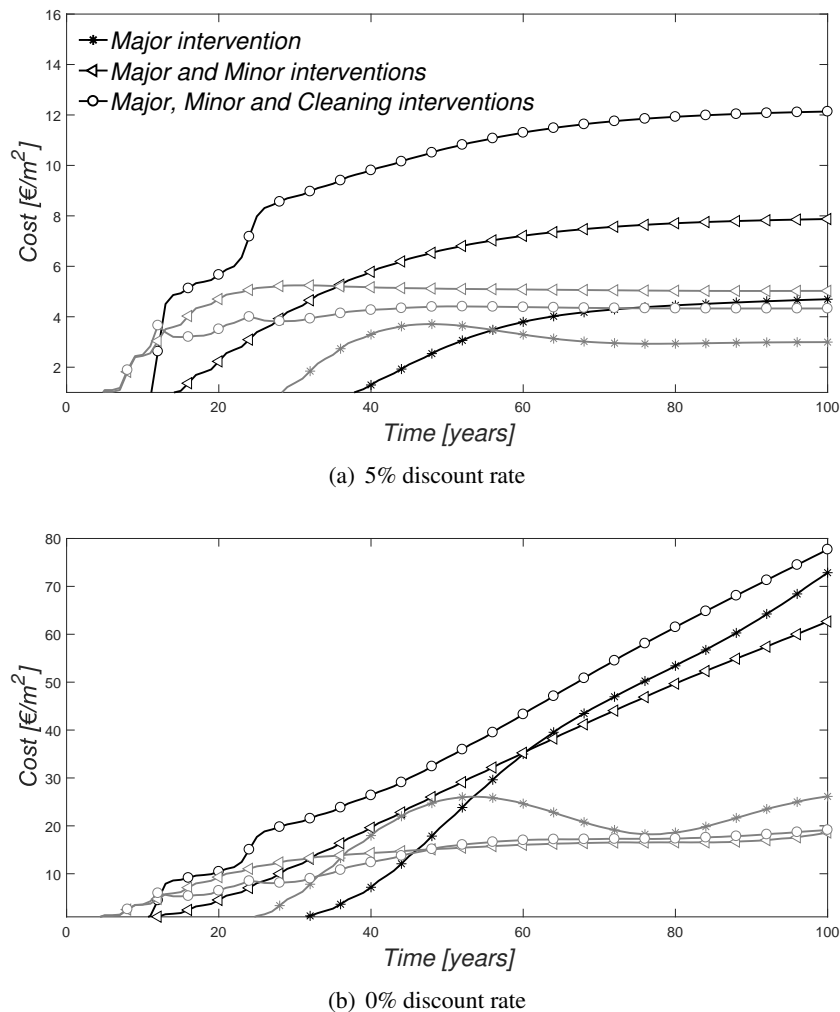
Figure 6.10 – Cumulative cost profiles for three maintenance strategies considered. Black lines represent the mean cumulative cost and the gray lines the standard deviation of the mean cumulative cost

Relatively to the environmental actions, claddings close to the coastal areas, with high exposure to damp and wind-rain actions, orientated to the North are more likely to be in the most unfavourable condition levels (approximately a probability of 70%). On the other hand, claddings far away from the sea are the more likely to remain in lower degradation conditions.

To evaluate the performance of ceramic claddings under maintenance actions, three maintenance strategies were considered: (1) only major intervention; (2) combination of minor and major interventions; and (3) combination of cleaning operations, minor and major interventions. The Weibull distribution was chosen as the appropriate distribution to sample the transition times in the deterioration process, and the Triangular distribution was chosen to model the interval between inspections.

Through the analysis of the predicted future condition profiles over time, it is possible to verify that any of the defined maintenance strategies has a significant impact on the mean condition. Results show that more regular interventions, through the application of minor intervention and cleaning operations improve the condition level even if causing an increase in life-cycle cost.

Chapter 7

Case Study 3: Transportation Network

7.1 Introduction

An extreme event, such as a hurricane, an earthquake, or a floods, can significantly affect the road network of any region (Bocchini and Frangopol, 2012). A road network, in addition to playing a major role in the socio-economic development of a region, is an extremely important means of emergency response and recovery activities after the occurrence of an extreme event. For these reasons, it is required that lifelines are designed to maintain their serviceability even in the case of so-called "low-probability high-consequence" events, to ensure prompt interventions and a fast restoration of the normal activities (Frangopol and Bocchini, 2012).

In a transportation network, bridges are the most fragile component (Frangopol and Bocchini, 2012). Indeed, bridges can suffer structural damage and cause severe disruptions in traffic flow. Therefore, it is very important that bridges, as crucial components, preserve their serviceability even in the case of extreme events. However, the ageing of network in the more developed countries and the scarcity of funding for maintenance and rehabilitation actions make it generally impossible to carry out simultaneous interventions in all infrastructures requiring care (Scherer and Glagola, 1994). Therefore, decision-makers have to prioritize the interventions that provide the most considerable contributions toward the restoration of the original performance in terms of traffic flow capacity (Bocchini and Frangopol, 2012).

In order to quantify the rapidity of rehabilitation of infrastructure and the restoration of traffic flow, it has become frequent the use of the concept of resilience. Over the years, several studies have addressed the problem of assessing resilience in different areas. For example, Rose and Liao (2005) worked on the theoretical formulation of resilience and applied the concept to water distribution systems. Bruneau and Reinhorn (2007) and Cimellaro et al. (2010b) studied resilience in the hospital system. Çağnan et al. (2006) and Xu et al. (2007) developed a technique for the restoration of the energy distribution system after an earthquake. Miles and Chang (2006) proposed a model for recovery of buildings and vital systems to the society after the occurrence of an earthquake.

7.2 Resilience in transport networks

According to Chen and Duan (2014), there are several parameters that can be used to quantify the performance of systems regarding tolerance to damage, such as: redundancy, vulnerability, robustness, resilience, among others.

However, today, resilience is the most accepted parameter by the scientific community as the best

way to measure the level of performance in transport networks. Resilience quantifies the capacity of a system to withstand an unusual perturbation and to recover from the damage caused quickly and economically efficient (Bocchini and Frangopol, 2012; Bocchini et al., 2014).

7.2.1 Conceptual definition of resilience

Several conceptual definitions of resilience have been proposed and discussed in the literature over the last years (Zhou et al., 2010). The first definition of resilience was introduced in the 1970s by Holling (1973). Holling (1973) studied resilience in ecological systems, and his definition focused only on one aspect: resilience can be measured by the magnitude of disturbance that a system can tolerate and still persist.

However, the definition of resilience that served as the basis for the most popular definition was only proposed years later by Timmennan (1981): resilience is the ability of human communities to withstand external shocks or perturbations and to recover from such perturbations. This definition introduces two important aspects: (1) when dealing with civil engineering, resilience is a property of communities rather than structures or infrastructure; (2) resilience is not only about being able to withstand a certain disturbance, but also about having resources and means for a prompt, efficient, and effective recovery (Bocchini et al., 2014).

These two aspects are clearly bonded. For example, the ability of a bridge to withstand an unusual external shock depends almost exclusively on its structural characteristics, but the recovery process is affected heavily by the technological, economic, and political conditions of the community interested in restoring the bridge. Moreover, the impact of the bridge damage and service condition in terms of traffic disruption and user costs, as well as the socio-economic benefits of a prompt recovery, are necessarily measured at the regional community level (Bocchini et al., 2014).

According to Bocchini et al. (2014), in the various conceptual definitions that have been proposed over the years, two general trends can be observed. The first is that the aspects of resistance to an unusual external shock (often referred as "robustness") and ability to recover quickly (often called "rapidity") have become a constant of almost all definitions. The second trend is the expansion of the definition by adding many other aspects. Starting from a single aspect considered in the first definition (Holling, 1973) and two aspects combined in the second definition (Timmennan, 1981), until Bruneau et al. (2003) provided a comprehensive description of resilience that accounts for at least 11 different aspects (Figure 7.1).

According to Bruneau et al. (2003), for the case of urban communities and infrastructure, resilience has four dimensions:

1. **Technical** – includes all the aspects associated with the construction and the other technological aspects;

2. **Organizational** – deals with the management plan, maintenance, and response to emergencies;

3. **Social** – involves the impact on the society and its mitigation; and

4. **Economic** – addresses indirect and direct costs associated with the reduction of functionality of the infrastructure and its rehabilitation.

These can be characterized by four properties:

1. **Robustness** – ability of elements, systems or other units of analysis to withstand a given extreme event without suffering disproportionate degradation or loss of function. This property is often measured by the level of residual functionality after the event occurrence;
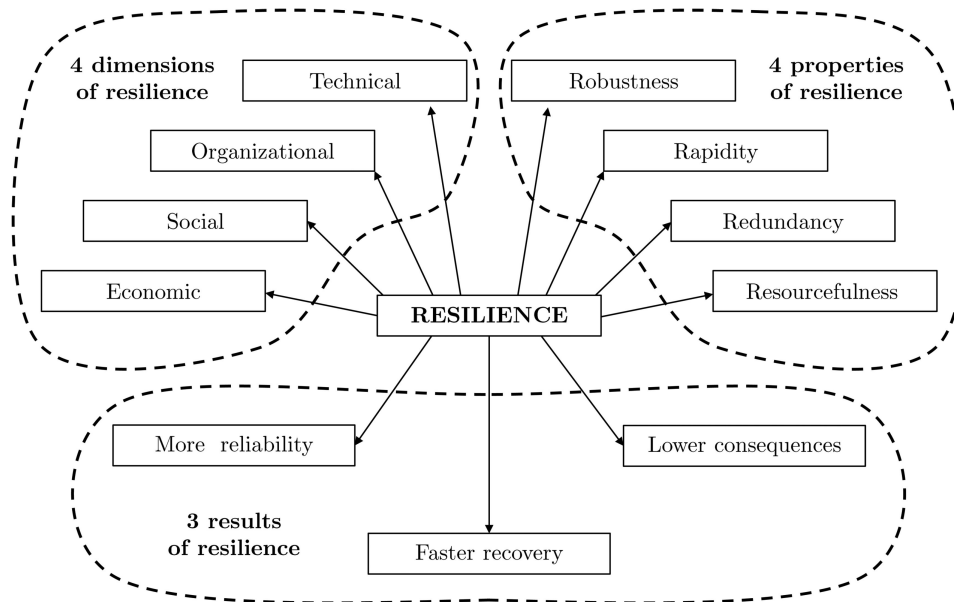
Figure 7.1 – Aspects of resilience considered in the definition of Bruneau et al. (2003) (Bocchini et al., 2014)

2. **Rapidity** – ability to meet priorities and achieve goals in a timely manner in order to contain losses and avoid future disruptions;

3. **Redundancy** – extension in which there are elements, systems or other units of analysis that are substitutable, that is, capable of satisfying functional requirements in the event of interruption, degradation or loss of functionality; and

4. **Resourcefulness** – ability to identify problems, prioritize and mobilize resources when conditions threaten to disturb any element, system or other unit of analysis. It may also consist of the ability to apply materials (i.e. monetary, physical, technological, among others) and human resources to meet established priorities and achieve goals.

And provides three results:

1. A resilient system is **more reliable**, since it has a lower probability of violating limit states. Robustness guarantees that even in case of extreme events, the extent of damage and the reduction of functionality are small;

2. Resilience is associated with **fast recovery**. The rapidity in the functionality restoration during a disaster is a paramount characteristic of resilient systems;

3. Resilience implies **low socio-economic consequences**. The reduced probability of significant service level reduction and fast recovery contributes to the reduction of the impact of extreme events on the society.

Other conceptual definitions of resilience have been proposed after 2003, specifically applying to lifelines (Chang and Shinozuka, 2004; Rose and Liao, 2005; Çağnan et al., 2006; Xu et al., 2007), distributed infrastructure systems (Miles and Chang, 2006; Bruneau and Reinhorn, 2007), and many other systems (Rose, 2004). All these definitions have common roots and traits, but each of them emphasizes different aspects, particularly those that are relevant for the considered application. However, the definition by Bruneau et al. (2003) remains the most popular among researchers.

7.2.2 Analytical definition of resilience

Bruneau et al. (2003), in addition to providing the most comprehensive conceptual definition of re-
silience accepted by the scientific community, have also introduced the so-called "resilience triangle".
This idea is the basis of a whole family of analytical definitions of resilience. The resilience triangle
is used to describe the loss of resilience rather than the resilience itself (Bocchini et al., 2014). Figure
7.2 illustrates the graphical interpretation of the triangle of resilience.
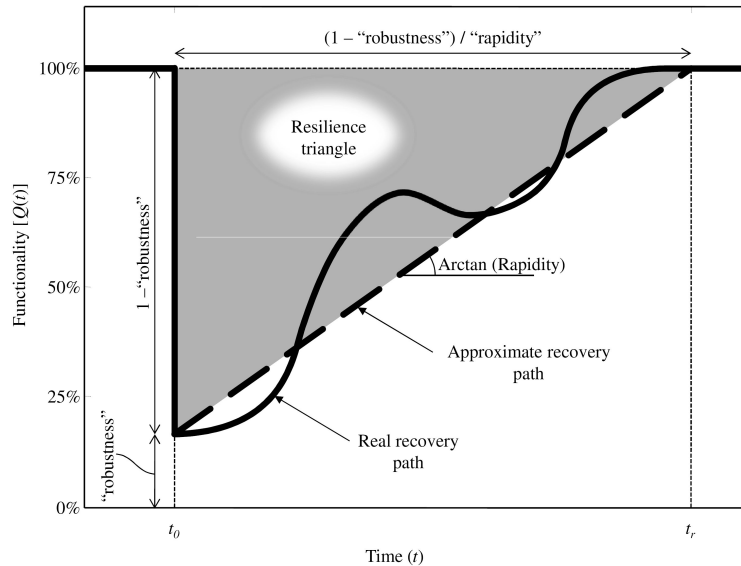
Figure 7.2 – Resilience triangle (shaded area); at $t = t_0$ the external event occurs, and at $t = t_r$ the
recovery is complete (Bocchini et al., 2014)

As can be seen in Figure 7.2, the quantification of resilience is strictly connected to the quantification
of functionality (the vertical axis) over time (the horizontal axis). After the occurrence of an extreme
event at time t_0, the quality of service of the investigated system (e.g. a bridge or a road network) is
immediately reduced. It is expected, however, that the system rehabilitation will occur gradually over
time, as shown in Figure 7.2, until time t_r, when the quality of service of the system is fully recovered
(Bruneau et al., 2003).

The resilience triangle is the shaded region above the linear approximation (dashed line) of the func-
tionality recovery path. The three edges of the triangle are particularly important:

- The vertical edge measures the quantity $(1 - robustness)$, which express the loss of functional-
  ity due to the extreme event;

- The horizontal edge represents the total recovery time, which can be expressed in terms of
  rapidity (average slope of the recovery path):

$$t_r - t_0 = \frac{1 - robustness}{rapidity} \tag{7.1}$$

- Finally, the hypotenuse represents the linear approximation of the functionality recovery path.

The area of the resilience triangle represents an approximation of the resilience lost by the investigated
system due to an extreme event. A more precise formulation to determine the resilience lost by the
system is given by (Bruneau et al., 2003):

$$R_L = \int_{t_0}^{t_r} [100 - Q(t)] \, dt \tag{7.2}$$

where R_L is the loss of resilience experienced by the system, t_0 is the time instant when the extreme event occurs, t_r is the time when the functionality of the system is fully restored, Q is the percentage "functionality" (or "quality", or "serviceability") of the system, and t is time.

In the conceptual definition introduced by Bruneau et al. (2003), resilience is defined as being dependent on four properties: robustness, rapidity, redundancy and resourcefulness. However, in the analytical definition only the first two properties are defined. Redundancy and resourcefulness, although strongly coupled with the definition of resilience, are two complex properties, since they depend on human factors and available resources, making them very difficult to model. However, it is recognized that a change in redundancy and/or resourcefulness can significantly affect the shape and slope of the recovery curve, as well as the recovery time t_r, which causes the robustness and rapidity properties to be directly affected (Cimellaro et al., 2010b).

For this reason, Bruneau et al. (2003) make a distinction of the properties between "means" and "ends". For example, robustness and rapidity are essential to the desired "ends" to be achieved through measures that improve resilience, and these outcomes are the ones that most deeply affect decisions made by managers. On the other hand, redundancy and resourcefulness are the measures that define the "means" by which resilience can be improved. That is, resilience can be increased by adding redundant elements to a system.

However, Equation 7.2 has the important merit of analytically connecting the concepts of resilience and functionality. This expression was used in several studies (Bruneau and Reinhorn, 2006, 2007; Bruneau, 2006).

After that, a different approach was proposed by Cimellaro et al. (2006) and Cimellaro et al. (2010b), this formulation focuses on the determination of resilience, not on the calculation of its loss:

$$R = \int_{t_0}^{t_r} Q(t)\, dt \tag{7.3}$$

This definition branches out from the resilience triangle and has the advantage of being able to take into account rehabilitation patterns that lead to a final functionality different of 100%, i.e. lower or even higher. However, this formulation has a drawback that makes it unsuitable for some applications, as the integral is calculated between t_0 and t_r, can result in low resilience values for fast rehabilitation strategies (Figure 7.3) (Bocchini and Frangopol, 2011b).

To overcome this limitation, Bocchini and Frangopol (2012) modified the expression of Equation 7.3 to a fixed time horizon, t_h:

$$R = \int_{t_0}^{t_0+t_h} Q(t)\, dt \tag{7.4}$$

Figure 7.4 shows that this definition correctly provides higher (i.e. better) values of resilience for the faster (i.e. better) recovery paths. The definition in Equation 7.4 can be used to compare, rank, and optimize the various disaster management strategies. The investigated time horizon, t_h does not need to be chosen larger than the longest recovery time. In fact, if the recovery is not complete at $t = t_0 + t_h$, Equation 7.4 is still applicable and yields, as expected, a small value of resilience (Bocchini and Frangopol, 2011b).

Unfortunately, Equation 7.4 still shares a shortcoming with Equations 7.2 – 7.3. In these three cases, resilience is measured in units of time, since the functionality of the system, $Q(t)$, is non-dimensional. Although Equation 7.4 calculates the correct values for resilience, expressed in units of time, these can be difficult to interpret and communicate to managers (Bocchini and Frangopol, 2011b). For this reason, the resilience index was normalized (Cimellaro et al., 2010a; Bocchini and Frangopol, 2011b):
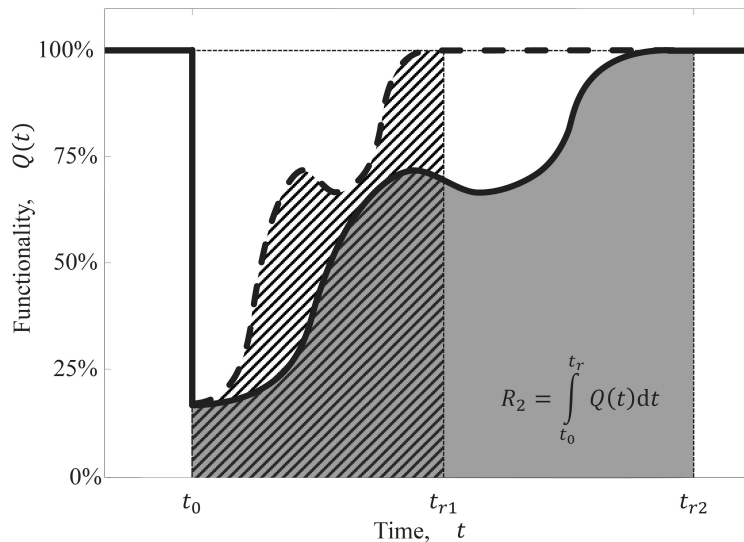
Figure 7.3 – Resilience according to Equation 7.3. The faster recovery path (dashed) yields a lower value of resilience (area with diagonal pattern) than the slower recovery path (solid) (Bocchini and Frangopol, 2011b)
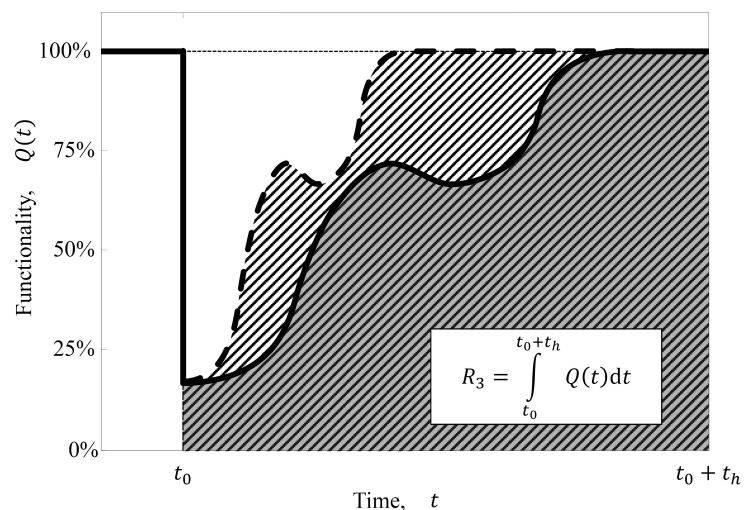
Figure 7.4 – Resilience according to Equation 7.4. The faster recovery path (dashed) correctly yields a higher value of resilience (area with diagonal pattern) than the slower recovery path (solid) (Bocchini and Frangopol, 2011b)

$$R = \frac{\int_{t_0}^{t_0+t_h} Q(t)\, dt}{t_h} \tag{7.5}$$

where the numerator represents the area underneath the recovery path, $Q(t)$ and the denominator represents the value of resilience in case the event did not occur or had no effects on functionality (i.e. $100\% \times t_h = t_h$). Figure 7.5 provides the graphical interpretation of Equation 7.5.

Depending on the general frameworks and applications where the analytical definitions of resilience in Equations 7.2 – 7.5 are used, each of them can be appropriate. However, Equation 7.5 is the most versatile and easy to use for decision-makers.

As previously noted, the definition of resilience is based on the concept of functionality and is defined as the integral in time of the system's functionality. However, there is some difficulty in defining and
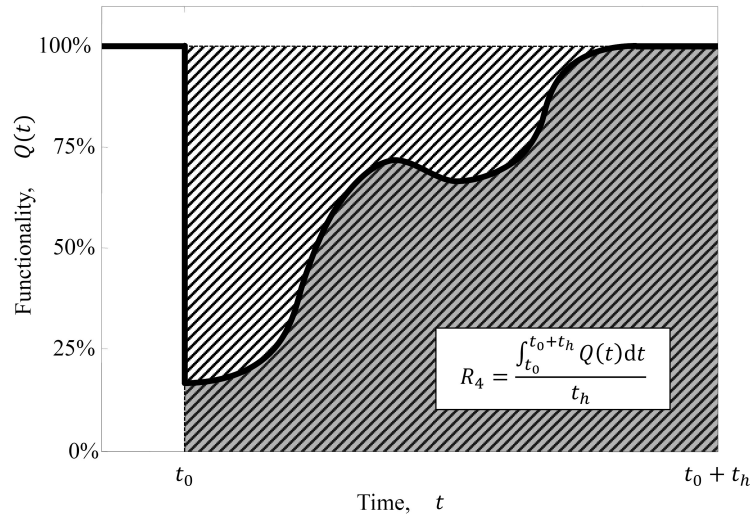
Figure 7.5 – Resilience according to Equation 7.5. The numerator of Equation 7.5 is the shaded area, the denominator is the area of the large rectangle (area with diagonal pattern) (Bocchini and Frangopol, 2011b)

quantifying this parameter for some types of systems, as clear measures of the functionality are not always available. Functionality can be measured in a number of ways according to the problem at hand (Bruneau et al., 2003; Cimellaro et al., 2010b). In the literature, several performance indicators and definitions of functionality that can be considered to quantify the service quality of road networks have been proposed (Scott et al., 2006; Liu and Frangopol, 2006; Ng and Efstathiou, 2006; Bocchini and Frangopol, 2012).

Bocchini and Frangopol (2012) proposed a computational framework based on multi-objective optimization for the rehabilitation of bridges after extreme events along a highway segment. In this methodology, the functionality of the network is determined through the following expression:

$$Q(t) = 100 \times \frac{\Gamma(t) - \Gamma^0}{\Gamma^{100} - \Gamma^0} \tag{7.6}$$

where $\Gamma(t)$ represents the performance of the network, Γ^{100} is the value of $\Gamma(t)$ when all bridges are in service, and Γ^0 is the value of $\Gamma(t)$ when none of bridges is in service. $\Gamma(t)$ is defined as:

$$\Gamma(t) = \frac{1}{\gamma_T \times TTT(t) + \gamma_D \times TTD(t)} \tag{7.7}$$

where γ_T is a balancing factor (cost) associated with the time spent by the users in the network, measured in $time^{-1}$, and γ_D is a similar factor associated with the distance travelled, measured in $length^{-1}$. For the present work the following values are considered (Bocchini and Frangopol, 2012):

$$\gamma_T = 2.00 \times 10^{-7} \; min^{-1} \tag{7.8}$$

$$\gamma_D = 6.21 \times 10^{-8} \; km^{-1} \tag{7.9}$$

In Equation 7.7, $TTT(t)$ and $TTD(t)$ represent, respectively, the total travel time and the total travel distance. The first parameter is the sum of all the time spent by the users to reach their destination

and the second parameter corresponds to the distance travelled by all users. Equations 7.10 and 7.11 illustrate, respectively, the parameters $TTT(t)$ and $TTD(t)$.

$$TTT(t) = \sum_{x \in X} \sum_{y \in Y} q_{xy}(t) \times c_{xy} \qquad (7.10)$$

$$TTD(t) = \sum_{x \in X} \sum_{y \in Y} q_{xy}(t) \times L_{xy} \qquad (7.11)$$

where X is the set of nodes of the network, Y is the subset of nodes connected to node x, $q_{xy}(t)$ is the traffic flow (number of equivalent vehicles per unit time) transiting over the highway segment between nodes x and y, c_{xy} is the time required to cover the highway segment x - y with traffic flow q_{xy}, and L_{xy} is the length of highway segment x - y.

The methodology used by Bocchini and Frangopol (2012) is based on the bottleneck assumption. That is, the traffic capacity of a segment of the network depends only on the residual traffic capacity of the most damaged bridge. In this model, the damage level of each bridge is described by a real value in the range $[0,4]$, where 0 and 4 represent, respectively, the condition state "no damage" and "collapse" (Frangopol and Bocchini, 2012).

The bridge damage level, $l_b(t)$, affects the functionality of the bridge, in terms of its ability to carry traffic flows. For example, when the damage level is moderate $(l_b \geq 2)$, the bridge in unsafe and should be prudentially closed to traffic. Therefore, its functionality, $q_b(t)$, is null (Table 7.1). On the other hand, if the damage is between minor and moderate $(1 \leq l_b < 2)$ the bridge can be partially open to traffic, but its capacity should be limited. In fact, by opening only some lanes, the parts of the structure more affected by damage can be protected and the overall traffic loads can be reduced, leading to a partial reduction of the bridge functionality. When the rehabilitation activities start on a bridge that has damage in this range (from minor to moderate), additional lanes have to be closed and the bridge is likely to be out of service. Finally, if a bridge has only very minor damages $(0 \leq l_b < 1)$, the rehabilitation activities require a partial reduction of the traffic flow capacity. However, while the rehabilitation works are not in progress, the bridge is fully open to traffic. Table 7.1 summarizes the bridge states and the bridge functionality for various damage levels (Frangopol and Bocchini, 2011).

Table 7.1 – Bridge functionality (Frangopol and Bocchini, 2011)

Damage level	Rehabilitation in progress	Bridge state	Functionality, q_b
$2 \leq l_b \leq 4$	Yes	Out of service	0
	No	Out of service	0
$1 \leq l_b < 2$	Yes	Out of service	0
	No	Partially in service	0.5
$0 \leq l_b < 1$	Yes	Partially in service	0.5
	No	In service	1

The methodology implemented by Bocchini and Frangopol (2012) is simple. The traffic capacity of the network segment depends only on the residual traffic capacity of the most damaged bridge and the bridge functionality is defined by three states (out of service, partially in service, or in service). This methodology can be improved with a traffic model, where it is possible to model the traffic behaviour of damaged bridges in a more realistic way, according to the constraints imposed for each situation.

7.3 Traffic model

The traffic model implemented is based on the macroscopic approach described by Tolba et al. (2005). It is a bottom-up approach, where the concept of continuous timed Petri net is used to build a modular model to describe a highway traffic system. This method is composed by two steps: decomposition and composition. Decomposition consists in partitioning a system into several systems, based on structural entities, i.e. highway segments, on-ramp and off-ramp links. On the other hand, composition involves the interconnections of these sub-models into a complete model, representing the whole system (Fanti et al., 2014). All these sub-models are modelled by CTPN.

As mentioned in Chapter 3, CTPN's are an extension of the original concept of Petri nets and are extensively used to model dynamic systems (Murata, 1989). A road network is considered a dynamic system, due to the complex interactions between the various temporal events, such as: arrivals and departures of vehicles at intersections, changing lanes, beginning and completion of the various phases in traffic lights, among others (Dotoli and Fanti, 2006).

7.3.1 Generic highway segment model

In this methodology, it is assumed that a highway network is discretized into smaller highway segments with length, L, between 100 - 3000 m, with a specified vehicle capacity C. Figure 7.6 illustrates the Petri net scheme for two generic highway segments of length L. Each highway segment is modelled by two places and one transition. The places intend to model the highway segment, while the transition stands for the separation between the segments i and $i+1$. The marking $m_i(t)$ of place p_i denotes the number of vehicles in highway segment i, the marking $m'_i(t)$ of place p'_i correspond to the number of available sites in the highway segment i, and $v_i(t)$ stands for the transition firing speed that represents the average flow rate $q_i(t)$ of the highway segment i (Tolba et al., 2005; Fanti et al., 2014).
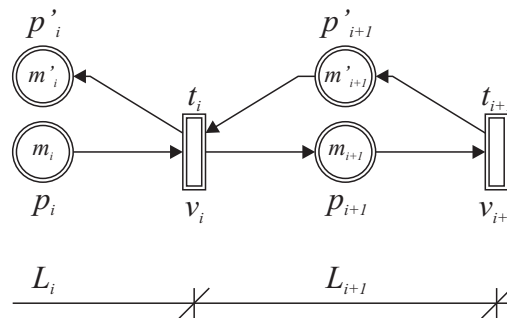
Figure 7.6 – Petri net scheme for a generic highway segment (adapted from Tolba et al., 2005 and Fanti et al., 2014)

Regarding Figure 7.6, vehicles that enter in segment $i+1$ are modelled by transition t_i and vehicles that exit from segment $i+1$ are modelled by transition t_{i+1}. When the transition t_i fires, the number of vehicles, $v_i(t)$, that exit from segment i is subtracted from places p_i and p'_{i+1} and added to places p'_i and p_{i+1}, modelling, in this way, the number of vehicles transiting from place p_i to place p_{i+1} and the number of available sites in each segment after the transition.

The transition firing speed, $v_i(t)$, is a piecewise linear function of the network marking, depending not only on the marking of the place p_i (i.e. on the number of the vehicles in the upstream segment i) but also on the marking of the place p'_{i+1} (i.e. the number of sites available in the downstream segment $i+1$) (Tolba et al., 2005):

$$v_i(t) = v_{max\,i} \times \min\left[\alpha_i,\, m_i(t),\, C_{i+1} - m_{i+1}(t)\right] \qquad (7.12)$$

where α_i and C_i correspond, respectively, to the maximum number of possible simultaneous firings for transition t_i and the limited capacity of place p_i. Both variables are related to the traffic parameters according to:

$$\alpha_i = \frac{q_{max\,i} \times L_i}{S_{free\,i}} \qquad (7.13)$$

$$C_i = \rho_{max\,i} \times L_i \qquad (7.14)$$

where $q_{max\,i}$, $S_{free\,i}$, and $\rho_{max\,i}$ represent, respectively, the maximum flow rate, the limited maximum speed, and the jam density in highway segment i. Finally, in Equation 7.12, $v_{max\,i}$ stands for the maximum firing frequency of transition t_i and is given by:

$$v_{max\,i} = \frac{S_{free\,i}}{L_i} \qquad (7.15)$$

The conservation of the number of vehicles in segment i is given by (Tolba et al., 2005):

$$\frac{dm_i(t)}{dt} = v_{i-1}(t) - v_i(t) \qquad (7.16)$$

this differential equation is responsible for the marking evolution of the place p_i in the traffic model.

Furthermore, each highway segment has marking invariants such that (Tolba et al., 2005):

$$m_i(t) + m_i'(t) = C_i \qquad \forall t \geq 0 \qquad (7.17)$$

The remain macroscopic parameters of the traffic flow model, average flow density $\rho_i(t)$ and average speed $S_i(t)$ for highway segment i, are given by (Tolba et al., 2005):

$$\rho_i(t) = \frac{m_i(t)}{L_i} \qquad (7.18)$$

$$S_i(t) = \frac{v_i(t) \times L_i}{m_i(t)} \qquad (7.19)$$

7.3.2   On-ramp model

The Petri net scheme for the on-ramp is shown in Figure 7.7. Transition t_{on} models the input of vehicles from the ramp to the network, being the vehicles routed from the ramp to the highway segment $i+1$ by the arc from transition t_{on} to place p_{i+1} and by the arc from place p_{i+1}' to transition t_{on}. Moreover, the marking $m_{on}(t)$ of place p_{on} represents the number of vehicles in ramp, and the marking $m_{on}'(t)$ of place p_{on}' the number of available sites in ramp (Fanti et al., 2014).

As can be seen, in the on-ramp model the highway segment $i+1$ have input traffic flow from two different segments: highway segment i and on-ramp. The transition firing speed, $v(t)$, for each input segment is computed using the same methodology presented in Section 7.3.1. For the present example, the transition firing speeds are given by:
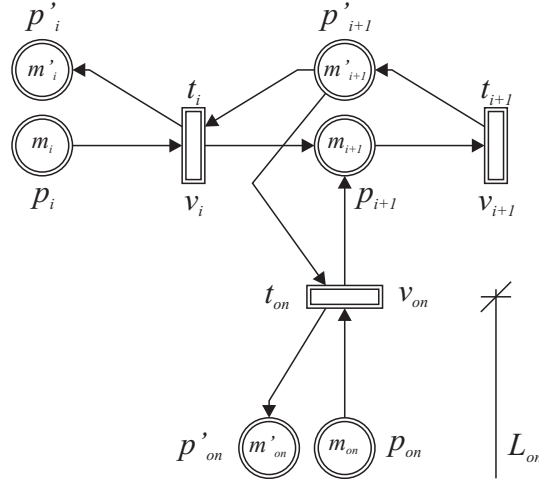
Figure 7.7 – Petri net scheme for the on-ramp (adapted from Fanti et al., 2014)

$$v_i(t) = v_{max\,i} \times \min\left[\alpha_i,\, m_i(t),\, C_{i+1} - m_{i+1}(t)\right] \tag{7.20}$$

$$v_{on}(t) = v_{max\,on} \times \min\left[\alpha_{on},\, m_{on}(t),\, C_{i+1} - m_{i+1}(t)\right] \tag{7.21}$$

The conservation of the number of vehicles in segment $i+1$ is given by:

$$\frac{dm_{i+1}(t)}{dt} = v_i(t) + v_{on}(t) - v_{i+1}(t) \tag{7.22}$$

In the on-ramp model, the marking invariant (Equation 7.17) is allows verified. The number of vehicles entering in the segment $i+1$ is never higher than the number of available sites in the segment, even in the situation of congestion. The number of vehicles that merge in the highway from each input segment is determined taking into account the number of available sites and the maximum firing frequency, since the maximum firing frequency is always less than 0.5, the number of vehicles flow to the segment $i+1$ is always less than the number of available sites.

7.3.3 Off-ramp model

The off-ramp model is very similar to the on-ramp model, and is illustrated in Figure 7.8. In this situation, the transition t_{off} models the output of vehicles from the network to the ramp, being the vehicles routed from the highway segment i to the ramp by the arc from place p_i to transition t_{off} and by the arc from transition t_{off} to place p'_i (Fanti et al., 2014).

In the off-ramp model, the highway segment i have two output segments: highway segment $i+1$ and off-ramp. In this case, the transition firing speed, $v(t)$, to each segment is weighted by the vehicle fraction that leaves at each ramp. For the present example, the transition firing speeds are given by:

$$v_i(t) = v_{max\,i} \times \min\left[\alpha_i,\, m_i(t),\, C_{i+1} - m_{i+1}(t)\right] \times OD_i \tag{7.23}$$

$$v_{off}(t) = v_{max\,i} \times \min\left[\alpha_i,\, m_i(t),\, C_{off} - m_{off}(t)\right] \times OD_{off} \tag{7.24}$$
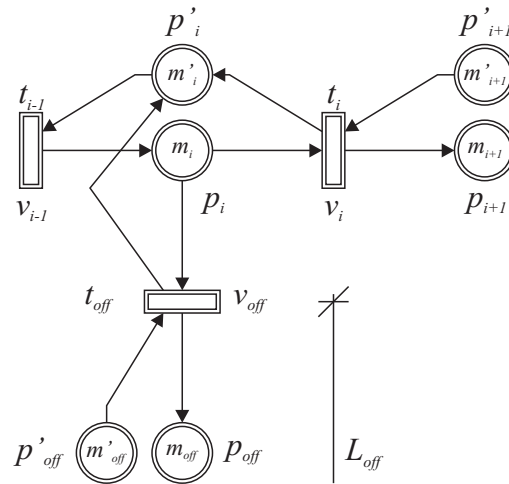
Figure 7.8 – Petri net scheme for the off-ramp (adapted from Fanti et al., 2014)

where OD_{off} and OD_i are, respectively, the percentage of vehicles that leaves the highway by the off-ramp and the continue in the highway obtained from the Origin-Destination matrix.

The conservation of the number of vehicles in segment i is given by:

$$\frac{\mathrm{d}m_i(t)}{\mathrm{d}t} = v_{i-1}(t) - v_i(t) - v_{off}(t) \tag{7.25}$$

7.3.4 Origin segment model

The Petri net scheme for the origin segment is shown in Figure 7.9. The origin segment is modelled by place p_i and transition t_i, and has the function of modelling the number of vehicles that enter in the network in each instant. Each input point of the network has associated an origin segment.
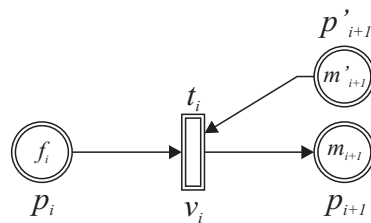
Figure 7.9 – Petri net scheme for the origin segment

The transition firing speed, $v_i(t)$, in this type of segment is slightly different, and is given by:

$$v_i(t) = \min\{f_i(t), v_{max\,i} \times [C_{i+1} - m_{i+1}(t)]\} \tag{7.26}$$

where $f_i(t)$ is the traffic flow that wants to enter in the network in each instant. The traffic flow that wants to enter the network is not constant over time and, in this model, it was considered that $f_i(t)$ follows an exponential distribution. This is, in each instant $f_i(t)$ is given by:

$$f_i(t) = -q_i(t) \times \log(1-p) \tag{7.27}$$

where $q_i(t)$ is the average flow rate of the input point i given by the Origin-Destination matrix and $p \in [0,1]$ is a probability randomly generated from a uniform distribution. An Origin-Destination

matrix is a table that specify the travel demands between different points in the network as a function of time (HCM, 2010).

In the situation of congestion, i.e. when $f_i(t)$ is larger than the capacity of next segment, $v_{max\,i} \times [C_{i+1} - m_{i+1}(t)]$, vehicles that cannot transit to the next segment are retained in the origin segment and have to wait for the next analysis instant, $t+1$, to enter the network. When this happens, the traffic flow available to enter the network at time $t+1$ is given by the sum of the traffic flow that wants to enter the network at time $t+1$, $f_i(t+1)$, plus the traffic flow that was retained in the origin segment in the previous instants.

7.3.5 Destination segment model

The Petri net for the destination segment is illustrated in Figure 7.10. The destination segment is just modelled by place p_i, and has the function of storing all the vehicles that leave the network. Each output point of the network has associated a destination segment.
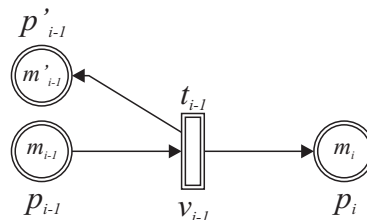
Figure 7.10 – Petri net scheme for the destination segment

In the highway segments that precede the destination segments, the Equation 7.12 can be simplified to:

$$v_{i-1}(t) = v_{max\,i-1} \times \min\left[\alpha_{i-1},\, m_{i-1}(t)\right] \tag{7.28}$$

7.4 Description of the road network

The case study is part of Portugal's highway network. It is composed by sections of three highways (A1, A9, and A10). Figure 7.11 illustrates the implementation of the network analysed in the case study in the Portuguese highway network.

The network analysed is composed by seven input points and two intersections between highways (Figure 7.12). The input points are identified by labels (1) to (7), while the intersections are identified by labels (A) and (B). All highway sections have traffic in both directions, and each direction there are three lanes. The maximum flow rate, q_{max}, is equal to 2 400 veh/h in each lane, for the limited maximum speed, S_{free}, of the 120 km/h as defined by HCM (2010). Table 7.2 contains all the information on the highway network.

7.5 Calibration and validation of the traffic model

Since the implemented traffic model is a macroscopic model, the calibration and validation of the traffic model is performed by comparing the values of the basic traffic parameters (speed, density, and flow rate) obtained through the traffic model implemented and the commercial micro-modelling software, Aimsun. The calibration of the model focuses on the adjustment of the basic traffic parameters
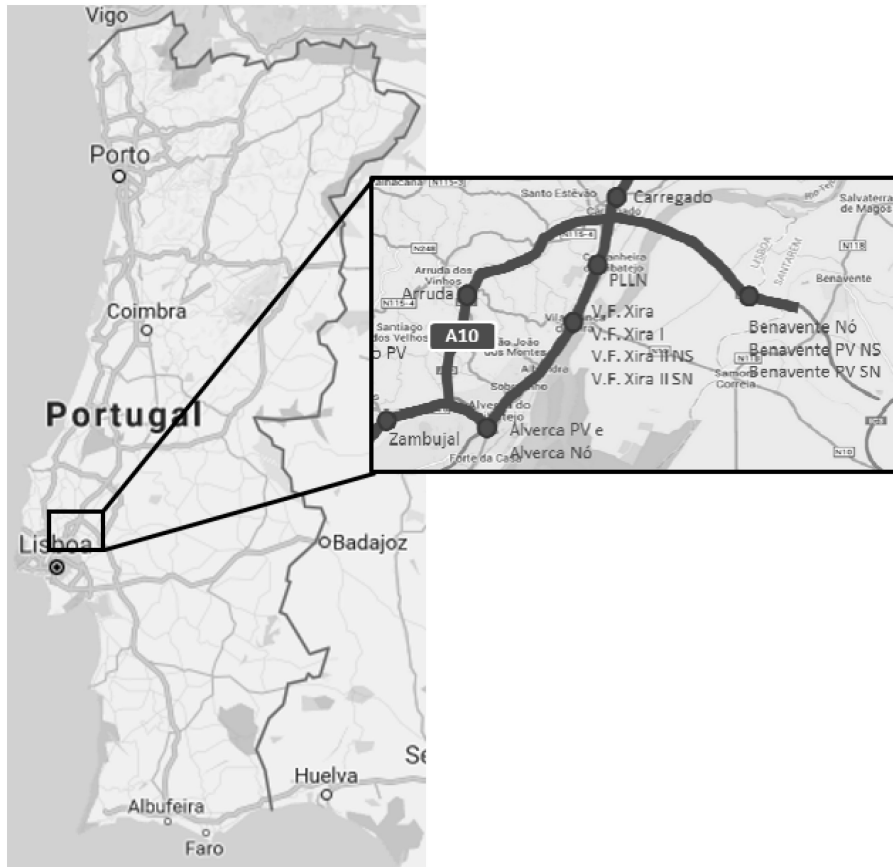
Figure 7.11 – Implementation the network studied in the case study in the Portuguese highway network
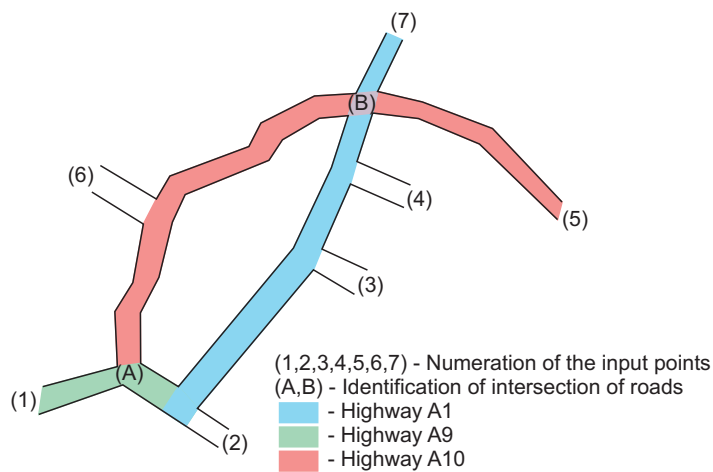
Figure 7.12 – Scheme of the network

in order to fit the local conditions, while validation focuses on demonstrating the ability of Petri nets to replicate the results obtained from traffic microsimulation tools (Toledo et al., 2003).

Aimsun is an integrated transport modelling software, developed, supported and marketed by TSS (Transport Simulation Systems) based in Barcelona, Spain. Aimsun is an open and extensible traffic modelling application, uniquely capable of fusing travel demand modelling, macroscopic functionalities and hybrid meso-micro approaches within a single environment. It is used by several entities, such as: government agencies, universities and private consultants to improve road infrastructure, re-

Table 7.2 – Network characteristics

Section		Length	Maximum flow rate	Limited maximum
Origin	Destination	[km]	by direction [veh/h]	speed [km/h]
(1) Zambujal	(A) Node A9/A10	3.50	7200	120
(A) Node A9/A10	(2) Alverca	3.40	7200	120
(2) Alverca	(3) V.F.Xira	10.90	7200	120
(3) V.F.Xira	(4) PLLN	3.90	7200	120
(4) PLLN	(B) Node A1/A10	1.20	7200	120
(B) A1/A10	(7) Carregado	0.90	7200	120
(A) Node A9/A10	(6) Arruda	8.30	7200	120
(6) Arruda	(B) Node A1/A10	3.00	7200	120
(B) Node A1/A10	(5) Benavente	6.90	7200	120

duce emissions, cut congestion, improve emergency evacuations, and design urban environments for vehicles and pedestrians (Aimsun, 2017).

7.5.1 Test network

A small sub-network extracted from the case study network was used to calibrate and validate traffic fundamental parameters. The sub-network is presented in Figure 7.13. The sub-network is localized on the northern highway (known as A1 highway) in the locality of V.F. Xira. In the sub-network, the flow occurs from South to North, has two input points (South and V.F. Xira) and two output points (North and V.F. Xira). All characteristics of the sub-network are those presented in the Table 7.3.
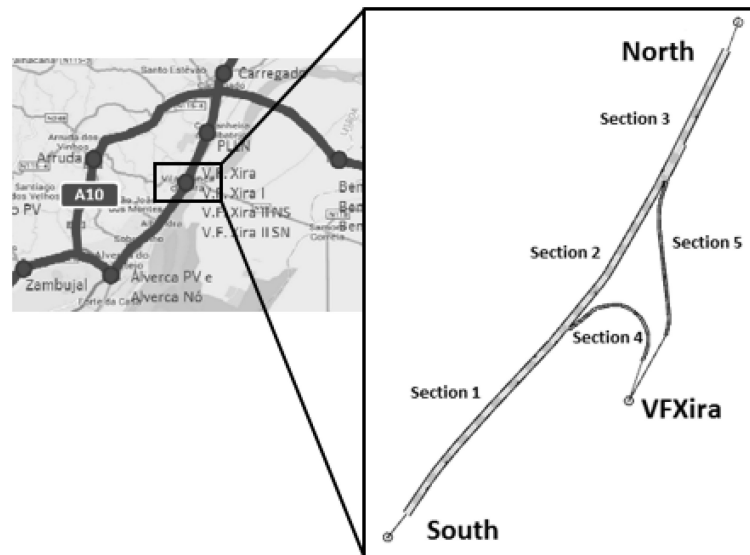
Figure 7.13 – Location of the sub-network

This sub-network was chosen for two reasons. Firstly, it is located in the highway with the highest traffic flow, making it easier to obtain the state of total congestion, and secondly because it contains the two main types of behaviour under analysis: on-ramp and off-ramp.

The Petri net of the traffic model for the test network is illustrated in Figure 7.14. Table 7.4 provided a full list with the description of places and transitions functions included in the traffic model. The Petri net scheme of the test network is composed by nine segments of variable length, fourteen places, and eight transitions. The places model the highway segments and the transitions have the function

Table 7.3 – Test network characteristics

Section	Type	Length [m]	S_{free} [km/h]	q_{max} [veh/h]	Number of lanes	ρ_{max} [veh/km]
1	Highway segment	341.1	120	2400	3	150
2	Highway segment	245.4	120	2400	3	150
3	Highway segment	194.9	120	2400	3	150
4	Off-ramp segment	178.5	60	900	1	150
5	On-ramp segment	218.4	60	900	1	150

of modelling the number of vehicles that transit between segments. The test network is constituted by three highway segments (Segments 2, 3, and 4), one off-ramp segment (Segment 5), one on-ramp segment (Segment 7), two origin segments (Segments 1 and 6), and two destination segments (Segments 8 and 9). The origin and destination segments are considered as having zero length. The length of the remain segments is presented in Table 7.3.
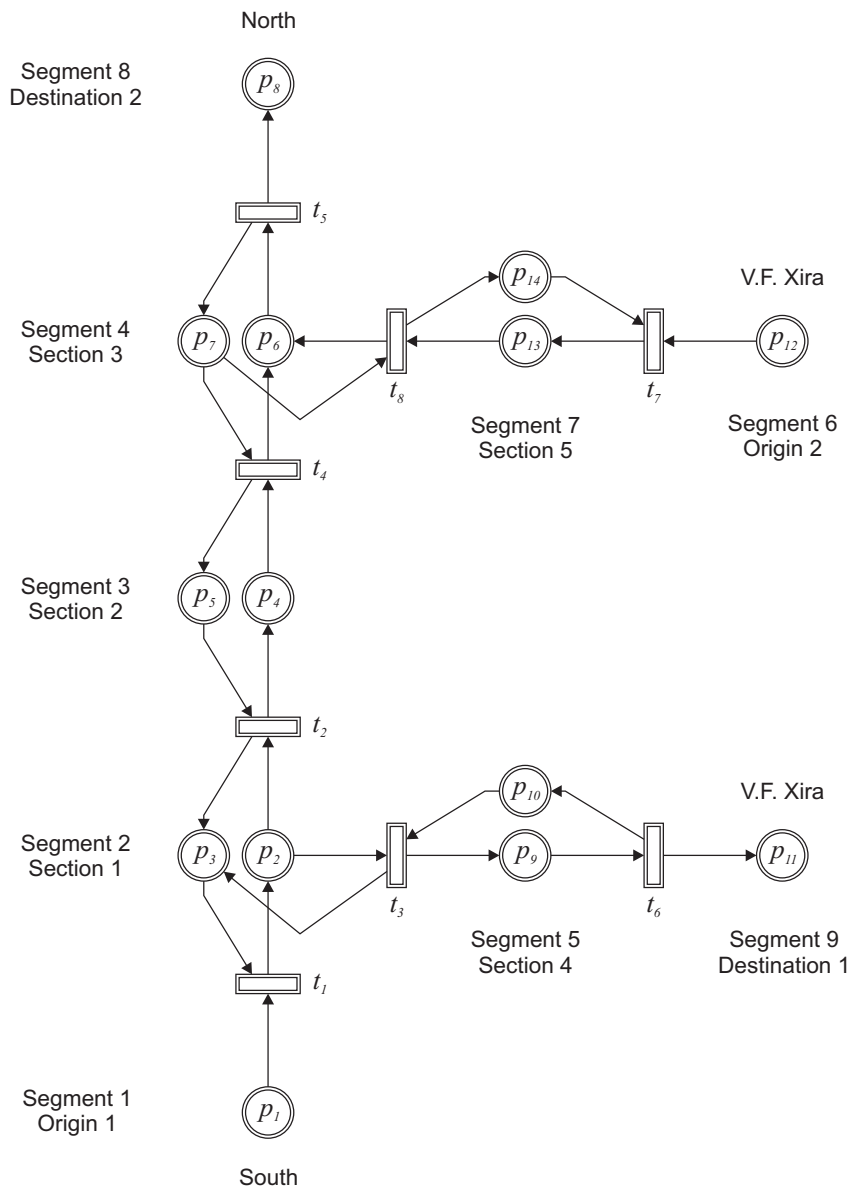
Figure 7.14 – Petri net scheme of the traffic model for the test network

Table 7.4 – Definition of places and transitions functions included in the traffic model for the test network

Element	Definition of the function
p_1	Input point 1 - South
p_2	Highway segment (Section 1)
p_3	Capacity of the highway segment (Section 1)
p_4	Highway segment (Section 2)
p_5	Capacity of the highway segment (Section 2)
p_6	Highway segment (Section 3)
p_7	Capacity of the highway segment (Section 3)
p_8	Output point 1 - North
p_9	Off-ramp segment
p_{10}	Capacity of the off-ramp segment (Section 4)
p_{11}	Output point 2 - V.F. Xira
p_{12}	Input point 2 - V.F. Xira
p_{13}	On-ramp segment
p_{14}	Capacity of the on-ramp segment (Section 5)
t_1	Vehicles that transit from input point 1 to Section 1
t_2	Vehicles that transit from Section 1 to Section 2
t_3	Vehicles that transit from Section 1 to off-ramp
t_4	Vehicles that transit from Section 2 to Section 3
t_5	Vehicles that transit from Section 3 to output point 1
t_6	Vehicles that transit from off-ramp to output point 2
t_7	Vehicles that transit from input point 2 to on-ramp
t_8	Vehicles that transit from on-ramp to Section 3

7.5.2 Calibration

The calibration of the traffic model is performed by analysing the graphs that relate the basic traffic parameters (speed, density, and flow rate). Figure 7.15 shows a generic representation of these relationships. The flow rate–density function is placed directly below the speed–density relationship because of their common horizontal scales, and the speed–flow rate function is placed next to the speed–density relationship because of their common vertical scales (HCM, 2010).

The form of the functions depends on the prevailing traffic and roadway conditions in the segment under study. However, from the curves illustrated in Figure 7.15 it is possible to identify several significant points. First, a zero flow rate occurs under two different conditions. One is when there are no vehicles on the facility – density is zero, and flow rate is zero. For this condition, speed is theoretical and would be selected by the first driver (presumably at a high value). The other one is when density becomes so high that all vehicles must stop – the speed is zero, and the flow rate is zero, because there is no movement and vehicles cannot pass a point on the roadway. The density at which all movements stops is called jam density, denoted by ρ_{max} in the diagrams (HCM, 2010).

Between these two extreme points, the behaviour of th traffic flow is dynamic. As flow rate increases from zero, density also increases, since more vehicles are on the roadway. When this happens, speed declines because of the interaction of vehicles. This decline is negligible at low and medium densities and flow rates. As density increases, the generic curves suggest that speed decreases significantly before the maximum capacity is achieved. Maximum capacity is reached when the product of density and speed results in the maximum flow rate. This condition is shown as critical speed, S_{cri}, critical density, ρ_{cri}, and maximum flow rate, q_{max}, (HCM, 2010). The three diagrams are redundant, since if any one relationship is known, the other two are uniquely defined. The speed–density function is
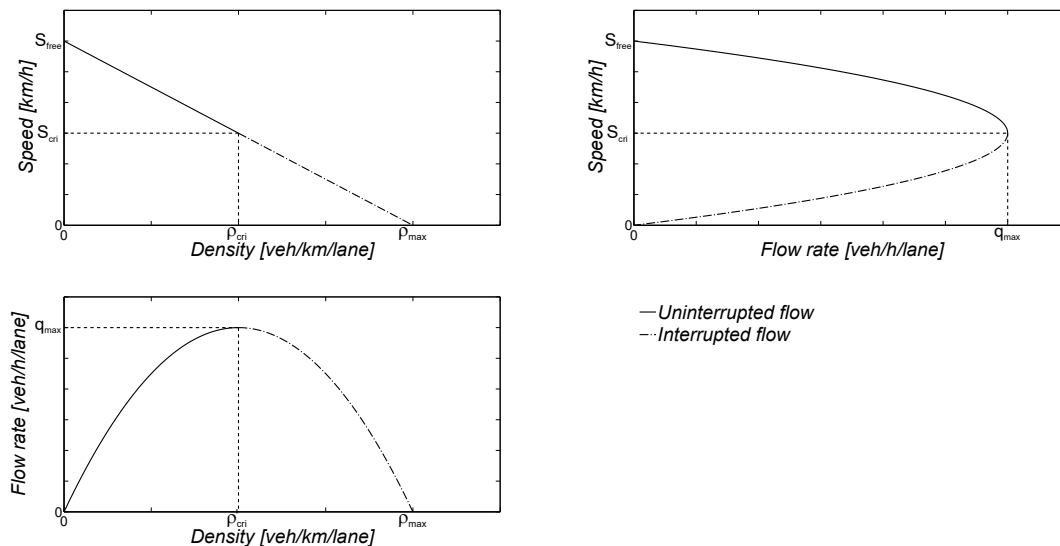
Figure 7.15 – Generic relationships between speed, density and flow rate (adapted from HCM, 2010)

used most frequently (HCM, 2010).

In order to analyse all possible behaviours in the network, three case studies are considered:

- Case study A – The traffic flow on the highway (Sections 1, 2, and 3) is continuously increased until the situation of congestion, being the traffic flow on the on- and off-ramp null. This case study allows studying traffic patterns in continuous highway segments;

- Case study B – Increase the traffic flow in segment South – V.F. Xira (Section 4), for constant traffic flows on the main road (Sections 1, 2, and 3). This case study allows studying traffic patterns in off-ramp segments (Section 4), and in the segment that precedes the bifurcation (Section 1);

- Case study C – Increase the traffic flow in segment V.F. Xira – North (Section 5), for constant traffic flows on the main road (Sections 1, 2, and 3). This case study allows studying traffic patterns in on-ramp segments (Section 5), in the segments that precedes the junction (Sections 1, and 2), and in the segment that follows the junction of the two flows (Section 3).

7.5.2.1   Case study A: Highway segments

In Figure 7.16, the results obtained using the traffic model proposed by Tolba et al. (2005) and the data obtained from the Aimsun for the Sections 1, 2, and 3 are compared. The relationships between speed, density, and flow rate for the traffic model implemented was computed, for a generic segment with a length of 1 000 m, through the methodology described in Section 7.3. The following characteristics of the segments were used: $S_{free} = 120$ km/h; $q_{max} = 2\,400$ veh/h/lane, and $\rho_{max} = 150$ veh/km/lane.

For this case study, Aimsun were run 8 times. The traffic flow data used in each simulation are presented in Table 7.5. Each simulation has a simulation time of 3 hours in order to ensure that the traffic flow is fully developed, with the data to be recorded every 10 minutes in each section.

From Figure 7.16 two main conclusions can be drawn. The first one is that the results obtained in Aimsun for the three sections are quite close, with only slight differences for higher traffic volumes (Simulation 6, 7, and 8). In these simulations, the input traffic flow is very close to or even higher than the capacity of the segments, making traffic flow along the network more unstable.

Figure 7.16 – Comparison of the relationships between speed, density, and flow rate between the traffic model proposed by Tolba et al. (2005) and the data obtained from the Aimsun – Case study A

Table 7.5 – Input traffic flow [veh/h] data used in each simulation for the Case study A

Simulation	$q_{South-North}$	Simulation	$q_{South-North}$
1	1200	5	6000
2	2400	6	7200
3	3600	7	8400
4	4800	8	9600

The second one is that the implemented traffic model (dashed line) does not fit the results obtained by Aimsun, mainly for the speed–density relationship and for the speed–flow rate relationship. However, the flow rate–density relationship shows a good agreement with the results obtained by Aimsun. In the traffic model described by Tolba et al. (2005), it is assumed that as flow rate increases from zero to maximum capacity, speed in the segment remains constant and equal to S_{free}. This result is unrealistic, since with the increase in the flow rate the interaction between vehicles causes the speed to be reduced. Furthermore, from the Aimsun data it can be seen that the maximum capacity of the segments is greater than the maximum flow rate, q_{max}, defined, approximately, 7.6%. For the maximum capacity, the Aimsun features a critical speed, S_{cri}, of, approximately, 98 km/h, and a critical density, ρ_{cri}, of 26 veh/km/lane. In addition, it can be observed that much higher it is the input traffic flow, the flow rate in the network is always equal to maximum capacity of the segment in uninterrupted flow. That is, there is no circulation in the network in interrupted conditions.

7.5.2.2 Case study B: Off-ramp segments

Figures 7.17 to 7.20 compare the traffic model implemented with the data obtained from Aimsun for Sections 1, 2, 3, and 4, respectively. As previously mentioned, in this case study the traffic flow in the segment South – V.F. Xira is increased for constant traffic flows in the segment South – North. Thus, each figure illustrates the variation of the basic traffic parameters in each section with the increase of traffic flow in the segment South – V.F. Xira for several traffic flow levels in the segment South – North.

For Sections 1, 2, and 3 the relationships between speed, density, and flow rate for the traffic model

implemented was computed, for a generic segment with a length of 1 000 m, through the methodology described in Section 7.3, with the following data: $S_{free} = 120$ km/h; $q_{max} = 2\,400$ veh/h/lane, and $\rho_{max} = 150$ veh/km/lane. While for Section 4, as it is an off-ramp segment, the relationships between the basic traffic parameters was computed, for a generic segment with a length of 1 000 m, and the following data were used as segment characteristics: $S_{free} = 60$ km/h; $q_{max} = 900$ veh/h/lane, and $\rho_{max} = 150$ veh/km/lane.

For this case study, Aimsun were run 36 times. The traffic flow data used in each simulation are presented in Table 7.6. Each simulation has a simulation time of 3 hours in order to ensure that the traffic flow is fully developed, with the data to be recorded every 10 minutes in each section.

Figure 7.17 – Comparison of the relationships between speed, density, and flow rate between the traffic model proposed by Tolba et al. (2005) and the data obtain from the Aimsun – Case study B, Section 1

Figure 7.18 – Comparison of the relationships between speed, density, and flow rate between the traffic model proposed by Tolba et al. (2005) and the data obtain from the Aimsun – Case study B, Section 2

In the same way as in case study A, the results for these four sections show that the traffic model

Figure 7.19 – Comparison of the relationships between speed, density, and flow rate between the traffic model proposed by Tolba et al. (2005) and the data obtain from the Aimsun – Case study B, Section 3

Figure 7.20 – Comparison of the relationships between speed, density, and flow rate between the traffic model proposed by Tolba et al. (2005) and the data obtain from the Aimsun – Case study B, Section 4

implemented (dashed line) does not fit the results obtained by Aimsun, presenting significant discrepancies. Mainly, in the speed–density relationships and in the speed–flow rate relationships, continuing the flow rate–density diagram the one that shows the best agreement in all sections. However, a careful analysis of these plots allows a better understanding of the behaviour of traffic in the network.

Figure 7.17 depicts the results obtained from Section 1; that is, the section that precedes the bifurcation in the network. From this figure, it is possible to observe that the increase in traffic level in the segment South – V.F. Xira has a great impact on the average speed of the section when compared with the same section of case study A. For example, for simulation 6 in case study B (Table 7.6), the average speed in Section 1 is, approximately, 80 km/h for an input flow rate, $q_{South-North}$, of 3900 veh/h, while the lower speed in Section 1 in case study A is, approximately, 98 km/h for flow rates

Table 7.6 – Input traffic flow [veh/h] data used in each simulation for the Case study B

$q_{South-North} = 1200$		$q_{South-North} = 2400$		$q_{South-North} = 3600$	
Simulation	$q_{South-VFXira}$	**Simulation**	$q_{South-VFXira}$	**Simulation**	$q_{South-VFXira}$
1	450	7	450	13	450
2	900	8	900	14	900
3	1350	9	1350	15	1350
4	1800	10	1800	16	1800
5	2250	11	2250	17	2250
6	2700	12	2700	18	2700
$q_{South-North} = 4800$		$q_{South-North} = 6000$		$q_{South-North} = 7200$	
Simulation	$q_{South-VFXira}$	**Simulation**	$q_{South-VFXira}$	**Simulation**	$q_{South-VFXira}$
19	450	25	450	31	450
20	900	26	900	32	900
21	1350	27	1350	33	1350
22	1800	28	1800	34	1800
23	2250	29	2250	35	2250
24	2700	30	2700	36	2700

higher than 7200 veh/h.

Figures 7.18 and 7.19 illustrate the results obtained for Sections 2, and 3, respectively. That is, the sections that follow the bifurcation in the network. For these two sections the results obtained are similar to the results presented for case study A, as these two sections are found after the bifurcation so only the traffic flow that follows to the North is considered to determine the relations between the three variables. In these plots each colour represents a traffic flow level in the segments.

Finally, Figure 7.20 shows the results obtained for the off-ramp segment (Section 4). As mentioned before, the traffic model (dashed line) does not fit the results obtained by Aimsun, showing significant differences in all plots. However, from this figure two main conclusions can be drawn. Firstly, according to Aimsun, the limited maximum speed, S_{free}, on the off-ramps is not 60 km/h but, approximately 70 km/h. And, has a maximum capacity of 2 400 veh/h (i.e. the maximum capacity is, approximately, 2.6 times higher than the maximum capacity defined).

7.5.2.3   Case study C: On-ramp segments

In Figures 7.21 to 7.24, the traffic model implemented and the data obtained from Aimsun for Sections 1, 2, 3, and 5 are compared, respectively. In this case study, the traffic flow in the segment V.F. Xira – North is increased for constant traffic flows in the segment South – North. That is, each figure illustrates the variation of the three fundamental traffic parameters in each section with the increase of the traffic flow in the segment V.F. Xira – North for several traffic flow levels in the segment South – North.

For Sections 1, 2, and 3 the relationships between speed, density, and flow rate for the traffic model implemented was computed, for a generic segment with a length of 1 000 m, through the methodology described in Section 7.3, with the following data: $S_{free} = 120$ km/h; $q_{max} = 2\,400$ veh/h/lane, and $\rho_{max} = 150$ veh/km/lane. While for Section 5, as it is an on-ramp segment, the relationships between the basic traffic parameters was computed, for a generic segment with a length of 1 000 m, and the following data were used as segment characteristics: $S_{free} = 60$ km/h; $q_{max} = 900$ veh/h/lane, and $\rho_{max} = 150$ veh/km/lane.

For this case study, 30 simulations were considered in Aimsun. The traffic flow data used in each simulation are presented in Table 7.7. Each simulation has a simulation time of 3 hours.
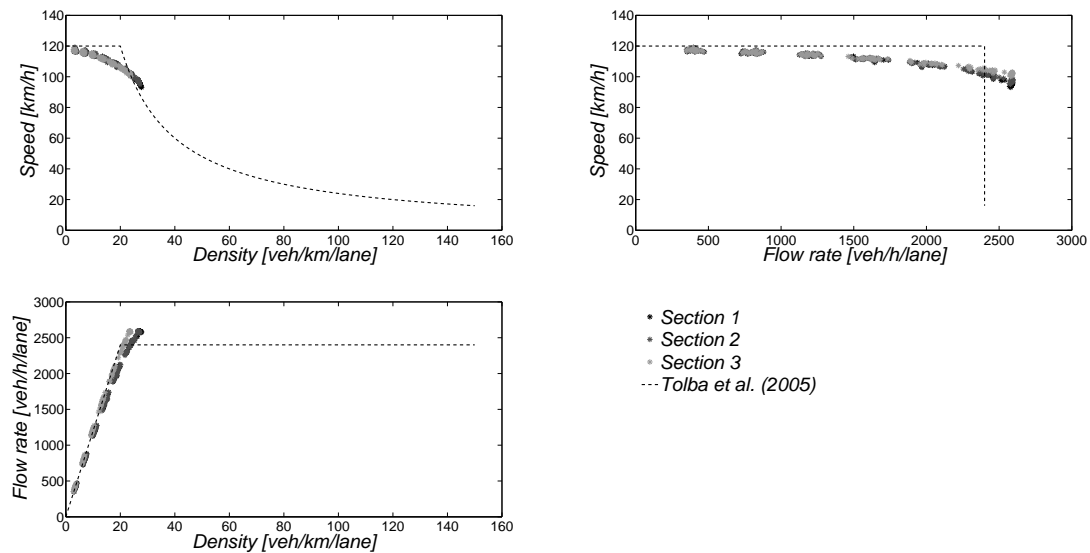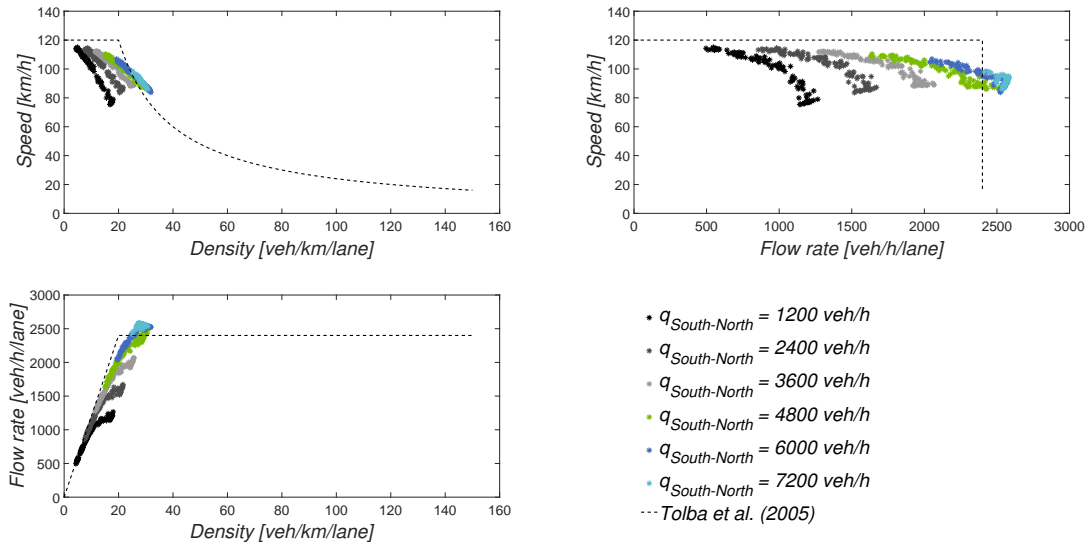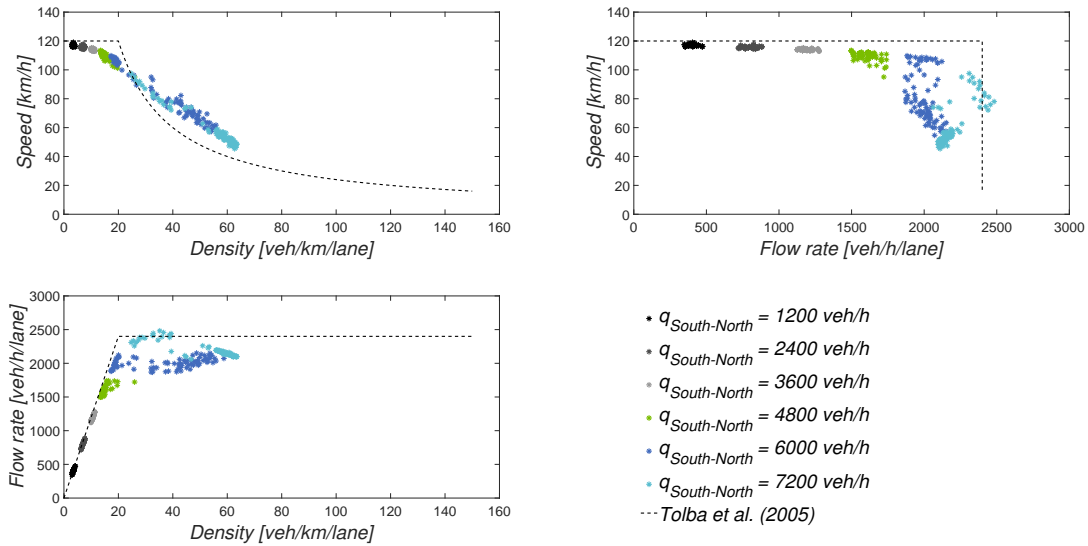

Figure 7.21 – Comparison of the relationships between speed, density, and flow rate between the traffic model proposed by Tolba et al. (2005) and the data obtain from the Aimsun – Case study C, Section 1
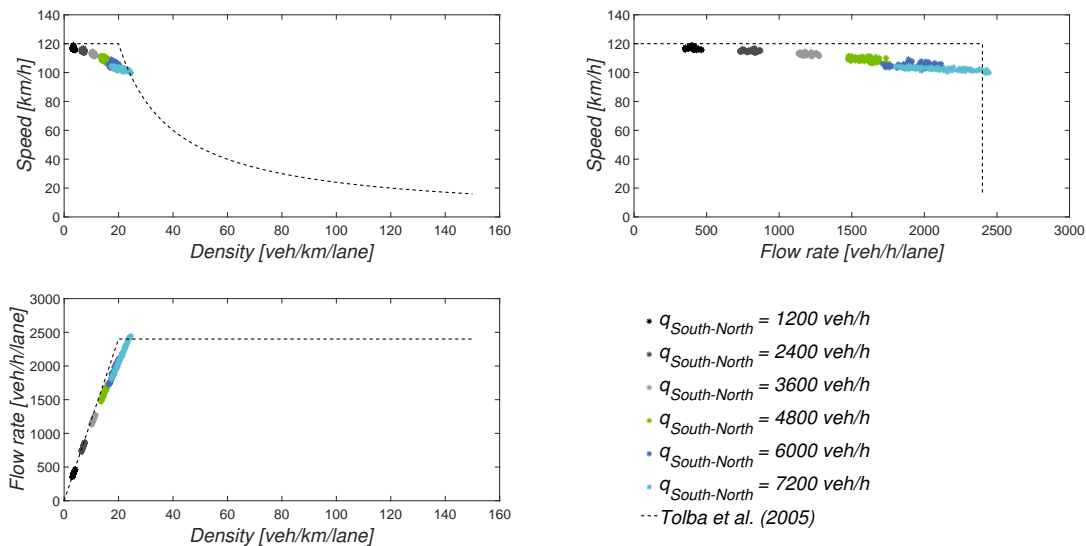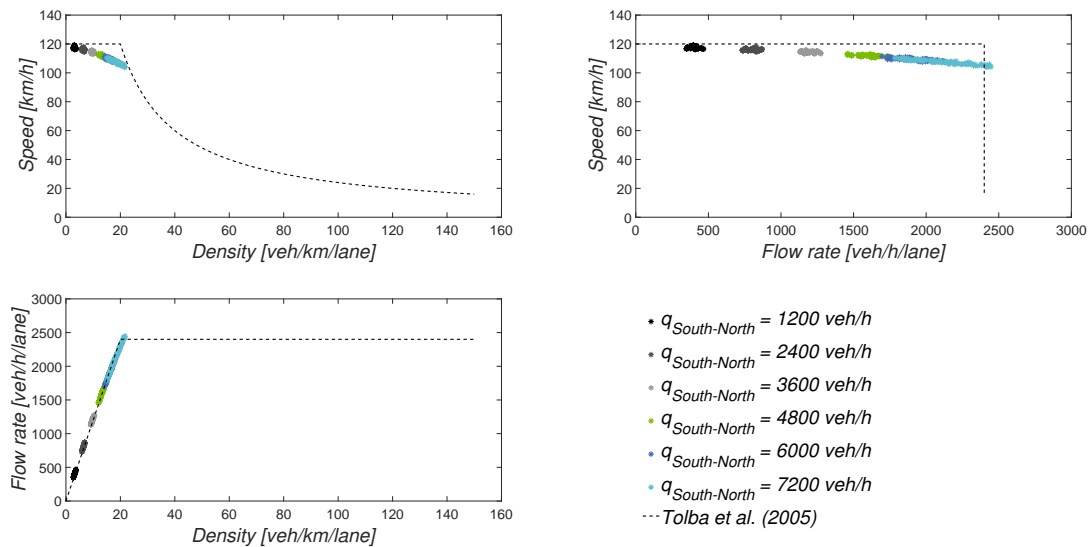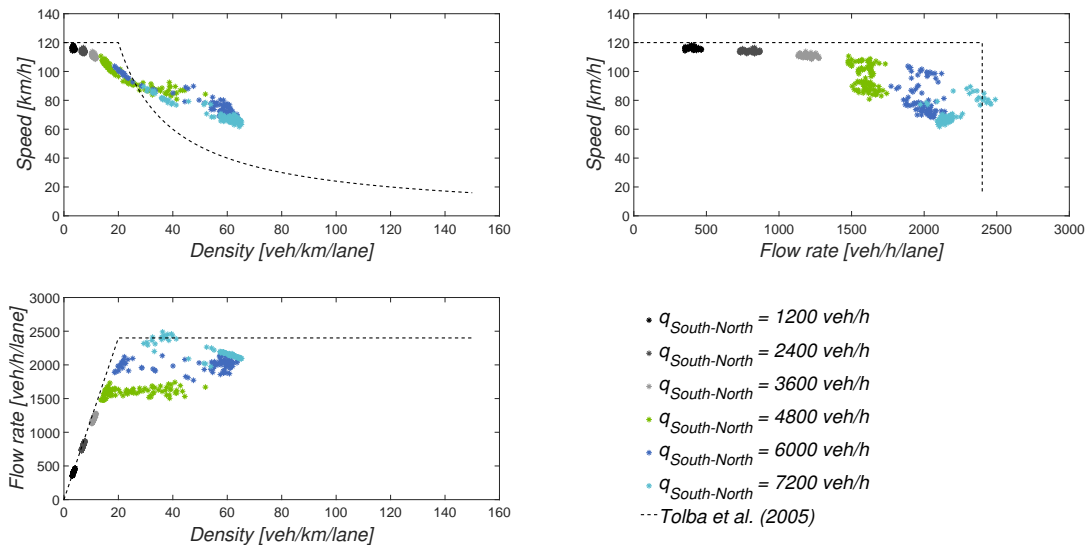

Figure 7.22 – Comparison of the relationships between speed, density, and flow rate between the traffic model proposed by Tolba et al. (2005) and the data obtain from the Aimsun – Case study C, Section 2

As in case study A and B, these figures show that, for these four sections, the traffic model implemented (dashed line) does not fit adequately the results obtained by Aimsun.

Figures 7.21 and 7.22 depict the results obtained for Sections 1, and 2, respectively. Both sections are located before the junction of the on-ramp with the main road. These results show that, for high traffic levels on the main road ($q_{South-North}$), the flow rate remains constant but the speed is considerably reduced due to the junction of the two flows. Also, it is possible to observe that for $q_{South-North} = 7200$ veh/h and for high traffic levels in segment V.F. Xira – North, the maximum capacity of these two sections is reduced by, approximately, 300 veh/h/lane. In parallel with these
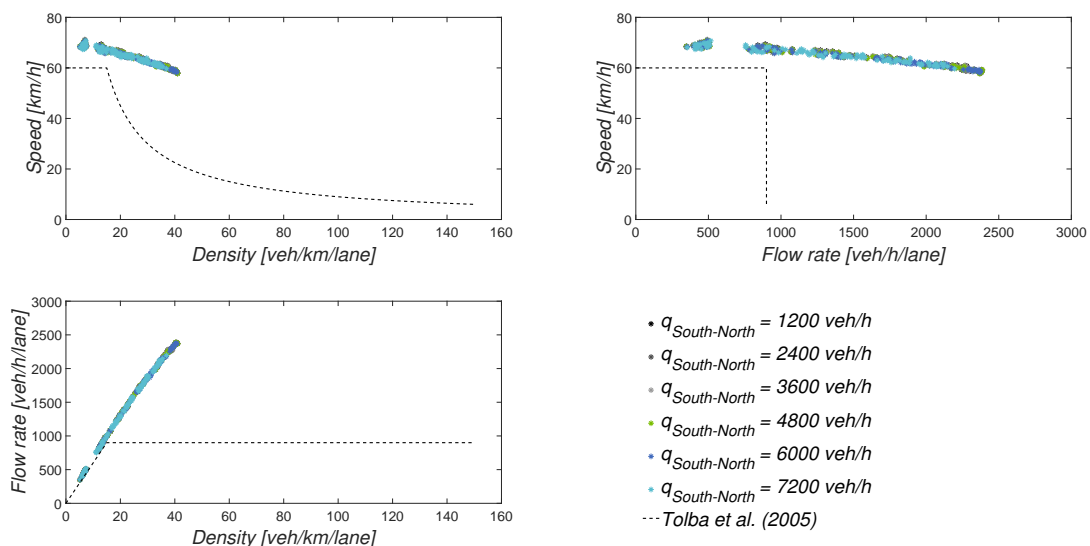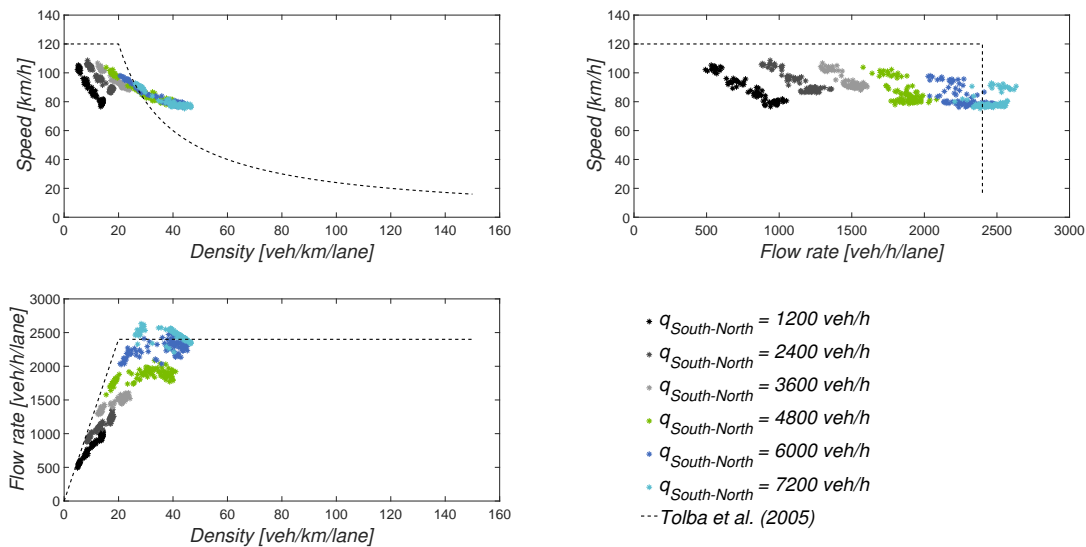
Figure 7.23 – Comparison of the relationships between speed, density, and flow rate between the traffic model proposed by Tolba et al. (2005) and the data obtain from the Aimsun – Case study C, Section 3
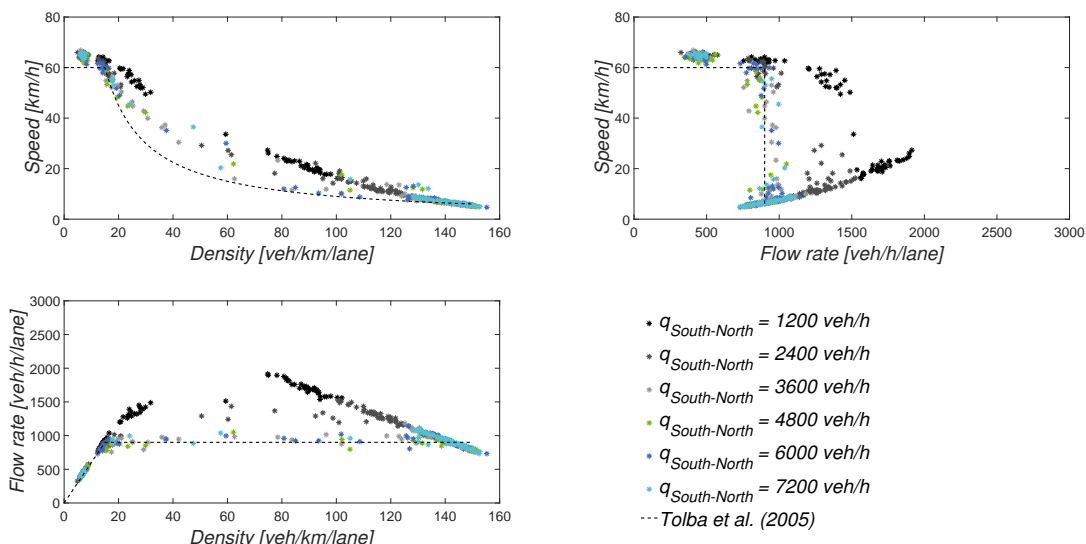
Figure 7.24 – Comparison of the relationships between speed, density, and flow rate between the traffic model proposed by Tolba et al. (2005) and the data obtain from the Aimsun – Case study C, Section 5

observations, it is possible to verify that the density in these two sections increases with the increase of traffic levels in the segment V.F. Xira – North.

By analysing the results obtained for Section 3 (Figure 7.23), the segment that follows the junction of the two flows, it can be concluded that the limited maximum speed, S_{free}, in this section is not 120 km/h but, approximately, 110 km/h. This leads us to conclude that, when there is junction of two flows, even at low traffic levels, drivers' instinct is to reduce their speed slightly as a road safety attitude.

Finally, Figure 7.24 shows the results obtained for the on-ramp segment (Section 5). In the same way as in Section 4 for case study B, similar conclusions can be taken. Firstly, according to Aimsun the

Table 7.7 – Input traffic flow [veh/h] data used in each simulation for the Case study C

$q_{South-North} = 1200$		$q_{South-North} = 2400$		$q_{South-North} = 3600$	
Simulation	$q_{VFXira-North}$	**Simulation**	$q_{VFXira-North}$	**Simulation**	$q_{VFXira-North}$
1	450	6	450	11	450
2	900	7	900	12	900
3	1350	8	1350	13	1350
4	1800	9	1800	14	1800
5	2250	10	2250	15	2250
$q_{South-North} = 4800$		$q_{South-North} = 6000$		$q_{South-North} = 7200$	
Simulation	$q_{VFXira-North}$	**Simulation**	$q_{VFXira-North}$	**Simulation**	$q_{VFXira-North}$
16	450	21	450	26	450
17	900	22	900	27	900
18	1350	23	1350	28	1350
19	1800	24	1800	29	1800
20	2250	25	2250	30	2250

limited maximum speed, S_{free}, on the on-ramps is not 60 km/h but, approximately 70 km/h. And secondly, the maximum capacity is only, approximately, 900 veh/h for situations where the traffic level on the main road is high ($q_{South-North} = 3600$ - 7200 veh/h). But, for low traffic levels, the maximum capacity is, approximately, 1300 veh/h for $q_{South-North} = 2400$ veh/h and 1700 veh/h for $q_{South-North} = 1200$ veh/h.

7.5.2.4 Discussion of the results

From the previously presented results, it is possible to conclude that the traffic model implemented does not fit adequately the results obtained through Aimsun, showing significant differences in the speed–density relationships and in the speed–flow rate relationships, being the relationships between flow rate and density the ones that show the highest agreement. However, the differences between the two models can be reduced by introducing three new parameters in the traffic model proposed by Tolba et al. (2005). These parameters were estimated from the results obtained by Aimsun, in order to approximate both models.

One of the first conclusions drawn is that the critical density obtained by the microsimulation model for the various sections analysed is higher than the critical density obtained by the implemented traffic model. Critical density, ρ_{cri}, defines the point at which traffic in the road network is no longer performed under an uninterrupted flow and is carried out under an interrupted flow. In the traffic model implemented, this point is defined by the α_i. Thus, the introduction of constant c_1 in Equation 7.13 is the first change in the traffic model:

$$\alpha_i = \underbrace{\frac{q_{max\,i} \times L_i}{S_{free\,i}}}_{\alpha_i^{theo}} \times c_1 \qquad (7.29)$$

where c_1 will allow the α_i to be increased, and α_i^{theo} is the α expression defined by Tolba et al. (2005), Equation 7.13.

However, by increasing the α_i, it is consequently increasing the value of the transition firing speed, $v_i(t)$. As can be seen in Equation 7.12, α_i is directly proportional to $v_i(t)$ for situations where the density of the segment is greater than the critical density, ρ_{cri}. Therefore, the introduction of the

constant c_2 in the model will allow reducing the average flow rate, $q_i(t)$, that leaves from the highway segment i:

$$q_i(t) = v_i(t) \times c_2 \tag{7.30}$$

Finally, the last parameter to be introduced in the traffic model is the critical speed, S_{cri}, that is not defined in the traffic model proposed by Tolba et al. (2005). Based on the results previously obtained and in order to simplify the expressions, it was assumed that the speed variation in the uninterrupted flows can be approximated by a linear function (Figure 7.25), obtaining Equation 7.31.
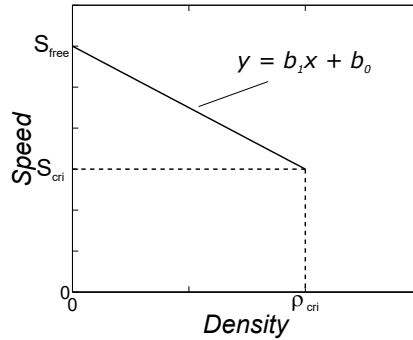
Figure 7.25 – First-degree polynomial used to describe the flow in uninterrupted conditions

$$S = \underbrace{\frac{S_{cri} - S_{free}}{\alpha_i}}_{b_1} \times \rho + \underbrace{S_{free}}_{b_0} \tag{7.31}$$

where the critical speed, S_{cri}, is given by:

$$S_{cri} = S_{free} + b_1 \times \alpha_i \tag{7.32}$$

The values of the variables b_0 and b_1 defined in Equation 7.31 were estimated using linear regression models applied to the results obtained through the microsimulation model. This change in the traffic model causes the expression proposed by Tolba et al. (2005) to calculate the average speed of the highway segment i (Equation 7.19) to be changed to:

$$S_i(t) = \begin{cases} \dfrac{S_{cri} - S_{free}}{\alpha_i} \times m_i(t) + S_{free}, & m_i(t) \leq \min[\alpha_i; C_{i+1} - m_{i+1}(t)] \\[3mm] \dfrac{v_i(t) \times c_2 \times L_i}{m_i(t)}, & m_i(t) > \min[\alpha_i; C_{i+1} - m_{i+1}(t)] \end{cases} \tag{7.33}$$

Through the results obtained from the three case studies previously analysed, it is possible to group the different segments that make up the network into four types:

- Type 1 – contains the generic highway segments and the segments that precede on- and off-ramps (Sections 1 and 2 in the test network);

- Type 2 – comprises the segments that follows the junction of the two flows (Section 3 in the test network);

- Type 3 – contains the on-ramp segments (Section 5 in the test network);

- Type 4 – comprises the off-ramp segments (Section 4 in the test network).

Type 1

From the results obtained for Sections 1, 2, and 3 in case study A, for Sections 1, 2, and 3 in case study B, and Sections 1, and 2 in case study C, it is possible to verify that in these eight sections the traffic behaviour in uninterrupted conditions is similar. These sections have, approximately, an average maximum capacity of 2600 veh/h/lane, an average critical density of 26 veh/km/lane, and an average critical speed of 98 km/h. However, in order to find the best parameters that fit to the Aimsun data, the linear regression model was applied to the speed–density relationship.

The linear regression equation was determined only on the basis of the data obtained for the Sections 1, 2, and 3 in the case study A. Only these sections were used because they are the only ones where it is possible to clearly observe the traffic behaviour in uninterrupted conditions. The following equation was obtained:

$$S = -0.8814 \times \rho + 122.2998 \tag{7.34}$$

where the coefficient of determination, r^2, is 0.9465, which means that the linear model is quite adequate to describe the speed–density relationship. In Table 7.8 the characteristics for the Type 1 segment are defined, and Figures 7.26 to 7.28 show the adjustment of the traffic model proposed based on the data obtained from Aimsun.

Table 7.8 – Type 1 segment characteristics

Variable	Value	Origin
S_{free} [km/h]	122.2998	Linear regression model, Equation 7.34
ρ_{cri} [veh/km]	25.6833	Average critical density obtained from Aimsun data
q_{max}^{theo} [veh/h]	2400.0	Theoretical maximum capacity defined from the Highway Capacity Manual (HCM, 2010)
q_{max} [veh/h]	2581.3706	Average maximum capacity obtained from Aimsun data
c_1 [–]	1.3088	$c_1 = \rho_{cri}/\alpha^{theo}$
α [veh/km]	25.6838	Equation 7.29
c_2 [–]	0.8218	$c_2 = q_{max}/(v_{max} \times \alpha)$
b_1 [–]	-0.8814	Linear regression model, Equation 7.34
S_{cri} [km/h]	99.6621	Equation 7.32

In Figure 7.26, the traffic model proposed by Tolba et al. (2005), the modified traffic model and the data obtained from Aimsun for Sections 1, 2, and 3 in case study A are compared. From this figure it is clear that the traffic model modified (black line) shows a good agreement with the data obtained from the microsimulation model.

Figures 7.27 and 7.28 depict the results obtained for Sections 1, 2, and 3 in case study B, and Sections 1, and 2 in case study C, respectively. The results for the traffic model implemented (original and modified) are determined on the assumption that the number of available sites in the downstream segment is always higher than the critical density. However, this assumption is not entirely realistic because the number of available sites in the downstream segment influence the transition firing speed (Equation 7.12).

For example, in Figure 7.27 for Section 1, the traffic model modified (black line) shows a good agreement with the data obtained from the microsimulation model for the situations where there is a low traffic level in the segment South – V.F. Xira. That is, for the situations where the flow in the main road and in the off-ramp are performed in uninterrupted conditions. However, with the increase of the traffic level in the segment South – V.F. Xira, the flow in the off-ramp begins to be carried out
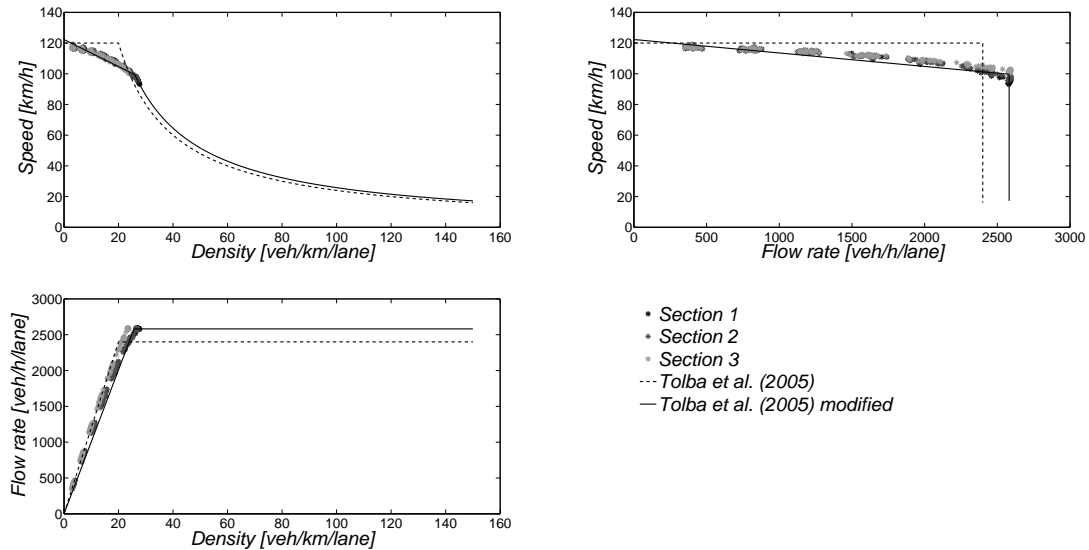
Figure 7.26 – Adjustment of the traffic model proposed to the data obtained from the Aimsun for type 1 segments (Sections 1, 2, and 3 of case study A)
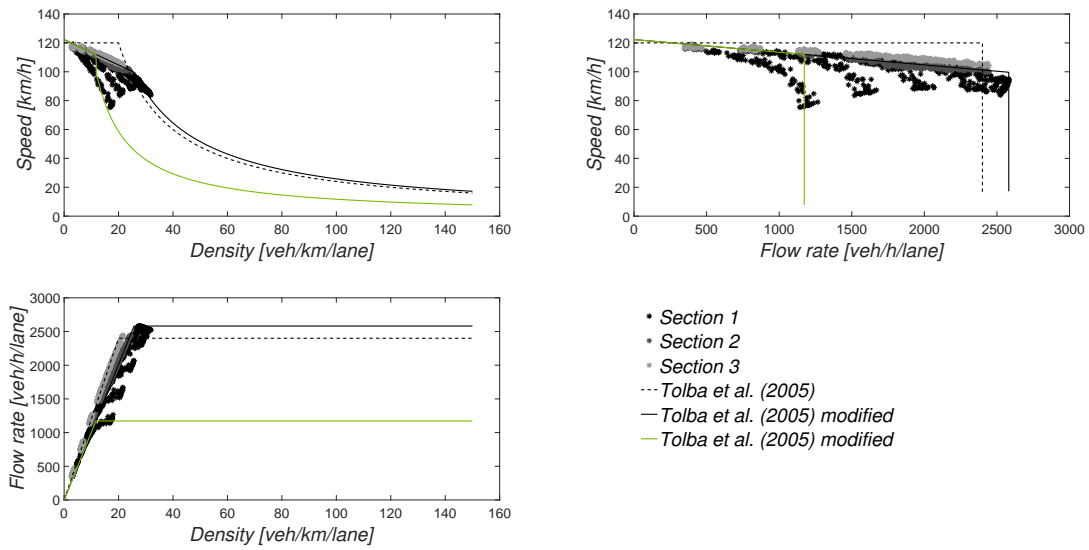
Figure 7.27 – Adjustment of the traffic model proposed to the data obtained from the Aimsun for type 1 segments (Sections 1, 2, and 3 of case study B)

in interrupted conditions, reducing the number of available sites in the downstream segment. This reduction of available sites will limit the transition firing speed of the Section 1 to the Section 4. This behaviour is not captured by the black line of the traffic model modified, since, in this study, the off-ramp is modelled by a generic segment and a destination segment. By definition, the destination segment does not have restriction on the maximum number of available sites, not allowing to model the uninterrupted flow in Section 4. However, it is possible to capture this behaviour with the Petri nets, as can be seen in Figure 7.27 through green line, only it is need to constrain the number of available sites in the downstream segment.
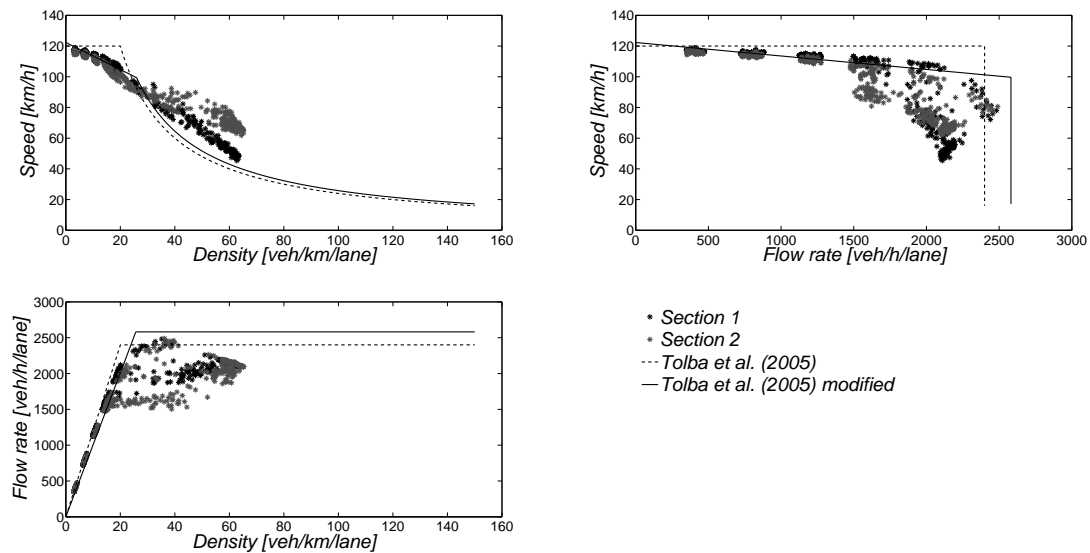
Figure 7.28 – Adjustment of the traffic model proposed to the data obtained from the Aimsun for type 1 segments (Sections 1, and 2 of case study C)

Type 2

From Section 3 (case study C) can be observed that this segment has, approximately, a critical density of 28 veh/km/lane, a maximum capacity of 2500 veh/h/lane, and a critical speed of 90 km/h (mean values of Simulation 26). Equation 7.35 shows the speed–density relationship obtained from the linear regression model.

$$S = -0.6262 \times \rho + 109.4279 \tag{7.35}$$

where the coefficient of determination, r^2, is 0.8265. Figure 7.29 shows the adjustment of the traffic model proposed to the data obtained from Aimsun and Table 7.9 the characteristics for the Type 2 segment.

Table 7.9 – Type 2 segment characteristics

Variable	Value	Origin
S_{free} [km/h]	109.4279	Linear regression model, Equation 7.35
ρ_{cri} [veh/km]	28.1567	Average critical density obtained from Aimsun data
q_{max}^{theo} [veh/h]	2400.0	Theoretical maximum capacity defined from the Highway Capacity Manual (HCM, 2010)
q_{max} [veh/h]	2538.8144	Average maximum capacity obtained from Aimsun data
c_1 [−]	1.2838	$c_1 = \rho_{cri}/\alpha^{theo}$
α [veh/km]	28.1566	Equation 7.29
c_2 [−]	0.8240	$c_2 = q_{max}/(v_{max} \times \alpha)$
b_1 [−]	−0.6262	Linear regression model, Equation 7.35
S_{cri} [km/h]	91.7962	Equation 7.32
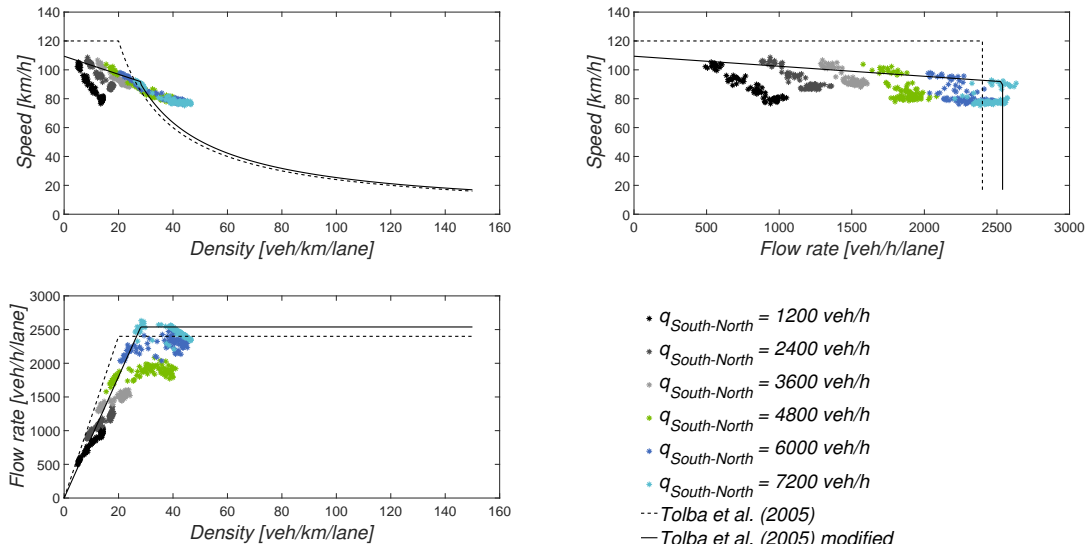
Figure 7.29 – Adjustment of the traffic model proposed to the data obtained from the Aimsun for type 2 segments (Section 3 of case study C)

Type 3

The speed–density relationship to segment Type 3 is presented in Equation 7.36, obtaining a coefficient of determination, r^2, of 0.7653 from the linear regression model. This relationship is computed from the data obtained in Section 5 in case study C (Simulation 2). This segment presents, on average, a critical density of 15 veh/km, a maximum capacity of 900 veh/h, and a critical speed of 62 km/h.

$$S = -0.2869 \times \rho + 66.9558 \tag{7.36}$$

Figure 7.30 and Table 7.10 present, respectively, the adjustment of the traffic model proposed to the data obtained from Aimsun and the characteristics for the Type 3 segment.

Table 7.10 – Type 3 segment characteristics

| Variable	Value	Origin
S_{free} [km/h]	66.9558	Linear regression model, Equation 7.36
ρ_{cri} [veh/km]	14.6000	Average critical density obtained from Aimsun data
q_{max}^{theo} [veh/h]	900.0	Theoretical maximum capacity defined from the Highway Capacity Manual (HCM, 2010)
q_{max} [veh/h]	900.2200	Average maximum capacity obtained from Aimsun data
c_1 [–]	1.0862	$c_1 = \rho_{cri}/\alpha^{theo}$
α [veh/km]	14.6004	Equation 7.29
c_2 [–]	0.9209	$c_2 = q_{max}/(v_{max} \times \alpha)$
b_1 [–]	−0.2869	Linear regression model, Equation 7.36
S_{cri} [km/h]	62.7670	Equation 7.32
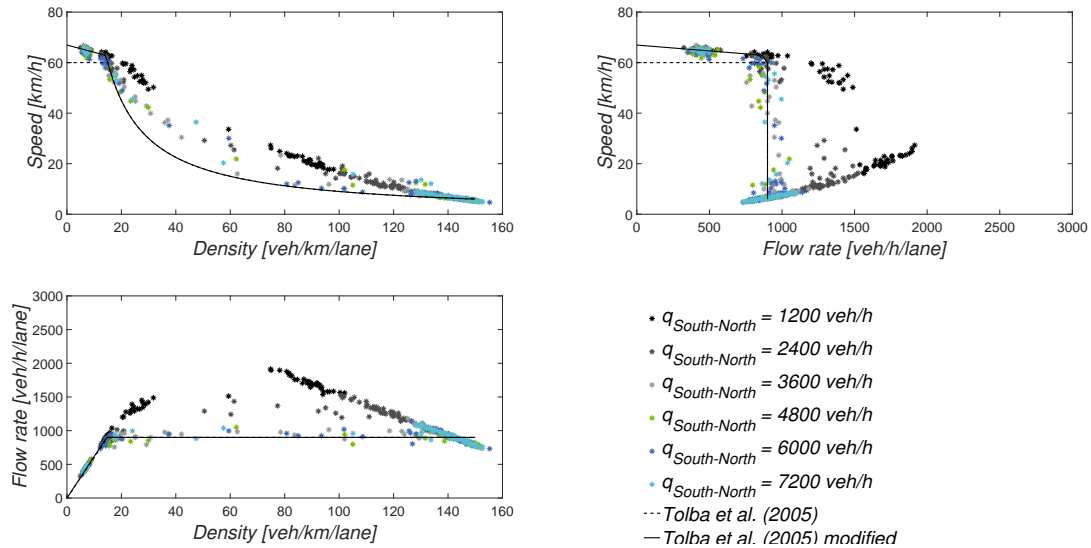
Figure 7.30 – Adjustment of the traffic model proposed to the data obtained from the Aimsun for type 3 segments (Section 5 of case study C)

Type 4

Finally, for the segment Type 4, the speed–density relationship was estimated from the data obtained in Section 4 of case study B (Simulations 6, 12, 18, 24, 30, and 36). From these data, it is possible to observe that this segment has, on average, a critical density of 39 veh/km, a maximum capacity of 2300 veh/h, and a critical speed of 59 km/h. By applying the linear regression model, the following equation was obtained:

$$S = -0.3121 \times \rho + 71.6746 \tag{7.37}$$

where the coefficient of determination, r^2, is 0.9641. Table 7.11 presents the characteristics for the Type 4 segment, and Figure 7.31 shows the adjustment of the traffic model proposed to the data obtained from Aimsun.

Table 7.11 – Type 4 segment characteristics

| Variable	Value	Origin
S_{free} [km/h]	71.6746	Linear regression model, Equation 7.37
ρ_{cri} [veh/km]	39.1153	Average critical density obtained from Aimsun data
q_{max}^{theo} [veh/h]	900.0	Theoretical maximum capacity defined from the Highway Capacity Manual (HCM, 2010)
q_{max} [veh/h]	2304.0556	Average maximum capacity obtained from Aimsun data
c_1 [–]	3.1151	$c_1 = \rho_{cri}/\alpha^{theo}$
α [veh/km]	39.1155	Equation 7.29
c_2 [–]	0.8218	$c_2 = q_{max}/(v_{max} \times \alpha)$
b_1 [–]	−0.3121	Linear regression model, Equation 7.37
S_{cri} [km/h]	59.4666	Equation 7.32
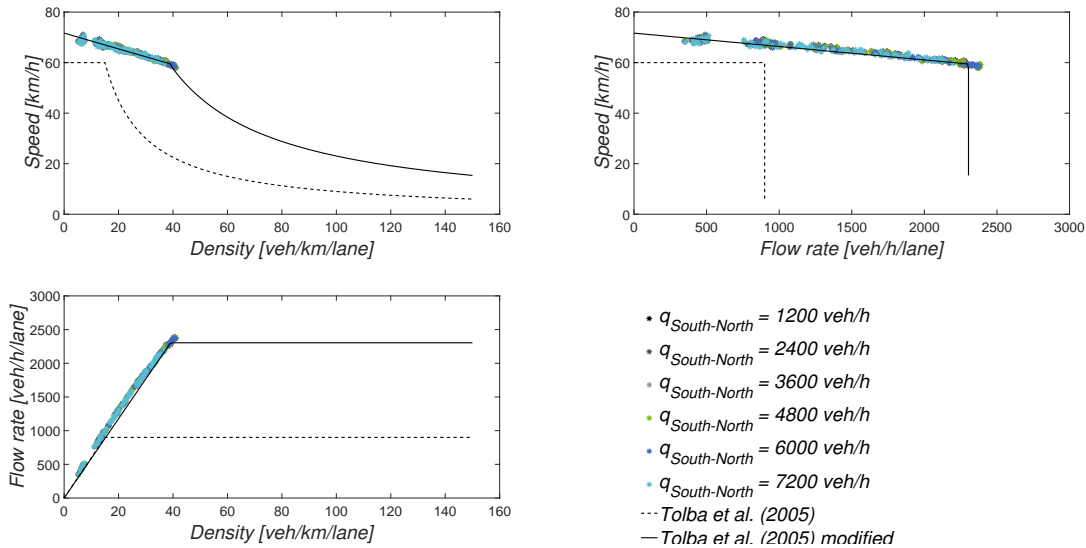
Figure 7.31 – Adjustment of the traffic model proposed to the data obtained from the Aimsun for type 4 segments (Section 4 of case study B)

7.5.3   Validation

For the validation at the macroscopic level, the average speed, density, and flow rate computed from the modified traffic model were compared with the results obtained from Aimsun. In the validation process, four Origin-Destination matrices (OD) were used (Tables 7.12 to 7.15). The Origin-Destination matrix 1 (OD1) is based on real data provided by BRISA (entity responsible for the highways that constitute the network being studied). The remaining OD matrices are linearly proportional to OD1.

Each simulation for both traffic models, modified traffic model and Aimsun, has a simulation time of 3 hours with the data to be recorded every 10 minutes in each section. In this study, 100 simulation were carried out for each traffic model.

Table 7.12 – Origin-Destination matrix 1 (OD1)

	V.F. Xira	North	Total
South	772	1263	2035
V.F. Xira	–	294	294
Total	772	1557	2329

Table 7.13 – Origin-Destination matrix 2 (OD2)

	V.F. Xira	North	Total
South	1544	2526	4070
V.F. Xira	–	588	588
Total	1544	3114	4658

7.5.3.1   Comparison of the fundamental parameters by section

In Tables 7.16 to 7.20, the average speed, density, and flow rate computed by the traffic model based on Petri nets is compared with the results obtained through the microsimulation model. Each table

Table 7.14 – Origin-Destination matrix 3 (OD3)

	V.F. Xira	North	Total
South	2316	3789	6105
V.F. Xira	–	882	882
Total	2316	4671	6987

Table 7.15 – Origin-Destination matrix 4 (OD4)

	V.F. Xira	North	Total
South	3088	5052	8140
V.F. Xira	–	1176	1176
Total	3088	6228	9316

presents the data obtained for each section defined in the test network (Figure 7.13). From these results it is possible to observe that there is a good agreement between the two models. Of the three analysed variables, density presents greater differences obtaining relative errors in the order of 30% for the higher traffic levels. The average speed has average relative errors of less than 10%, while the flow rate has average relative errors of less than 5%.

Table 7.16 – Comparison of the fundamental parameters in Section 1

	Aimsun			**Petri nets**			**Relative error [%]**		
	Speed	Den-sity	Flow rate	Speed	Den-sity	Flow rate	Speed	Den-sity	Flow rate
OD1	111.6	6.1	2026.5	117.4	5.6	2036.5	5.2	9.1	0.5
OD2	105.7	13.1	4064.8	112.5	11.1	4072.9	6.4	14.9	0.2
OD3	91.2	24.3	6092.4	105.8	17.0	6109.2	16.0	30.0	0.3
OD4	86.5	30.7	7418.8	86.2	27.6	7746.9	0.4	10.1	4.4

Table 7.17 – Comparison of the fundamental parameters in Section 2

	Aimsun			**Petri nets**			**Relative error [%]**		
	Speed	Den-sity	Flow rate	Speed	Den-sity	Flow rate	Speed	Den-sity	Flow rate
OD1	116.3	3.6	1257.3	119.2	3.4	1263.1	2.5	5.1	0.5
OD2	113.6	7.5	2523.1	116.2	6.9	2526.3	2.2	7.6	0.1
OD3	109.0	11.6	3785.2	113.0	10.5	3839.1	3.7	10.1	1.4
OD4	102.6	16.5	5044.8	110.0	13.9	5115.2	7.2	15.2	1.4

Table 7.18 – Comparison of the fundamental parameters in Section 3

	Aimsun			**Petri nets**			**Relative error [%]**		
	Speed	Den-sity	Flow rate	Speed	Den-sity	Flow rate	Speed	Den-sity	Flow rate
OD1	107.2	4.8	1551.7	106.5	4.7	1556.3	0.7	0.6	0.3
OD2	103.1	10.3	3107.0	103.5	9.5	3112.7	0.4	7.8	0.2
OD3	95.6	18.7	4660.7	100.4	14.4	4718.4	5.1	23.0	1.2
OD4	91.1	27.1	6004.1	97.8	18.5	6088.2	7.4	31.6	1.4

Table 7.19 – Comparison of the fundamental parameters in Section 4

	Aimsun			**Petri nets**			**Relative error [%]**		
	Speed	Den-sity	Flow rate	Speed	Den-sity	Flow rate	Speed	Den-sity	Flow rate
OD1	68.0	11.4	767.5	68.3	10.8	771.9	0.5	5.4	0.6
OD2	64.6	24.0	1538.2	65.0	21.5	1543.7	0.6	10.2	0.4
OD3	59.1	39.0	2301.7	61.8	31.6	2265.6	4.5	19.0	1.6
OD4	58.4	40.6	2367.4	60.2	36.6	2626.0	3.1	9.7	10.9

Table 7.20 – Comparison of the fundamental parameters in Section 5

	Aimsun			**Petri nets**			**Relative error [%]**		
	Speed	Den-sity	Flow rate	Speed	Den-sity	Flow rate	Speed	Den-sity	Flow rate
OD1	65.3	4.6	295.4	65.7	4.4	294.2	0.7	3.6	0.4
OD2	64.0	9.2	586.1	64.4	8.8	588.3	0.7	4.8	0.4
OD3	51.0	22.4	879.6	55.2	16.1	882.2	8.4	28.2	0.3
OD4	8.6	132.3	965.5	6.9	139.9	976.7	20.4	5.8	1.2

7.5.3.2   Comparison of the flow rate by node

Tables 7.21 and 7.22 compare the flow rates in the bifurcation and in the junction for the four OD matrices, respectively. In Table 7.21, column "South" presents the flow rate from Section 1, column "North" shows the flow rate that goes North (Section 2), and column "V.F. Xira" displays the flow rate that enters the off-ramp (Section 4). While in Table 7.22, column "South" presents the flow rate that leaves Section 2, column " V.F. Xira" shows the flow rate that leaves the on-ramp (Section 5), and column "North" exhibits the flow rate that goes North (Section 3).

The main purpose of these two tables is to show that Petri nets are able to model traffic behaviour at the macroscopic level, even in oversaturate conditions. From these results it is clear that, for all traffic levels, that there is a good agreement between the two models, presenting low relative errors.

Table 7.21 – Comparison of the flow rate [veh/h] in the bifurcation

	Aimsun			**Petri nets**			**Relative error [%]**		
	South	North	V.F. Xira	South	North	V.F. Xira	South	North	V.F. Xira
OD1	2026.5	1258.2	768.2	2036.5	1263.9	772.6	0.5	0.5	0.6
OD2	4064.8	2525.0	1539.7	4072.9	2527.9	1545.0	0.2	0.1	0.3
OD3	6092.4	3788.2	2304.0	6109.2	3841.7	2267.5	0.3	1.4	1.6
OD4	7418.8	5048.9	2369.8	7746.9	5118.7	2628.2	4.4	1.4	10.9

7.6   Performance evaluation of the road network

The main aim of this methodology is to evaluate the performance of the road network described in Section 7.4. The performance of the road network is evaluated by calculating the resilience index. In this problem, the resilience index is computed through Equation 7.5, and the functionality of the network, $Q(t)$, is defined by Equation 7.6.

Table 7.22 – Comparison of the flow rate [veh/h] in the junction

	Aimsun			Petri nets			Relative error [%]		
	South	V.F. Xira	North	South	V.F. Xira	North	South	V.F. Xira	North
OD1	1257.3	295.4	1552.7	1263.1	294.2	1557.2	0.5	0.4	0.3
OD2	2523.1	586.1	3109.1	2526.3	588.3	3114.6	0.1	0.4	0.2
OD3	3785.2	879.6	4664.6	3839.1	882.2	4721.3	1.4	0.3	1.2
OD4	5044.8	965.5	6009.8	5115.2	976.7	6091.9	1.4	1.2	1.4

The calculations were performed for a time horizon, t_h, of 24 hours. The traffic data used in the traffic model was provided by a Portuguese company – BRISA and corresponds to January 20, 2014 (Table 7.23). The Petri net modelling the network is presented in Appendix B – Section B.1.

Table 7.23 – Daily traffic flow of the road network for January 20, 2014

	(1) Zambujal	(2) Alverca	(3) V.F.Xira	(4) PLLN	(5) Benavente	(6) Arruda	(7) Carregado
(1) Zambujal	–	1 355	556	71	223	32	3 128
(2) Alverca	1 522	–	8 303	403	615	1 537	18 146
(3) V.F.Xira	718	10 928	–	110	122	18	3 379
(4) PLLN	64	416	87	–	72	4	215
(5) Benavente	231	719	112	61	–	4	1 037
(6) Arruda	40	1 276	12	5	5	–	226
(7) Carregado	3 432	21 282	3 429	247	1 221	251	–

In this example only two levels of damage were considered for the bridges. Either they are in service and the road traffic takes place in the section without any restrictions, or they are totally out of service and the traffic flow in the section is equal to zero.

7.6.1 Calculation of Γ^{100}

The first step is to determine the performance of the network over a 24-hour time horizon for the situation in which all bridges are in service by Equation 7.7:

$$\Gamma^{100}(24\,h) = \frac{1}{2 \times 10^{-7} \cdot TTT^{100}(24\,h) + 6.21 \times 10^{-8} \cdot TTD^{100}(24\,h)} \qquad \text{(7.7 revisited)}$$

The total travel time, $TTT^{100}(24\,h)$, and the total travel distance, $TTD^{100}(24\,h)$, are obtained directly from the traffic model through Equations 7.10 and 7.11.

$$TTT^{100}(24\,h) = \sum_{i=1}^{24\,h} \sum_{x \in X} \sum_{y \in Y} q_{xy}(i) \cdot c_{xy}(i) \qquad \text{(7.10 revisited)}$$

$$TTD^{100}(24\,h) = \sum_{i=1}^{24\,h} \sum_{x \in X} \sum_{y \in Y} q_{xy}(i) \cdot L_{xy} \qquad (7.11\ \text{revisited})$$

where $q_{xy}(i)$ is the traffic flow transiting over the highway segment x - y during the hour i, and $c_{xy}(i)$ is the time required to cover the highway segment x - y during the hour i computing by;

$$c_{xy}(i) = \frac{L_{xy}}{S_{xy}(i)} \qquad (7.38)$$

where L_{xy} denotes the length of the highway segment x - y and $S_{xy}(i)$ the average speed of the highway segment x - y during the hour i. The traffic flow circulation to the situation where all bridges are in service is shown in Figure 7.32.

The performance of the network, for the situation in which all bridges are in service is 5.16, i.e. $\Gamma^{100} = 5.16$.

7.6.2   Calculation of Γ^0

For the situation in which the network is totally out of service, the performance of the network is null, i.e. $\Gamma^0 = 0$.

7.6.3   Calculation of Γ for other situations

In addition to the two situations mentioned above, the overall performance of the network was determined for additional six scenarios. In order to be able to examine the resilience index of the road network and to identify the section that most affects the performance of the network.

Although the road network is composed by 18 sections, sections (1) Zambujal – (A) Node A9/A10, (A) Node A9/A10 – (1) Zambujal, (B) Node A1/A10 - (5) Benavente, (5) Benavente – (B) Node A1/A10, (B) Node A1/A10 - (7) Carregado, and (7) Carregado – (B) Node A1/A10 were not analysed. Because, in the road network in study, it is not present an alternative route solution for these sections. The identification of the 12 sections analysed is presented in Figure 7.33.

Table 7.24 presents the results obtained when each pair of sections is unavailable. Through the traffic model, the values for the total travel time, TTT, (column 3) and the total travel distance, TTD, (column 4) were obtained. The overall performance of the network (column 5) is computed using Equation 7.7 and the values of the resilience index for a 24-hours time horizon (column 7) are determined using Equations 7.5 and 7.6. The traffic flow circulation for each pair of sections unavailable is illustrated in Appendix B – Section B.2.

7.6.4   Discussion of the results

From the results presented in Table 7.24, it is possible to observe that the road network has an average resilience index of 0.77. Whatever the pair of sections closed, the road network has a resilience index greater than 0.58. Regarding the critical sections, the sections on the highway A1 are those with the lowest resilience index for the road network, with sections 5 and 8 being the most unfavourable. These results are in line with expectations, since the highway A1 is the road with highest traffic flow.

The closure of a section in highway A1 considerably reduces the resilience index when compared to the closure of sections in highways A9 or A10, because the traffic flow that is required to diverge is

(a) Input (1) Zambujal

(b) Input (2) Alverca

(c) Input (3) V.F.Xira

(d) Input (4) PLLN

(e) Input (5) Benavente
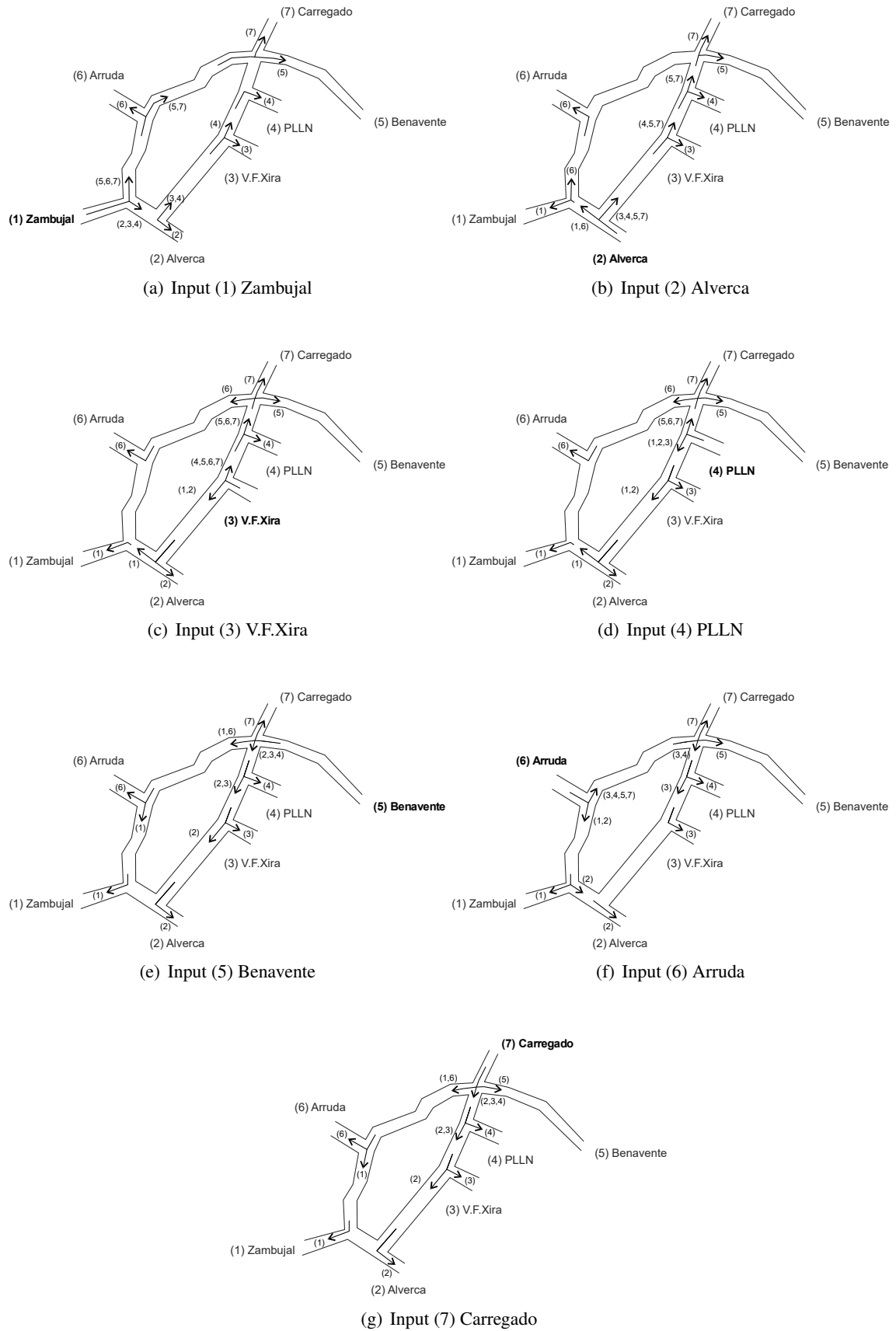
(f) Input (6) Arruda

(g) Input (7) Carregado

Figure 7.32 – Scheme of the traffic flow circulation to the situation in which all bridges are in service
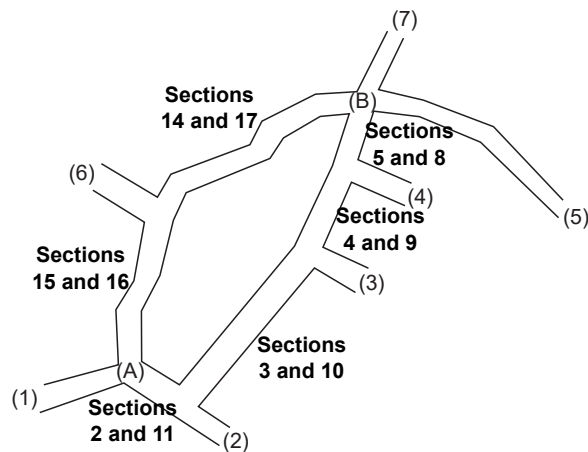
Figure 7.33 – Identification of the sections in the road network

Table 7.24 – Results: total travel time, total travel distance, performance network, functionality, and resilience of the road network for each of the studied situations

Sections closed	L [km]	TTT [min]	TTD [km]	Γ [–]	Q [%]	R [–]
No restrictions	–	603326	1176999	5.16	100.0	1.000
2 and 11	3.40	651415	1268200	4.78	92.7	0.927
3 and 10	10.90	1059769	1297971	3.42	66.2	0.662
4 and 9	3.90	1234770	1273447	3.07	59.4	0.594
5 and 8	1.20	1251617	1285843	3.03	58.7	0.587
14 and 17	3.00	641846	1246452	4.86	94.2	0.942
15 and 16	8.30	647326	1255362	4.82	93.4	0.934

much higher than the maximum capacity of the ramp between highways A9 and A10. That is, when a section in the highway A1 is closed, vehicles from the Southern input points of the highway A1 that wish to move North, or vice versa, are forced to use the alternative A9 + A10. The access ramp between highways A9 and A10 are a Type 3 segment in the traffic model with a maximum capacity of 900 veh/h. However the traffic flow that is required to use this alternative is much higher than this value as is depicted in Figure 7.34, increasing the time spend by users to travel between two points in the road network, and consequently reduces the overall performance of the road network according to Equation 7.7.

Figure 7.34 shows the variation of hourly traffic flow over January 20, 2014 on the ramp between highways A9 and A10 in the South – North direction (i.e. between Sections 11 and 16). As can be seen, the solid black, gray and green lines representing the traffic flow variation when sections in the highway A1 are closed. During the daytime period, flow rates exceeding the maximum capacity of the ramp (dotted black line). The dashed black line represents the hourly traffic flow for the situation in which all sections are in service. The solid blue line represents the traffic volume for the situation in which Sections 14 and 17 are closed. The situations in which Sections 2 and 11, and 15 and 16 are closed are not represented in the figure because the flow rate on the ramp between highways A9 and A10 in the South – North direction is null.
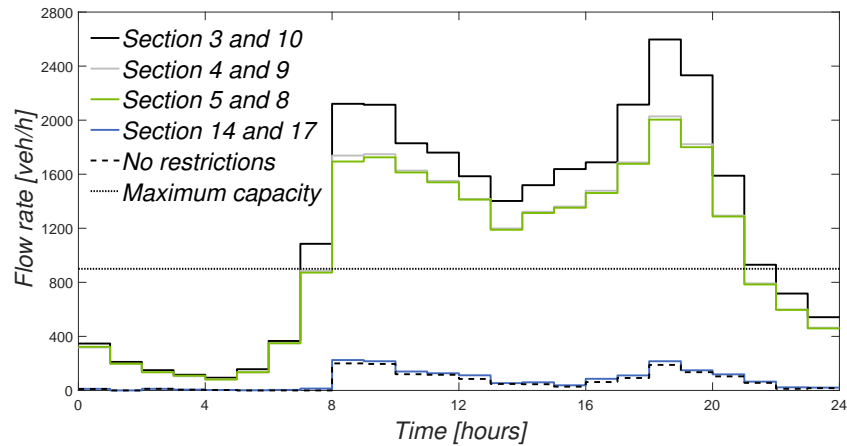
Figure 7.34 – Variation of the flow rate on the ramp between highway A9 and A10 in the South – North direction (from Section 11 to Section 16) over time

7.7 Summary

The main purpose of this chapter was to define a measure of the impact of maintenance on users. Through a literature review it can be observed that the resilience is one of the most used performance indicators to quantify the damage to networks.

The definition of resilience provided by Bruneau et al. (2003) is considered the most comprehensive definition and the most popular in the scientific community. This definition is composed by 11 different aspects: four dimensions (technical, organizational, social, economic), four properties (robustness, rapidity, redundancy, resourcefulness), and three results (more reliability, faster recovery, lower consequences). This definition introduces important aspects in the analysis of a transport network, although the ability of a bridge to withstand a disturbance depends almost exclusively on its structural characteristics, the recovery process is strongly affected by the technical, economic and political conditions of the community concerned in rehabilitating the bridge.

The road network used in the case study is part of the Portuguese highway network. The methodology implemented for the calculation of the resilience index is based on the work of Bocchini and Frangopol (2012). In this methodology, the system's functionality, $Q(t)$, is based on the concept of overall network performance, $\Gamma(t)$, which in turn is based on the concept of total travel time, $TTT(t)$, and total travel distance, $TTD(t)$. The last two parameters are easily obtained from a traffic model. The traffic model implemented is based on the concept of continuous Petri nets proposed by Tolba et al. (2005), being posteriorly calibrated and validated through the commercial software Aimsun.

From the obtained results it was observed that, in general, the road network presents a reasonable level of resilience. It can be concluded that the sections present in highway A1 are the most critical in the road network, which has the greatest socioeconomic consequences for the users in case traffic disturbance. In this sense, maintenance and/or rehabilitation actions should be planned in order to make this section more reliable and robust.

Chapter 8

Multi-objective Optimization

8.1   Introduction

The main purpose of a bridge manager is to find the best maintenance plan for a group of bridges over a time horizon. The definition of a maintenance plan usually results in a conflict of objectives. Bridge manager seeks to achieve a maintenance strategy that minimizes maintenance costs and maintain the structure in a safe and low deterioration condition. This problem can be studied as a single-objective optimization problem where cost is minimizes keeping performance above pre-defined thresholds (Neves, 2005). However, a single-objective optimization problem involves a single objective function and usually results in a single solution, called optimal solution (Branke et al., 2008). This methodology does not show the advantages and disadvantages of considering other objectives and constraints. On the other hand, a multi-objective optimization procedure considers several conflicting objectives simultaneously. In such a case, a set of maintenance scenarios with different trade-offs between objectives, called Pareto optimal solutions or non-dominated solutions is obtained (Branke et al., 2008). From these and considering the available budget, as well as the importance of the individual bridge and/or network, the decision-maker can make a more informed decision to prioritize the interventions that provide more benefits for the network (Neves, 2005).

A multi-objective optimization problem involves two or more objective functions which are to be either minimized or maximized. As in a single-objective optimization problem, the multi-objective optimization problem may contain a number of constraints that any feasible solution must satisfy. A multi-objective optimization problem can be expressed as follows (Branke et al., 2008):

$$\text{Minimize/Maximize:} \qquad f_m(x) \qquad m = 1, 2, ...M$$

$$\text{Subject to:} \qquad \begin{aligned} g_j(x) &\geq 0 \qquad j = 1, 2, ...J \\ h_k(x) &= 0 \qquad k = 1, 2, ...K \\ x_i^L \leq x_i &\leq x_i^U \qquad i = 1, 2, ...I \end{aligned} \qquad (8.1)$$

where $f_m(x)$ are the objective functions, and $g_j(x)$, $h_k(x)$, x_i^L, x_i^U are the constraints.

As mentioned before, in this type of problems the concept of optimal solution is replaced by the concept of non-dominated solutions. By definition, a feasible solution $x^{(1)}$ is said dominate the feasible solution $x^{(2)}$, if both the following conditions are true (Branke et al., 2008):

1. The solution $x^{(1)}$ is no worse than $x^{(2)}$ in any objectives.

2. The solution $x^{(1)}$ is strictly better than $x^{(2)}$ in at least one objective.

For a given set of solutions, a pair-wise comparison can be made using the above definition and whether one solution dominates the other can be established. All solutions that are not dominated by any other solution of the set are called non-dominated solution. In Figure 8.1, an example of a multi-objective optimization problem is shown. From the set of six solutions shown in the figure, solution 3, 5, and 6 are non-dominated solutions. The improvement in one objective, f_1, requires a sacrifice in the other objective, f_2. These solutions make up a non-dominated front when viewed together on the objective space (Branke et al., 2008).
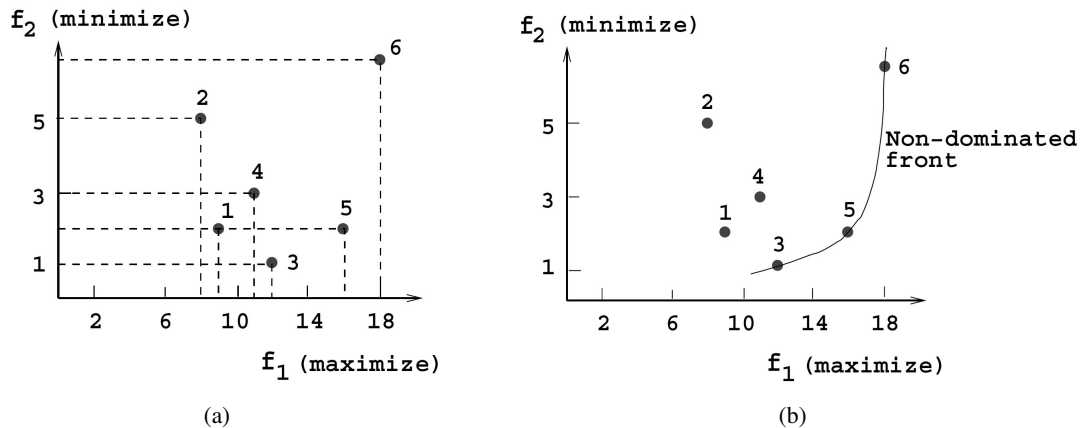

Figure 8.1 – Example of a set of solutions and the first non-dominated front of a multi-objective optimization problem (Branke et al., 2008)

In this study, the multi-objective optimization is performed using genetic algorithms available in software MalLab® (MatLab, 2017). One distinguishing feature of this methodology is the use of a population of solutions. This is of particular advantage because they search for several Pareto optimal solutions simultaneously (Branke et al., 2008).

In this chapter, the multi-objective optimization is applied to bridge maintenance. Two bridge components, pre-stressed concrete deck and bearings, are analysed. Since in the maintenance model it was defined that maintenance can only be applied after a major inspection has been carried out, the main goal of the multi-objective problem is to understand if there is an optimal time interval for performing the maintenance actions. This study is carried out for all maintenance strategies analysed in Section 5.6.

8.2   Formulation of the optimization problem

In this work, the optimization problem is formulated as a tri-objective optimization. The multi-objective algorithm is used to optimize the time intervals between major inspections. Therefore, in this optimization problem, the time interval between major inspections is considered as design variable, while the objective functions are the maximization of the mean condition state, the minimization of the total maintenance cost at time horizon, and the minimization of the impact of maintenance on users.

The mean condition state of the infrastructure is computed through the Petri net maintenance model described in Section 4.3. The total maintenance cost is a function of all maintenance actions performed in the infrastructure, being the Equation 4.9 adopted to compute the present value of cumulative maintenance cost. Finally, the concept of resilience is used to quantify the impact of maintenance on users (Equation 7.5), where the network functionality over time is computed through flow analyses provided by the traffic model (Section 7.3).

The design variable is subject to a constraint, the (optimal) time interval between major inspections should vary between a maximum and a minimum value. The analytical formulation of this optimization problem is given by:

> **Find:** The (optimal) time interval between major inspections, t_{insp}
>
> **So that:** Maximize the mean condition state during the time horizon
>
> Minimize the total maintenance cost at time horizon
>
> Minimize the impact of maintenance on users during the time horizon, through the maximization of the resilience index of the network
>
> **Subject to:** $2 \geq t_{insp} \geq 20$ [years]

Figure 8.2 presents the main interactions between the models of the methodology proposed. The maintenance model manages the effects of ageing and maintenance interventions over the time horizon, being also used to compute the maintenance cost. The traffic model is used to compute the traffic flow. The optimization model is the core of the procedure. In this model, multi-objective genetic algorithms are employed.

Figure 8.2 – Flowchart of the main interactions between the models of the tri-objective optimization problem

The optimization procedure has, as inputs, the initial condition state, C_0; the deterioration rate vector, Θ; the time horizon, t_h; the information about the maintenance strategy, *PM data* and *CM data*; and the information regarding the network characteristics, bridge location and traffic data. As the time interval between major inspection, t_{insp}, is the design variable, the multi-objective optimization begins by setting a value for this variable. The oncoming step is in the maintenance model, a performance and a cumulative maintenance cost profile are computed for each bridge present on the network, according to the maintenance strategy defined. The procedure followed in the maintenance model is described in Figure 4.12. When maintenance is applied, the traffic model is used to compute the functionality of the network, $Q(t)$, during maintenance. Functionality is computed through Equation 7.6. In the next step, the mean condition state of the infrastructure, the total maintenance cost, and the

mean resilience of the network are computed. This process is repeated iteratively until the predefined stopping criteria in the genetic algorithm is satisfied. The output of this procedure is a Pareto surface that relates the three objectives.

The parameters used in the optimization problems are the following:

- Size of the population: 150 individuals;

- Stopping criteria: the algorithm stops if the average relative change in the best fitness function value over 100 generations is less than or equal to 10^{-4};

- Mutation procedure was performed using the Adaptive Feasible algorithm implemented in MalLab$^{®}$;

- Crossover procedure was performed using the Intermediate algorithm implemented in MalLab$^{®}$.

8.3   Pre-stressed concrete decks

According to experts' judgement, the three maintenance works analysed in Section 5.6 for pre-stressed concrete deck do not affect the road traffic. So, the optimization problem for this bridge component can be simplified into a bi-objective optimization problem (Figure 8.3), being the analytical formulation of the optimization problem given by:

Find: The (optimal) time interval between major inspections, t_{insp}

So that: Maximize the mean condition state during the time horizon

Minimize the total maintenance cost at time horizon

Subject to: $2 \geq t_{insp} \geq 20$ [years]
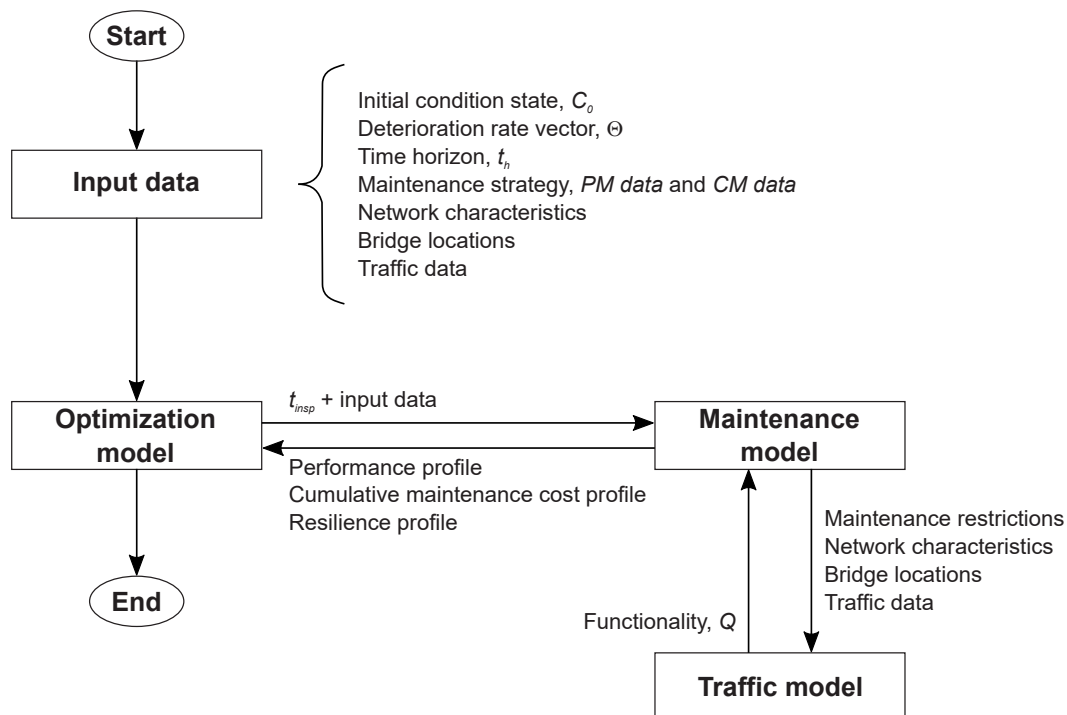

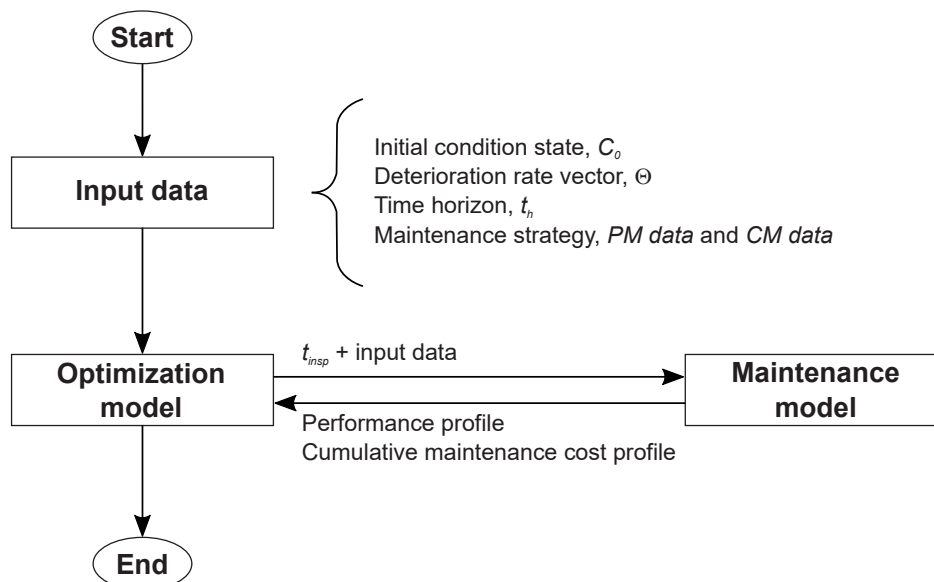Figure 8.3 – Flowchart of the main interactions between the models of the bi-objective optimization problem

Furthermore, the following data are considered for this optimization problem: (i) the deterioration of condition state under no maintenance follows a Weibull distribution with parameters (α_i, β_i), with $i = 1, 2, 3, 4, 5$, shown in Table 5.20; and, (ii) the effects on condition state and cost of application are

presented in Table 5.18. The condition state and the cumulative cost profiles are computed using the Monte Carlo simulation with 1 000 samples.

8.3.1 Optimization of performance indicators through the application of Maintenance D5

The set of non-dominated solutions obtained, considering the partial or full-depth concrete repair (Maintenance D5) as the only maintenance action, is shown in Figure 8.4. This figure relates the mean condition state and the total maintenance cost at time horizon. The relationship between these two objectives is slightly non-linear.
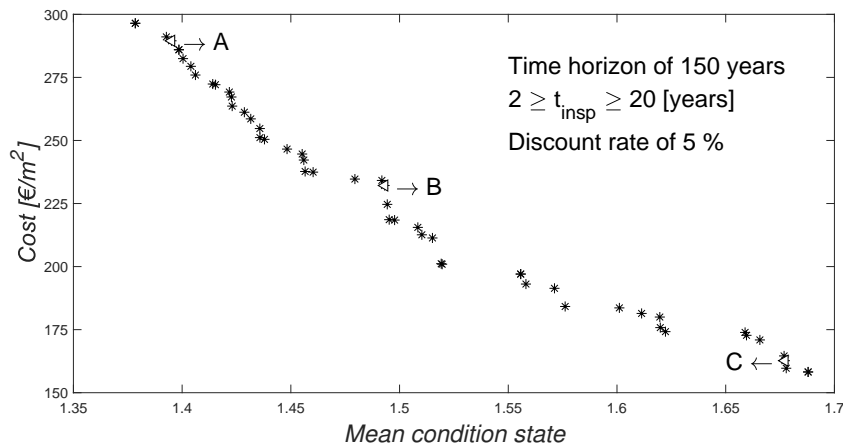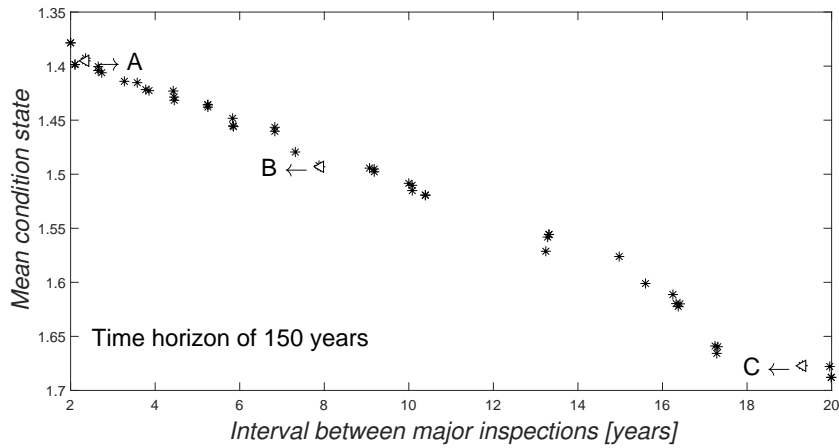

Figure 8.4 – Relationship between mean condition state and total maintenance cost at time horizon – Maintenance D5 – Pre-stressed concrete decks
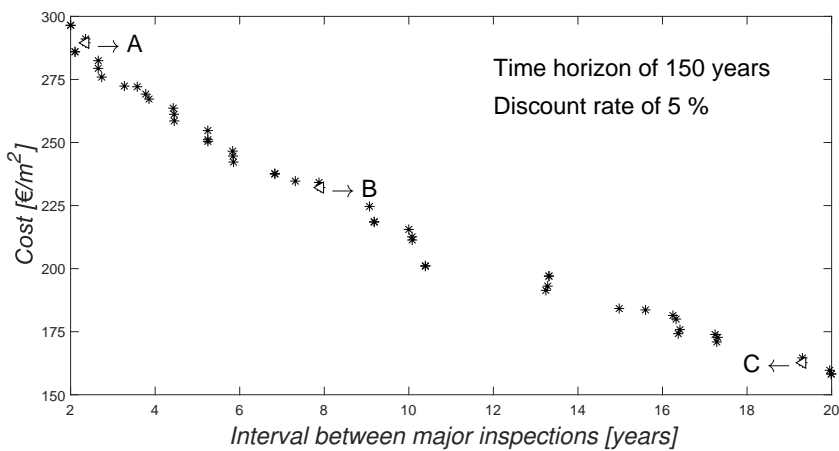
In Figure 8.5, the design variable, t_{insp}, is compared with the two objective functions. These results show that the correlation between the mean condition state and the time interval between major inspections (Figure 8.5(a)), and between the total maintenance cost and the time interval between major inspections (Figure 8.5(b)) is very strong.

In Figures 8.4 and 8.5, three different solutions (A, B, and C) are highlighted. These three solutions were selected amongst all optimal solutions because they are associated with high, medium and low cost, respectively. The analysis of these three solutions allows a clearer understanding of the impact of the interval between inspections on the cost and condition state. From these two figures, it is possible to stress that lower (i.e. better) values of mean condition state are associated with small time intervals between major inspections and higher maintenance cost. Small time intervals between major inspections mean that the verification of the condition state of the deck is performed more frequently and, consequently, the application of Maintenance D5 is performed at early condition states.

These observations can be corroborated by the results presented in Figure 8.6 and Table 8.1. In Figure 8.6, the condition and cumulative cost profiles of the three solutions are compared. In Table 8.1, the mean number of interventions for the three solutions are presented. Solution A is associated with a small time interval between major inspections and, consequently, with more frequent maintenance interventions (on average, 3.34 Maintenance D5 are applied over the time horizon). But, a higher frequency has a great disadvantage, a higher maintenance costs. On the other hand, solution C is associated with longer time intervals between major inspections. That is, the frequency of maintenance action application, in this solution, is the lowest of the three (on average, 2.44 Maintenance D5 are applied over the time horizon). Consequently, this solution is associated with higher deterioration levels and smaller maintenance costs. Solution B is an intermediate solution.

(a) Relationship between mean condition state and time interval between major inspections

(b) Relationship between total maintenance cost and time interval between major inspections

Figure 8.5 – Comparison of the design variable (time interval between major inspections, t_{insp}) with the two objective functions (mean condition state and total maintenance cost at the time horizon) – Maintenance D5 – Pre-stressed concrete decks

Table 8.1 – Mean number of intervention for solutions A, B, and C – Maintenance D5 – Pre-stressed concrete decks

Solution	Maintenance D5
A	3.34
B	2.97
C	2.44

In Table 8.2, the design variable, t_{insp}, and the values of the two objective functions (mean condition state and total maintenance cost) for the three solutions are presented. These results show, once again, the impact of the time interval between major inspections on the condition and cost values.

(a) Condition profiles

(b) Cumulative cost profiles
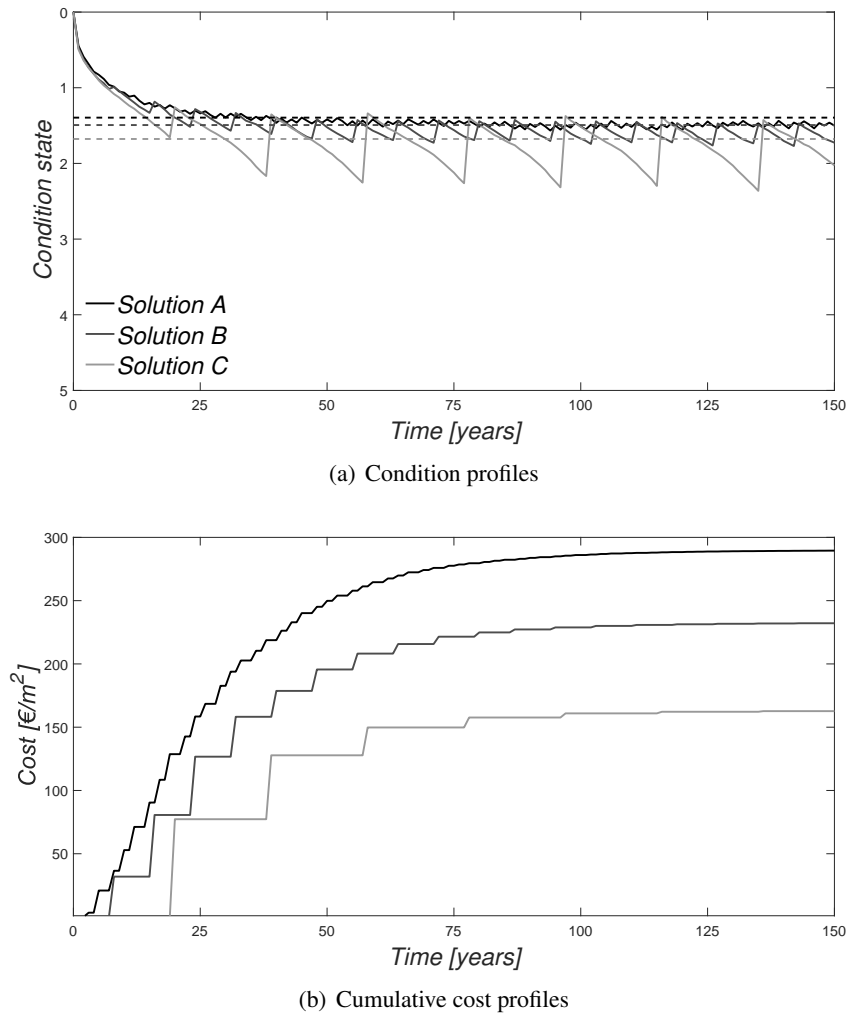
Figure 8.6 – Comparison of the condition and cumulative cost profiles for solutions A, B, and C. Solid lines represent the variation of the condition and cumulative cost profiles over time and the dashed lines the mean condition state – Maintenance D5 – Pre-stressed concrete decks

Table 8.2 – Comparison of the performance indicators for solutions A, B, and C – Maintenance D5 – Pre-stressed concrete decks

Solution	Mean condition state	Total maintenance cost [€/m^2]	Time interval between major inspections [years]
A	1.40	289.52	2.36
B	1.49	232.14	7.91
C	1.68	162.69	19.31

8.3.2 Optimization of performance indicators through the application of Maintenances D4 and D5

For the maintenance strategy that combines partial or full-depth concrete repair (Maintenance D5) and minor patching (Maintenance D4), the set of optimal solutions is shown in Figure 8.7. The results obtained show that there is a slight non-linearity between the two objective functions.

Figure 8.7 – Relationship between mean condition state and total maintenance cost at time horizon – Maintenance D4 and D5 – Pre-stressed concrete decks

In Figure 8.8, it is shown an almost linear relation between the mean condition state and the time interval between major inspections (Figure 8.8(a)), and between the total maintenance cost and the time interval between major inspections (Figure 8.8(b)).

In Figures 8.7 and 8.8, three optimal solutions (A, B, and C) are highlighted. The values of the design variable and objective functions associated with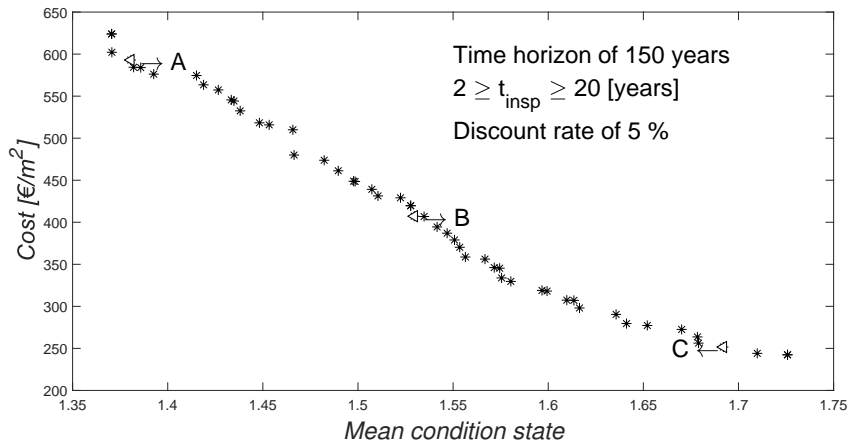 these three solutions are shown in Table 8.3. From these two figures and Table 8.3, it is possible to verify that, as before, lower (i.e. better) values of mean condition state are associated with small time intervals between major inspections and higher maintenance cost.

Table 8.3 – Comparison of the performance indicators for solutions A, B, and C – Maintenance D4 and D5 – Pre-stressed concrete decks

Solution	Mean condition state	Total maintenance cost [€/m^2]	Time interval between major inspections [years]
A	1.38	592.97	2.33
B	1.52	407.24	9.99
C	1.69	251.63	18.74

In Figure 8.9, the condition and cumulative cost profiles of the three solutions are compared and, in Table 8.4, the mean number of interventions for each of the three solutions is presented. Solution A is associated with a small time interval between major inspections. By comparing this solution with the other two solutions, it is possible to observe that solution A presents a lower mean condition state and a higher total maintenance cost. As can be seen from Table 8.4, small time intervals between major inspections are associated with a large number of maintenance interventions, increasing the overall maintenance cost. In total, in solution A, 10.74 maintenance actions are applied, on average, over time. On the other hand, solution C is associated with a longer time interval between major inspections. From the three solutions, solution C presents a higher mean condition state, a lower maintenance cost and, consequently, a lower frequency of maintenance actions application. In total, in solution C, 6.54 maintenance actions are applied, on average, over time. Solution B is an intermediate solution.

Furthermore, it should also be mentioned that for time intervals between major interventions lower
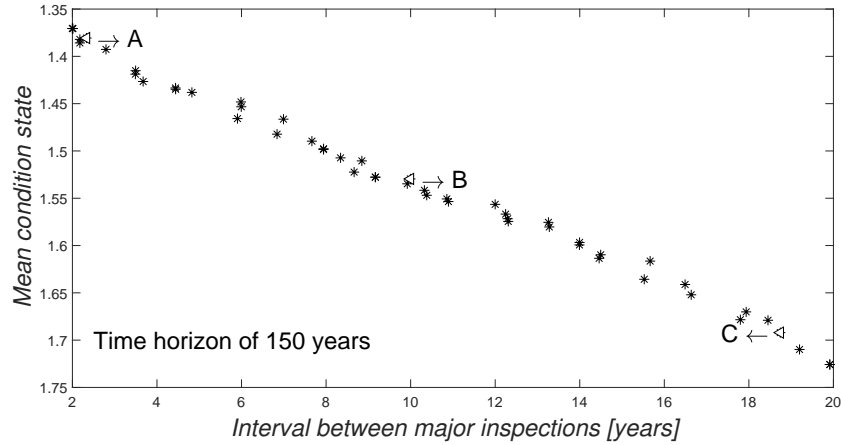
(a) Relationship between mean condition state and time interval between major inspections
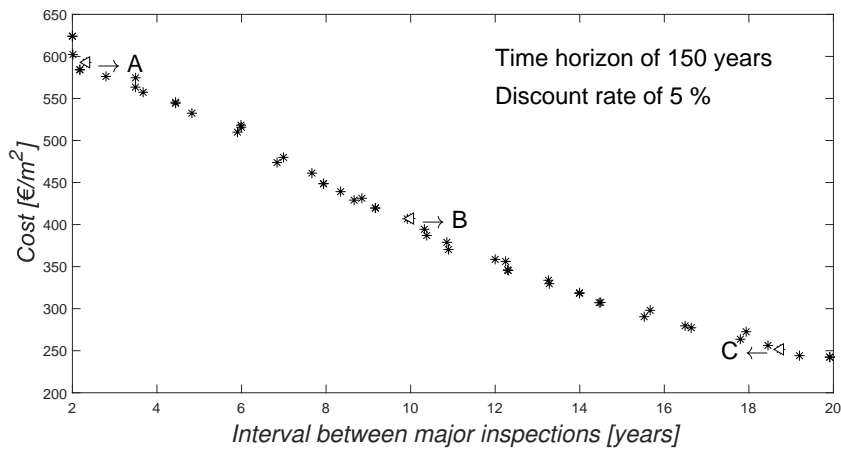
(b) Relationship between total maintenance cost and time interval between major inspections

Figure 8.8 – Comparison of the design variable (time interval between major inspections, t_{insp}) with the two objective functions (mean condition state and total maintenance cost at the time horizon) – Maintenance D4 and D5 – Pre-stressed concrete decks

Table 8.4 – Mean number of intervention for solutions A, B, and C – Maintenance D4 and D5 – Pre-stressed concrete decks

Solution	Maintenance D4	Maintenance D5
A	7.62	3.12
B	5.74	3.28
C	3.65	2.89

than 3 years, the superposition of effects of Maintenance D4 is possible. However, this superposition does not have great impact on the results because of the restrictions imposed in the number of consecutive maintenance actions of the same type (Section 5.6).

(a) Condition profiles
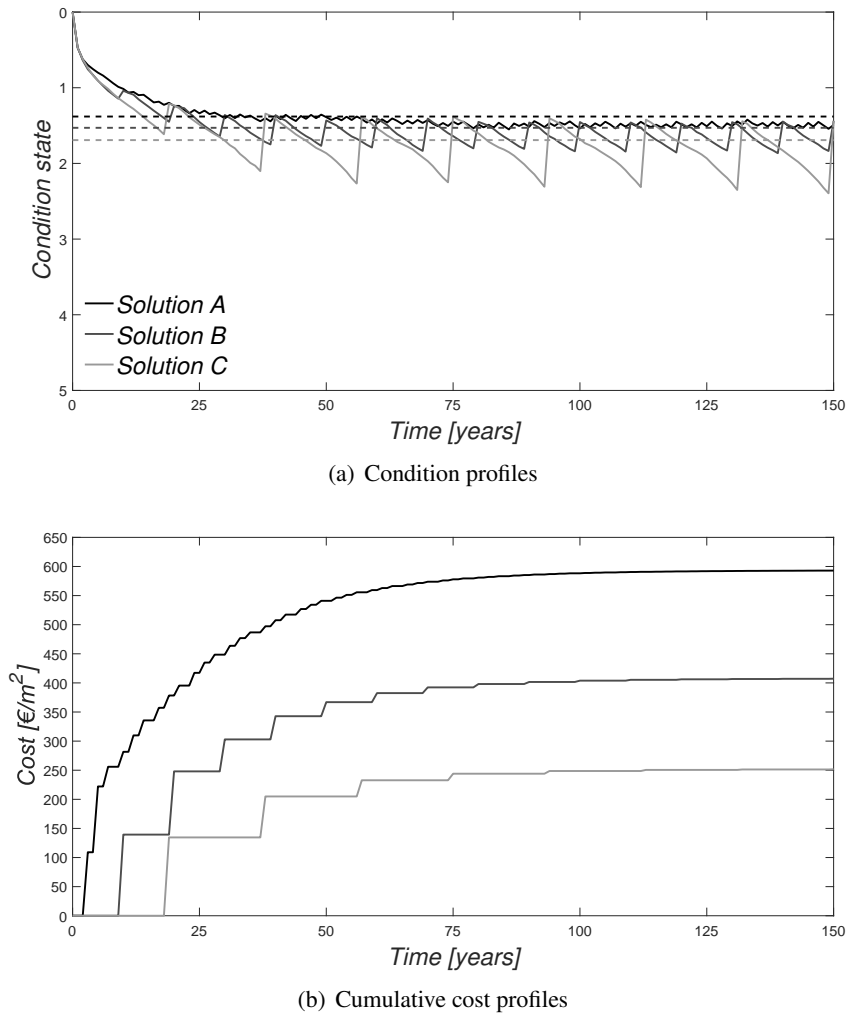

(b) Cumulative cost profiles

Figure 8.9 – Comparison of the condition and cumulative cost profiles for solutions A, B, and C. Solid lines represent the variation of the condition and cumulative cost profiles over time and the dashed lines the mean condition state – Maintenance D4 and D5 – Pre-stressed concrete decks

8.3.3 Optimization of performance indicators through the application of Maintenances D2, D4 and D5

As for previous maintenance strategies, the set of optimal solutions obtained under partial or full depth repair (Maintenance D5), minor patching (Maintenance D4) and spot painting of concrete elements (Maintenance D2) is presented in Figure 8.10. In this figure, the relationship between the mean condition state and the total maintenance cost at time horizon are assessed. The Pareto front is discontinuous, being possible to divide the feasible set of solutions into two regions. The first region is associated with lower (i.e. better) values of mean condition state and higher total maintenance costs, and the second region associated with higher mean condition states and lower total maintenance costs.

In order to understand the reason for this discontinuity and to observe the evolution of the performance indicators throughout the entire domain, non-dominated and dominated solutions were plotted in the same figure (Figure 8.11). In Figure 8.11, four non-dominated solutions (A, B, C, and D) and two dominated solutions (C', and C'') are highlighted. The values of the design variables and the objective functions associated with these six solutions are shown in Table 8.5.

In Figure 8.12, that relates the design variable, t_{insp}, with the two objective functions, the discontinuity
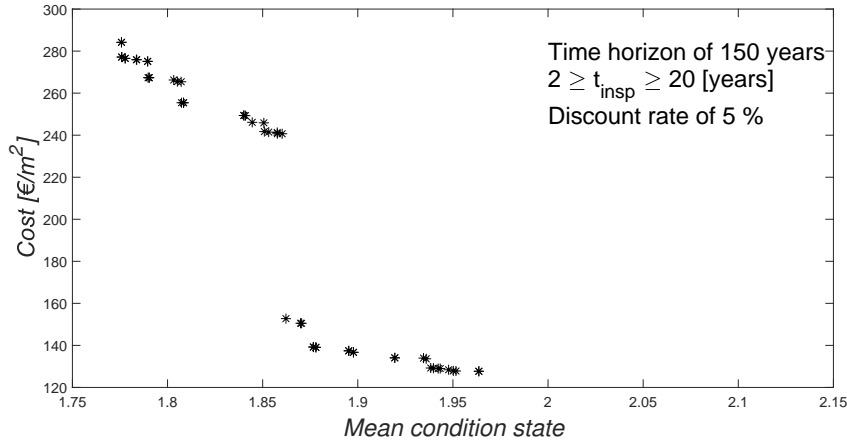
Figure 8.10 – Relationship between mean condition state and total maintenance cost at time horizon – Maintenance D2, D4 and D5 – Pre-stressed concrete decks
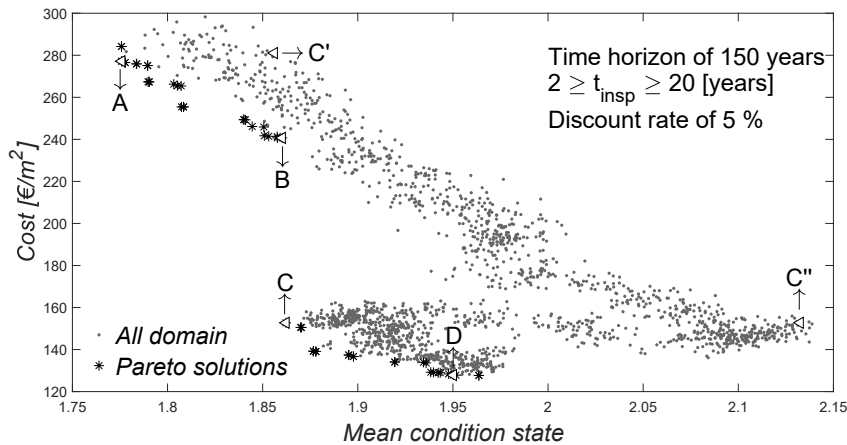
Figure 8.11 – Non-dominated and dominated solutions – Maintenance D2, D4 and D5 – Pre-stressed concrete decks

Table 8.5 – Comparison of the performance indicators for all solutions – Maintenance D2, D4 and D5 – Pre-stressed concrete decks

Solution	Mean condition state	Total maintenance cost [€/m^2]	Time interval between major inspections [years]
A	1.77	277.17	2.05
B	1.86	240.68	3.76
C	1.86	152.73	14.98
C'	1.86	281.06	3.03
C"	2.13	152.73	10.45
D	1.95	127.87	19.44

referred to above remains visible. In addition, it is possible to observe from these results that time intervals between major inspections among 4 and 15 years do not belong to the Pareto front.

In Figure 8.13 and Table 8.6, the condition and cumulative cost profiles of the four optimal solu-

(a) Relationship between mean condition state and time interval between major inspections
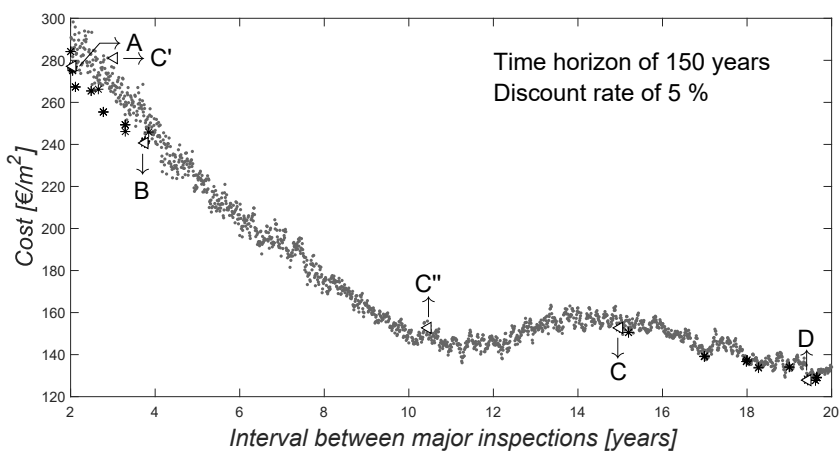
(b) Relationship between total maintenance cost and time interval between major inspections

Figure 8.12 – Comparison of the design variable (time interval between major inspections, t_{insp}) with the two objective functions (mean condition state and total maintenance cost at the time horizon) – Maintenance D2, D4 and D5 – Pre-stressed concrete decks

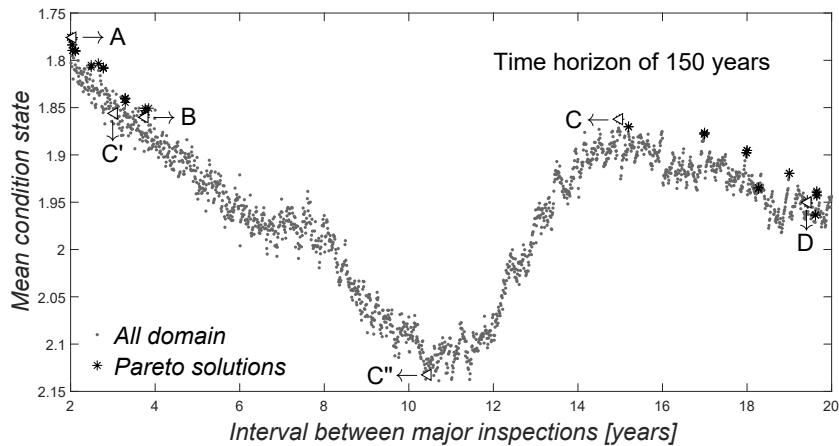tions and the mean number of interventions for each optimal solution are presented, respectively. By comparing this four solutions, solution A is associated with a small time interval between major inspections and, consequently, presents a lower mean condition state, a higher total maintenance cost and a higher frequency of maintenance actions application (13.11 maintenance actions are applied, on average, over time). In opposition, solution D is associated with a longer time interval between major inspections, presenting a higher mean condition state, a lower cumulative maintenance cost and a lower frequency of maintenance actions application (5.88 maintenance actions are applied, on average, over time). Solution B and C are intermediate solutions. These results show that, although resulting in similar mean condition state, solution B is associated with a lower time interval between major inspections, resulting in higher maintenance costs. From Table 8.6, it can be seen that small time intervals are associated with a large number of applications of maintenance. In solution C, 7.78 maintenance actions are applied while, in solution B, 11.8 maintenance actions are applied. Also, it can be observed that in solution C the number of applications of Maintenance D2 and D4 decreases and the number of applications of Maintenance D5 increases.

The performance indicators associated with solutions C, C' and C" in Figure 8.11 are compared in Figure 8.14. These results show that although solutions C and C' have similar mean condition states, solution C' is associated with a smaller time interval between major inspections and, consequently,

(a) Condition profiles
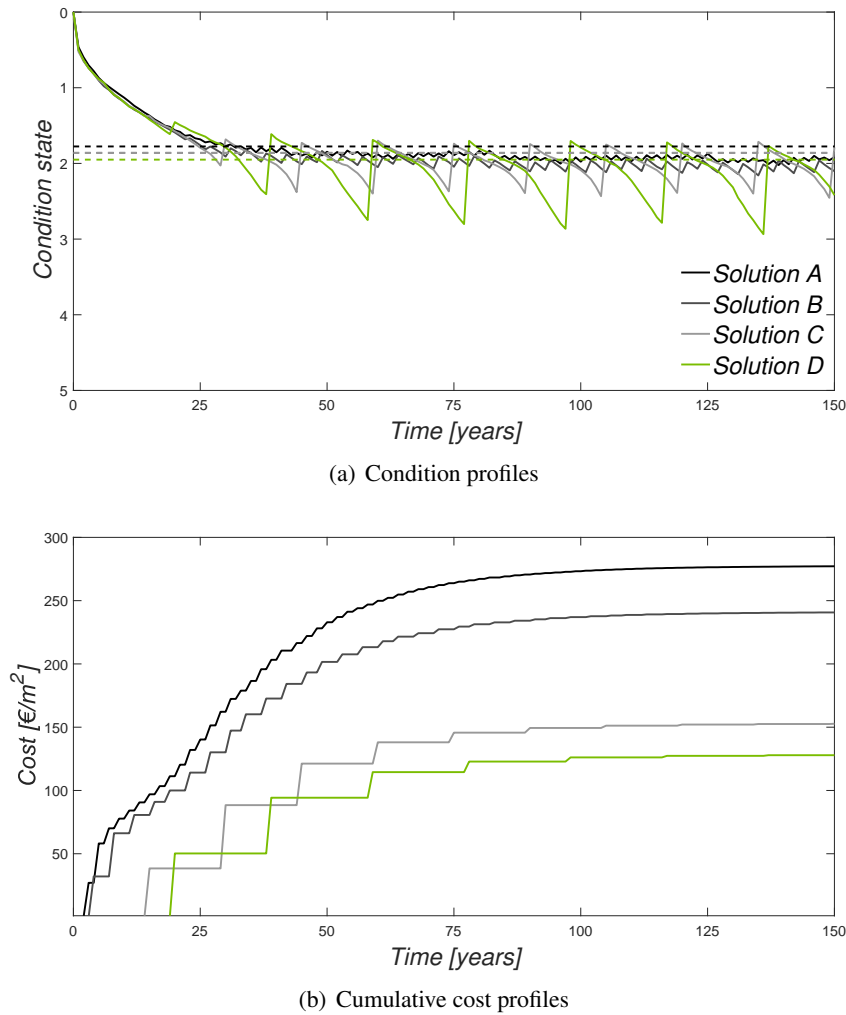

(b) Cumulative cost profiles

Figure 8.13 – Comparison of the condition and cumulative cost profiles for solutions A, B, C and D. Solid lines represent the variation of the condition and cumulative cost profiles over time and the dashed lines the mean condition state – Maintenance D2, D4 and D5 – Pre-stressed concrete decks

Table 8.6 – Mean number of intervention for all solutions – Maintenance D2, D4 and D5 – Pre-stressed concrete decks

Solution	Maintenance D2	Maintenance D4	Maintenance D5
A	5.97	4.95	2.19
B	5.24	4.56	2.00
C	3.64	1.90	2.24
C'	5.66	4.92	2.17
C''	3.59	3.69	1.67
D	2.75	1.16	1.97

a higher frequency of maintenance actions application (on average, 12.75 maintenance actions are applied over time for solution C') and a higher cumulative maintenance cost. On the other hand, if solutions C and C'' are compared, it is possible to verify that these two solutions have similar cumulative maintenance cost, but solution C'' is associated with worse mean condition state. The time interval between major inspections, in solution C'', is lower when compared to solution C.

(a) Condition profiles
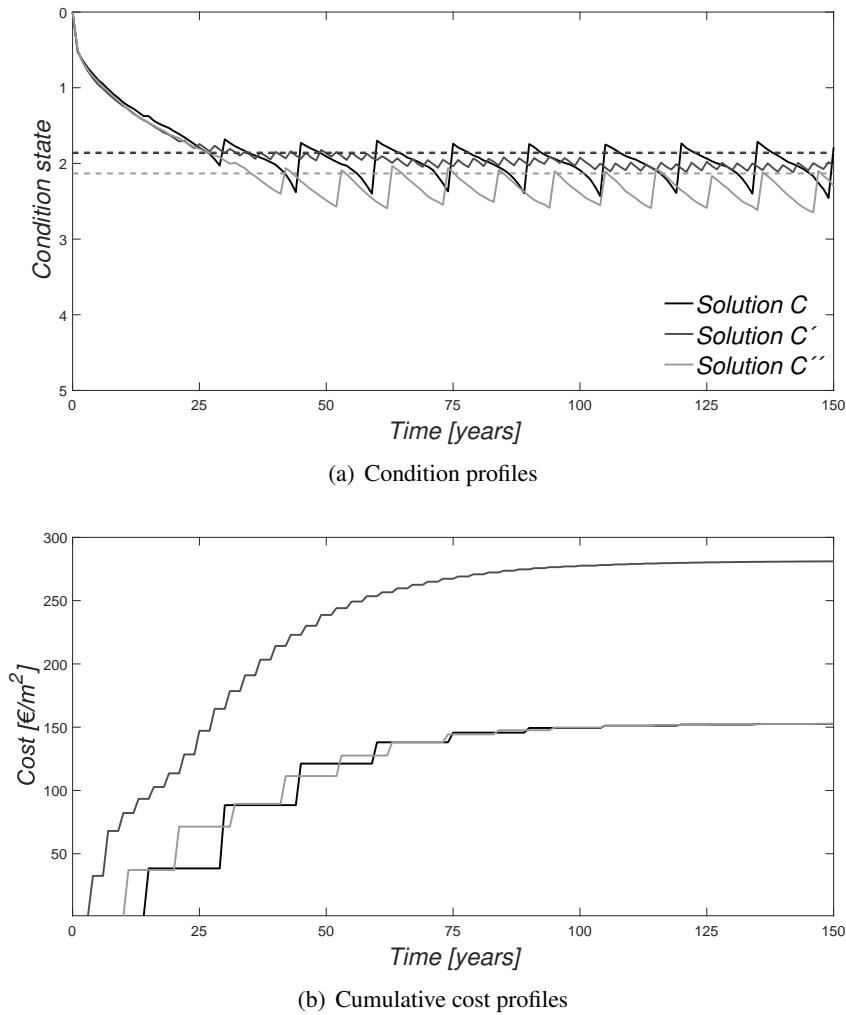

(b) Cumulative cost profiles

Figure 8.14 – Comparison of the condition and cumulative cost profiles for solutions C, C', and C''. Solid lines represent the variation of the condition and cumulative cost profiles over time and the dashed lines the mean condition state – Maintenance D2, D4 and D5 – Pre-stressed concrete decks

8.3.4 Comparison of different optimal maintenance strategies for pre-stressed concrete decks

In the present section, a multi-objective optimization algorithm based on genetic algorithm was used to compute the optimal time intervals between major inspections, considering different combinations of maintenance actions for pre-stressed concrete decks. In Figure 8.15, the Pareto fronts of these maintenance strategies are compared.

For this bridge component, the use of one type of maintenance actions show some advantages when compared with the other strategies. When the Pareto solutions associated with maintenance strategy 1 (Maintenance D5) and maintenance strategy 2 (Maintenance D5 and D4) are compared, differences in the objective functions become apparent. For similar mean condition states, the maintenance strategy that combines Maintenance D5 and D4 leads to higher maintenance costs than those that only include Maintenance D5. In maintenance strategy 2 costs are approximately double.

In short, the application of Maintenance D4 (minor patching) together with Maintenance D5 (partial or full-depth concrete repair) is not a very effective maintenance strategy, as mentioned in Section 5.6. Since the period of time that the deterioration process is suppressed in Maintenance D4 (Table
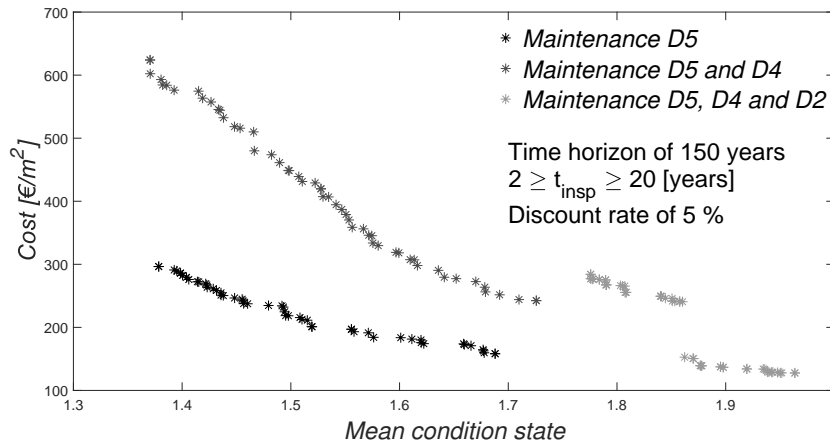
Figure 8.15 – Comparison of the dominated solutions of the three maintenance strategies – Prestressed concrete decks

5.18) is short, making this maintenance alone has little or no impact on the mean condition state of the deck and has a significant impact on costs.

On the other hand, when maintenance strategy 1 and maintenance strategy 3 (Maintenance D5, D4 and D2) are compared, maintenance strategy 3 shows worst mean condition states for similar maintenance costs. By comparing Tables 8.1 and 8.6, it can be seen that the inclusion of Maintenance D2 allows reducing the number of applications of Maintenance D5, reducing slightly the maintenance costs but without great advantage in the mean condition state.

8.4 Bearings

For bearings, based on experts' judgement, from the three maintenance works analysed in Section 5.6, only Maintenance B4 affects the road traffic. According to the information gathered, in a replacement of the bearings in a bridge, there is the closure of the more external lanes for 3 days (on average) to avoid instabilities in the deck. In addition, it has been explained that during this period the limited maximum speed is only casually reduced when the elevation of the deck is performed for the bearings to be replaced. So, for this bridge component, the second optimization problem described in Section 8.2 is implemented.

Furthermore, the following data and assumptions are considered for this optimization problem: (i) the deterioration of condition state under no maintenance follows a Weibull distribution with parameters (α_i, β_i), with $i = 1, 2, 3, 4, 5$, shown in Table 5.21; (ii) the effects on condition state and costs of application are presented in Table 5.19; and, (iii) the traffic data used in the traffic model are presented in Table 8.7, corresponding to the average daily traffic flow in January 2014.

The present application example is applied to the road network described in Section 7.4. In order to be able to evaluate the resilience index of the road network and to analyse which is the section that most affects the performance of the network, six case studies were examined for each maintenance strategy. It was considered that in each case studies only one bridge is under maintenance. The identification of the six different case studies analysed is presented in Figure 8.16.

As mentioned in Section 7.6, although the road network is composed by 18 sections, sections (1) Zambujal – (A) Node A9/A10, (A) Node A9/A10 – (1) Zambujal, (B) Node A1/A10 - (5) Benavente, (5) Benavente – (B) Node A1/A10, (B) Node A1/A10 - (7) Carregado, and (7) Carregado – (B) Node A1/A10 were not analysed. Once, in the road network in study, an alternative route solution for these

Table 8.7 – Average daily traffic flow of the road network on January 2014

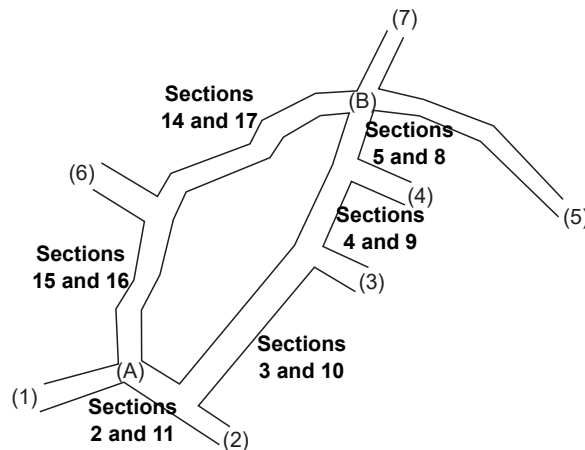|	(1) Zam-bujal	(2) Alverca	(3) V.F.Xira	(4) PLLN	(5) Be-navente	(6) Arruda	(7) Car-regado
(1) Zam-bujal	–	1 554	491	48	229	33	3 175
(2) Alverca	1 764	–	7 538	324	627	1 161	19 523
(3) V.F.Xira	626	9 857	–	83	107	18	2 909
(4) PLLN	44	333	73	–	53	4	178
(5) Be-navente	216	669	104	45	–	4	1 025
(6) Arruda	35	1 293	13	5	5	–	206
(7) Car-regado	2 929	20 282	2 746	192	1 081	241	–

Figure 8.16 – Identification of the sections in the road network

sections is not presented. The calculations of the resilience index were performed for a 24-hour time horizon, and the methodology used is described in Section 7.6. The results obtained are presented in Table 8.8.

Table 8.8 – Results: total travel time, total travel distance, performance network, and resilience of the road network for the situation in which all bridges are in service

Sections closed	L [km]	TTT [min]	TTD [km]	Γ [–]	R [–]
No restrictions	–	582486	1139171	5.3407	1.0000

In each case study analysed, the overall performance of the network was determined imposing only the constraints on a segment of the concerned sections, modelling the extension of the bridge under maintenance. In Table 8.9, the numbers of restricted segments in each section are identified (see those locations in Appendix B – Section B.1).

In order to model the traffic constraints provided by expert opinion, the following characteristics are considered in each segment: only the more external lane is closed and the traffic behaviour considered

Table 8.9 – Identification of the restricted segments in each section

Section	Segment	Section	Segment
2	8	11	65
3	17	10	55
4	27	9	46
5	33	8	41
14	86	17	115
15	93	16	106

is of the type 2 (Section 7.5.2). That is, when there is a junction or a bottleneck in the network, the drivers' instinct is to reduce their speed slightly as a road safety attitude. Table 8.10 presents the results obtained when each pair of sections is constrained. Through the traffic model, the values for the total travel time, TTT, (column 3) and the total travel distance, TTD, (column 4) were obtained. The overall performance of the network, Γ, (column 5) is computed using Equation 7.7. Finally, the values of the resilience index, R, for a 24-hours time horizon (column 6) are determined using Equations 7.5 and 7.6.

Table 8.10 – Results: total travel time, total travel distance, performance network, and resilience of the road network for each of the studies situations

Sections closed	L [km]	TTT [min]	TTD [km]	Γ [–]	R [–]
2 and 11	3.40	582746	1139171	5.3393	0.9997
3 and 10	10.90	585675	1139171	5.3226	0.9966
4 and 9	3.90	584701	1139171	5.3281	0.9976
5 and 8	1.20	583255	1139171	5.3364	0.9992
14 and 17	3.00	582889	1139171	5.3385	0.9996
15 and 16	8.30	582928	1139171	5.3382	0.9995

Since the traffic flows of the road network are not very high and traffic constrains are not very significant, the influence of Maintenance B4 on the performance of the network is reduced. Resilience values range from 0 to 1, where 1 means that road traffic is unconstrained and 0 means that network is out of service. However, from Table 8.10 it can be seen that the impact to users, when there is application of Maintenance B4, is reduced.

Considering the differences between resilience values are minimal, in the following sections, so that the results are more understandable for resilience, a logarithmic scale is used. Resilience, R, and logarithmic resilience, R_{Log}, follow the relation:

$$R_{Log} = -\log\left(1 - R\right) \tag{8.2}$$

Furthermore, the traffic analyses for each maintenance strategy were considered in a deterministic way, in order to reduce the computational time of the optimization problem. The results of this analysis will enable decision-makers to know, in an expeditious way, which are the most critical segments of the road network and, in this way, prioritize maintenance actions so that the road network becomes more reliable and that the socioeconomic consequences are minimized.

The condition, cumulative cost, and resilience profiles are computed using the Monte Carlo simulation with 1 000 samples.

8.4.1   Optimization of performance indicators through the application of Maintenance B4

The set of non-dominated solutions obtained, for the situation where the replacement of the bearings (Maintenance B4) is the only maintenance action considered, is shown in Figure 8.17, for the six situations analysed. The projections of these results in bi-dimensional space are presented in Figure 8.18. These three figures relate the three objective functions (mean condition state, total maintenance cost at time horizon and resilience).
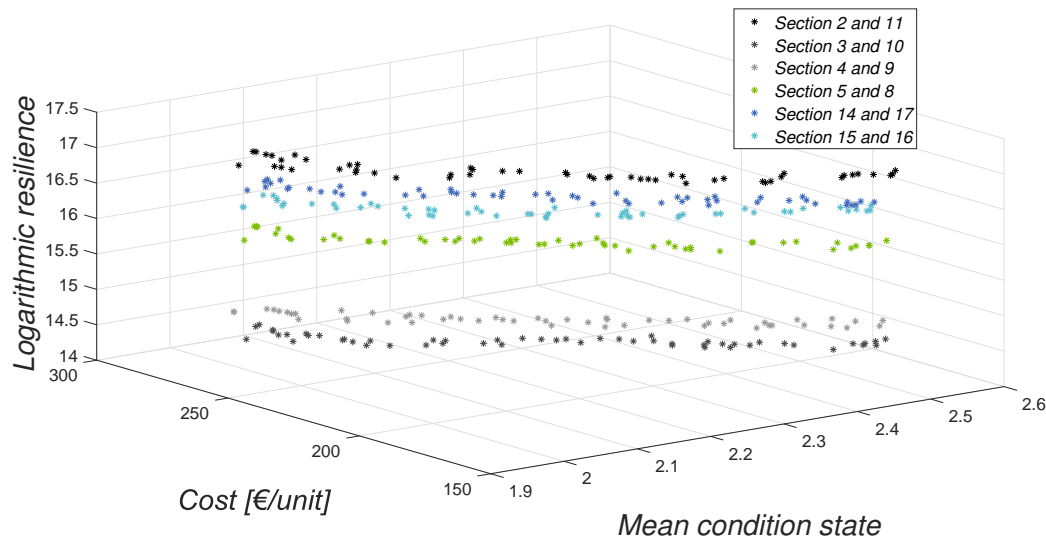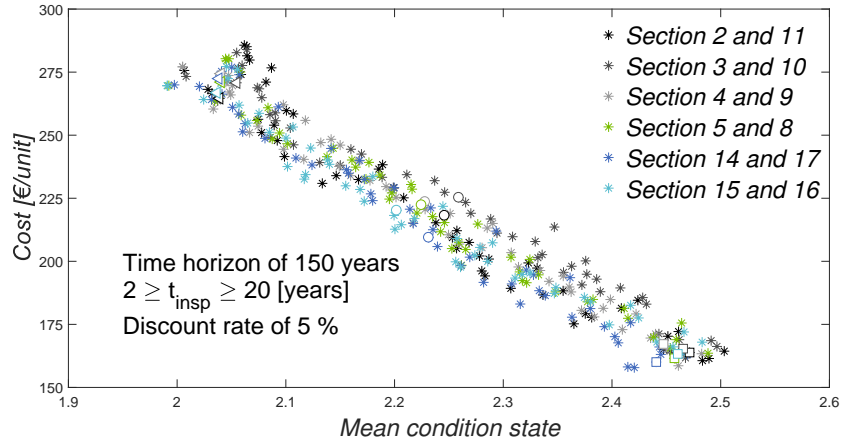

Figure 8.17 – Relationship between three objective functions (mean condition state, total maintenance cost at time horizon and resilience) – Maintenance B4 – Bearings

From these figures, it can be seen that Sections 3 and 10 produce higher impact to users when Maintenance B4 is applied, since they are the sections with the highest traffic flows (see Figure 7.32 and Table 8.7). In addition, through the relationships between the three objective functions, it can be seen that better resilience values are associated with lower maintenance costs and higher average condition states. These conclusions are visible for the six case studies, being most noticeable for Sections 3 and 10.

In Figure 8.19, the design variable, t_{insp}, is compared with the three objective functions. These results show a linear relation between all objective functions. The results presented in this figure corroborate the above observations. It is possible to verify that longer time intervals between major inspections mean worse mean condition states, lower total maintenance costs, and better resilience indices. That is, longer time intervals are associated with a smaller number of maintenance interventions, reducing maintenance costs and traffic disruptions.

These observations are also visible in Figures 8.20 to 8.22 and Table 8.11. In Figures 8.18 and 8.19, several optimal solutions are highlighted. More precisely, for each case study, three non-dominated solutions are highlighted through three different symbols. The triangular, circular, and quadricular symbols correspond, respectively, to optimal solutions with shorter, intermediate, and longer time intervals between major inspections. In Figures 8.20 to 8.22, the condition, cumulative cost and resilience profiles of the six case studies analysed for the three time intervals are compared, respectively. And, in Table 8.11, the mean number of interventions for each optimal solution are presented. The triangular solutions are associated with short time intervals between major inspections. This means that the verification of the condition state of the bearings is carried out more frequently and, consequently, Maintenance B4 is performed earlier, being more likely that more maintenance actions are implemented over the years, thereby increasing the overall maintenance cost and decreasing the

(a) Relationship between mean condition state and total maintenance cost at time horizon
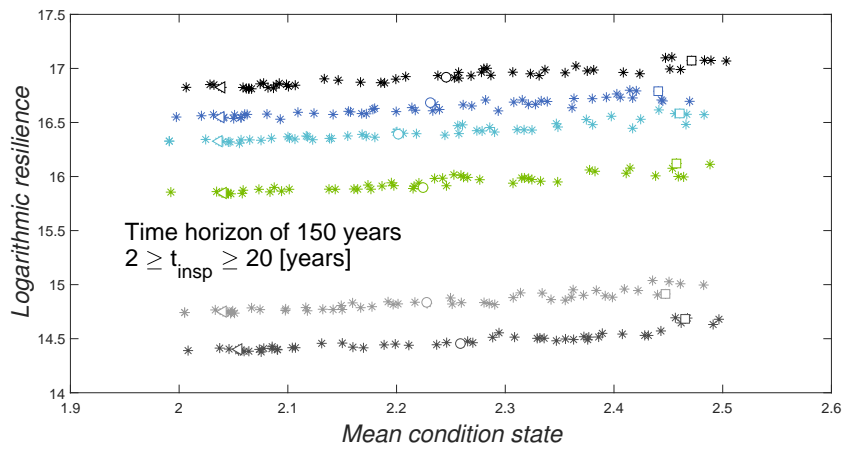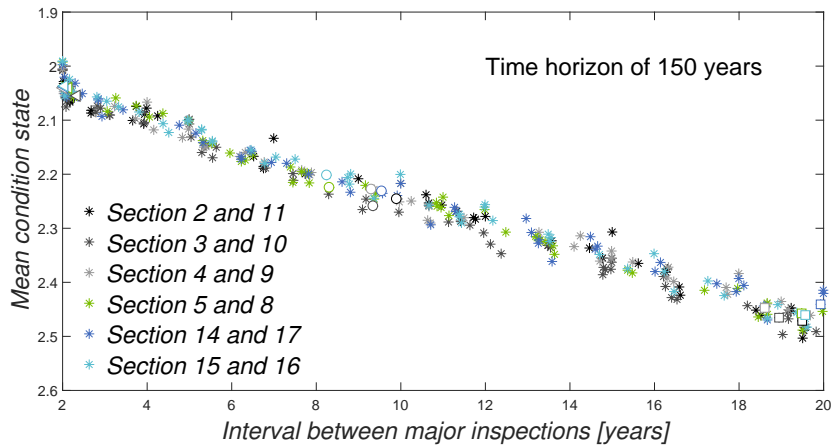

(b) Relationship between mean condition state and logarithmic resilience at time horizon
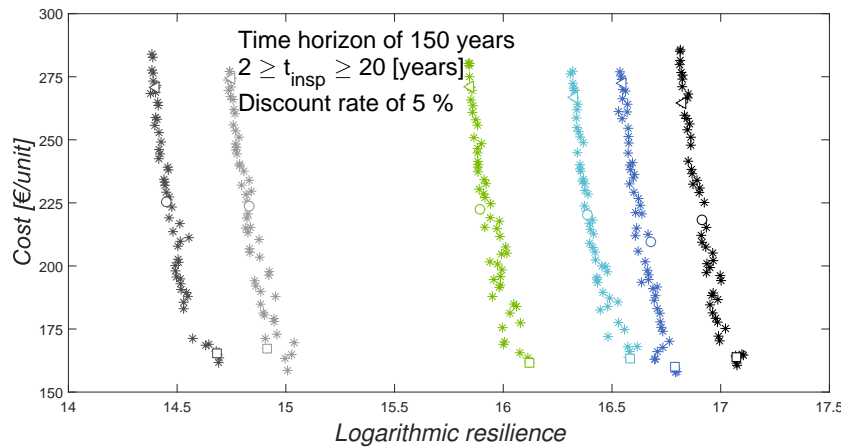
(c) Relationship between logarithmic resilience and total maintenance cost at time horizon

Figure 8.18 – Projections of the objective functions in bi-dimensional space – Maintenance B4 – Bearings

resilience of the network. On the other hand, quadricular solutions are associated with longer time intervals between major inspections. In this solution, the frequency of application of Maintenance B4 is lowest, resulting in fewer maintenance actions to be implemented over the years, decreasing the overall maintenance cost and increasing the resilience of the network.

(a) Relationship between mean condition state and time interval between major inspections
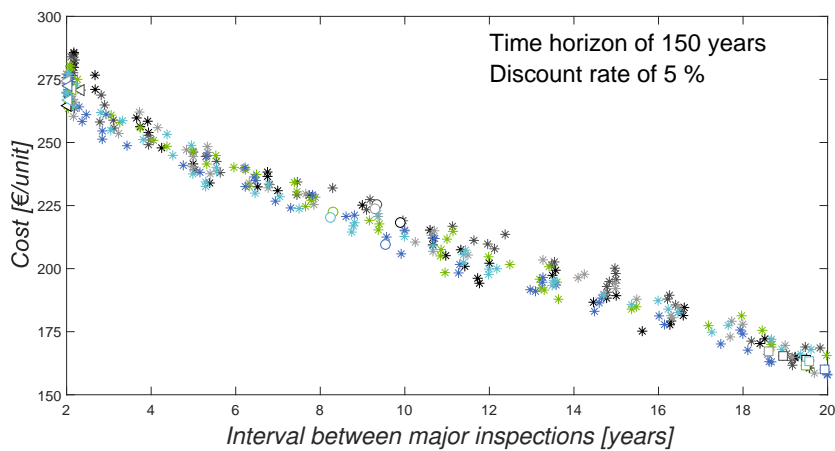
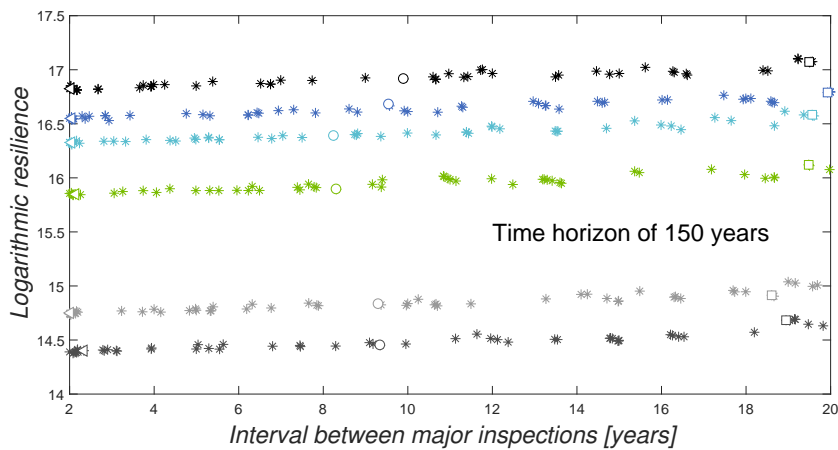(b) Relationship between total maintenance cost and time interval between major inspections

(c) Relationship between logarithmic resilience and time interval between major inspections

Figure 8.19 – Comparison of the design variable (time interval between major inspections, t_{insp}) with the three objective functions (mean condition state, total maintenance cost at the time horizon and resilience) – Maintenance B4 – Bearings

In Table 8.12, the design variable, t_{insp}, and the values of the three objective functions (mean condition state, total maintenance cost, and mean resilience) for all highlighted solutions are presented. These results show, once again, the impact of the time interval between major inspections on the condition,

(a) Condition profiles

(b) Cumulative cost profiles

(c) Resilience profiles

Figure 8.20 – Comparison of the condition, cumulative cost and resilience profiles for solutions with shorter time intervals between major inspections for the six situations analysed. Solid lines represent the variation of the condition, cumulative cost and resilience profiles over time and the dashed lines the mean condition state and resilience, respectively – Maintenance B4 – Bearings

cost, and resilience values.

(a) Condition profiles

(b) Cumulative cost profiles
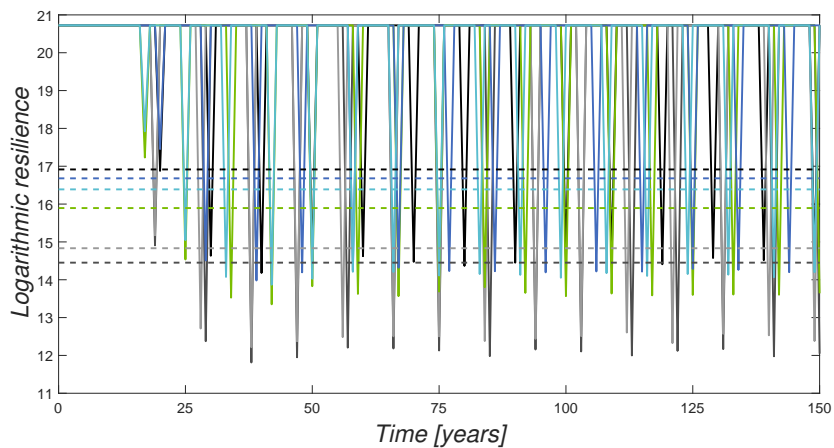
(c) Resilience profiles

Figure 8.21 – Comparison of the condition, cumulative cost and resilience profiles for solutions with intermediate time intervals between major inspections for the six situations analysed. Solid lines represent the variation of the condition, cumulative cost and resilience profiles over time and the dashed lines the mean condition state and resilience, respectively – Maintenance B4 – Bearings
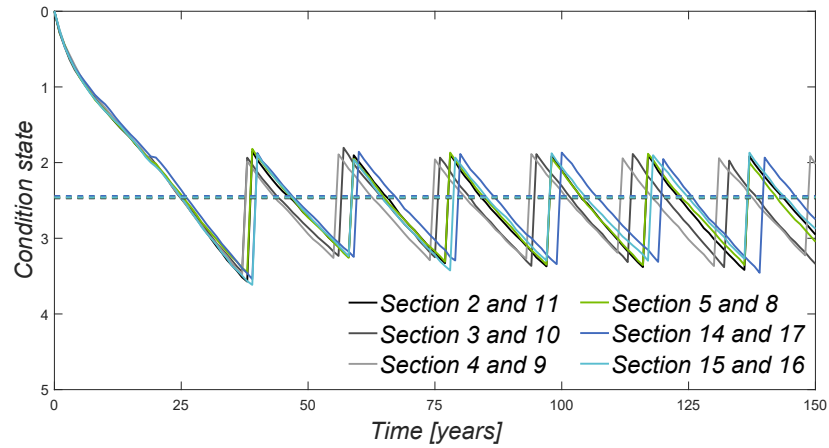
(a) Condition profiles
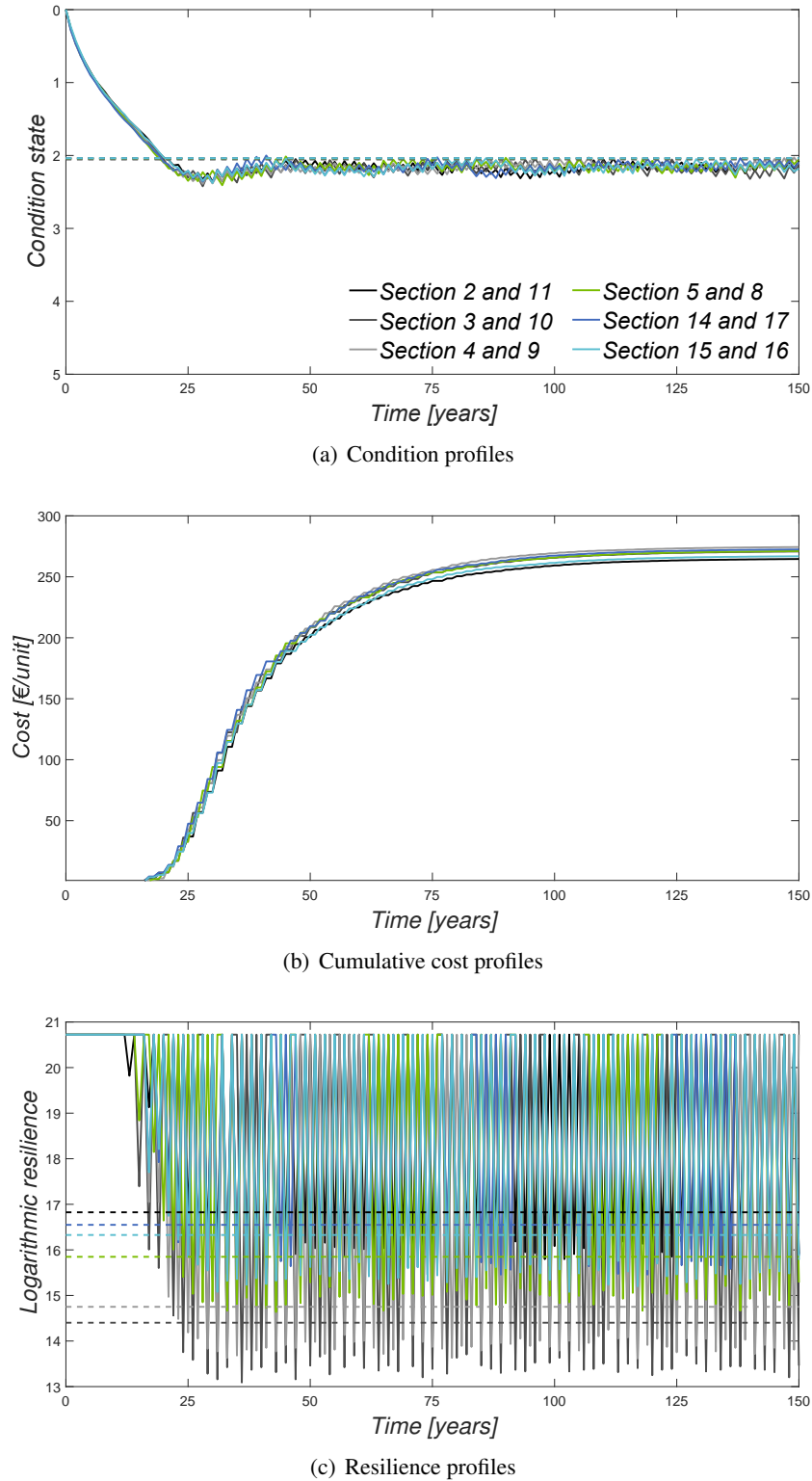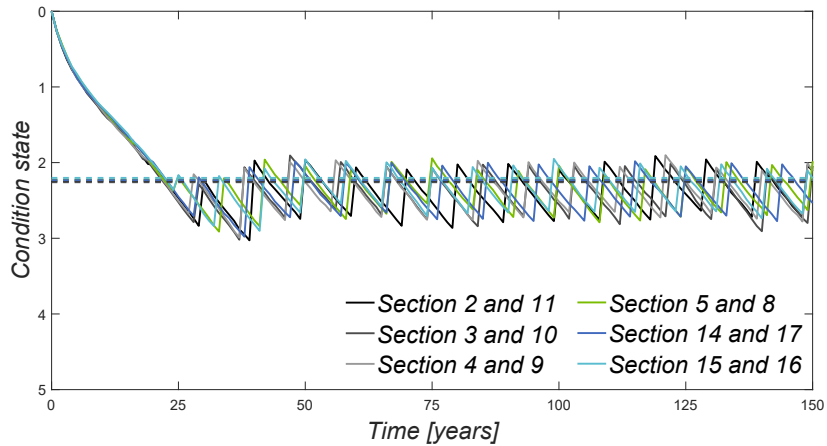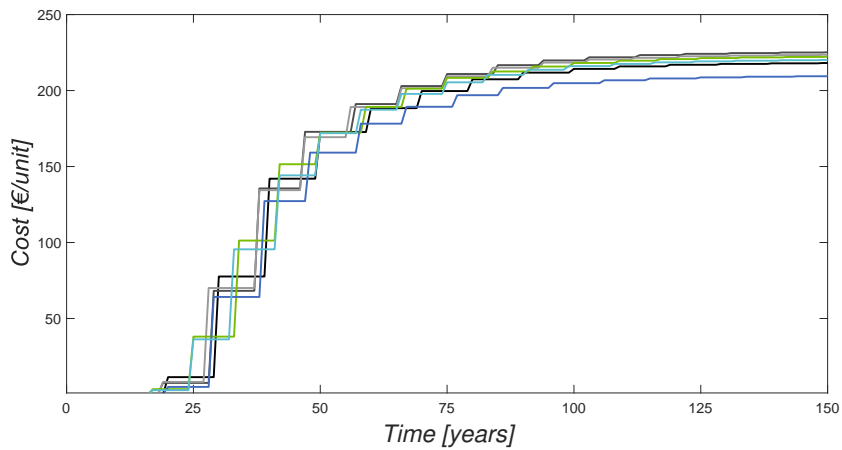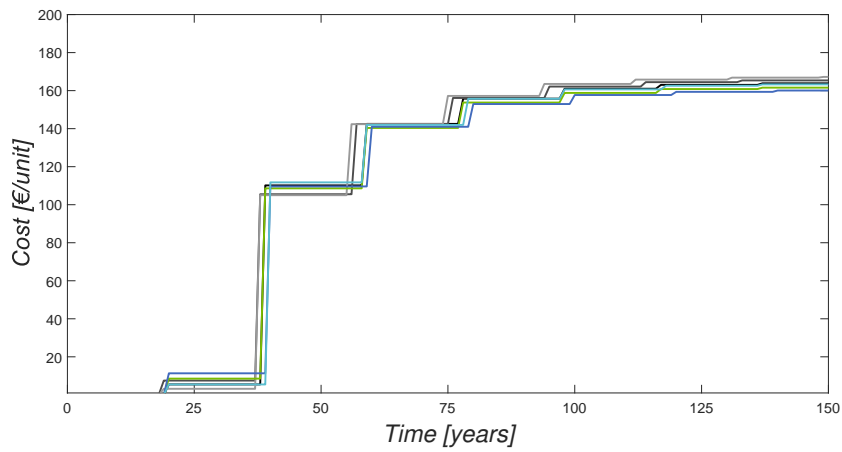

(b) Cumulative cost profiles
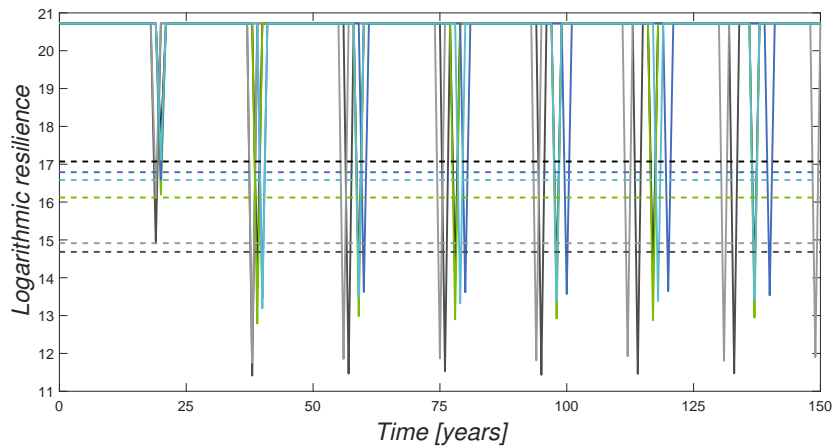
(c) Resilience profiles

Figure 8.22 – Comparison of the condition, cumulative cost and resilience profiles for solutions with longer time intervals between major inspections for the six situations analysed. Solid lines represent the variation of the condition, cumulative cost and resilience profiles over time and the dashed lines the mean condition state and resilience, respectively – Maintenance B4 – Bearings

Table 8.11 – Mean number of intervention for all solutions – Maintenance B4 – Bearings

Sections	Solution	Maintenance B4
2 and 11	Triangular	3.02
	Circular	2.76
	Quadricular	2.36
3 and 10	Triangular	3.01
	Circular	2.86
	Quadricular	2.27
4 and 9	Triangular	3.01
	Circular	2.77
	Quadricular	2.55
5 and 8	Triangular	3.01
	Circular	2.87
	Quadricular	2.29
14 and 17	Triangular	2.98
	Circular	2.62
	Quadricular	2.34
15 and 16	Triangular	2.98
	Circular	2.80
	Quadricular	2.31

Table 8.12 – Comparison of the performance indicators for all solutions – Maintenance B4 – Bearings

Sections	Solution	Mean condition state	Total maintenance cost [€/unit]	Mean resilience	Time interval between major inspections [years]
2 and 11	Triangular	2.04	264.61	16.82	2.03
	Circular	2.25	218.12	16.92	9.90
	Quadricular	2.47	163.84	17.07	19.49
3 and 10	Triangular	2.05	270.78	14.40	2.34
	Circular	2.26	225.26	14.45	9.35
	Quadricular	2.47	165.36	14.68	18.95
4 and 9	Triangular	2.04	274.40	14.75	2.01
	Circular	2.23	223.57	14.83	9.30
	Quadricular	2.45	167.22	14.91	18.61
5 and 8	Triangular	2.04	271.06	15.85	2.14
	Circular	2.22	222.31	15.89	8.31
	Quadricular	2.46	161.57	16.12	19.48
14 and 17	Triangular	2.04	272.45	16.55	2.05
	Circular	2.23	209.41	16.68	9.55
	Quadricular	2.44	160.06	16.79	19.93
15 and 16	Triangular	2.04	266.84	16.33	2.05
	Circular	2.20	220.16	16.39	8.25
	Quadricular	2.46	163.29	16.58	19.56

8.4.2 Optimization of performance indicators through the application of Maintenances B4 and B3

For the maintenance strategy that combines replacement (Maintenance B4) and total repair of the bearings (Maintenance B3), the set of optimal solutions is shown in Figure 8.23, for the six case studies. This figure relates the three objective functions (mean condition state, total maintenance cost at time horizon and resilience). The projections of these results in bi-dimensional space are presented in Figure 8.24.
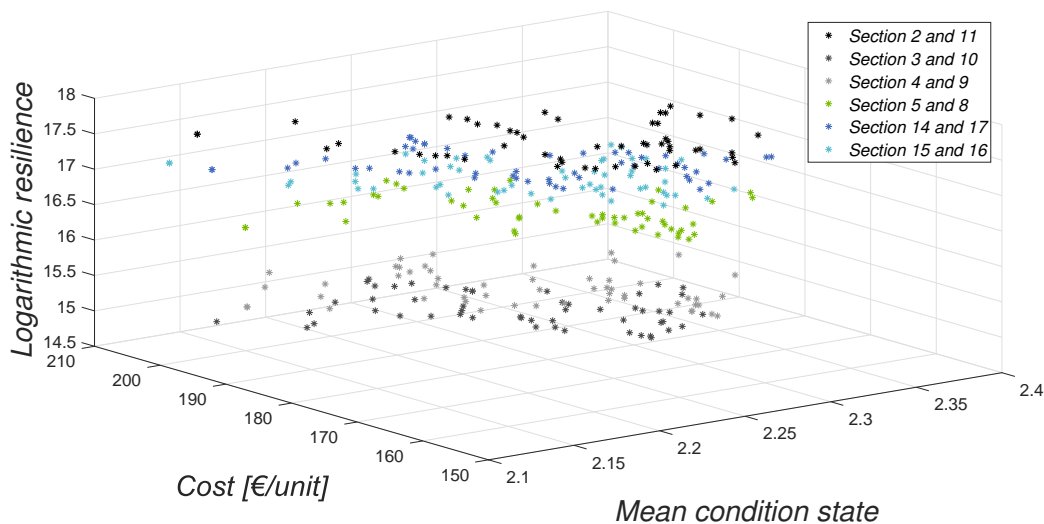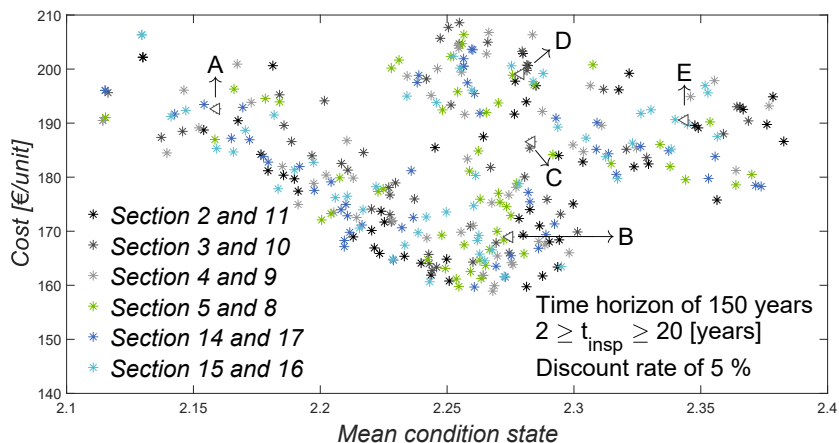

Figure 8.23 – Relationship between three objective functions (mean condition state, total maintenance cost at time horizon and resilience) – Maintenance B4 and B3 – Bearings

The relationship between the non-dominated solutions of the three objective functions is not as linear as in the maintenance strategy previously presented (Section 8.4.1). In Figure 8.24(a), that relates the mean condition state and the total maintenance cost at time horizon, it is possible to divide the feasible set of solutions into three regions. The first region is for mean condition states between 2.1 and 2.25. For this region, the total maintenance cost decreases with increasing mean condition state. The second region is located around mean condition state 2.25. In this region, there are several non-dominated solutions which have approximately the same mean condition state and different total maintenance costs (amounts ranging between 160 and 210 €/unit). Finally, the third region is for mean condition states between 2.25 and 2.4, and shows the same behaviour as the first region.

These behaviours are also visible in Figures 8.24(b) and 8.24(c). Figure 8.24(b) shows the relationship between the mean condition state and the resilience. In this figure, it is possible to see that the resilience of the network increases very slightly with the mean condition state 2.25–2.3. After that, verifies the resilience values drop, remaining substantially constant with the increase of the mean condition state. Lastly, in Figure 8.24(c), the total maintenance cost at time horizon and the resilience are compared. In this figure, the behaviour of the optimal solutions can be also divided into three regions. In the first region, there is a slight increase in the network resilience with decreasing of the total maintenance costs. In the second region, there is an increase in total maintenance costs with decreasing of the network resilience. Finally, in the third region there is a decrease in total maintenance costs for similar values of resilience.

In Figure 8.25, the design variable, t_{insp}, and the objective functions are related. From these figures, it is possible to understand better the behaviour of the performance indicators for different time intervals between major inspections. It is possible to observe that: (i) small time intervals are associated with lower mean condition states and high total maintenance costs; (ii) longer time intervals between major

(a) Relationship between mean condition state and total maintenance cost at time horizon
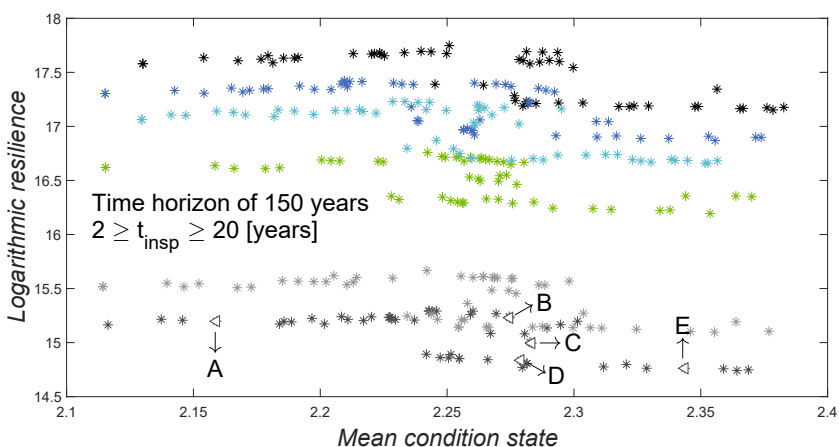
(b) Relationship between mean condition state and logarithmic resilience at time horizon
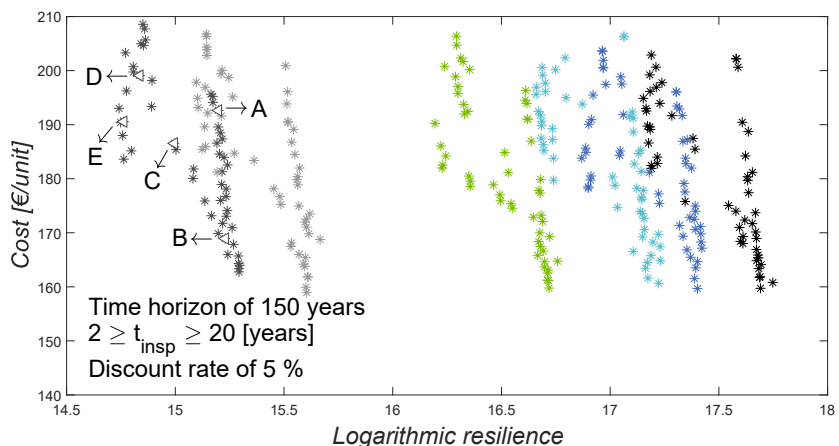
(c) Relationship between logarithmic resilience and total maintenance cost at time horizon

Figure 8.24 – Projections of the objective functions in bi-dimensional space – Maintenance B4 and B3 – Bearings

inspections are associated with high mean condition states and high total maintenance costs, being the maintenance costs for longer time intervals of the same order of the maintenance costs for small time intervals; (iii) the lowest maintenance costs occur for time intervals between major inspections between 6 and 8 years; and (iv) small time intervals between major inspections are associated with

better resilience indices.
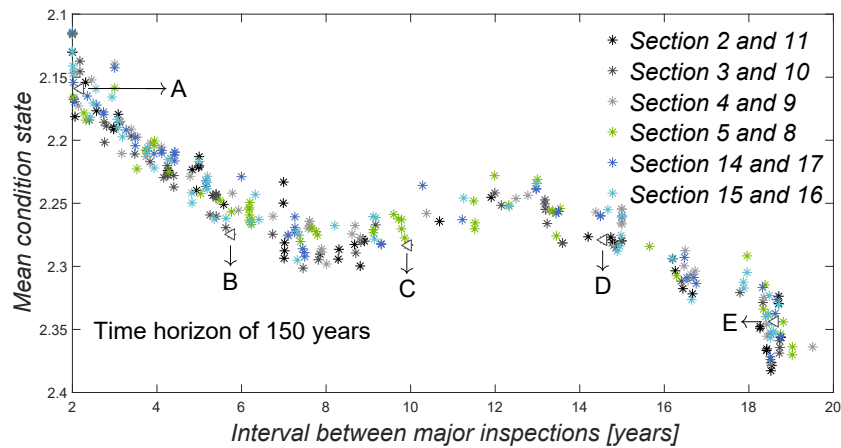
(a) Relationship between mean condition state and time interval between major inspections
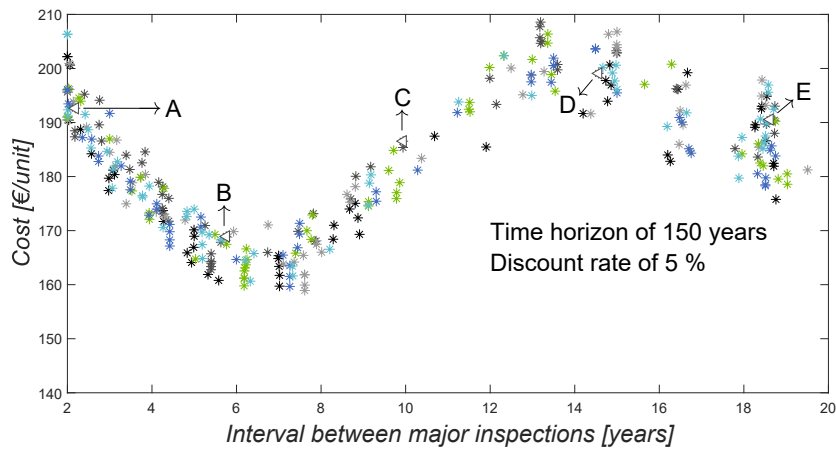
(b) Relationship between total maintenance cost and time interval between major inspections
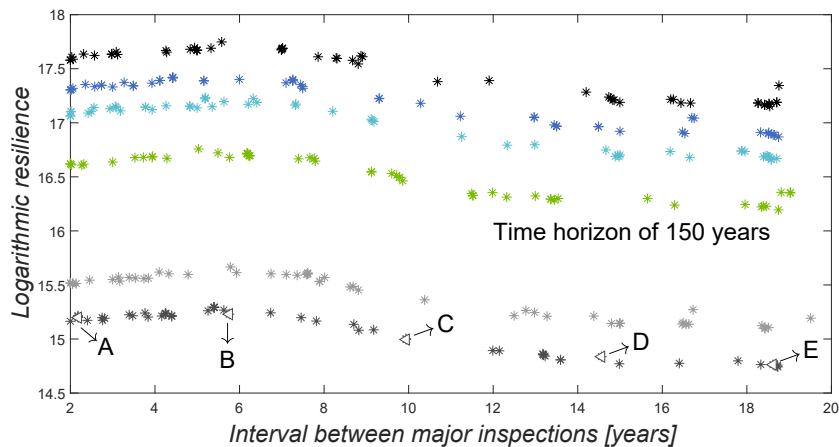
(c) Relationship between logarithmic resilience and time interval between major inspections

Figure 8.25 – Comparison of the design variable (time interval between major inspections, t_{insp}) with the three objective functions (mean condition state, total maintenance cost at the time horizon and resilience) – Maintenance B4 and B3 – Bearings

As before, from Figures 8.24 and 8.25 it can be observed that Sections 3 and 10 continue to be those with greater impact on users when Maintenance B4 is applied. From the six case studies analysed,

this pair of sections is the one that presents lower values of resilience.

In order to better understand the behaviour and evolution of performance indicators throughout the entire domain, as well as the variation of the mean number of interventions for different time intervals, five optimal solutions (A, B, C, D, and E) are highlighted in Figures 8.24 and 8.25. Since the behaviour of the six case studies are similar, it was chosen to analyse in more detail the results obtained for Sections 3 and 10. The design variables and objective functions associated with these solutions are shown in Table 8.13, whereas Table 8.14 presents the mean number of interventions for each solution.

Table 8.13 – Comparison of the performance indicators for all solutions – Maintenance B4 and B3 – Bearings

Solution	Mean condition state	Total maintenance cost [€/unit]	Mean resilience	Time interval between major inspections [years]
A	2.16	192.64	15.20	2.19
B	2.27	168.93	15.23	5.76
C	2.28	186.55	14.99	9.94
D	2.28	199.09	14.84	14.56
E	2.34	190.56	14.76	18.62

Table 8.14 – Mean number of intervention for all solutions – Maintenance B4 and B3 – Bearings

Solution	Maintenance B3	Maintenance B4
A	3.62	1.36
B	3.48	1.31
C	2.64	1.66
D	1.76	1.95
E	1.51	2.10

In Figure 8.26, the condition, cumulative cost and resilience profiles of the five highlighted solutions are compared. Solution A is associated with shorter time intervals between major inspections, solution E is associated with longer time intervals between major inspections, and the remaining three solutions (B, C, and D) are associated with intermediate time intervals between major inspections.

By comparing solution A with the other four solutions, it is possible to observe that solution A is the one with the best mean condition state. However, it is not the solution with the worst maintenance costs. This solution is also associated with better resilience indices. Shorter time intervals between major inspections mean that the verification of the condition state of the bearings is carried out more frequently, being more likely that there are more Maintenance B3 applications and thus reducing the number of applications of Maintenance B4. As can be seen from Table 5.19, the total repair of the bearings (Maintenance B3) is also a corrective maintenance, performed when deterioration levels reach the CS4 and allows improving the condition state of the bearings to CS2.

On the other hand, solution E is the one with the worst mean condition state. Also, it can be seen that the maintenance costs are similar to those of solution A. Besides, this solution is also associated with worst resilience indices. Since it is associated with longer time intervals between major inspections, the verification of the condition state of the bearings is carried out less frequently. The bearings are more likely to have worse deterioration levels requiring Maintenance B4 more often. For this solution, Maintenance B4 is applied, on average, 2.1 times, while for solution A it is applied, on average, 1.36 times.
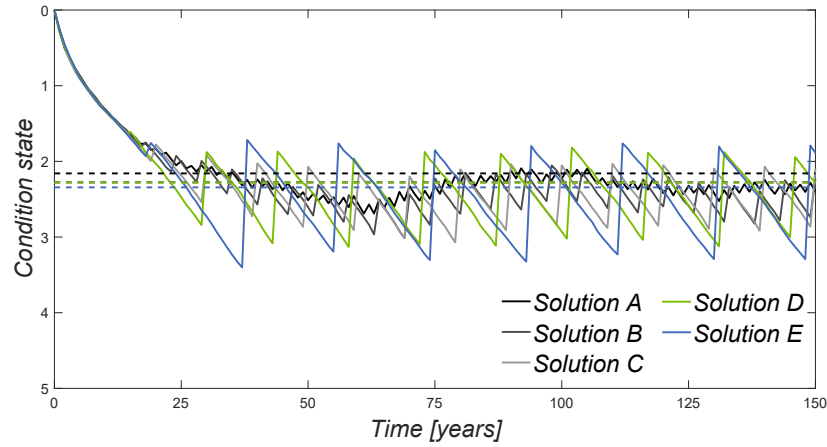
(a) Condition profiles
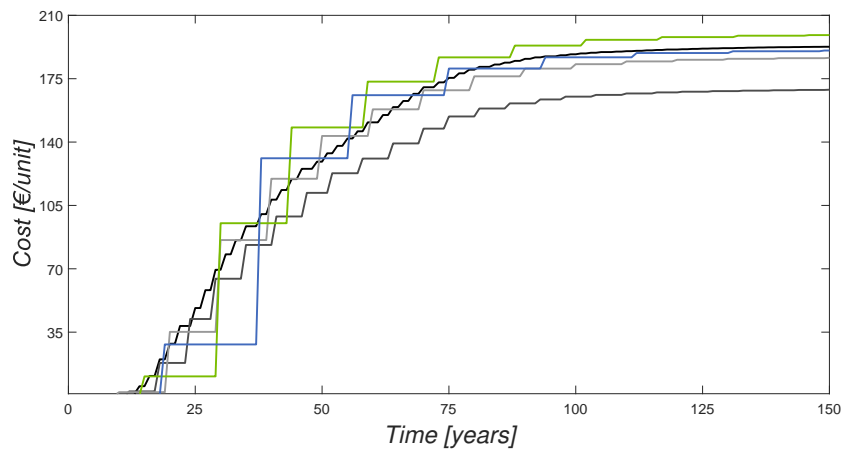
(b) Cumulative cost profiles
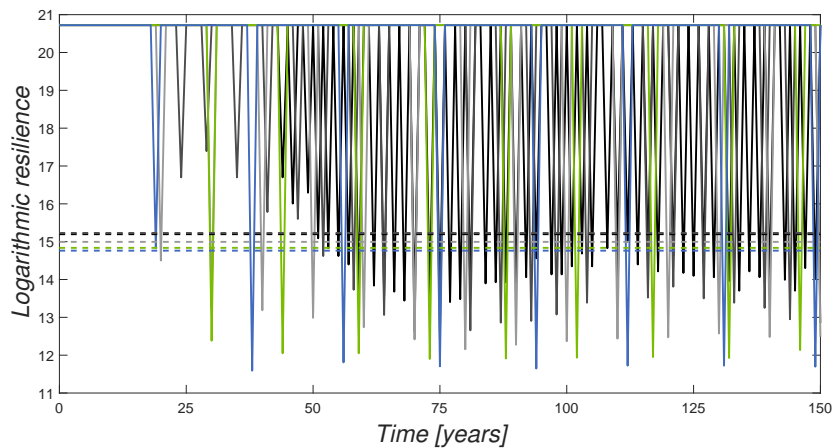
(c) Resilience profiles

Figure 8.26 – Comparison of the condition, cumulative cost and resilience profiles for all solutions. Solid lines represent the variation of the condition, cumulative cost and resilience profiles over time and the dashed lines the mean condition state and resilience, respectively – Maintenance B4 and B3 – Bearings

For the intermediate solutions, the results show that, although resulting in a similar mean condition state, differences in costs and resilience indices exist, and solution B is the one that has lowest

maintenance costs. Moreover, from Table 8.14, it is clear that with the increase in the time interval between major inspections the average number of Maintenance B3 decreases and the average number of Maintenance B4 increases, being the increase of the time interval between major inspections the main responsible for the reduction of the network performance.

8.4.3 Optimization of performance indicators through the application of Maintenances B4, B3 and B2

As for previous maintenance strategies, the set of optimal solutions obtained under combination of replacement (Maintenance B4), total repair (Maintenance B3) and maintenance of the bearings' components (Maintenance B2) is presented in Figure 8.27, for the six case studies. The projections of these results in bi-dimensional space are presented in Figure 8.28.
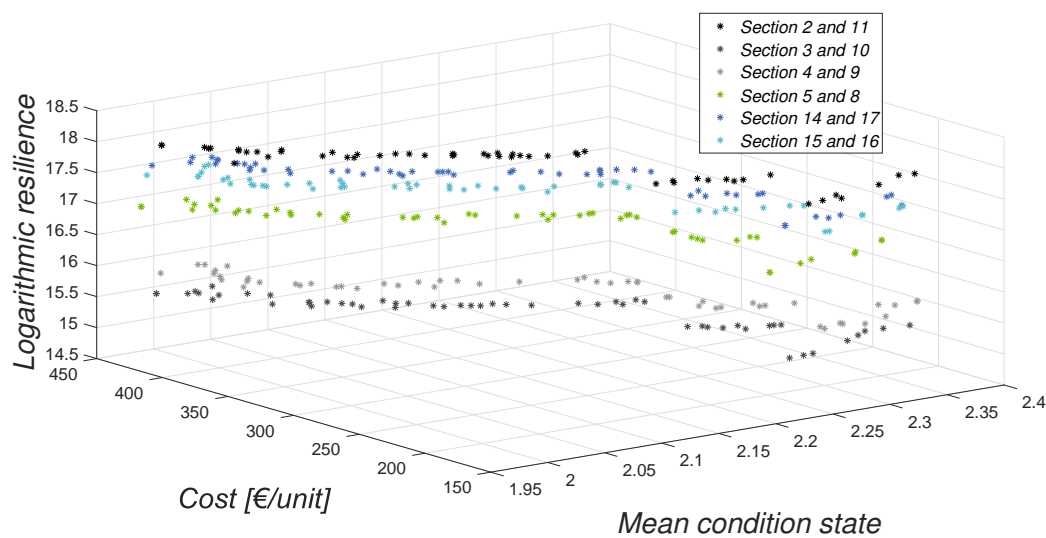
Figure 8.27 – Relationship between three objective functions (mean condition state, total maintenance cost at time horizon and resilience) – Maintenance B4, B3 and B2 – Bearings

Figure 8.28(a) relates the mean condition state and the total maintenance cost at time horizon. In this figure, the feasible set of solutions is discontinuous. In general, it can be observed that maintenance costs decrease with the increase in the mean condition cost of the bearings. However, around the mean condition state 2.2–2.25 there is a drop in total maintenance costs.

The same discontinuity is also present in Figures 8.28(b) and 8.28(c). Figure 8.28(b) shows the relationship between the mean condition state and the resilience. In this figure, it is possible to see that the resilience of the network increases slightly with the mean condition state in the region 2.2–2.25. In this range, there is a decrease in the values of the resilience and the optimal solutions present a less uniform behaviour. Lastly, in Figure 8.28(c), the total maintenance cost at time horizon and the resilience are compared. The behaviour of the optimal solutions can be divided into two regions. In first region there is a slightly increase in the network resilience with decreasing of the total maintenance costs. In second region, the behaviour of the optimal solutions is less uniform. However, around the total maintenance cost of 250 €/unit, a decrease in resilience is also observed.

From Figure 8.29, that relates the design variable, t_{insp}, with the three objective functions, it is possible to observe that: (i) the behaviour of the performance indicators can be divided into three regions, between years 7–9 and 12–14 there are no optimal solutions in the feasible space; (ii) the results obtained for the three performance indicators exhibit a parabolic shape; (iii) small time intervals between major inspections are associated with high total maintenance costs, lower mean condition
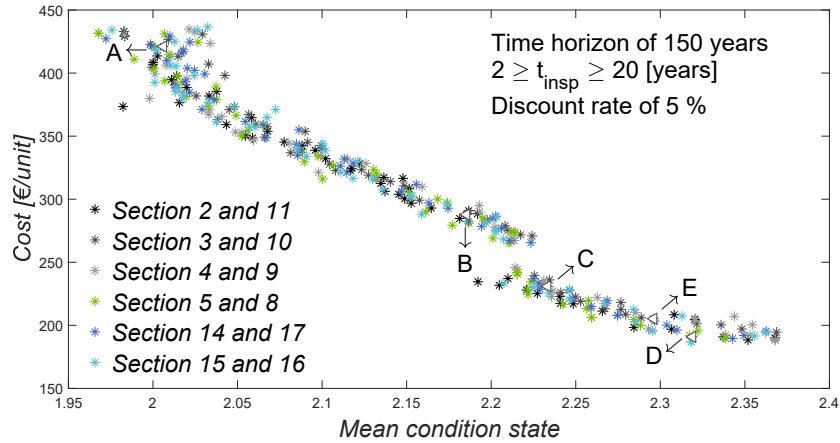
(a) Relationship between mean condition state and total maintenance cost at time horizon
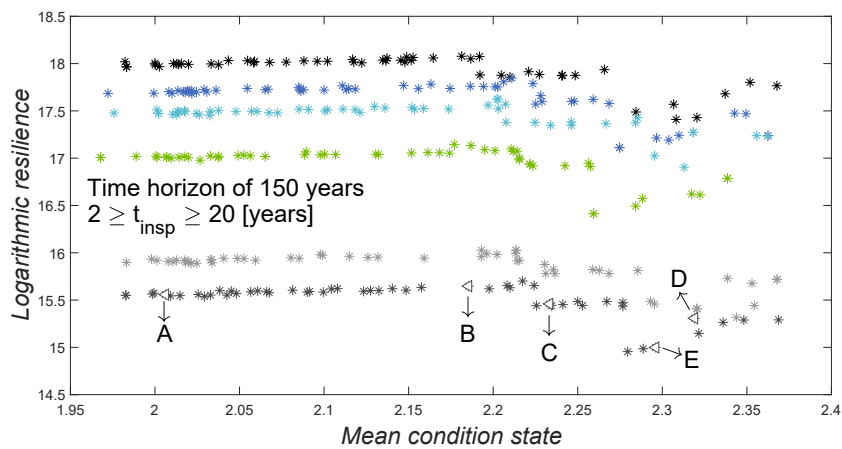
(b) Relationship between mean condition state and logarithmic resilience at time horizon
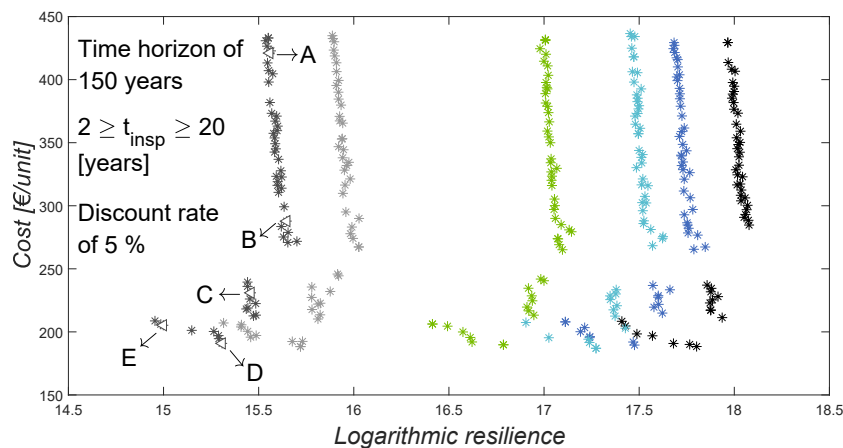
(c) Relationship between logarithmic resilience and total maintenance cost at time horizon

Figure 8.28 – Projections of the objective functions in bi-dimensional space – Maintenance B4, B3 and B2 – Bearings

states and better resilience indices; (iv) the lowest maintenance costs occur for time intervals equal to 16 years, but the mean condition states for this time interval are the worst; and (v) longer time intervals between major inspections are associated with worst resilience indices.
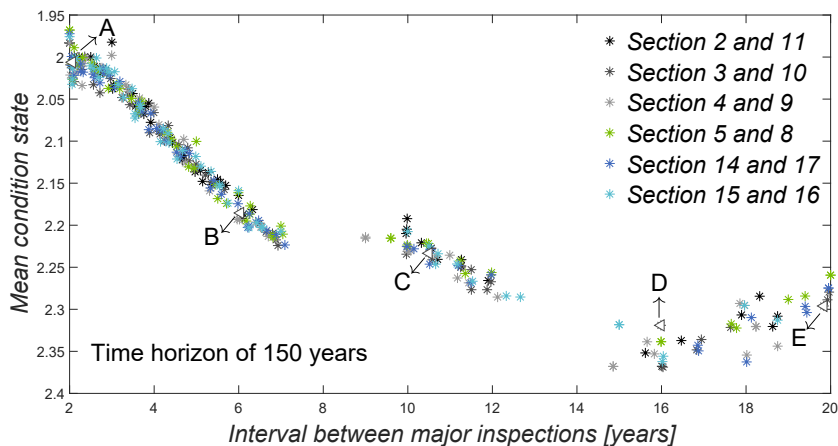
(a) Relationship between mean condition state and time interval between major inspections
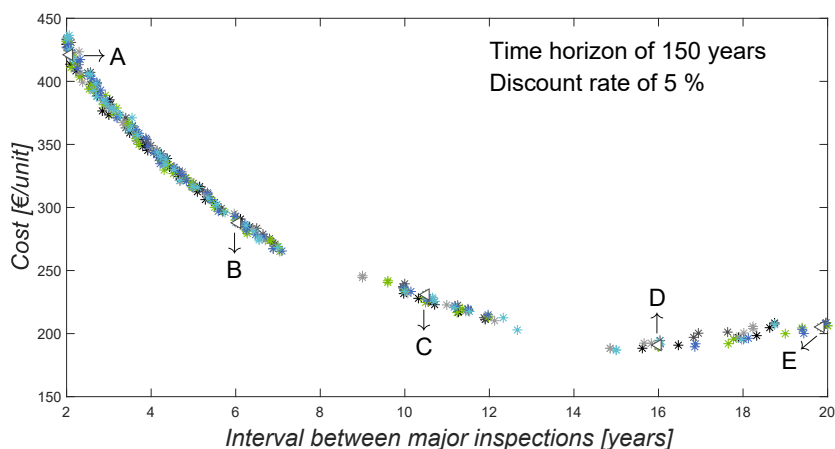
(b) Relationship between total maintenance cost and time interval between major inspections
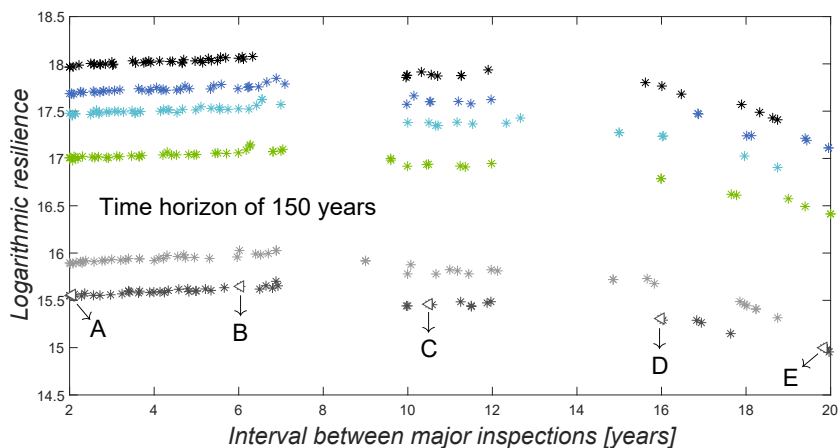
(c) Relationship between logarithmic resilience and time interval between major inspections

Figure 8.29 – Comparison of the design variable (time interval between major inspections, t_{insp}) with the three objective functions (mean condition state, total maintenance cost at the time horizon and resilience) – Maintenance B4, B3 and B2 – Bearings

In Figures 8.28 and 8.29, five optimal solutions (A, B, C, D, and E) are highlighted for Sections 3 and 10. This pair of sections is what has a greater impact to users when Maintenance B4 is applied. In Figure 8.30 and Table 8.15, the design variables and objective functions associated with the five

highlighted solutions are compared, and, in Table 8.16, the mean number of interventions for each solution is presented.

Table 8.15 – Comparison of the performance indicators for all solutions – Maintenance B4, B3 and B2 – Bearings

Solution	Mean condition state	Total maintenance cost [€/unit]	Mean resilience	Time interval between major inspections [years]
A	2.01	421.08	15.56	2.06
B	2.19	287.83	15.65	6.04
C	2.23	230.98	15.46	10.50
D	2.32	190.87	15.31	15.99
E	2.30	205.24	15.00	19.84

Table 8.16 – Mean number of intervention for all solutions – Maintenance B4, B3 and B2 – Bearings

Solution	Maintenance B2	Maintenance B3	Maintenance B4
A	13.77	2.78	0.95
B	10.97	2.09	0.87
C	8.12	2.01	1.04
D	4.71	2.14	1.22
E	3.42	1.56	1.66

By comparing this five solutions, solution A is associated with shorter time intervals between major inspections and, consequently, presents a lower mean condition state and a higher total maintenance cost. However, it is not the solution that has the better resilience indices. Through Figure 8.30(c) and Table 8.16, it is possible to see that solution B with time interval between major inspections of 6 years has a lower number of applications of Maintenance B4 and, consequently, a better network performance.

In opposition, Solution E is associated with longer time intervals between major inspections and worst resilience indices. However, it is not the solution that has the worst mean condition state. The worst mean condition state, as well as the best maintenance costs, are associated with solution D.

8.4.4   Comparison of different optimal maintenance strategies for bearings

In the present section, a multi-objective optimization problem based on genetic algorithm was used to compute the optimal time intervals between major inspections, considering different combinations of maintenance actions for bearings. In Figure 8.31, the non-dominated solutions for the sections 3 and 10 are compared.

For this bridge component, the results show that the different maintenance strategies lead to different outcomes. By comparing the three maintenance strategies, it is possible to observe that the three lead, approximately, to the same condition states (mean condition state vary between 2 and 2.5), but the maintenance strategy 3 (Maintenance B4, B3 and B2) lead to higher maintenance costs. However, the combination of the three maintenance actions in maintenance strategy 3 reduces the number of applications of Maintenance B4 and, consequently, improves the resilience of the network.

On the other hand, maintenance strategy 2 (Maintenances B4 and B3) is the one that presents lower maintenance costs, leading to much lower mean condition states for the same maintenance costs. As
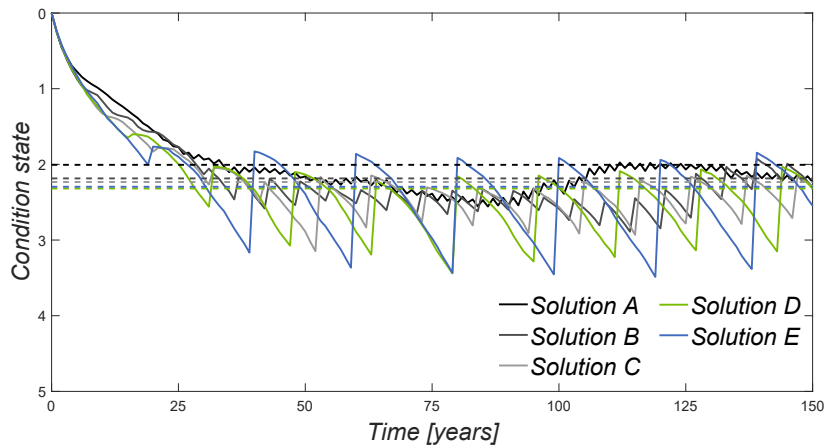
(a) Condition profiles
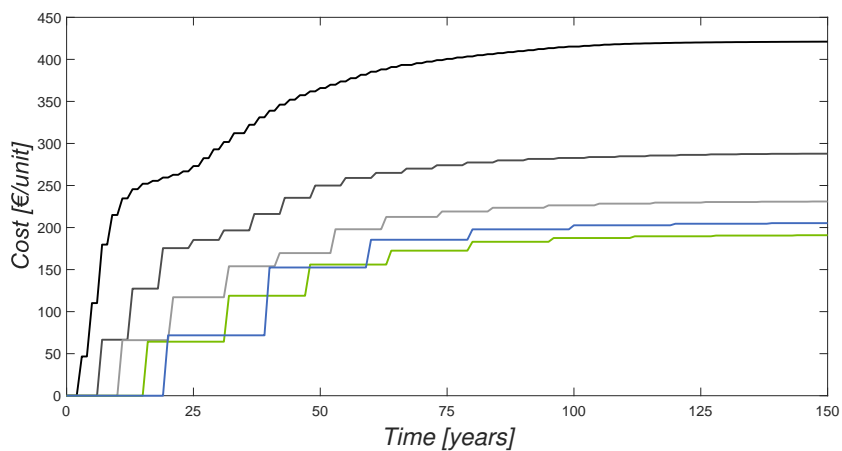
(b) Cumulative cost profiles
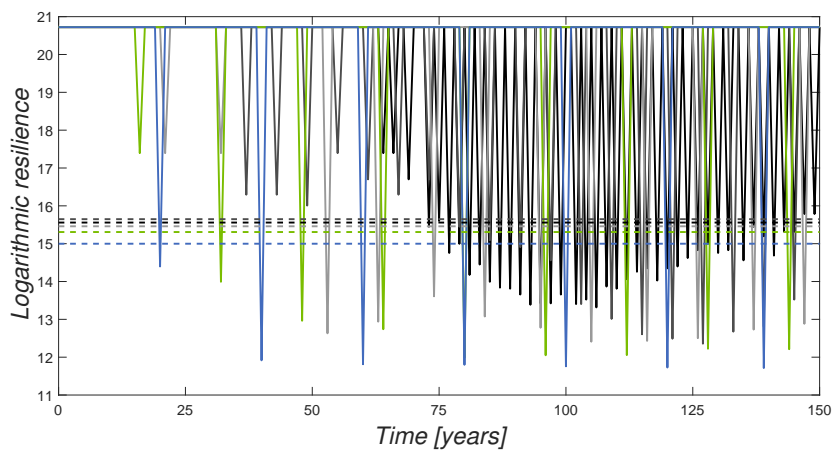
(c) Resilience profiles

Figure 8.30 – Comparison of the condition, cumulative cost and resilience profiles for all solutions. Solid lines represent the variation of the condition, cumulative cost and resilience profiles over time and the dashed lines the mean condition state and resilience, respectively – Maintenance B4, B3 and B2 – Bearings

mentioned before, the combination of Maintenances B4 and B3 allows reducing of the number of applications of Maintenance B4 and increasing the resilience values of the network.
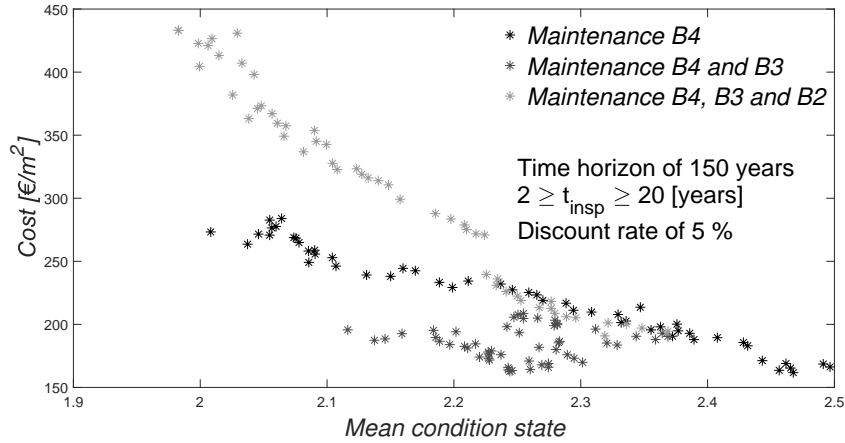
(a) Relationship between mean condition state and total maintenance cost at time horizon
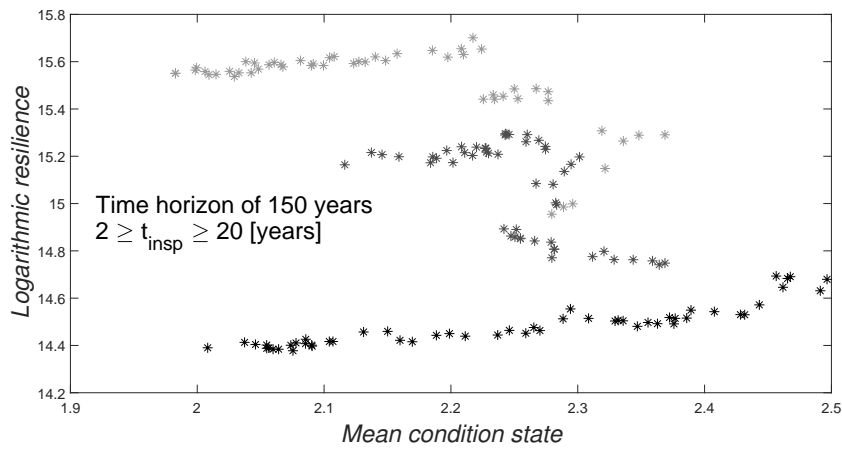
(b) Relationship between mean condition state and logarithmic resilience at time horizon
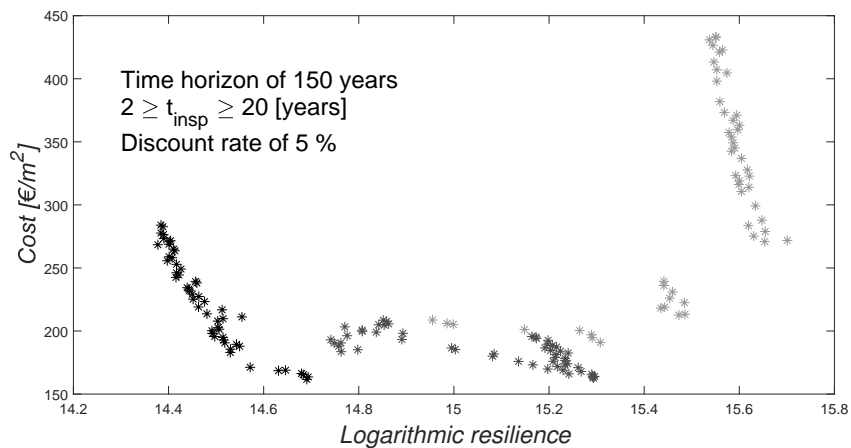
(c) Relationship between logarithmic resilience and total maintenance cost at time horizon

Figure 8.31 – Comparison of the non-dominated solution of the three maintenance strategies – Bearings

Finally, for this bridge component, the use of one type of maintenance does not have many advantages. Although it has relatively low maintenance costs compared to maintenance strategy 3, it is the solution that has the greatest impact on network resilience. However, it is a simple maintenance strategy and can be advantageous for structures in remote locations or difficult access.

8.5   Summary

An optimization framework based on genetic algorithm was used in this chapter as a decision-making approach to optimize maintenance strategies for two bridge components, pre-stressed concrete deck and bearings.

For each component analysed, three maintenance strategies were considered, as described in Chapter 5. The optimization problem is formulated as a tri-objective optimization, in order to optimize the time intervals between major inspections. The objective functions are the maximization of the mean condition state during the time horizon, the minimization of the total maintenance cost at time horizon, and the minimization of the impact of maintenance on users during the time horizon through the maximization of the resilience index of the network. However, since the maintenance strategies analysed for the pre-stressed concrete deck do not affect the road traffic, for this bridge component, the optimization problem was simplified for a bi-objective optimization problem. The probabilistic performance indicators including the condition state, cumulative maintenance cost, and resilience of the network are computed using the Monte Carlo simulation.

For pre-stressed concrete decks, the results obtained showed that the two preventive maintenance actions (Maintenance D4 – minor patching and Maintenance D2 – spot painting of concrete elements) are not very effective combined with Maintenance D5 – partial or full-depth concrete repair. The use of only Maintenance D5 show advantages when compared with the other maintenance strategies. However, in order to keep the bridge deck in a safe and serviceable condition during its lifetime, the realization of preventive maintenance is of fundamental importance.

Regarding bearings, the results showed that maintenance strategy 3 (combination of the three maintenance actions) leads to better mean condition states and better resilience indices, but it is associated with higher total maintenance costs.

However, it should be mentioned that the differences in the performance indicators between all maintenance strategies, for the two bridge components, are minimal. No single maintenance strategy is better than any other in all respects. The choice of the best maintenance strategy can only be made by the manager, considering all the parameters available, such as: location, available budget, constraints, among others (Neves, 2005).

Chapter 9

Conclusions and Future Developments

9.1 Conclusions

In this thesis, an infrastructure management system is described. In this methodology, the assessment of the future performance is based on inspection data (condition states). The proposed framework was developed with the assumption of implementing a transversal management system to different types of civil engineering infrastructures, while minimizing the impact of interventions, allowing the maximization of the performance level and the functionality of the infrastructure without incurring in disproportionate costs.

After a brief introduction where the problem of deterioration of the built heritage in developed countries and the need of maintenance and rehabilitation actions was contextualized, a detailed literature review on infrastructure management systems is introduced. In the second chapter, the definition of infrastructure management systems and the enumeration of its main components are made, including an extensive literature review of the main management system developed over the years. It was noted that the main research area of management systems are still bridges, but it is no longer a restricted area. There is already a reasonable amount of research in other civil infrastructures, such as buildings, pavements, wasterwater, among others. Furthermore, it was possible to observe that the methodologies used by the different management systems and their basic components are similar for all types of infrastructures and that the deterioration models are considered a critical component in a management system. The first observation came to solidify the main premise of this work, that it is possible to develop a management system transversal to all types of civil engineering infrastructures.

In a management system, a deterioration model has the function of simulating the deterioration process of the assets and, in order to capture the variability of the degradation process, stochastic deterioration models should be used to predict the future performance of the structures. The majority of the management systems have adopted deterioration models based on Markov chains; however, there are also a considerable number of studies based on reliability-based approaches and, more recently, Petri nets also has been used to model the deterioration process. Markov chains are characterized for their simplicity, the use of exponential distribution to describe the transition between condition state, and the existence of analytical expressions for the probability distribution that facilitates the computational work. However, exponential distributions are not very versatile, can result in a gross approximation of the system characteristics, the model size becomes unmanageable when the problem is too complex, and the effects of maintenance are not directly captured by the transition probability matrix. In contrast with the Markov chains, the application of Petri nets to define degradation models is a recent research field, but Petri nets have been used in many different applications areas. This modelling technique shows several advantages: (i) provides a graphical and mathematical formalism. These two characteristics are of high importance as the system development process needs

graphical representation to describe the problem in an intuitive way, as well as, the algorithmic tools; (ii) abstraction is crucial for the effective design of large scale and complex systems; (iii) different variants of Petri net models have been developed that are all related to the basic net formalism which they are built upon. This allows them to meet the needs in different application domains on the one hand, but, on the other hand, provides facilities for communication and the transfer of methods and tools from one field to another. This flexibility allows the incorporation of many rules in the model to accurately simulate complex situations, while keeping the model size within manageable limits. Currently, besides the basic model, there are extensions such as timed, stochastic, high-level, object-oriented Petri nets, meeting the specific need for (almost) every applications area; and (iv) with this modelling technique, transition times are not required to be exponential distributed.

In the third chapter, all extensions and components of the Petri net implemented in this thesis are discussed. The concepts of Petri nets described in this work are an extension of the original Petri nets. These extensions correspond to models to which functioning rules have been added, in order to enrich the initial model, thereby enabling a greater number of applications to be treated, while making the model more concise and efficient.

In Chapter 4, a probabilistic Petri nets is developed to model the deterioration of civil engineering infrastructure under no maintenance, preventive and corrective maintenance. The probabilistic model is divided into deterioration and maintenance model. The methodology used in the deterioration model is based on the ESPN formalism proposed by Dugan et al. (1984), where the firing rate assigned to each transition can be modelled by a different types of probabilistic distributions. The maintenance model was built from the deterioration model, including inspection, maintenance and renewal processes. The uncertainly related with the deterioration process and the effect of the maintenance actions is considered through the use of probability distributions and Monte Carlo simulation.

In Chapter 5, the deterioration and maintenance model based on Petri net formalism described in Chapter 4 is applied to the analysis of the life-cycle performance to two bridge components, pre-stressed concrete deck and bearings, based on historic data provided by a Portuguese company – Ascendi. In the first part of the chapter, the validation of the Petri net deterioration model is carried out. The validation is accomplished taking into account the existing isomorphism between bounded Petri net with exponentially distributed transition rates and a finite Markov process. The results presented show that both models are equivalents and there is a good agreement between observed and predicted data in each condition state, for both bridge components. Additionally, both for pre-stressed concrete decks and for bearings, Petri nets show a better agreement with the historic data than Markov chains.

After that, the Petri net deterioration model was applied to analyse the deterioration process over time without consideration of maintenance actions. In this probabilistic analyse, in addition to the Exponential distribution, four additional distributions were studied: Weibull, Gumbel, Normal, and Lognormal. The results obtained show that the Exponential distribution does not describe adequately the deterioration process, in particular, the transition between the more advanced deterioration states. The poor fit of the Exponential distribution can be explained by two aspects: (a) the limitation of being a one-parameter distribution that may contribute to the difficulty in modelling the deterioration process; and (b) the rare or non-existent samples in the more advanced deterioration states that influence the performance of the optimization algorithm. Furthermore, the Lognormal distribution does not describe adequately the transition between the more advanced deterioration states. The poor fit of the Lognormal distribution is, mainly, related to the low number of elements in the database. The Lognormal distribution shows unrealistic mean times in each condition state, which leads to believe that this distribution requires more observations to estimate, properly, the parameters that best describe the process of deterioration. Finally, for both bridge elements, the Weibull distribution shows a larger log-likelihood value and, consequently, a better fit to the historical data. The Gumbel and Normal distributions show results very close to the results obtained by the Weibull distribution, in

terms of predicted future condition profile and predicted probabilities, however, the log-likelihood values and the mean relative errors are worse for these distributions.

To evaluate the performance of bridge components under maintenance, four and three maintenance strategies were considered for pre-stressed concrete decks and bearings, respectively. For both bridge components, the Weibull distribution was chosen as the appropriate distribution to sample the transitions times in the deterioration process, and the triangular distribution was chosen to model inspections intervals. The choice of the Weibull distribution was made based on the results obtained in the probabilistic analysis performed in this chapter, while the Triangular distribution was defined based on experts' judgement.

Through the analysis of the predicted future condition profiles over time, it is possible to observe that any of the defined maintenance strategies, for both components, has a significant impact on the mean condition level comparing with the profile without maintenance. For pre-stressed concrete decks, maintenance strategy 4 (partial or full-depth concrete repair) shows better balance between performance and cost. However, this maintenance strategy is only based on corrective maintenance, which is frequently associated high user costs. However, when the 95-, and 99-percentiles of the cumulative cost for the four maintenance strategies are compared, it can be observed that maintenance strategy 3, that combines preventive and corrective maintenance, presents smaller costs than maintenance strategy 1 and 2, and similar costs to maintenance strategy 4, and continues to present an acceptable deterioration level.

Regarding bearings, the results presented show that maintenance strategy 2 (combination of replacement and total repair of the bearings' component) results in better relationship between performance and cost. But, if the 95- or 99-percentiles are analysed, it becomes clear that the cumulative costs of maintenance strategy 3 (combination of replacement, total repair and maintenance of the bearings' component) are similar, and is likely that, in the long-term, maintenance strategy 3 is the one that presents the best relation between performance and cost.

In Chapter 6, the Petri net model developed in Chapter 4 is applied to analyse the deterioration process of ceramic claddings located in Lisbon (Portugal). In the first part of this chapter, the Petri net model is used to predict the deterioration of ceramic claddings over time and to understand how the different environmental exposures contribute impact the degradation. As for the bridge components, five probability distributions (Exponential, Weibull, Gumbel, Lognormal and Normal) were analysed in order to examine which distribution has a better fit to the historical date. The results obtained from the probabilistic analysis show that the use of distributions with two parameters improves the value of the log-likelihood. The log-likelihood values of the four distributions are quite similar; however, the Weibull distributions shows a larger log-likelihood value and, consequently, a better fit to the historical date.

Relatively to the environmental actions, the results presented show that the claddings close to the coastal areas, exposed to damp and wind-rain actions, and orientated North show more tendency to belong to the most unfavourable condition levels (approximately a probability of 70%). On the other hand, claddings more than 5 km from the sea, are the most prone to remain in lower degradation conditions. These results show that the division of the original sample by environmental characteristic is important. The results demonstrate that each variable is strongly independent of the complete sample, only the intermediate situations (intermediate distance from the sea and moderate wind-rain action) show same dependency as the complete sample.

To evaluate the performance of ceramic claddings under maintenance actions, three maintenance strategies were considered. As in case study of the bridges, the Weibull distribution was chosen as the appropriate distribution to sample the transition times in the deterioration process and the Triangular distribution was chosen to model inspection intervals.

Through the analysis of the predicted future condition profiles over time, it is possible to verify that

any of the defined maintenance strategies has a significant impact on the mean condition level. Maintenance strategy 1 (major intervention) represents the strategy currently implemented by the owners. The results presented show that more regular interventions in cladding, through the application of minor intervention and cleaning operations, allow improving the condition level, extending the estimated service life. The combination of cleaning, minor and major interventions (maintenance strategy 3) leads to increased costs compared with major intervention alone. However, the mean condition profile of this two maintenance strategy is considerably different. Maintenance strategy 3 results in a significant improvement in the mean condition index when compared to maintenance strategy 1.

From results obtained in Chapters 5 and 6, it is verified that the Weibull distribution is the one that shows a better fit in the three components (pre-stressed concrete decks, bearings, and ceramic claddings). However, the choice of the model for each component and/or structure requires a probabilistic analysis, because the model will depend on its structural characteristics, age, load, environmental conditions, and amount of information available.

In Chapter 7, a model to evaluate the impact of maintenance on users was developed. Through a literature review it was found that resilience is one of the most used performance indicators to quantify damage to networks. The definition of resilience introduces important aspects in the analysis of a traffic network. Although the ability of bridge to withstand a disturbance depends almost exclusively on its structural characteristics, the recovery process is strongly affected by the technical, economic and political conditions of the community concerned in rehabilitating the bridge.

In this chapter, a methodology for the calculation of the resilience index was implemented. The road network used in this case study is part of the Portuguese highway network. The results obtained show that, in general, the road network presents a reasonable level of resilience. It can be concluded that the sections present in highway A1 are the most critical in the road network, which has the greatest socioeconomic consequences for the users in case of traffic disturbance. In this sense, maintenance and/or rehabilitation actions should be planned in order to make this section more reliable and robust.

In Chapter 8, a multi-objective optimization procedure based on genetic algorithm was used to optimize maintenance strategies for two bridge components, pre-stressed concrete deck and bearings. In this work, the optimization problem is formulated as a tri-objective optimization. The multi-objective algorithm is used to optimize the time intervals between major inspections. The objective functions are the maximization of the mean condition state during the time horizon, the minimization of the total maintenance cost at time horizon, and the minimization of the impact of maintenance on users during the time horizon through the maximization of the resilience index of the network.

For the pre-stressed concrete deck, the results obtained showed that the two preventive maintenance actions (Maintenance D4 – minor patching and Maintenance D2 – spot painting of concrete elements) are not very effective when combined with Maintenance D5 – partial or full-depth concrete repair, since the use of only of the Maintenance D5 show advantages when compared with the other maintenance strategies. However, in order to keep the bridge deck in a safe and serviceable condition during their lifetime, the realization of preventive maintenance is of fundamental importance. With regard to bearings, the results showed that maintenance strategy 3 (combination of the three maintenance actions) leads to better mean condition states and better resilience indices, but it is associated with higher total maintenance costs.

In short, the proposed methodology is a useful tool for management authorities and decision-makers to assess the degradation process and investigate the effects of different maintenance policies on civil infrastructures, and can be employed to determine cost-effective maintenance strategies while maintaining a desirable condition state and functionality.

9.2 Future developments

The present dissertation is a further contribution to the development of an efficient management system for civil engineering infrastructures. However, future research works continue to be required to make these systems useful and reliable to infrastructure managers. Among these, the following, are considered the most significant:

- Whatever the researchers' efforts in developing better infrastructure management systems, its efficiency is always uncertain due the limitation of visual inspections to reveal structural anomalies. This limitation can lead to costly and inadequate maintenance actions to cover the uncertainty resulting from visual inspections. In addition, visual inspections are a very subjective evaluation procedure, where often two inspectors under the same conditions assess the structure differently. Furthermore, the classification systems used are based on qualitative information. So, it is needed to define new classification systems that incorporate more quantitative information from visual inspections, so that subjectivity can be reduced in the process of assessing the structural condition.

- Following the previous point, more research into quantifying the effects of maintenance works, as well as the degradation process after each intervention, is also needed. Currently, there is little information on the effects of maintenance actions on structures, and the information available is based on expert opinion.

- Petri nets have the ability to model more complete and realistic maintenance models, through the consideration of more rules. Therefore, future works should be focused on considering the dependence between different elements.

- Finally, the macroscopic traffic model based on Petri nets, implemented in this work, shows promising results. However, further research is needed to improve the traffic analysis.

References

AASHTO (1993). Guidelines for bridge management systems. Technical report, American Association of State Highway and Transportation Officials.

Abaza, K. A., Ashur, S. A., and Al-Khatib, I. A. (2004). Integrated pavement management system with a markovian prediction model. *Journal of Transportation Engineering*, 130(1):24–33.

Abraham, D. M., Wirahadikusumah, R., Short, T., and Shahbahrami, S. (1998). Optimization modeling for sewer network management. *Journal of Construction Engineering and Management*, 124(5):402–410.

Aguirre-Hernández, R. and Farewell, V. (2002). A pearson-type goodness-of-fit test for stationary and time-continuous Markov regression models. *Statistics in Medicine*, 21(13):1899–1911.

Aimsun (2017). https://www.aimsun.com/. (Page consulted on June, 14, 2017).

Al-Ahmari, A. (2016). Optimal robotic cell scheduling with controllers using mathematically based timed Petri nets. *Information Sciences*, 329(1):638–648.

Alla, H. and David, R. (1998). A modelling and analysis tool for discrete events systems: Continuous Petri net. *Performance Evaluation*, 33(3):175–199.

Amaro, B., Saraiva, D., de Brito, J., and Flores-Colen, I. (2013). Inspection and diagnosis system of etics on walls. *Construction and Building Materials*, 47:1257–1267.

Andersen, N. H. (1990). Danbro – A bridge management system for many levels. In: Nowak A. S. (eds) Bridge Evaluation, Repair and Rehabilitation. NATO ASI Series (Series E: Applied Sciences), volume 187. Springer, Dordrecht.

Andrews, J. (2013). A modelling approach to railway track asset management. *Journal of Rail and Rapid Transit*, 227(1):56–73.

Ariaratnam, S. T., El-Assaly, A., and Yang, Y. (2001). Assessment of infrastructure inspection needs using logistic models. *Journal of Infrastructure Systems*, 7(4):160–165.

ASCE (2017). 2017 Infrastructure Report Card - A comprehensive assessment of America's infrastructure. Technical report, America Society of Civil Engineers.

Barros, P. (2013). Bridge management and current state condition of Brisa's highway network bridges. In *Condition assessment of bridges: past, present and future - A complementary approach*, Lisbon, Portugal.

Baskocagil, C. and Kurtulan, S. (2011). Generalized state equation for Petri nets. *WSEAS Transactions on Systems*, 10(9):295–305.

Baur, R. and Herz, R. (2002). Selective inspection planning with ageing forecast for sewer types. *Water Science and Technology*, 46(6-7):389–396.

Berardinelli, U., Neves, L. C., Matos, J. C., and Guimarães, H. (2014). An advanced highway asset management system. In *Proceedings of the 4th International Symposium on Life-Cycle Civil Engineering*, Tokyo, Japan.

BETAR (2017). http://www.betar.pt/pt/content/10-goa. (Page consulted on May 23, 2017).

Bocchini, P. and Frangopol, D. M. (2011a). A probabilistic computational framework for bridge network optimal maintenance scheduling. *Reliability Engineering & System Safety*, 96(2):332–349.

Bocchini, P. and Frangopol, D. M. (2011b). Resilience-driven disaster management of civil infrastructure. In *Computational Methods in Structural Dynamics and Earthquake Engineering*, Island of Corfu, Greece.

Bocchini, P. and Frangopol, D. M. (2012). Optimal resilience-and cost-based postdisaster intervention prioritization for bridges along a highway segment. *Journal of Bridge Engineering*, 17(1):117–129.

Bocchini, P., Frangopol, D. M., Ummenhofer, T., and Zinke, T. (2014). Resilience and sustainability of civil infrastructure: Toward a unified approach. *Journal of Infrastructure Systems*, 20(2):1–16.

Bordalo, R., de Brito, J., Gaspar, P. L., and Silva, A. (2011). Service life prediction modelling of adhesive ceramic tiling systems. *Building Research & Information*, 39(1):66–78.

Bowden, F. D. J. (2000). A brief survey and synthesis of the roles of time in Petri nets. *Mathematical and Computer Modelling*, 31(10):55–68.

Branco, F. A. and de Brito, J. (2004). Handbook of concrete bridge management. American Society of Civil Engineers.

Branke, J., Deb, K., and Miettinen, K. (2008). *Multiobjective optimization: Interactive and evolutionary approaches*. Springer Science & Business Media.

Brownjohn, J. M. W. (2007). Structural health monitoring of civil infrastructure. *Mathematical, Physical and Engineering Sciences*, 365(1851):589–622.

Bruneau, M. (2006). Enhancing the resilience of communities against extreme events from an earthquake engineering perspective. *Journal of Security Education*, 1(4):159–167.

Bruneau, M., Chang, S. E., Eguchi, R. T., Lee, G. C., O'Rourke, T. D., Reinhorn, A. M., Shinozuka, M., Tierney, K., Wallace, W. A., and von Winterfeldt, D. (2003). A framework to quantitatively assess and enhance the seismic resilience of communities. *Earthquake Spectra*, 19(4):733–752.

Bruneau, M. and Reinhorn, A. (2006). Overview of the resilience concept. In *Proceedings of the 8th US National Conference on Earthquake Engineering*, San Francisco, United States of America.

Bruneau, M. and Reinhorn, A. (2007). Exploring the concept of seismic resilience for acute care facilities. *Earthquake Spectra*, 23(1):41–62.

Butt, A. A., Shahin, M. Y., Feighan, K. J., and Carpenter, S. H. (1987). Pavement performance prediction model using the Markov process. *Transportation Research Record*, 1123:12 – 19.

Çağnan, Z., Davidson, R. A., and Guikema, S. D. (2006). Post-earthquake restoration planning for Los Angeles electric power. *Earthquake Spectra*, 22(3):589–608.

Caleyo, F., Velázquez, J. C., Valor, A., and Hallen, J. M. (2009). Markov chain modelling of pitting corrosion in underground pipelines. *Corrosion Science*, 51(9):2197–2207.

CEN (2002). EN 1990: Basis of structural design.

Cesare, M. A., Santamarina, C., Turkstra, C., and Vanmarcke, E. H. (1992). Modeling bridge deterioration with Markov chains. *Journal of Transportation Engineering*, 118(6):820–833.

Chai, C., de Brito, J., Gaspar, P., and Silva, A. (2013). Predicting the service life of exterior wall painting: techno-economic analysis of alternative maintenance strategies. *Journal of Construction Engineering and Management*, 140(3):04013057.

Chang, S. E. and Shinozuka, M. (2004). Measuring improvements in the disaster resilience of communities. *Earthquake Spectra*, 20(3):739–755.

Chen, W.-F. and Duan, L. (2014). *Bridge Engineering Handbook: Fundamentals*. CRC press.

Chen, Y., Li, Z., and Barkaoui, K. (2014). Maximally permissive liveness-enforcing supervisor with lowest implementation cost for flexible manufacturing systems. *Information Sciences*, 256(6):74–90.

Cheng, F., Wang, Y., Ling, X., and Bai, Y. (2011). A Petri net simulation model for virtual construction of earthmoving operations. *Automation in Construction*, 20(2):181–188.

Choi, E. C. (1999). Wind-driven rain on building faces and the driving-rain index. *Journal of Wind Engineering and Industrial Aerodynamics*, 79(1):105–122.

Chughtai, F. and Zayed, T. (2008). Infrastructure condition prediction models for sustainable sewer pipelines. *Journal of Performance of Constructed Facilities*, 22(5):333–341.

Cimellaro, G. P., Reinhorn, A. M., and Bruneau, M. (2006). Quantification of seismic resilience. In *Proceedings of the 8th US National conference on Earthquake Engineering*, San Francisco, United States of America.

Cimellaro, G. P., Reinhorn, A. M., and Bruneau, M. (2010a). Framework for analytical quantification of disaster resilience. *Engineering Structures*, 32(11):3639–3649.

Cimellaro, G. P., Reinhorn, A. M., and Bruneau, M. (2010b). Seismic resilience of a hospital system. *Structure and Infrastructure Engineering*, 6(1-2):127–144.

Corotis, R. B., Ellis, J. H., and Jiang, M. (2005). Modeling of risk-based inspection, maintenance and life-cycle cost with partially observable Markov decision processes. *Structure and Infrastructure Engineering*, 1(1):75–84.

Das, P. C. (1999). *Management of Highway Structures*. Thomas Telford.

David, R. and Alla, H. (2010). *Discrete, Continuous, and Hybrid Petri Nets*. Springer Science & Business Media.

de Brito, J. (1992). *Desenvolvimento de um sistema de gestão de obras de arte em betão*. PhD thesis, Instituto Superior Técnico, Portugal.

de Brito, J. and Branco, F. (1994). Bridge management policy using cost analysis. *Proceedings of the Institution of Civil Engineers: Structures and Buildings*, 104(4):431–9.

de Brito, J., Branco, F., Thoft-Christensen, P., and Sørensen, J. D. (1997). An expert system for concrete bridge management. *Engineering Structures*, 19(7):519–526.

de Brito, J., Branco, F. A., and Ibañez, M. (1994). A knowledge-based system for concrete bridge inspection. *Concrete International, ACI, Detroit, MI*.

Dehghanian, P., Fotuhi-Firuzabad, M., Aminifar, F., and Billinton, R. (2013). A comprehensive scheme for reliability centered maintenance in power distribution systems - Part I: Methodology. *IEEE Transactions on Power Delivery*, 28(2):761–770.

Denysiuk, R., Matos, J. C., Tinoco, J., Miranda, T., and Correia, A. G. (2016). Multiobjective optimization of maintenance scheduling: Application to slopes and retaining walls. *Procedia Engineering*, 143:666–673.

Di Febbraro, A., Giglio, D., and Sacco, N. (2016). A deterministic and stochastic Petri net model for traffic-responsive signaling control in urban areas. *IEEE Transactions on Intelligent Transportation Systems*, 17(2):510–524.

Dias, J., Silva, A., Chai, C., Gaspar, P., and de Brito, J. (2014). Neural networks applied to service life prediction of exterior painted surfaces. *Building Research & Information*, 42(3):371–380.

Dotoli, M. and Fanti, M. P. (2006). An urban traffic network model via coloured timed Petri nets. *Control Engineering Practice*, 14(10):1213–1229.

Dugan, J. B., Trivedi, K. S., Geist, R. M., and Nicola, V. F. (1984). Extended stochastic Petri nets: Applications and analysis. Technical report, Duke University, United States of America.

Elbehairy, H. (2007). *Bridge management system with integrated life cycle cost optimization*. PhD thesis, University of Waterloo, Canada.

Emídio, F., de Brito, J., Gaspar, P. L., and Silva, A. (2014). Application of the factor method to the estimation of the service life of natural stone cladding. *Construction and Building Materials*, 66:484–493.

Fanti, M., Iacobellis, G., Mangini, A., and Ukovich, W. (2014). Freeway traffic modeling and control in a first-order hybrid Petri net framework. *IEEE Transactions on Automation Science and Engineering*, 11(1):90–102.

Fenner, R. (2000). Approaches to sewer maintenance: A review. *Urban Water*, 2(4):343–356.

FHWA (2013). Status of the nation's highways, bridges and transit: Conditions and performance. Technical report, Federal Highway Administration.

Frangopol, D. M. (1998). A probabilistic model based on eight random variables for preventive maintenance of bridges. Presented at the progress meeting "Optimum maintenance strategies for different bridge types", highways agency, London, United Kingdom.

Frangopol, D. M. and Bocchini, P. (2011). Resilience as optimization criterion for the rehabilitation of bridges belonging to a transportation network subject to earthquake. In *Structures Congress 2011*, Las Vegas, United States of America.

Frangopol, D. M. and Bocchini, P. (2012). Bridge network performance, maintenance and optimisation under uncertainty: Accomplishments and challenges. *Structure and Infrastructure Engineering*, 8(4):341–356.

Frangopol, D. M., Kallen, M. J., and van Noortwijk, J. M. (2004). Probabilistic models for life-cycle performance of deteriorating structures: Review and future directions. *Progress in Structural Engineering and Materials*, 6(4):197–212.

Frangopol, D. M., Kong, J. S., and Gharaibeh, E. S. (2001). Reliability-based life-cycle management of highway bridges. *Journal of Computing in Civil Engineering*, 15(1):27–34.

Frangopol, D. M. and Neves, L. C. (2004). *Probabilistic maintenance and optimization strategies for deteriorating civil infrastructures*, chapter 14 in Progress In Computational Structures Technology, pages 353–377. Saxe-Coburg Publications.

Freire, L. M., de Brito, J., and Correia, J. R. (2013). Inspection survey of support bearings in road bridges. *Journal of Performance of Constructed Facilities*, 29(4):04014098.

Freire, L. M., de Brito, J., and Correia, J. R. (2014). Management system for road bridge structural bearings. *Structure and Infrastructure Engineering*, 10(8):1068–1086.

Gaal, G. (2004). *Prediction of deterioration of concrete bridges*. PhD thesis, Delft University of Technology, Netherlands.

Galbusera, M., de Brito, J., and Silva, A. (2014). Application of the factor method to the prediction of the service life of ceramic external wall cladding. *Journal of Performance of Constructed Facilities*, 29(3):04014086.

Gandelheid, A. (2007). https://www.123rf.com/photo_65737761_stock-illustration-illustration-of-an-hourglass-with-sand.html. (Page consulted on May 23, 2017).

Garcez, N., Lopes, N., de Brito, J., and Silvestre, J. (2012). System of inspection, diagnosis and repair of external claddings of pitched roofs. *Construction and Building Materials*, 35:1034–1044.

Gaspar, P. L. (2009). *Vida útil das construções: Desenvolvimento de uma metodologia para a estimativa da durabilidade de elementos da construção. Aplicação a rebocos de edifícios correntes*. PhD thesis, Instituto Superior Técnico, Portugal.

Gaspar, P. L. and de Brito, J. (2008a). Quantifying environmental effects on cement-rendered facades: A comparison between different degradation indicators. *Building and Environment*, 43(11):1818–1828.

Gaspar, P. L. and de Brito, J. (2008b). Service life estimation of cement-rendered façades. *Building Research & Information*, 36(1):44–55.

Gaspar, P. L. and de Brito, J. (2011). Limit states and service life of cement renders on façades. *Journal of Materials in Civil Engineering*, 23(10):1396–1404.

Girault, C. and Valk, R. (2013). *Petri Nets for Systems Engineering: A guide to modeling, verification, and applications*. Springer Science & Business Media.

GOA (2008). Manual de aplicação informática do GOA. Technical report, Betar Consultores.

Golabi, K., Kulkarni, R. B., and Way, G. B. (1982). A statewide pavement management system. *Interfaces*, 12(6):5–21.

Grigg, N. S. (2012). *Water, Wastewater, and Stormwater Infrastructure Management*. CRC Press.

Guimarães, H. and Matos, J. C. (2015). Bridge maintenance models using expert opinion. In *FIB 2015 Symposium*.

Hajdin, R. (2008). Kuba 4.0: The swiss road structure management system. In *Proceedings of the 10th International Conference on Bridge and Structure Management*, Buffalo, New York.

Hanji, T. and Tateishi, K. (2007). Review of recent bridge asset management systems. In *Proceedings of International Symposium on EcoTopia Science*, Nagoya, Japan.

Harper, W. V. and Majidzadeh, K. (1991). Use of expert opinion in two pavement management systems. *Transportation Research Record*, 1311:242 – 247.

Hatami, A. and Morcous, G. (2011). Developing deterioration models for Nebraska bridges. Technical report, Nebraska Department of Roads.

Hawk, H. (1999). Bridgit: User-friendly approach to bridge management. *Transportation Research Circular*, 498(1).

Hawk, H. and Small, E. P. (1998). The BRIDGIT bridge management system. *Structural Engineering International*, 8(4):309–314.

HCM (2010). Highway capacity manual. Technical report, Transportation Research Board.

Hill, L., Cheetham, A., and Haas, R. (1991). Development and implementation of a pavement management system for Minnesota. *Transportation Research Record*, 1311:230–241.

Hochberg, Y. and Tamhane, A. C. (1987). *Multiple Comparison Procedures*. John Wiley & Sons.

Holland, J. H. (1992). *Adaptation in Natural and Artificial Systems: An Introductory Analysis with Applications to Biology, Control, and Artificial Intelligence*. The MIT Press.

Holling, C. S. (1973). Resilience and stability of ecological systems. *Annual Rview of Ecology and Systematics*, 4(1):1–23.

Hossain, K. M., Lachemi, M., and Şahmaran, M. (2009). Performance of cementitious building renders incorporating natural and industrial pozzolans under aggressive airborne marine salts. *Cement and Concrete Composites*, 31(6):358–368.

Hovde, P. J. (2002). The factor method for service life prediction from theoretical evaluation to practical implementation. In *Proceedings of the 9th International Conference on Durability of Buildings Materials and Components*, Brisbane, Australia.

Jackson, C. (2007). Multi-state modelling with R: the msm package. Technical report, Department of Epidemiology and Public Health, Imperial College, United Kingdom.

Jackson, C. (2011). Multi-state models for panel data: The msm package for R. *Journal of Statistical Software*, 38(8):1–29.

Jensen, K. (1992). *Coloured Petri Net: Basic concepts, analysis methods and practical use, Volume 1*. Springer-Verlag.

Jeong, H. S., Baik, H.-S., and Abraham, D. M. (2005). An ordered probit model approach for developing Markov chain based deterioration model for wastewater infrastructure systems. In *Pipelines 2005: Optimizing Pipeline Design, Operations, and Maintenance in Today's Economy*, Houston, United States of America.

Jiang, Y., Saito, M., and Sinha, K. C. (1988). Bridge performance prediction model using the Markov chain. *Transportation Research Record*, 1180:25–32.

Kalbfleisch, J. D. and Lawless, J. F. (1985). The analysis of panel data under a Markov assumption. *Journal of the American Statistical Association*, 80(392):863–871.

Kallen, M.-J. (2007). *Markov processes for maintenance optimization of civil infrastructure in the Netherlands*. PhD thesis, Delft University of Technology, Netherlands.

Kallen, M. J. and van Noortwijk, J. M. (2006). Statistical inference for Markov deterioration models of bridge conditions in the Netherlands. In *Proceedings of the 3rd International Conference on Bridge Maintenance, Safety and Management*, Oporto, Portugal.

Kielhauser, C., Adey, B. T., and Lethanh, N. (2017). Investigation of a static and a dynamic neighbourhood methodology to develop work programs for multiple close municipal infrastructure networks. *Structure and Infrastructure Engineering*, 13(3):361–389.

Kobayashi, K., Do, M., and Han, D. (2010). Estimation of markovian transition probabilities for pavement deterioration forecasting. *KSCE Journal of Civil Engineering*, 14(3):343–351.

Kong, J. S. and Frangopol, D. M. (2003). Life-cycle reliability-based maintenance cost optimization of deteriorating structures with emphasis on bridges. *Journal of Structural Engineering*, 129(6):818–828.

Le, B. (2014). *Modelling railway bridge asset management*. PhD thesis, The University of Nottingham, United Kingdom.

Le, B. and Andrews, J. (2015). Petri net modelling of bridge asset management using maintenance-related state conditions. *Structure and Infrastructure Engineering*, 12(6):730–751.

Le, B. and Andrews, J. (2016). Modelling wind turbine degradation and maintenance. *Wind Energy*, 19(4):571–591.

Leigh, J. and Dunnett, S. (2016). Use of Petri nets to model the maintenance of wind turbines. *Quality and Reliability Engineering International*, 32(1):167–180.

Liu, M. and Frangopol, D. M. (2006). Probability-based bridge network performance evaluation. *Journal of Bridge Engineering*, 11(5):633–641.

Lounis, Z. and Madanat, S. M. (2002). Integrating mechanistic and statistical deterioration models for effective bridge management. In *Proceedings of the 7th ASCE International Conference on Applications of Advanced Technology in Transportation*, Boston, United States of America.

Madureira, S., Flores-Colen, I., de Brito, J., and Pereira, C. (2017). Maintenance planning of façades in current buildings. *Construction and Building Materials*, 147:790–802.

Magos, M., de Brito, J., Gaspar, P. L., and Silva, A. (2016). Application of the factor method to the prediction of the service life of external paint finishes on façades. *Materials and Structures*, 49(12):5209–5225.

Man, K. F., Tang, K. S., and S., K. (1999). *Genetic Algorithms: Concepts and designs*. Springer-Verlag London.

Marques, C., de Brito, J., and Silva, A. (2018). Application of the factor method to the service life prediction of etics. *International Journal of Strategic Property Management*, 22(3):204–222.

Marsan, M. A., Balbo, G., Conte, G., Donatelli, S., and Franceschinis, G. (1994). *Modelling with Generalized Stochastic Petri Nets*. John Wiley & Sons, Inc.

Marsan, M. A. and Chiola, G. (1986). On Petri nets with deterministic and exponentially distributed firing times. In *Proceedings of the European Workshop on Applications and Theory in Petri Nets*.

Marsan, M. A., Conte, G., and Balbo, G. (1984). A class of generalized stochastic Petri nets for the performance evaluation of multiprocessor systems. *ACM Transactions on Computer Systems*, 2(2):93–122.

MatLab (2017). https://www.mathworks.com/help/gads/genetic-algorithm.html. (Page consulted on January 17, 2017).

McDuling, J. J. (2006). *Towards the development of transition probability matrices in the Markovian model for predicted service life of buildings*. PhD thesis, University of Pretoria, South Africa.

Meegoda, J., Juliano, T., Ratnaweera, P., and Abdel-Malek, L. (2005). Framework for inspection, maintenance, and replacement of corrugated steel culvert pipes. *Transportation Research Record: Journal of the Transportation Research Board*, 1911:22–30.

Meng, X. (2010). Modeling of reconfigurable manufacturing systems based on colored timed object-oriented Petri nets. *Journal of Manufacturing Systems*, 29(2):81–90.

Micevski, T., Kuczera, G., and Coombes, P. (2002). Markov model for storm water pipe deterioration. *Journal of Infrastructure Systems*, 8(2):49–56.

Miles, S. B. and Chang, S. E. (2006). Modeling community recovery from earthquakes. *Earthquake Spectra*, 22(2):439–458.

Miyamoto, A., Kawamura, K., and Nakamura, H. (2000). Bridge management system and maintenance optimization for existing bridges. *Computer-Aided Civil and Infrastructure Engineering*, 15(1):45–55.

Miyamoto, A., Kawamura, K., and Nakamura, H. (2001). Development of a bridge management system for existing bridges. *Advances in Engineering Software*, 32(10):821–833.

Molloy, M. K. (1982). Performance analysis using stochastic Petri nets. *IEEE Transactions on computers*, 100(9):913–917.

Morcous, G. (2006). Performance prediction of bridge deck systems using Markov chains. *Journal of Performance of Constructed Facilities*, 20(2):146–155.

Morcous, G. and Lounis, Z. (2005). Maintenance optimization of infrastructure networks using genetic algorithms. *Automation in construction*, 14(1):129–142.

Morcous, G., Lounis, Z., and Mirza, M. (2002a). Life-cycle assessment of highway bridges. In *Proceedings of the Taiwan-Canada Workshop on Bridges*, Taipei, Taiwan.

Morcous, G., Rivard, H., and Hanna, A. M. (2002b). Modeling bridge deterioration using case-based reasoning. *Journal of Infrastructure Systems*, 8(3):86–95.

Morgado, J., Flores-Colen, I., de Brito, J., and Silva, A. (2017). Maintenance planning of pitched roofs in current buildings. *Journal of Construction Engineering and Management*, 143(7):05017010.

Mousavi, S., Silva, A., de Brito, J., Ekhlassi, A., and Hosseini, S. (2017). Service life prediction of natural stone claddings with an indirect fastening system. *Journal of Performance of Constructed Facilities*, 31(4):04017014.

Murata, T. (1989). Petri nets: Properties, analysis and applications. In *Proceedings of the IEEE*.

Najafi, M. and Kulandaivel, G. (2005). Pipeline condition prediction using neural network models. In *Pipelines 2005: Optimizing Pipeline Design, Operations, and Maintenance in Today's Economy*, Houston, United States of America.

Neter, J., Kutner, M. H., Nachtsheim, C. J., and Wasserman, W. (1996). *Applied Linear Statistical Models*. Irwin Press.

Neto, N. and de Brito, J. (2011). Inspection and defect diagnosis system for natural stone cladding. *Journal of Materials in Civil Engineering*, 23(10):1433–1443.

Neto, N. and de Brito, J. (2012). Validation of an inspection and diagnosis system for anomalies in natural stone cladding (NSC). *Construction and Building Materials*, 30:224–236.

Neves, L. C. (2005). *Life-cycle analysis of bridges considering condition, safety and maintenance cost interaction*. PhD thesis, Universidade do Minho, Portugal.

Neves, L. C. (2011). Sistemas de gestão de infraestruturas. *Construção Magazine*, 43:4 – 6.

Neves, L. C. and Frangopol, D. M. (2005). Condition, safety and cost profiles for deteriorating structures with emphasis on bridges. *Reliability Engineering and System Safety*, 89(2):185–198.

Neves, L. C., Frangopol, D. M., and Petcherdchoo, A. (2006). Probabilistic lifetime-oriented multiobjective optimization of bridge maintenance: Combination of maintenance types. *Journal of Structural Engineering*, 132(11):1821–1834.

Ng, A. K. and Efstathiou, J. (2006). Structural robustness of complex networks. *Physical Review*, 3:175–188.

O'Connor, A., Sheils, E., Breysse, D., and Schoefs, F. (2011). Markovian bridge maintenance planning incorporating corrosion initiation and nonlinear deterioration. *Journal of Bridge Engineering*, 18(3):189–199.

OECD (2006). Infrastructure to 2030 - Telecom, land transport, water and electricity. Technical report, Organisation for Economic Co-operation and Development.

OECD (2007). Infrastructure to 2030 - Mapping policy for electricity, water and transport. Technical report, Organisation for Economic Co-operation and Development.

Orcesi, A. D., Frangopol, D. M., and Kim, S. (2010). Optimization of bridge maintenance strategies based on multiple limit states and monitoring. *Engineering Structures*, 32(3):627–640.

Ortiz-García, J. J., Costello, S. B., and Snaith, M. S. (2006). Derivation of transition probability matrices for pavement deterioration modeling. *Journal of Transportation Engineering*, 132(2):141–161.

Pandey, M. (1998). Probabilistic models for condition assessment of oil and gas pipelines. *NDT & E International*, 31(5):349–358.

Paulo, P., Branco, F., de Brito, J., and Silva, A. (2016). BuildingsLife – The use of genetic algorithms for maintenance plan optimization. *Journal of Cleaner Production*, 121:84–98.

Paulo, P. V., Branco, F., and de Brito, J. (2014). BuildingsLife: a building management system. *Structure and Infrastructure Engineering*, 10(3):388–397.

Petcherdchoo, A. and Frangopol, D. M. (2004). Maintaining condition and safety of deteriorating bridges by probabilistic models and optimization. Technical report, Department of Civil, Environmental, and Architectural Engineering, University of Colorado, United States of America.

Peterson, J. L. (1977). Petri nets. *Computing Surveys*, 9(3):223–252.

Petri, C. A. (1962). *Kommunikation mit Automaten*. PhD thesis, Institut für Instrumentelle Mathematik, Germany. Also, English translation: Petri, C. A. (1966). Communication with Automata. Technical report RADC-TC-65-377, Griffiss Air Force Base, New York, United States of America.

Phares, B. M., Washer, G. A., Rolander, D. D., Graybeal, B. A., and Moore, M. (2004). Routine highway bridge inspection condition documentation accuracy and reliability. *Journal of Bridge Engineering*, 9(4):403–413.

Pilson, C., Hudson, W. R., and Anderson, V. (1999). Multi-objective optimization in pavement management using genetic algorithms and efficient surfaces. *Transportation Research Record*, 1644(1):42–48.

Pires, R., de Brito, J., and Amaro, B. (2013). Inspection, diagnosis, and rehabilitation system of painted rendered façades. *Journal of Performance of Constructed Facilities*, 29(2):04014062.

Plšková, I., Chobola, Z., and Matysik, M. (2011). Assessment of ceramic tile frost resistance by means of the frequency inspection method. *Ceramics-Silikáty*, 55(2):176–182.

Rama, D. and Andrews, J. (2013). A system-wide modelling approach to railway infrastructure asset management. In *Proceedings of the 20th Advances in Risk and Reliability Technology Symposium*, Loughborough, United Kingdom.

Rama, D. and Andrews, J. (2016). Railway infrastructure asset management: The whole-system life cost analysis. *IET Intelligent Transport Systems*, 10(1):58–64.

Ramamoorthy, C. V. and Ho, G. S. (1980). Performance evaluation of asynchronous concurrent systems using Petri nets. *IEEE Transactions on Software Engineering*, SE-6(5):440–449.

Ramos, R., Silva, A., de Brito, J., and Gaspar, P. L. (2018). Methodology for the service life prediction of ceramic claddings in pitched roofs. *Construction and Building Materials*, 166:386–399.

Rirsch, E., MacMullen, J., and Zhang, Z. (2011). Evaluation of mortar samples obtained from UK houses treated for rising damp. *Construction and Building Materials*, 25(6):2845–2850.

Rose, A. (2004). Defining and measuring economic resilience to disasters. *Disaster Prevention and Management: An International Journal*, 13(4):307–314.

Rose, A. and Liao, S.-Y. (2005). Modeling regional economic resilience to disasters: A computable general equilibrium analysis of water service disruptions. *Journal of Regional Science*, 45(1):75–112.

Ryall, M. J. (2010). *Bridge Management*. CRC Press.

Sá, G., Sá, J., de Brito, J., and Amaro, B. (2014). Inspection and diagnosis system for rendered walls.

Salman, B. (2010). *Infrastructure management and deterioration risk assessment of wastewater collection systems*. PhD thesis, University of Cincinnati, United States of America.

Sánchez-Silva, M. and Klutke, G.-A. (2016). *Reliability and Life-Cycle Analysis of Deteriorating Systems*. Springer.

Scherer, W. T. and Glagola, D. M. (1994). Markovian models for bridge maintenance management. *Journal of Transportation Engineering*, 120(1):37–51.

Schneeweiss, W. G. (2004). *Petri Net Picture Book: An elementary introduction to the best pictorial description of temporal changes*. LiLoLe - Verlag GmbH.

Scott, D. M., Novak, D. C., Aultman-Hall, L., and Guo, F. (2006). Network robustness index: A new method for identifying critical links and evaluating the performance of transportation networks. *Journal of Transport Geography*, 14(3):215–227.

Serralheiro, M. I., de Brito, J., and Silva, A. (2017). Methodology for service life prediction of architectural concrete facades. *Construction and Building Materials*, 133:261–274.

Shahin, M. Y. and Kohn, S. D. (1982). Overview of the 'PAVER' pavement management system and economic analysis of field implementing the 'PAVER' pavement management system. Technical report, DTIC Document.

Shamir, U., Howard, C., et al. (1979). An analytical approach to scheduling pipe replacement (PDF). *Journal-American Water Works Association*, 71(5):248–258.

Shohet, I. M. and Paciuk, M. (2004). Service life prediction of exterior cladding components under standard conditions. *Construction Management and Economics*, 22(10):1081–1090.

Shohet, I. M., Puterman, M., and Gilboa, E. (2002). Deterioration patterns of building cladding components for maintenance management. *Construction Management & Economics*, 20(4):305–314.

Silva, A., de Brito, J., and Gaspar, P. (2011a). Service life prediction model applied to natural stone wall claddings (directly adhered to the substrate). *Construction and Building Materials*, 25(9):3674–3684.

Silva, A., de Brito, J., and Gaspar, P. (2012a). Application of the factor method to maintenance decision support for stone cladding. *Automation in Construction*, 22:165–174.

Silva, A., de Brito, J., and Gaspar, P. (2015). Stochastic approach to the factor method: durability of rendered façades. *Journal of Materials in Civil Engineering*, 28(2):04015130.

Silva, A., de Brito, J., and Gaspar, P. L. (2016a). Comparative analysis of service life prediction methods applied to rendered façades. *Materials and Structures*, 49(11):4893–4910.

Silva, A., de Brito, J., and Gaspar, P. L. (2016b). *Methodologies for service life prediction of buildings: with a focus on façade claddings*. Springer.

Silva, A., Dias, J., Gaspar, P., and de Brito, J. (2011b). Service life prediction models for exterior stone cladding. *Building Research & Information*, 39(6):637–653.

Silva, A., Dias, J., Gaspar, P., and de Brito, J. (2013). Statistical models applied to service life prediction of rendered façades. *Automation in Construction*, 30:151–160.

Silva, A., Gaspar, P., and de Brito, J. (2012b). Probabilistic analysis of the degradation evolution of stone wall cladding (directly adhered to the substrate). *Journal of Materials in Civil Engineering*, 25(2):227–235.

Silva, A., Gaspar, P. L., de Brito, J., and Neves, L. C. (2016c). Probabilistic analysis of degradation of façade claddings using Markov chain models. *Materials and Structures*, 49(7):2871–2892.

Silva, A., Neves, L. C., Gaspar, P. L., and de Brito, J. (2016d). Probabilistic transition of condition: render façades. *Building Research & Information*, 44(3):301–318.

Silva, A., Vieira, S., de Brito, J., and Gaspar, P. (2016e). Fuzzy systems in the service-life prediction of exterior natural stone claddings. *Journal of Performance of Constructed Facilities*, 30(5):04016005.

Silva, C. d., Coelho, F., de Brito, J., Silvestre, J., and Pereira, C. (2017). Inspection, diagnosis, and repair system for architectural concrete surfaces. *Journal of Performance of Constructed Facilities*, 31(5):04017035.

Silvestre, J. D. and de Brito, J. (2005). Development of an expert system for inspection and diagnosis of ceramic wall of floor tiling laid on mortar or adhesive. In *Proceedings of the Congress CIB W102: Meeting on Information and Knowledge Management in Building*.

Silvestre, J. D. and de Brito, J. (2009). Ceramic tiling inspection system. *Construction and Building Materials*, 23(2):653–668.

Stillman, R. (2003). Power line maintenance with minimal repair and replacement. In *Annual Reliability and Maintainability Symposium*, Tampa, United States of America.

Tang, F., Guo, M., Dong, M., Li, M., and Guan, H. (2008). Towards context-aware workflow management for ubiquitous computing. In *Proceedings of the International Conference on Embedded Software and Systems*, Sichuan, China.

Tavakoli, A., Lapin, M. S., and Figueroa, J. L. (1992). PMSC: Pavement management system for small communities. *Journal of Transportation Engineering*, 118(2):270–280.

Thai-Ker, L. and Chung-Wan, W. (2006). Challenges of external wall tiling in singapore. In *Qualicer 2006: IX World Congress on Ceramic Tile Quality*, Castellón, Spain.

Thoft-Christensen, P. (1998). Assessment of the reliability profiles for concrete bridges. *Engineering Structures*, 20(11):1004–1009.

Thompson, P. D., Small, E. P., Johnson, M., and Marshall, A. R. (1998). The Pontis bridge management system. *Structural Engineering International*, 8(4):303–308.

Timmennan, P. (1981). Vulnerability, resilience and the collapse of society: A review of models and possible climatic applications. *Environmental Monograph. Toronto: Institute for Environmental Studies*.

Tolba, C., Lefebvre, D., Thomas, P., and El Moudni, A. (2005). Continuous and timed Petri nets for the macroscopic and microscopic traffic flow modelling. *Simulation Modelling Practice and Theory*, 13(5):407–436.

Toledo, T., Koutsopoulos, H., Davol, A., Ben-Akiva, M., Burghout, W., Andréasson, I., Johansson, T., and Lundin, C. (2003). Calibration and validation of microscopic traffic simulation tools: Stockholm case study. *Transportation Research Record: Journal of the Transportation Research Board*, 1831:65–75.

Uzam, M., Gelen, G., and Saleh, T. L. (2016). Think-globally-act-locally approach with weighted arcs to the synthesis of a liveness-enforcing supervisor for generalized Petri nets modeling FMSs. *Information Sciences*, 363:235–260.

van der Aalst, W. M. (2002). Making work flow: On the application of petri nets to business process management. In *Proceedings of the 23rd International Conference on Application and Theory of Petri Nets*, Adelaide, Australia.

van Noortwijk, J. M. and Frangopol, D. M. (2004). Two probabilistic life-cycle maintenance models for deteriorating civil infrastructures. *Probabilistic Engineering Mechanics*, 19(4):345–359.

Vieira, S., Silva, A., Sousa, J., de Brito, J., and Gaspar, P. (2015). Modelling the service life of rendered facades using fuzzy systems. *Automation in Construction*, 51:1–7.

Walski, T. M. and Pelliccia, A. (1982). Economic analysis of water main breaks. *Journal (American Water Works Association)*, pages 140–147.

Wang, Y., Moselhi, O., and Zayed, T. (2009). Study of the suitability of existing deterioration models for water mains. *Journal of Performance of Constructed Facilities*, 23(1):40–46.

Wirahadikusumah, R., Abraham, D., and Iseley, T. (2001). Challenging issues in modeling deterioration of combined sewers. *Journal of Infrastructure Systems*, 7(2):77–84.

Wirahadikusumah, R. and Abraham, D. M. (2003). Application of dynamic programming and simulation for sewer management. *Engineering, Construction and Architectural Management*, 10(3):193–208.

Wirahadikusumah, R., Abraham, D. M., and Castello, J. (1999). Markov decision process for sewer rehabilitation. *Engineering, Construction and Architectural Management*, 6(4):358–370.

Wu, C. F. J. and Hamada, M. S. (2011). *Experiments: Planning, analysis, and optimization*. John Wiley & Sons.

Ximenes, S., De Brito, J., Gaspar, P., and Silva, A. (2015). Modelling the degradation and service life of etics in external walls. *Materials and Structures*, 48(7):2235–2249.

Xu, N., Guikema, S. D., Davidson, R. A., Nozick, L. K., Çağnan, Z., and Vaziri, K. (2007). Optimizing scheduling of post-earthquake electric power restoration tasks. *Earthquake Engineering & Structural Dynamics*, 36(2):265–284.

Yang, S. I., Frangopol, D. M., Kawakami, Y., and Neves, L. C. (2006). The use of lifetime functions in the optimization of interventions on existing bridges considering maintenance and failure costs. *Reliability Engineering & System Safety*, 91(6):698–705.

Yianni, P. C., Rama, D., Neves, L. C., Andrews, J. D., and Castlo, D. (2017). A Petri-net-based modelling approach to railway bridge asset management. *Structure and Infrastructure Engineering*, 13(2):287–297.

Zayed, T. and Mohamed, E. (2013). Budget allocation and rehabilitation plans for water systems using simulation approach. *Tunnelling and Underground Space Technology*, 36:34–45.

Zhou, H., Wan, J., Jia, H., et al. (2010). Resilience to natural hazards: A geographic perspective. *Natural Hazards*, 53(1):21–41.

Zuberek, W. M. (1980). Timed Petri nets and preliminary performance evaluation. In *Proceedings of the 7th annual symposium on Computer Architecture*, La Baule, France.

Appendix A

Definition of Places and Transitions

A.1   List of places

A full list of places included in the Petri net maintenance model (Figure 4.10) is provided in Table A.1.

Table A.1 – Definition of places

Place	Definition of the function
p_1	System in a *Very good condition*
p_2	System in a *Good condition*
p_3	System in a *Poor condition*
p_4	System in a *Very poor condition*
p_5	No major inspection is being performed
p_6	Major inspection is being performed
p_7	*Very good condition* of the system is revealed
p_8	*Good condition* of the system is revealed
p_9	*Poor condition* of the system is revealed
p_{10}	*Very poor condition* of the system is revealed
p_{11}	System needs a preventive maintenance in the *Very good condition*
p_{12}	System needs a preventive maintenance in the *Good condition*
p_{13}	System needs a preventive maintenance in the *Poor condition*
p_{14}	System needs a preventive maintenance in the *Very poor condition*
p_{15}	System needs a corrective maintenance in the *Very good condition*
p_{16}	System needs a corrective maintenance in the *Good condition*
p_{17}	System needs a corrective maintenance in the *Poor condition*
p_{18}	System needs a corrective maintenance in the *Very poor condition*
p_{19}	No maintenance action is performed on the system
p_{20}	Preventive maintenance is performed on the system
p_{21}	Corrective maintenance is performed on the system
p_{22}	System ready to return to the process of deterioration
p_{23}	Indication that preventive maintenance improves the condition of the system after the application of the maintenance action
p_{24}	Indication that preventive maintenance suppresses the deterioration process during a period of time after the application of the maintenance action
p_{25}	Indication that preventive maintenance reduces the deterioration rate during a period of time after the application of the maintenance action
p_{26}	System after preventive maintenance is performed

Place	Definition of the function
p_{27}	Indication that corrective maintenance improves the condition of the system after the application of the maintenance action
p_{28}	Indication that corrective maintenance suppresses the deterioration process during a period of time after the application of the maintenance action
p_{29}	Indication that corrective maintenance reduces the deterioration rate during a period of time after the application of the maintenance action
p_{30}	System after corrective maintenance is performed
p_{31}	Indication that a preventive maintenance is available in the *Very good condition*
p_{32}	Indication that a preventive maintenance is available in the *Good condition*
p_{33}	Indication that a preventive maintenance is available in the *Poor condition*
p_{34}	Indication that a preventive maintenance is available in the *Very poor condition*

A.2   List of transitions

A full list of transitions included in the Petri net maintenance model (Figure 4.10) is provided in Table A.2.

Table A.2 – Definition of transitions

Transition	Definition of the function
t_1	It is a stochastic transition and models the transition between *Very good condition* and *Good condition*, representing the time that the system spends in *Very good condition* before moving to *Good condition*
t_2	It is a stochastic transition and models the transition between *Good condition* and *Poor condition*, representing the time that the system spends in *Good condition* before moving to *Poor condition*
t_3	It is a stochastic transition and models the transition between *Poor condition* and *Very poor condition*, representing the time that the system spends in *Poor condition* before moving to *Very poor condition*
t_4	It is an immediate transition and returns the token present in place p_6 to place p_5 after the major inspection has been performed and the true condition of the system has been revealed
t_5	It is a stochastic transition and manages the moments of realization of the major inspections
t_6	It is an immediate transition and removes the token from the deterioration process, place p_1, and reveals the true condition of the system - *Very good condition*
t_7	It is an immediate transition and removes the token from the deterioration process, place p_2, and reveals the true condition of the system - *Good condition*
t_8	It is an immediate transition and removes the token from the deterioration process, place p_3, and reveals the true condition of the system - *Poor condition*
t_9	It is an immediate transition and removes the token from the deterioration process, place p_4, and reveals the true condition of the system - *Very poor condition*
t_{10}	It is an immediate transition and its firing means that no maintenance is taken when the system has a *Very good condition*

Transition	Definition of the function
t_{11}	It is an immediate transition and its firing means that no maintenance is taken when the system has a *Good condition*
t_{12}	It is an immediate transition and its firing means that no maintenance is taken when the system has a *Poor condition*
t_{13}	It is an immediate transition and its firing means that no maintenance is taken when the system has a *Very poor condition*
t_{14}	It is an immediate transition and its firing means that a preventive maintenance is taken when the system has a *Very good condition*
t_{15}	It is an immediate transition and its firing means that a preventive maintenance is taken when the system has a *Good condition*
t_{16}	It is an immediate transition and its firing means that a preventive maintenance is taken when the system has a *Poor condition*
t_{17}	It is an immediate transition and its firing means that a preventive maintenance is taken when the system has a *Very poor condition*
t_{18}	It is an immediate transition and its firing means that a corrective maintenance is taken when the system has a *Very good condition*
t_{19}	It is an immediate transition and its firing means that a corrective maintenance is taken when the system has a *Good condition*
t_{20}	It is an immediate transition and its firing means that a corrective maintenance is taken when the system has a *Poor condition*
t_{21}	It is an immediate transition and its firing means that a corrective maintenance is taken when the system has a *Very poor condition*
t_{22}	It is an immediate transition and its firing means that the system no need maintenance and is ready to return to the process of deterioration
t_{23}	It is an immediate transition and its firing means that a preventive maintenance was applied to the system and this is ready to return to the process of deterioration
t_{24}	It is an immediate transition and its firing means that a corrective maintenance was applied to the system and this is ready to return to the process of deterioration
t_{25}	It is an immediate transition and returns the system to *Very good condition* in the deterioration process
t_{26}	It is an immediate transition and returns the system to *Good condition* in the deterioration process
t_{27}	It is an immediate transition and returns the system to *Poor condition* in the deterioration process
t_{28}	It is an immediate transition and returns the system to *Very poor condition* in the deterioration process
t_{29}	It is an immediate transition and its firing means that the preventive maintenance only improves the condition state of the system
t_{30}	It is a immediate transition and its firing means that the preventive maintenance only suppresses the deterioration process over a period of time
t_{31}	It is an immediate transition and its firing means that the preventive maintenance improves the condition state and suppresses the deterioration process over a period of time
t_{32}	It is an immediate transition and its firing means that the preventive maintenance only reduces the deterioration rate over a period of time
t_{33}	It is an immediate transition and its firing means that the preventive maintenance improves the condition state and reduces the deterioration rate over a period of time

Transition	Definition of the function
t_{34}	It is an immediate transition and its firing means that the corrective maintenance only improves the condition state of the system
t_{35}	It is an immediate transition and its firing means that the corrective maintenance improves the condition state and suppresses the deterioration process over a period of time
t_{36}	It is an immediate transition and its firing means that the corrective maintenance improves the condition state and reduces the deterioration rate over a period of time
t_{37}	It is a deterministic transitions and its firing means that the preventive maintenance is available in *Very good condition*
t_{38}	It is a deterministic transitions and its firing means that the preventive maintenance is available in *Good condition*
t_{39}	It is a deterministic transitions and its firing means that the preventive maintenance is available in *Poor condition*
t_{40}	It is a deterministic transitions and its firing means that the preventive maintenance is available in *Very poor condition*

Appendix B

Network Description

B.1 Petri net schemes

Figure B.1 shows the network analysed. The network is composed by seven input points and two intersections between highways. The input points are identified by number from (1) to (7), while the intersections are identified by the letters (A) and (B). All highway sections have traffic in both directions.
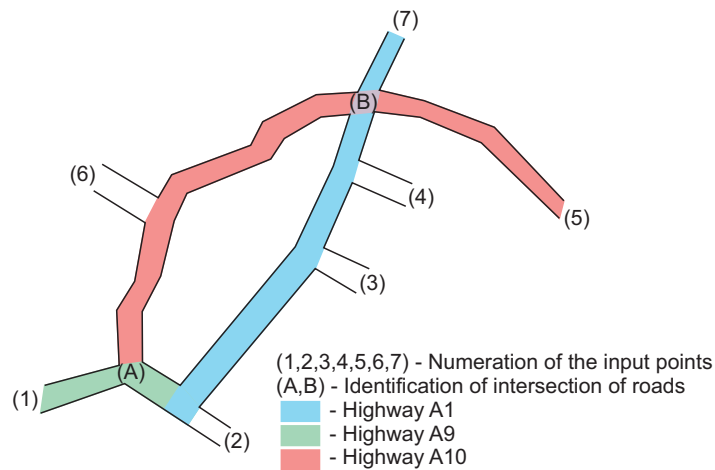
Figure B.1 – Network analysed

Figures B.2 – B.19 present the Petri net schemes for the 18 sections that comprise the network analysed, and Figures B.20 – B.21 present the Petri net schemes for the two intersections between highways. The Petri net scheme is composed by 132 segments of variable length, 246 places and 144 transitions.
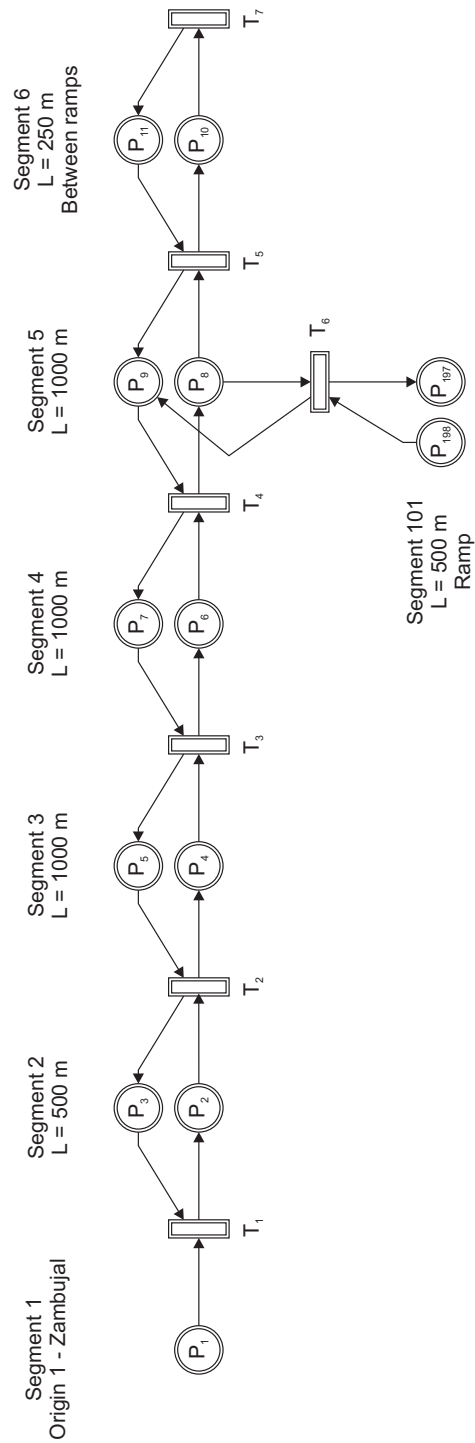
Figure B.2 – Petri net scheme of Section 1 of the network – Section (1) – (A)
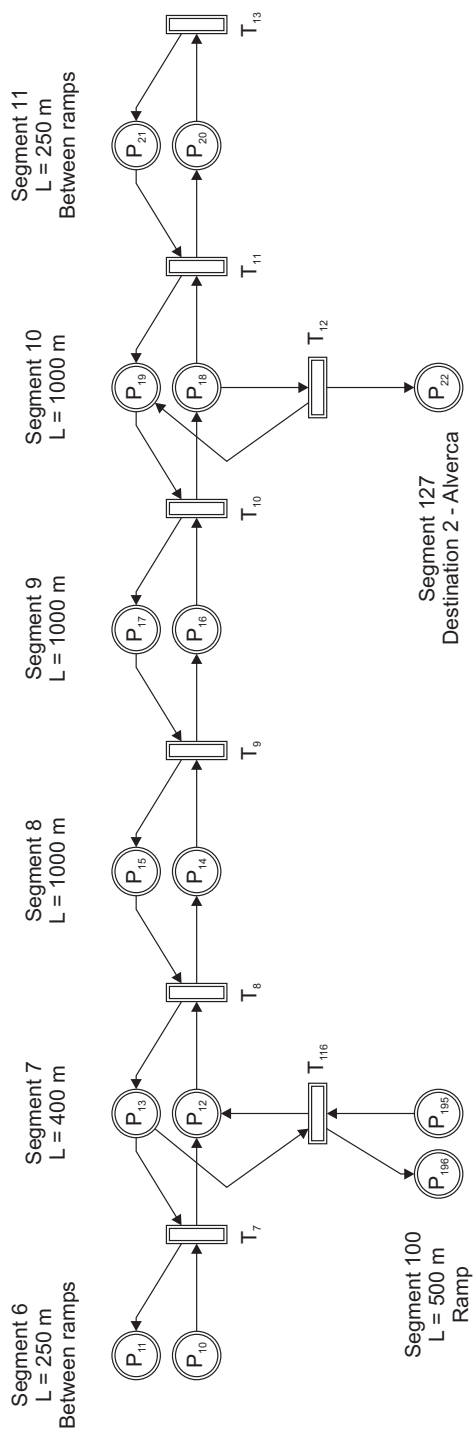
Figure B.3 – Petri net scheme of Section 2 of the network – Section (A) – (2)
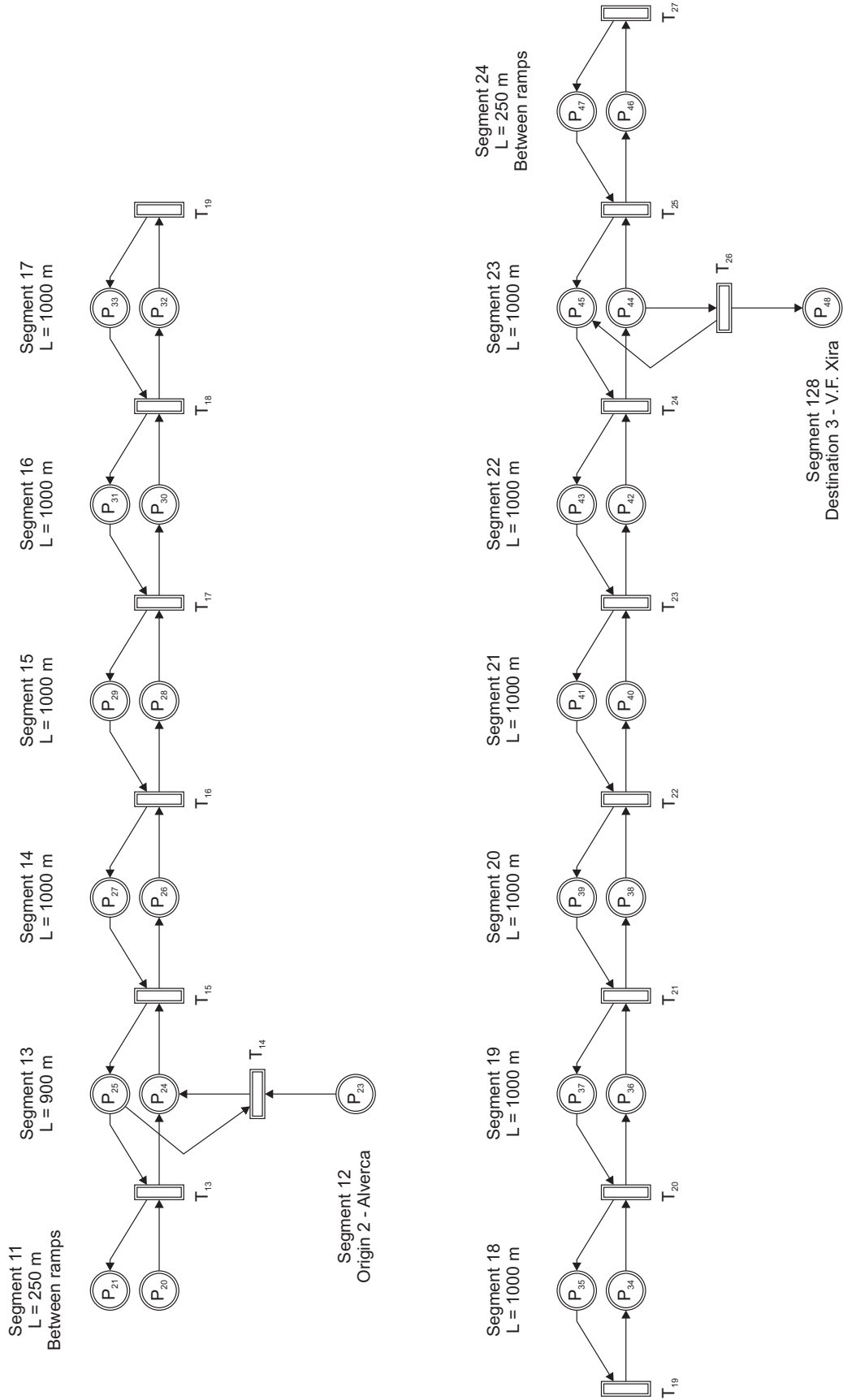
Figure B.4 – Petri net scheme of Section 3 of the network – Section (2) – (3)
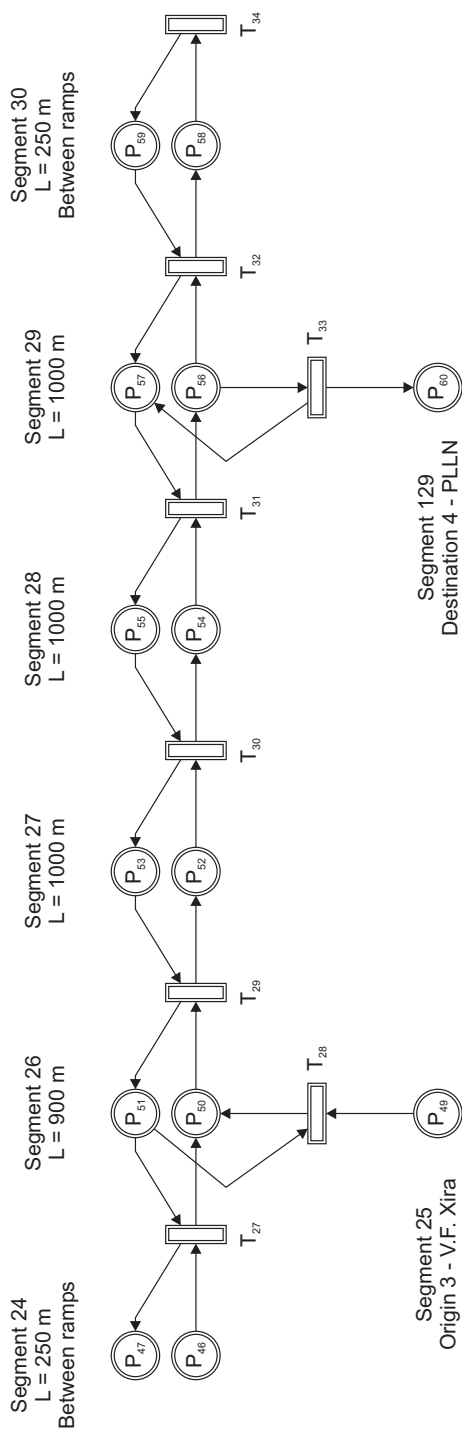
Figure B.5 – Petri net scheme of Section 4 of the network – Section (3) – (4)
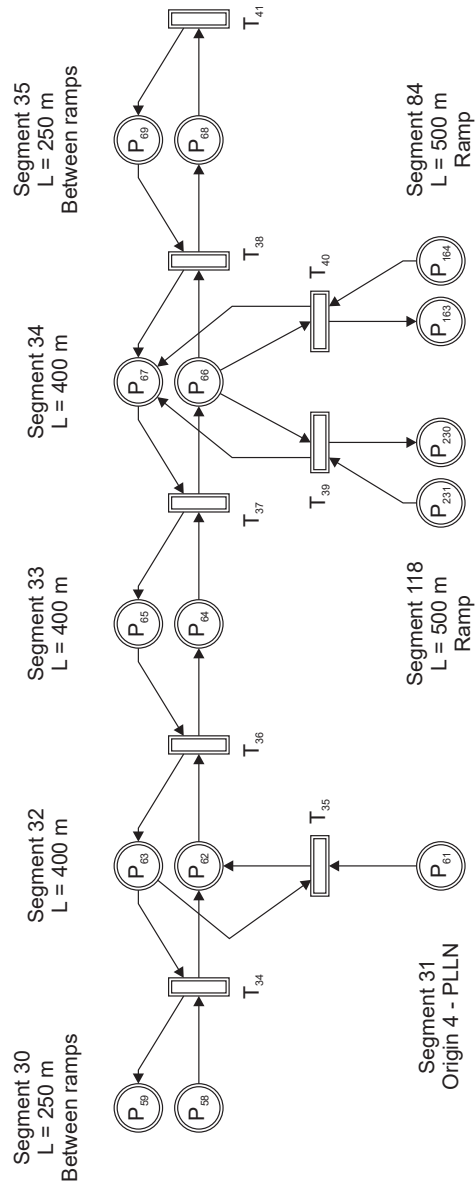
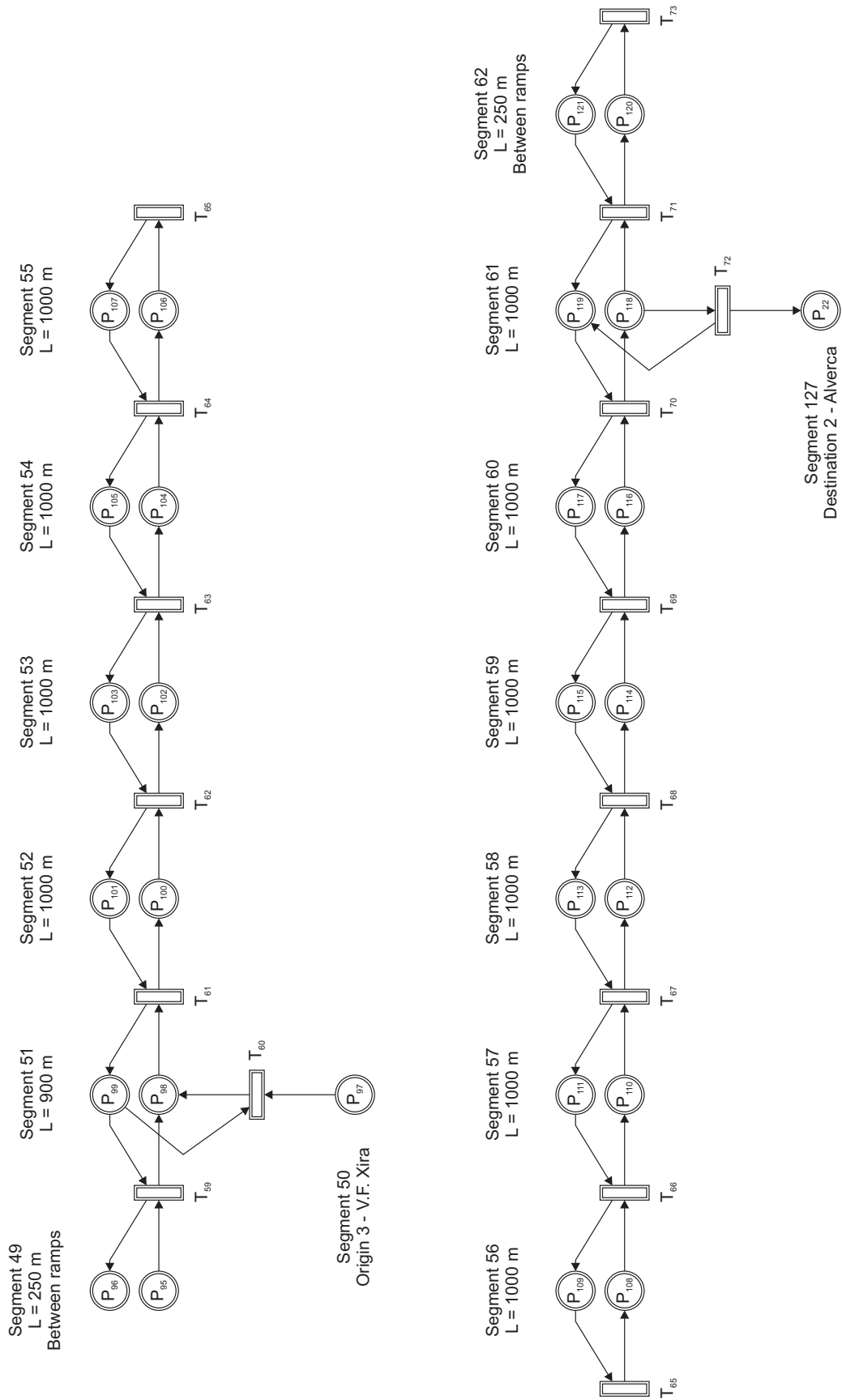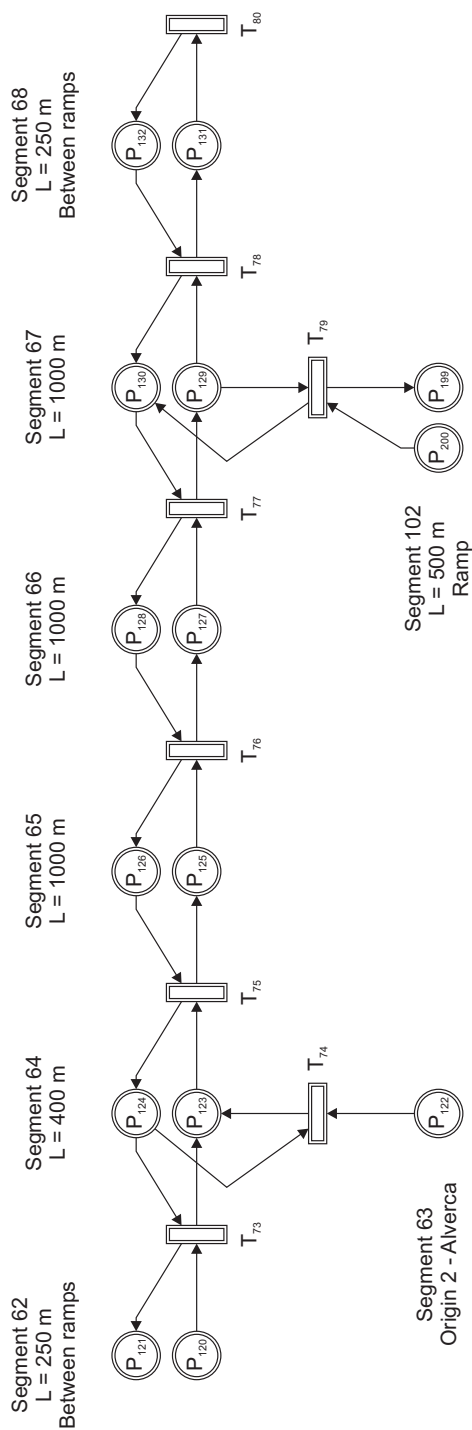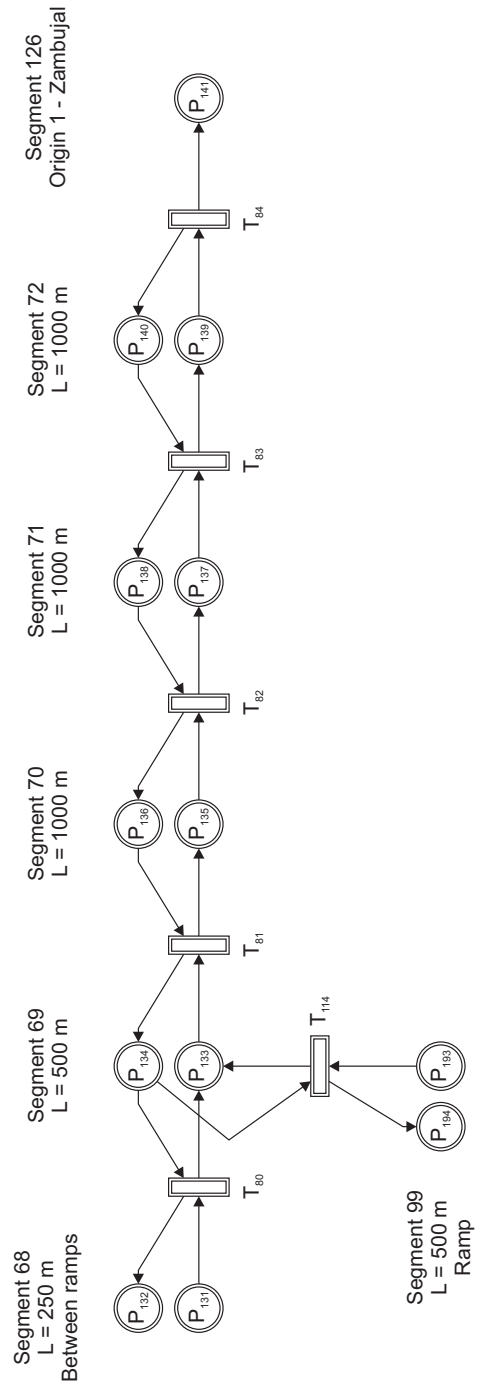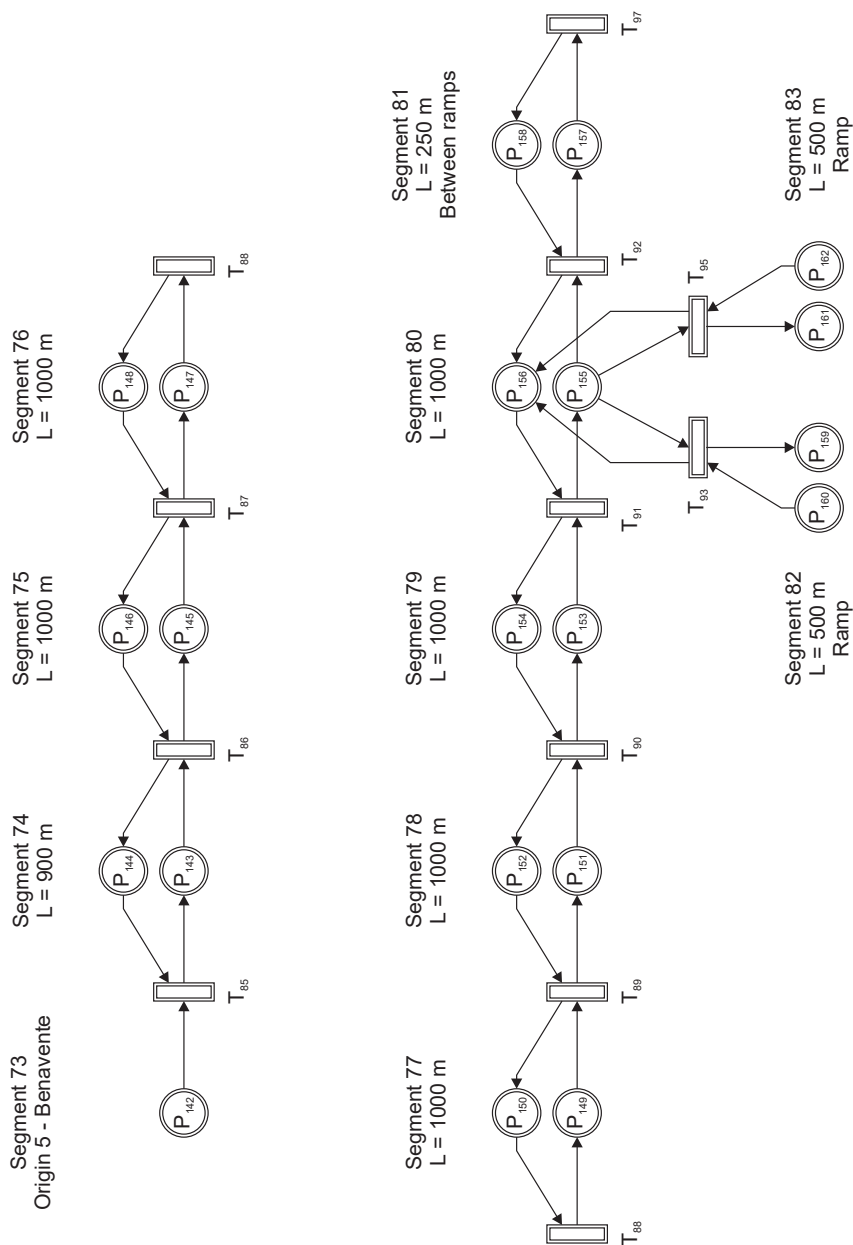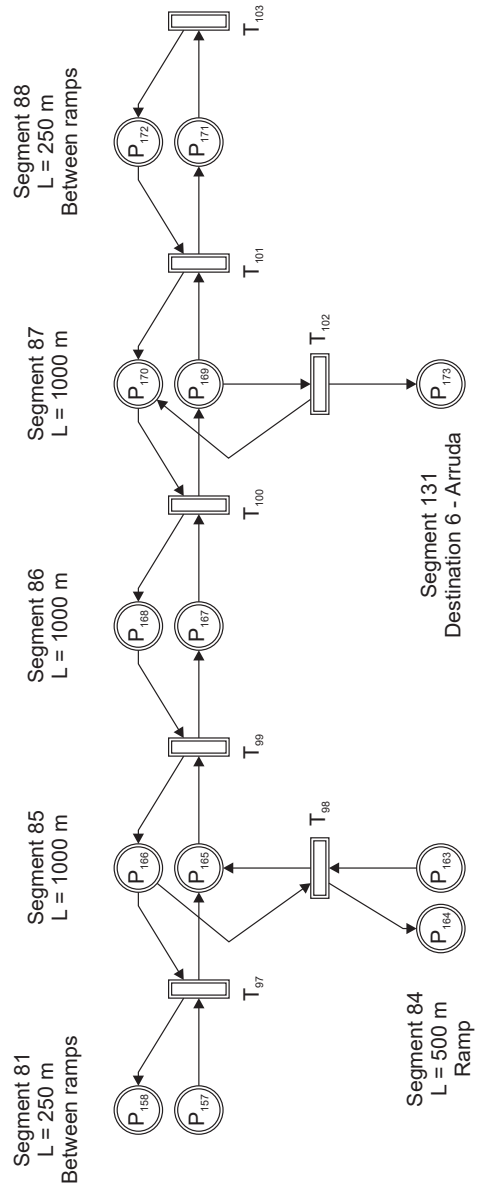Figure B.6 – Petri net scheme of Section 5 of the network – Section (4) – (B)
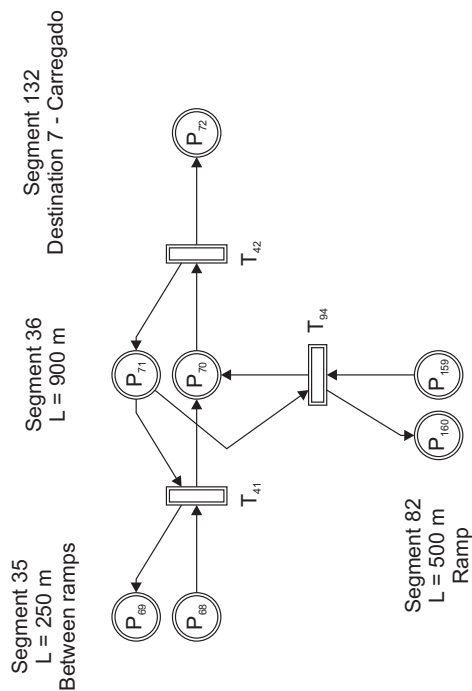
Figure B.7 – Petri net scheme of Section 6 of the network – Section (B) – (7)
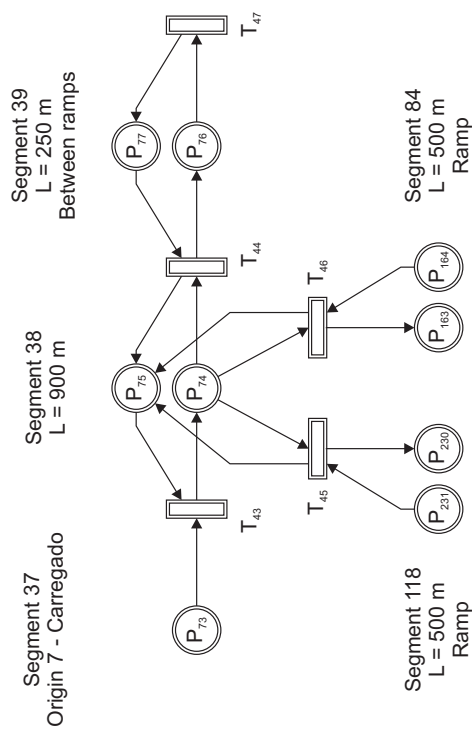
Figure B.8 – Petri net scheme of Section 7 of the network – Section (7) – (B)
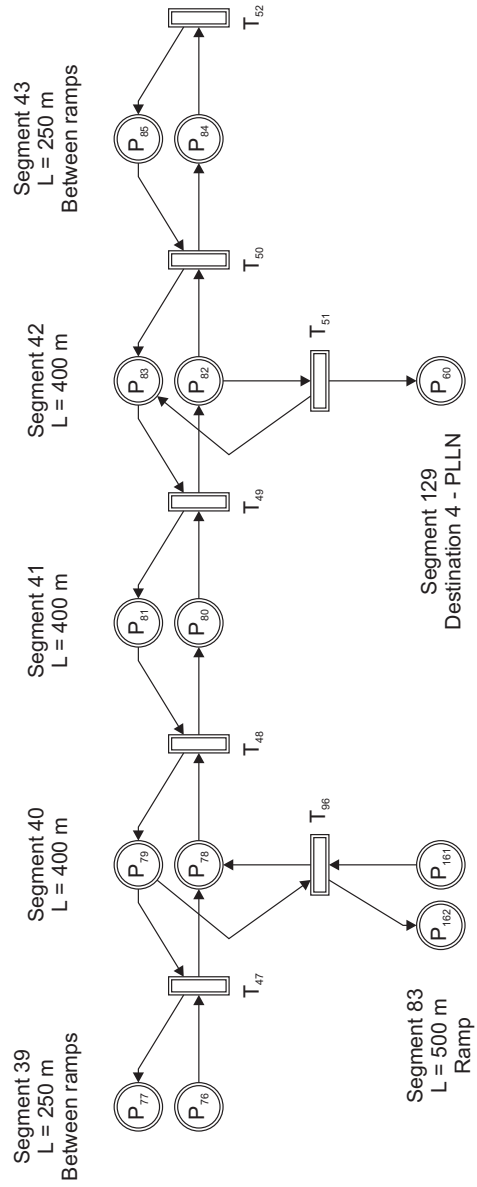
Figure B.9 – Petri net scheme of Section 8 of the network – Section (B) – (4)
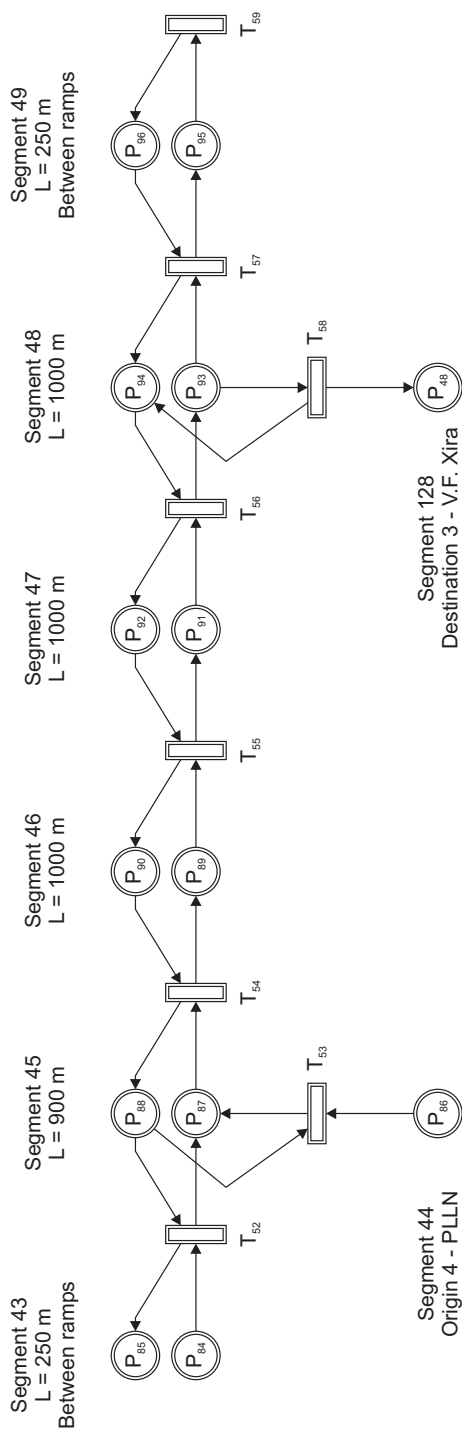
Figure B.10 – Petri net scheme of Section 9 of the network – Section (4) – (3)

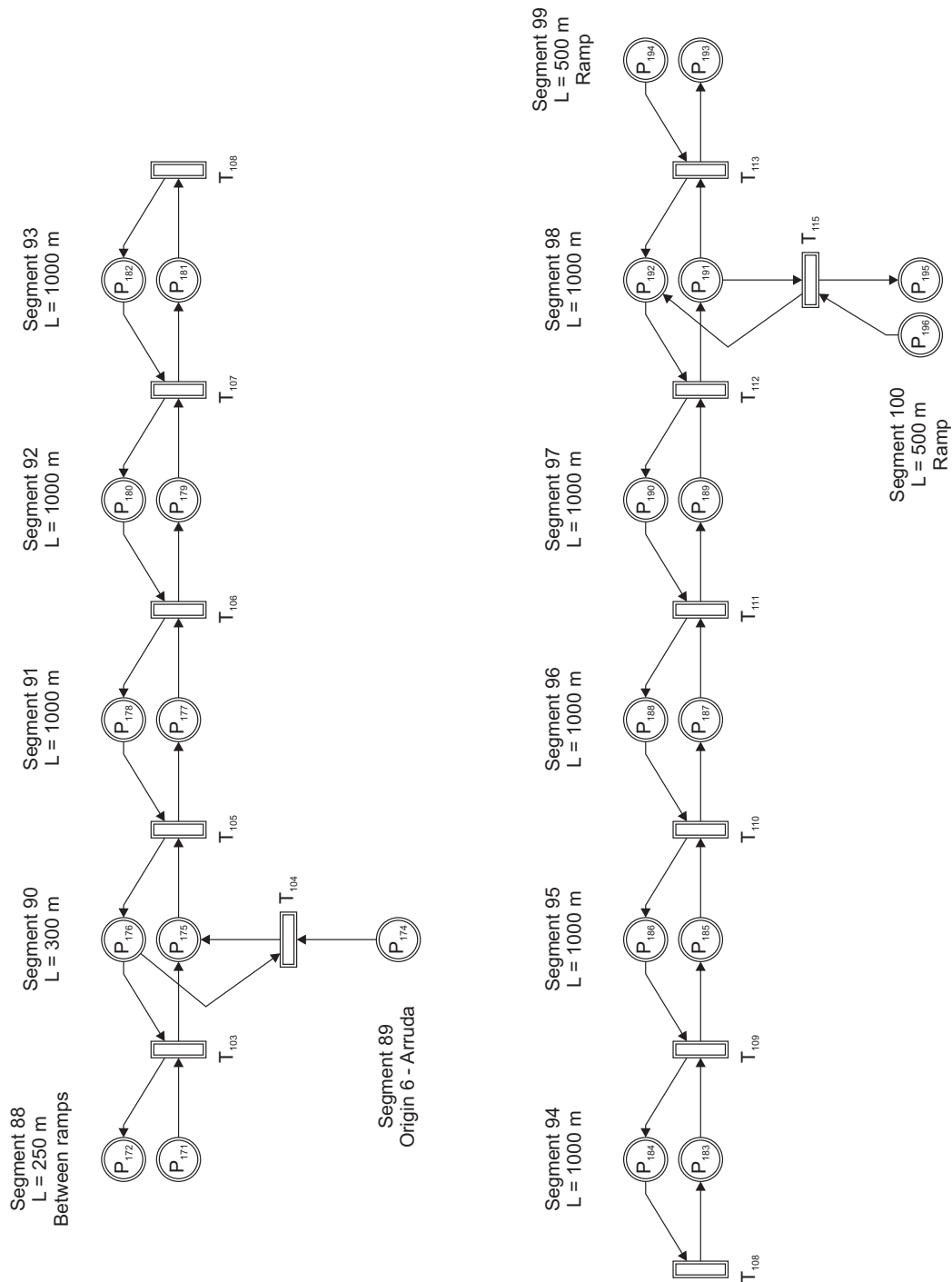Figure B.11 – Petri net scheme of Section 10 of the network – Section (3) – (2)

Figure B.12 – Petri net scheme of Section 11 of the network – Section (2) – (A)

Figure B.13 – Petri net scheme of Section 12 of the network – Section (A) – (1)

Figure B.14 – Petri net scheme of Section 13 of the network – Section (5) – (B)

Figure B.15 – Petri net scheme of Section 14 of the network – Section (B) – (6)

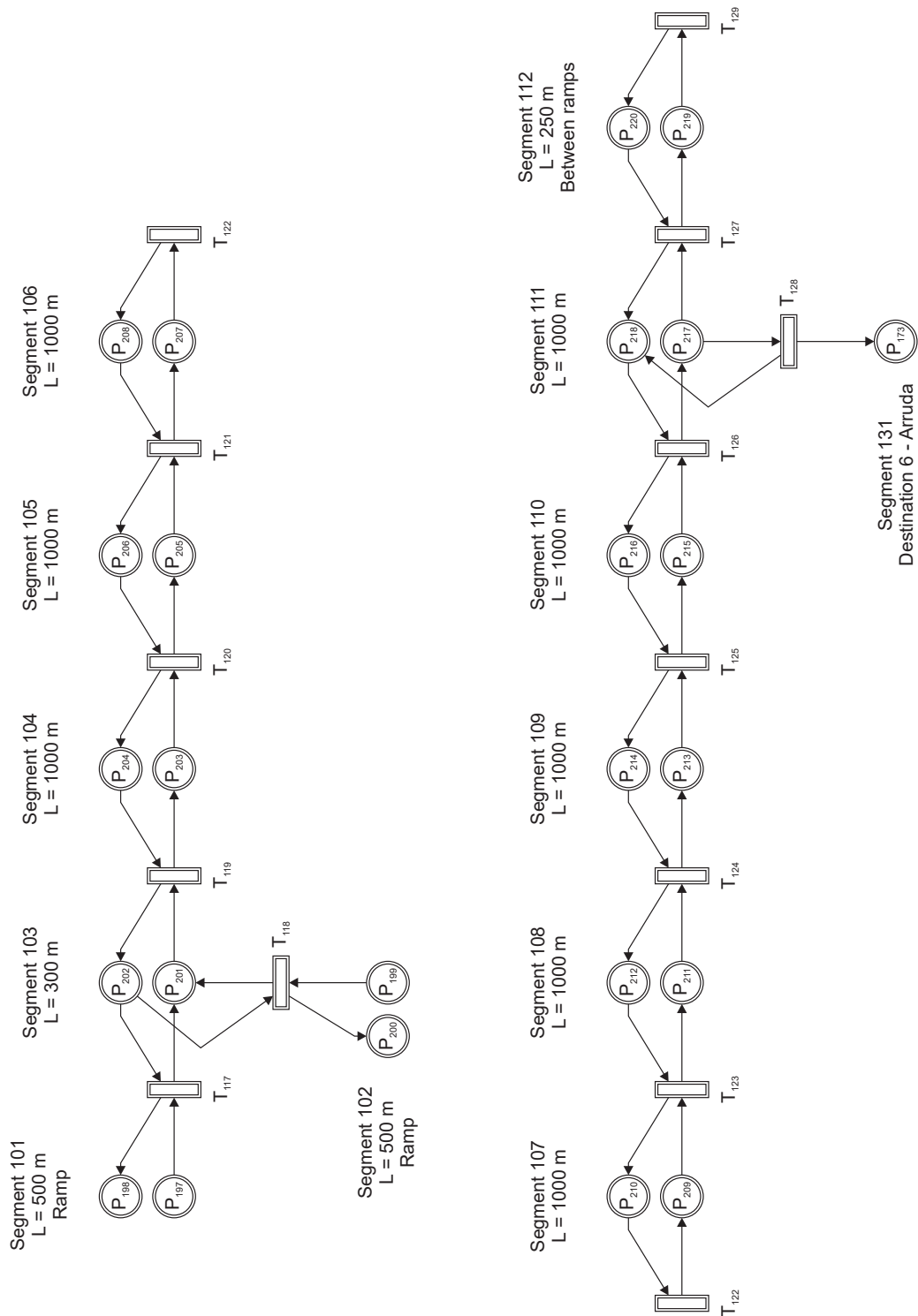Figure B.16 – Petri net scheme of Section 15 of the network – Section (6) – (A)

Figure B.17 – Petri net scheme of Section 16 of the network – Section (A) – (6)
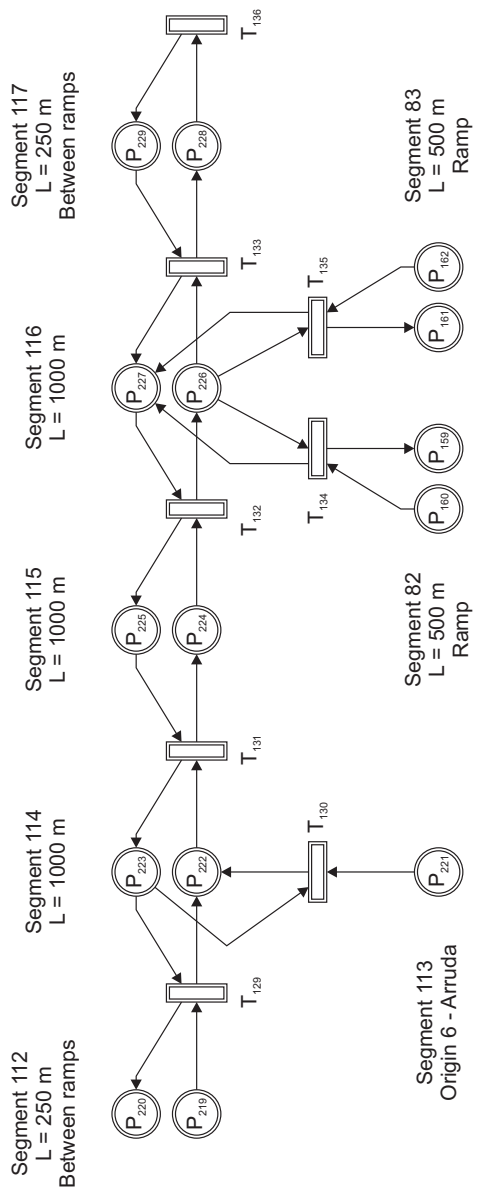
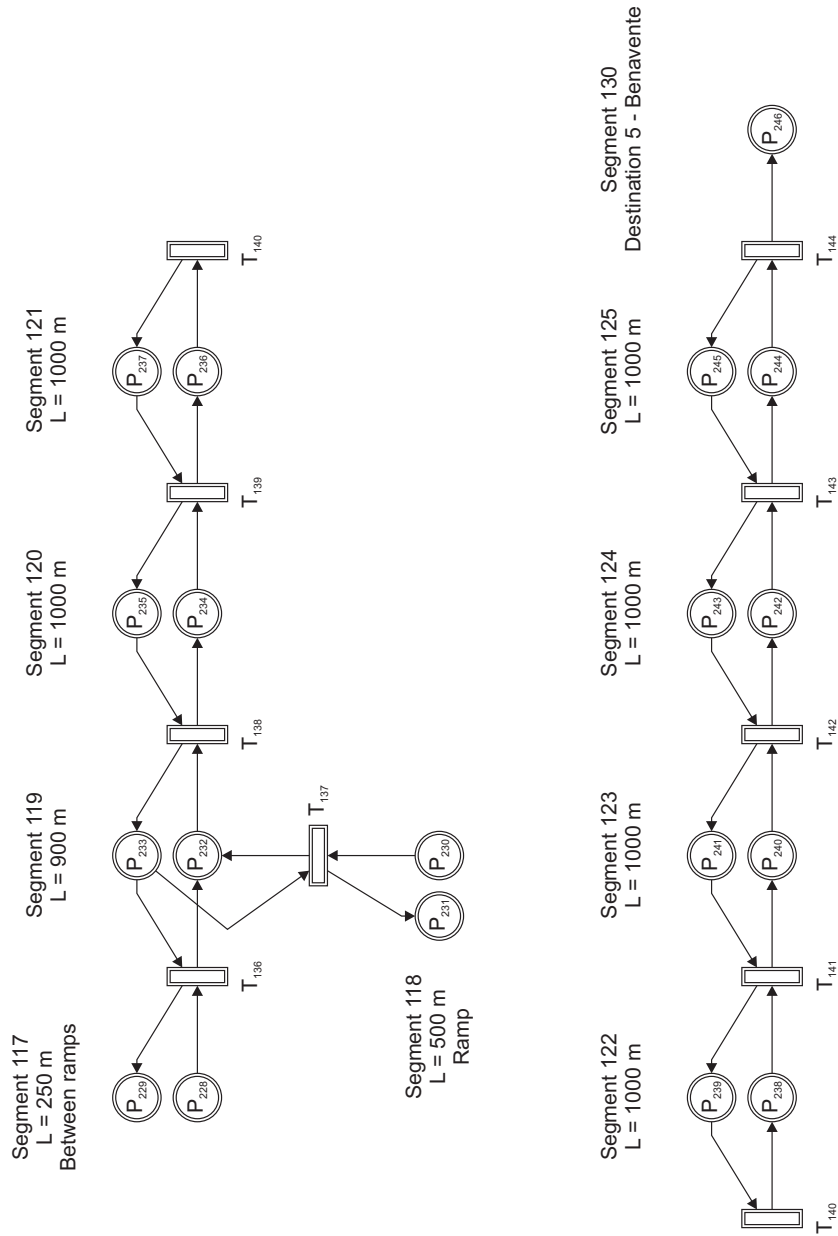Figure B.18 – Petri net scheme of Section 17 of the network – Section (6) – (B)

Figure B.19 – Petri net scheme of Section 18 of the network – Section (B) – (5)
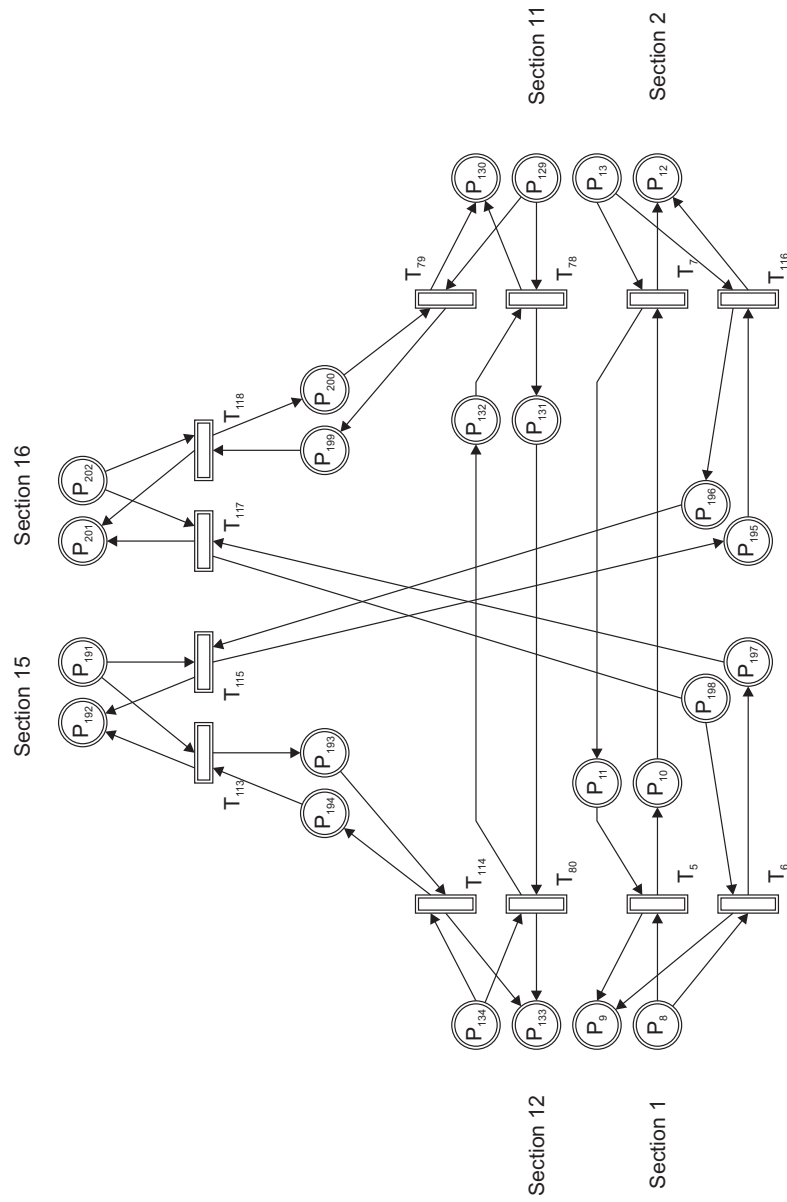
Figure B.20 – Petri net scheme of the intersection between A9 and A10 – Intersection (A)

Figure B.21 – Petri net scheme of the intersection between A1 and A10 – Intersection (B)

B.2 Traffic flow circulation schemes

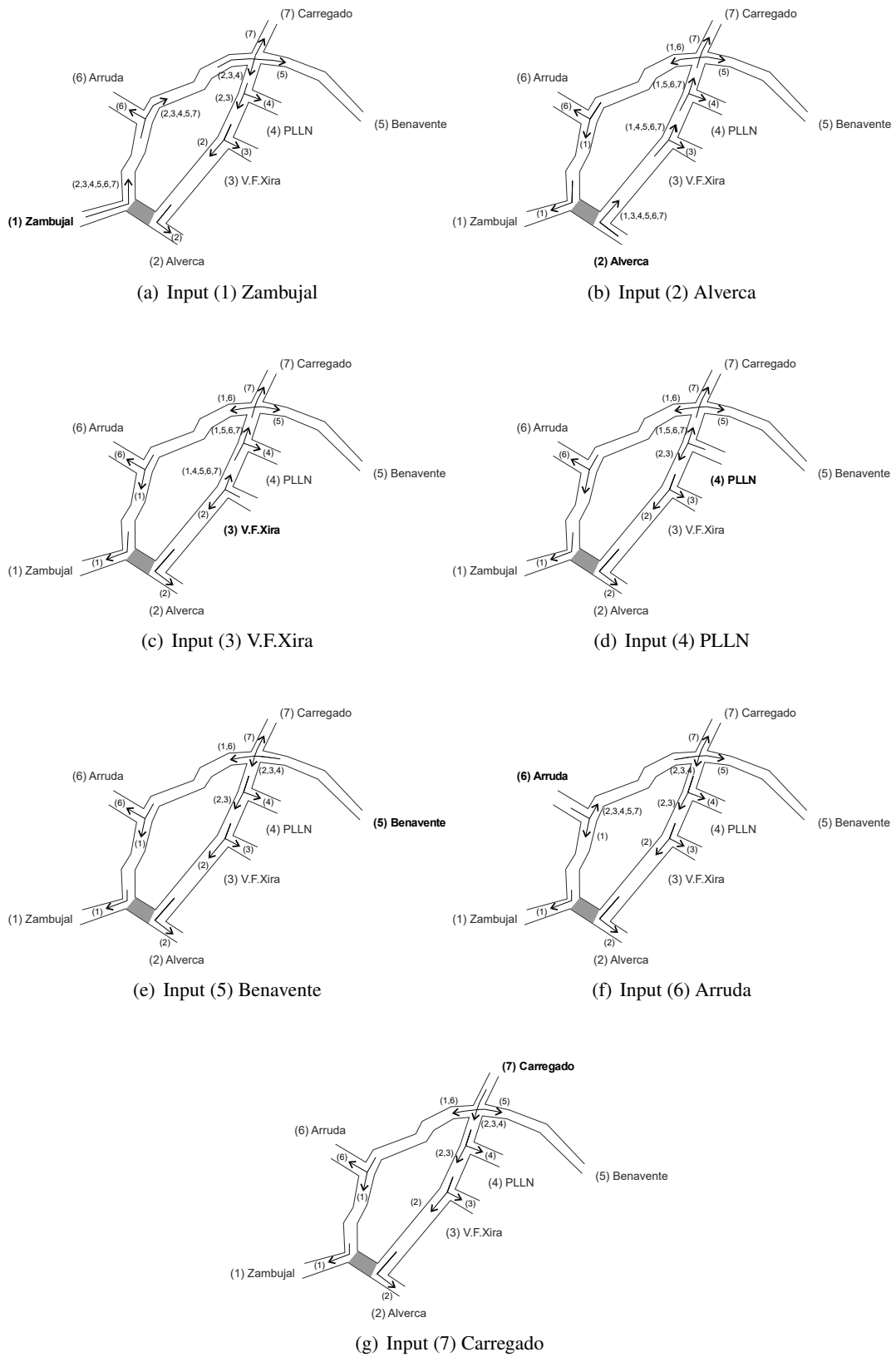(a) Input (1) Zambujal

(b) Input (2) Alverca

(c) Input (3) V.F.Xira

(d) Input (4) PLLN

(e) Input (5) Benavente

(f) Input (6) Arruda

(g) Input (7) Carregado

Figure B.22 – Scheme of the traffic flow circulation in the situation in which Sections 2 and 11 are unavailable

(a) Input (1) Zambujal

(b) Input (2) Alverca

(c) Input (3) V.F.Xira
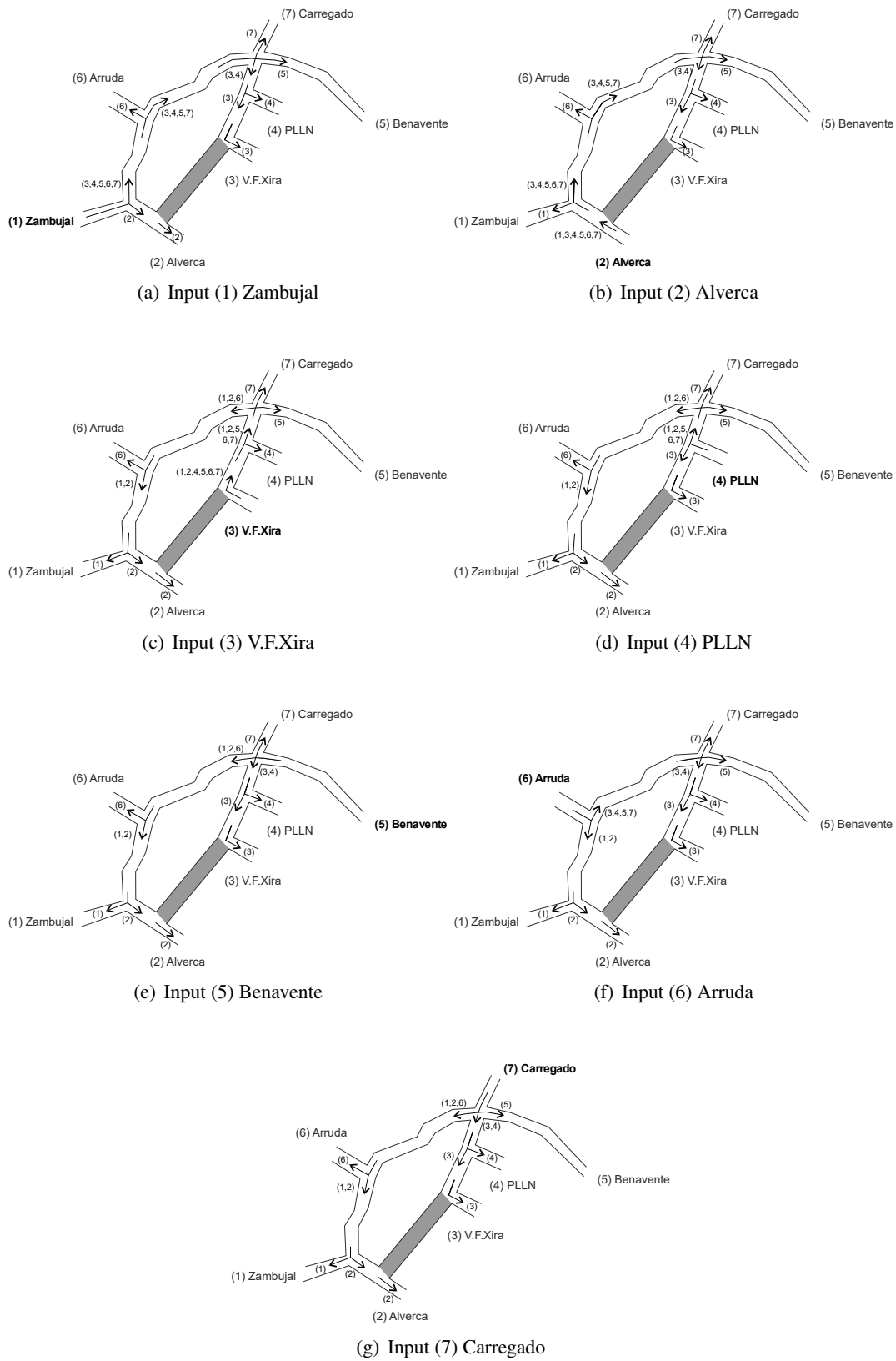
(d) Input (4) PLLN

(e) Input (5) Benavente

(f) Input (6) Arruda

(g) Input (7) Carregado

Figure B.23 – Scheme of the traffic flow circulation in the situation in which Sections 3 and 10 are unavailable

(a) Input (1) Zambujal

(b) Input (2) Alverca

(c) Input (3) V.F.Xira

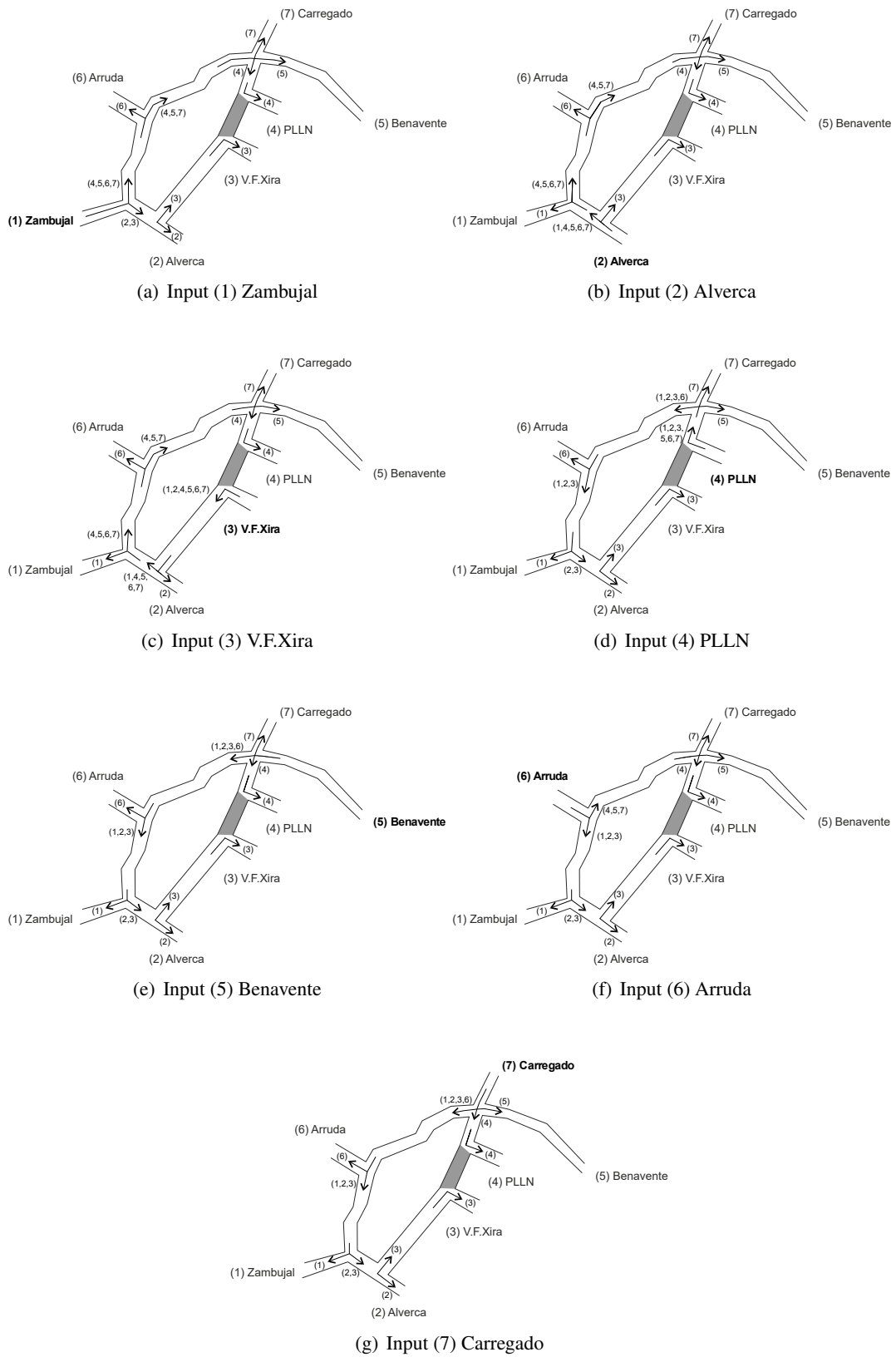(d) Input (4) PLLN

(e) Input (5) Benavente

(f) Input (6) Arruda

(g) Input (7) Carregado

Figure B.24 – Scheme of the traffic flow circulation in the situation in which Sections 4 and 9 are unavailable

(a) Input (1) Zambujal

(b) Input (2) Alverca

(c) Input (3) V.F.Xira
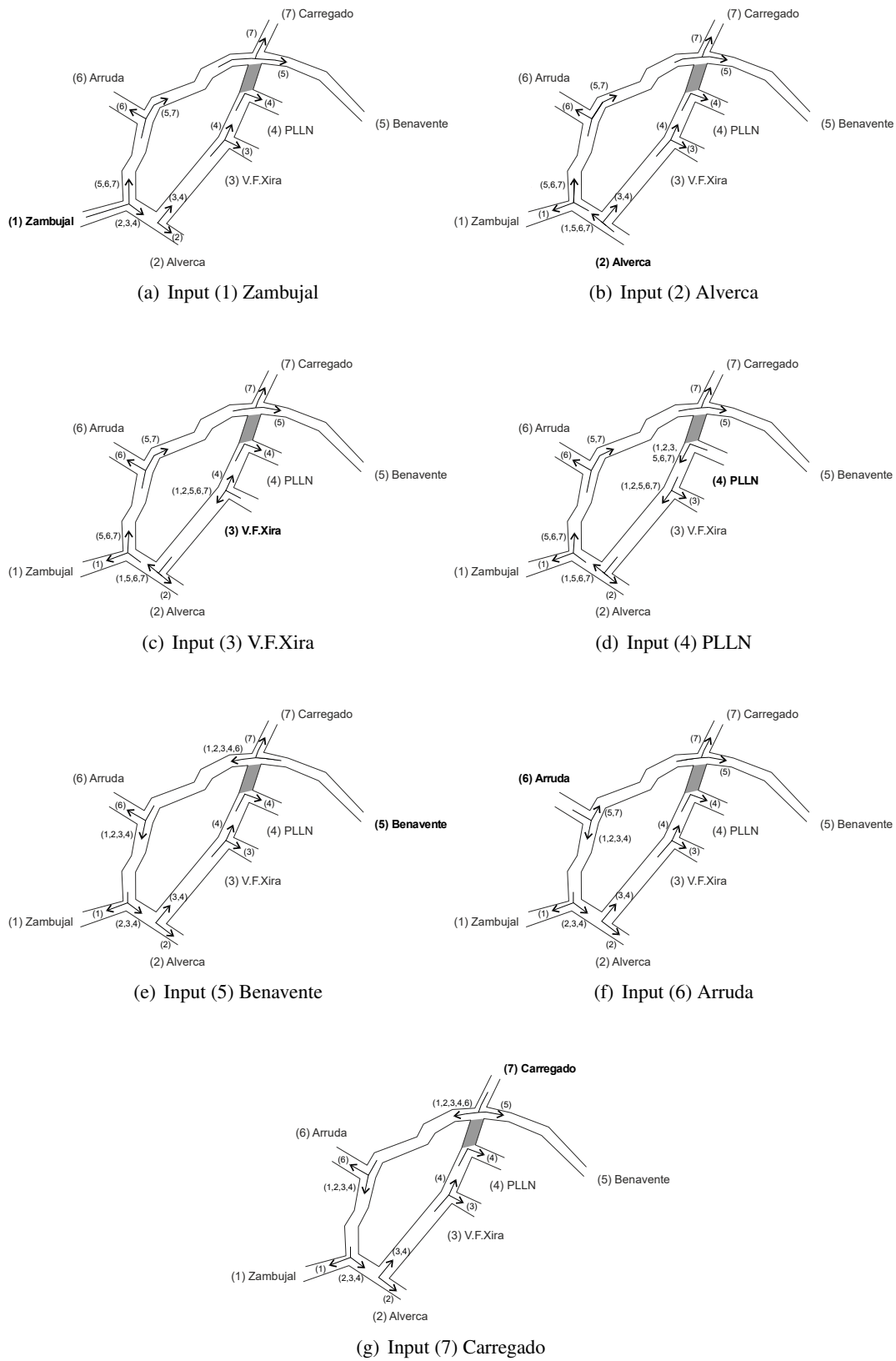
(d) Input (4) PLLN

(e) Input (5) Benavente

(f) Input (6) Arruda

(g) Input (7) Carregado

Figure B.25 – Scheme of the traffic flow circulation in the situation in which Sections 5 and 8 are unavailable

(a) Input (1) Zambujal

(b) Input (2) Alverca

(c) Input (3) V.F.Xira

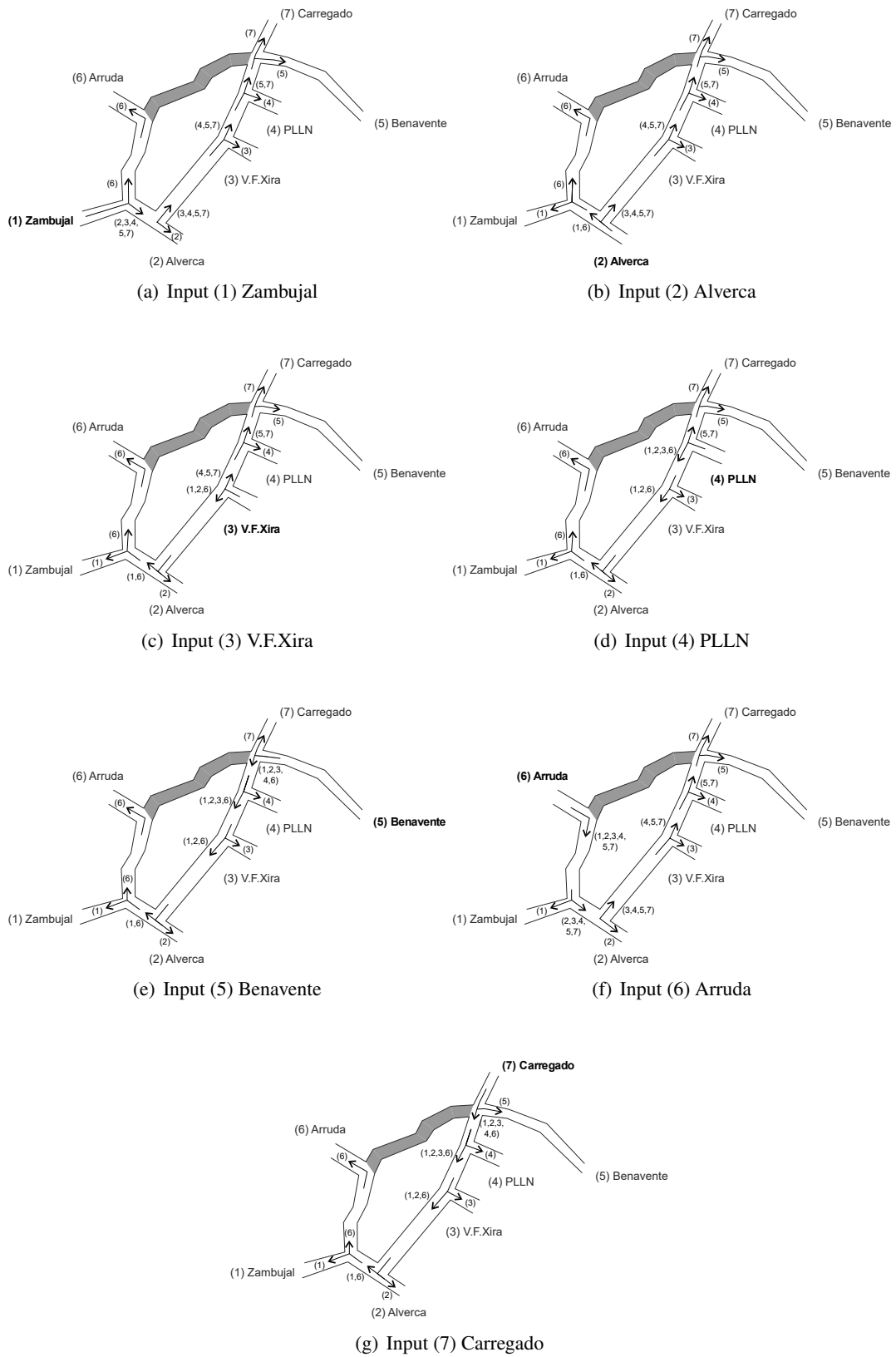(d) Input (4) PLLN

(e) Input (5) Benavente

(f) Input (6) Arruda

(g) Input (7) Carregado

Figure B.26 – Scheme of the traffic flow circulation in the situation in which Sections 14 and 17 are unavailable

(a) Input (1) Zambujal

(b) Input (2) Alverca

(c) Input (3) V.F.Xira

(d) Input (4) PLLN

(e) Input (5) Benavente
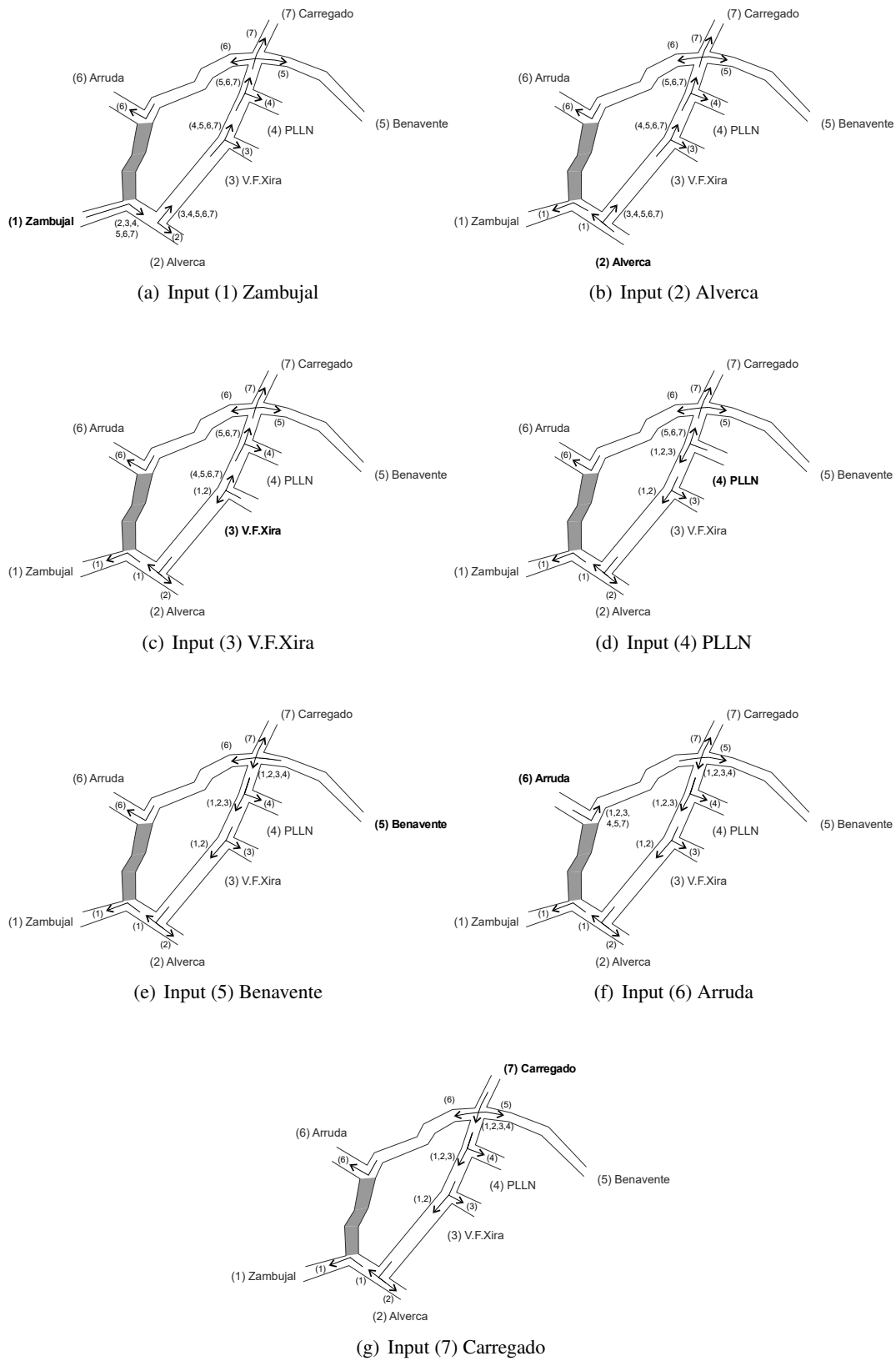
(f) Input (6) Arruda

(g) Input (7) Carregado

Figure B.27 – Scheme of the traffic flow circulation in the situation in which Sections 15 and 16 are unavailable